FLEXOR TENDON HEALING

EVALUATION OF PERITENDINOUS ADHESION FORMATION

AND TENDON STRENGTH AFTER TENOTOMY AND PRIMARY REPAIR

IN AN OVINE MODEL

BY

K. Elaine Davidson MB, ChB, MRCS

M.D. Thesis – The University of Edinburgh – A.D 2005

DECLARATION OF ORIGINALITY

I, Elaine Davidson, declare that this thesis has been composed by myself and that the work reported here is my own work.

This work has not previously formed any part of a degree submitted at this or at another University

Ms K Elaine Davidson

Surgical Research Fellow
Department of Clinical Neurosciences
Western General Hospital NHS Trust
Edinburgh

16th December 2005

Acknowledgements

First, I wish to thank Mr Michael Glasby for having taken the time to come and speak with me after my Membership examination at the Royal College of Surgeons of Edinburgh, as this was the turning point which guided me toward the pursuit of this research project and M.D. I am extremely grateful for his continued support, guidance and enthusiasm which have enabled me to fulfil this goal.

Many thanks to Mr Tom Gilchrist and all the team at Giltech Limited for having given me this opportunity to research their new product, for allowing me such freedom of design and management of the project and for making me feel so welcome a part of their team.

Thanks to Miss Gail Valler for her daily assistance in theatre and for her support throughout my time with the Peripheral Nerve Research Group. I wish her every success in her change of career and hope that she finds happiness and fulfilment.

My thanks to Professor Peter Sandercock, Head of the Department of Clinical Neurosciences at the Western General Hospital in Edinburgh; the department with which I have been affiliated for the duration of this project.

To Mr Dennis Doogan and all of the team at the Marshall Building in Roslin I wish to extend special thanks: for always brightening up the day with cheerful warm friendship; for all the laughter, the camaraderie and the help in overcoming difficulties; for the Christmas celebrations, the barbeque, and for simply making me feel so welcome as a part of 'the family'. In particular, I wish to thank Mrs Joan Docherty, with whom I shall always enjoy keeping in touch. I feel particularly privileged to have had the opportunity to meet and begin to know the delightful, colourful and ingenious character of the late Norah who, I know, is sorely missed by the whole team.

My special thanks also go to Brendan Hawes for his technical help and positive approach to all the challenges faced. Thanks also to Professor Joseph McGeough, Head of the Department of Engineering, for his support and selection of Brendan to

assist with this work, and to Jim Hutcheson for granting access to the Instron machine.

My heartfelt thanks go out to all my family, without whom none of this would have been possible. For their love, support and countless hours of magnificent childcare, I am most grateful.

Above all, however, I wish to thank my husband for his endless love, support and enthusiasm for all that I choose to pursue in life, for always being there, especially when the road gets tough and for believing in us and our future.

This thesis is dedicated to our son, Matteo.

Abstract

This experimental study was designed to assess the effects of different surgical repair techniques on the process of flexor tendon healing. In particular it aimed to evaluate the effects of incorporating a novel biocompatible, biodegradable 'wrap' into the process of tendon repair. This inorganic polymer wrap, Controlled Release Glass, (Giltech Limited, Ayr, Scotland, UK) was composed of a combination of sodium and calcium cations with phosphate and oxide anions and degraded into simple ionic substances normally found in tissue fluid. The hypothesis to be tested stated that 'the addition of this potentially anti-adhesiogenic substance to the process of flexor tendon repair would result in no difference in musculoskeletal function or tendon characteristics after recovery'.

Tenotomy and primary repair of the ovine Flexor Digitorum Superficialis Pars Superficialis slip was performed using a variety of different repair methods, involving combinations of the following elements of repair; modified Kessler core suture, circumferential epitenon suture, CRG wrap, triamcinolone paste. Eleven experimental groups of twelve cases each were set-up and evaluated in two time cohorts; six weeks and six months after surgery. A control group of twelve non-operated cases was also assessed.

Outcome was measured using a combination of standard *in vitro* tests (tensile strength, morphometry and percent composition) and in addition two *in vivo* assessments (Laser Doppler Blood Flowmetry and dynamic testing of displacement, velocity and acceleration).

Results of statistical analyses showed that for the experimental groups containing CRG wrap, the proliferative vascular response to injury was diminished toward 'normal' range at six weeks, and within 'normal' range by six months after repair. This occurred in the absence of any significant difference in superficial blood flow beyond the site of repair or in the strength of these groups of repaired tendons.

Also, at six weeks after operation these experimental groups showed a reduction in fibrous tissue at the sites of tendon repair without any other significant differences in morphological features of the healing tendons. The implications for clinical practice of these findings are discussed.

CONTENTS

LIST OF FIGURES

LIST OF TABLES

Identification codes & variables

GROUP	PRIMARY PROCEDURE
AEarly	= KC repair at 6 Weeks
BEarly	= KCE repair 6 Weeks
CEarly	= KCW repair 6 Weeks
DEarly	= KCEW repair 6 Weeks
ALate	= KC repair 6 Months
BLate	= KCE repair 6 Months
CLate	= KCW repair 6 Months
DLate	= KCEW repair 6 Months
N	= **N**ormal
S	= Dissection only
W	= **W**rap only
T	= KCEW repair + **T**riamcinolone

Doppler

R/LF1	= **R**ight / **L**eft **F**lux 1	(proximal probe)
R/LF2	= **R**ight / **L**eft **F**lux 2	(distal probe)
R/LF1-2	= **R**ight / **L**eft **F**lux 1- Flux 2	
L/RF1	= **L**eft / **R**ight **F**lux 1	
L/RF2	= **L**eft / **R**ight **F**lux 2	
L/RF1-2	= **L**eft / **R**ight **F**lux 1- Flux 2	

In vivo tendon dynamics

DmR/L	= **m**aximum **D**isplacement, **R**ight / **L**eft
tDmR/L	= **t**ime to **m**aximum **D**isplacement, **R**ight / **L**eft
DhrR/L	= **D**isplacement at **h**alf **r**elaxation, **R**ight / **L**eft
tDhrR/L	= **t**ime to **D**isplacement at **h**alf **r**elaxation, **R**ight / **L**eft
tTTR/L	= **t**ime for **T**otal **T**witch, **R**ight / **L**eft
VmR/L	= **m**aximum **V**elocity, **R**ight / **L**eft
tVmR/L	= **t**ime to **m**aximum **V**elocity, **R**ight / **L**eft
t0AccelR/L	= **t**ime to zero **Accel**eration, **R**ight / **L**eft

Instron

R/LF	= maximum **F**orce, **R**ight / **L**eft
R/LD	= maximum **D**isplacement, **R**ight / **L**eft

Histological

R/LA	=**R**ight/**L**eft **A**rea
R/LP	=**R**ight/**L**eft **P**erimeter
R/LL	=**R**ight/**L**eft **L**ength
R/LXF	=**R**ight/**L**eft **X**Feret
R/LYF	=**R**ight/**L**eft **Y**Feret
R/LFF	=**R**ight/**L**eft **F**orm **F**actor

RT	=**R**ight **T**endon fibres
RS	=**R**ight **S**uture material
RV	=**R**ight blood **V**essels
RO	=**R**ight **O**ther/fibrous substance

(also see Appendix 6)

CHAPTER 1

INTRODUCTION

This project was designed to assess the effects of several different surgical techniques, including the use of a new product – Controlled Release Glass wrap (CRG, see Biodegradable Glass, page 37) in the process of flexor tendon healing. The hypothesis set out to be tested stated that ***'the addition of a potentially anti-adhesiogenic agent to the process of tendon repair would result in no difference in musculoskeletal function or tendon characteristics after recovery'***.

GENERAL AIM

The principle aim of this research was to use a large animal model (ovine) to ascertain if, after division of a tendon (tenotomy) and primary repair, peritendinous adhesions could be reduced by the incorporation of anti-adhesiogenic agents, with a consequent improvement in motor function.

DEFINITION OF A TENDON

A tendon may be defined as a cord of inelastic fibrous tissue connecting a muscle to its point of insertion.

FUNCTIONS OF TENDONS

Tendons transmit the force generated by contraction of their respective muscle to effect movement of the appropriate joint(s). They also store elastic strain energy.

HISTORICAL BACKGROUND

Hippocrates (469 – 399 BC) was author of the first recorded description of the function of tendons, to move joints (Peri arthron III:17). Several centuries later the second century Greek physician and philosopher Claudius Galen (131-201 AD) of Pergamum (Pearcy 2004) wrote about tendons though he described the white cords of tendons as being those of nerves. In his doctrine, the Ars Parva, he warned of the dangers inherent in injuring or even touching nerves (or tendons) cautioning that this could result in pain, convulsions and even gangrene (Kleinert & Pickford 1997). Thus Galen advocated the avoidance of tendon operation after division or injury. His opinion heavily influenced physicians in Europe for many centuries and it was not until the tenth century that the first operation to repair a divided tendon was believed to have been performed. This was carried out by the Arabian surgeon, Avicenna, but his valuable observations remained ignored for nearly 600 years (Kleinert, Spokevicius, & Papas 1995). A new generation of physicians then began to re-examine Galen's theories and in 1752 Albreecht Von Haller published results of his work on sensibility and irritability of various tissues, surmising that tendons had no sensibility (Seiler & Fogle 2004). Backed by the French Academy of Science and along with the emergence of other authors' publications (such as Syme's successful primary tendon repair in England in 1850), the primary repair of a tendon (tenorrhaphy) gradually began to become accepted as the treatment for division of tendons (Kleinert, Spokevicius, & Papas 1995). From this time reports of different methods of tendon repair began to emerge including the description of a locking suture method by Kirchmayr, of which the Kessler (see Core Suture, page 33) and Tsuge sutures are close variants and still in use today.

In 1918 Sterling Bunnell, founder of the speciality of hand surgery in the United States of America published a pioneering paper (Newmeyer 2003). In his manuscript he introduced the concept of 'no man's land'[1] (see Zone Classification, page 23) and

---

[1] *so called since results of primary repair performed in this zone (within the flexor sheath) were extremely poor*

advocated tendon grafts in this zone rather than simply avoiding any attempt at surgical repair. He also reinforced the concepts of meticulous surgical technique, the importance of the pulley system (see Flexor sheaths, page 21), the need for careful postoperative rehabilitation and early mobilization regimens. In 1944 he published his first edition of *Surgery of the Hand,* a highly prominent text at the foundation of the speciality of hand surgery. The 1940s and 1950s heralded the publication of many papers from authors such as Mason, Boyes, Koch, Pulvertaft, Allan, and Verdan, in which the authors described their own observations and techniques for dealing with tendon injuries. Then in the late 1950s and in early 1960 respectively, Verdan (in Swizerland) and Kleinert (in USA) published results of their first series of primary repairs performed on cleanly divided tendons, contrary to the generally accepted practice of tendon grafting. The presentations of these encouraging operative outcomes led to further inspection by the members of the American Society for Surgery of the Hand. The Society then gave its approval of this practice of tenorrhaphy, which has since become the 'gold standard' treatment for severed tendons. Since the 1960s a vast amount of literature has been published describing different methods of suturing, types of suture material used, protocols for post-operative mobilization and in-depth studies of the anatomy, physiology and biomechanics of normal and healing tendons, including many papers by distinguished authors such as Gelberman, Manske, Lundborg.

However, despite this increase in knowledge and understanding of the mechanical and physiological properties of tendons and improvements in suture technique the treatment of flexor tendons lacerated within their digital sheaths remains one of the most challenging problems in hand surgery today (Beredjiklian 2003;Leddy 1988).

The major clinical problem is that of the development of restrictive post-operative adhesions (see Healing & Sequelae, page 26) and much research continues to address the balance of the multitude of factors which influence the outcome of surgical intervention and the natural healing process.

Many novel techniques have been explored to-date in an attempt to overcome this problem of adhesions. However, none has become widely accepted into clinical practice and as such the search for this 'Holy Grail' in hand surgery continues.

ANATOMY OF TENDONS

Detailed anatomy of human tendons may be found in any comprehensive anatomy textbook (*e.g* Gray's Anatomy) thus for the purposes of this thesis description will be limited to a few basic principles and some salient points related to the tendon under examination; the flexor digitorum superficialis (FDS).

Structure of a tendon

Tendons are composed of a strictly ordered hierarchy of successively larger structural units. The most basic element is that of a collagen fibril (Type I). The fibrils are aggregated into bundles to create 'fibres' which in turn link together to form subfascicles. The subfascicles are grouped together along with fibroblast cells and enclosed in a covering known as endotenon, thus forming a tendon fascicle. These fascicles are then bound together in an outer layer of epitenon which completes the hierarchical structure of a tendon.

Figure 1: Structure of a tendon

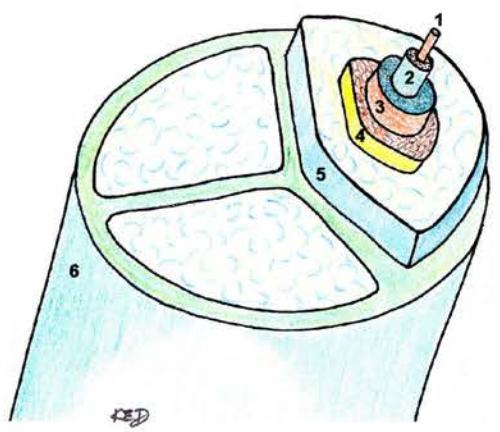

Classification of type

A muscle and its respective tendon may be classified as either 'flexor' or 'extensor' dependent upon the action of joint movement effected as a result of contraction; flexors bend the joint whilst extensors straighten it.

Flexor tendons of the human hand

The flexor tendons of the hand commence at their musculotendinous junctions in the distal third of the forearm and are derived from the following muscles; flexor digitorum superficialis (FDS), flexor digitorum profundus (FPD), flexor carpi ulnaris, flexor carpi radialis, flexor pollicis longus and palmaris longus (though often the latter muscle is absent). For the purpose of this study however, description of anatomical course will be restricted to only that of the FDS and FDP tendons.

The FDS muscle is supplied by the median nerve and arises from two distinct origins; a 'humeroulnar' head and a 'radial' head. The humeroulnar head arises from the medial epicondyl of the humerus and the medial margin of the coronoid process of the ulna. The radial head arises from the oblique line of the anterior surface of the shaft of the radius. The FDS muscle divides into four tendons which ultimately insert into the base of the middle phalanx of each of the four fingers of the hand.

Figure 2: Origin and insertions of human right FDS muscle

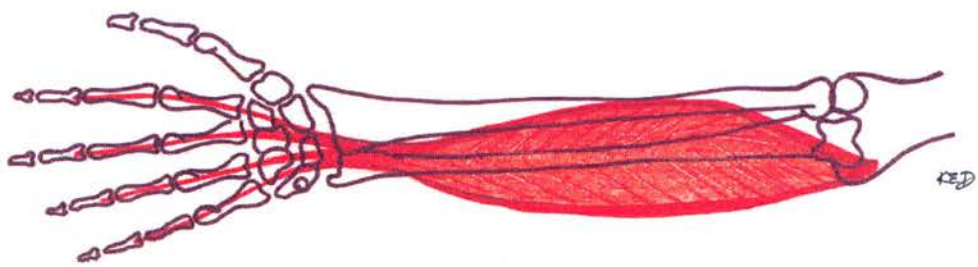

View of palmar aspect of right forearm. FDS muscle and tendons shown in red.

The FDP muscle is supplied by both the ulnar and median nerves and arises from the upper part of the anterior and medial surfaces of the shaft of the ulna along with the adjoining part of the interosseous membrane. It divides into four tendons which are ultimately inserted into the base of the distal phalanx of each of the four fingers of the hand.

Figure 3: Origin and insertions of human right FDP muscle

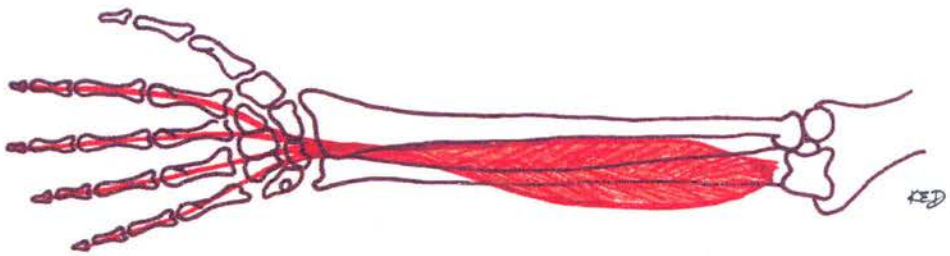

View of palmar aspect of right forearm. FDP muscle and tendons shown in red.

From their commencement at the musculotendinous junctions the tendons are divided into two groups. If dissecting from the volar aspect of the forearm, the superficialis group is identified first, lying as a group of independent tendons. Deep to these lies the conjoined tendon of the profundus group. Continuing distally, to the level where the tendons traverse the wrist, the eight tendons of the FDS and FDP enter into a large synovial sheath, the common flexor sheath (see Flexor sheaths, page 21). The tendons continue to course distally within the common flexor sheath, through the tight space of the carpal tunnel; formed by the flexor retinaculum overlying the carpal bones of the hand. The FDS tendons maintain a consistent arrangement with the tendons to the middle and ring finger lying palmar to those of index and little, with FDP deep to these. They then fan out into the palm with the FDS tendons in the same plane and FDP remaining deep. At the level of the proximal transverse crease of the palm, the superficialis and profunda tendons to the index, middle and ring fingers emerge for a short distance before entering into individual digital synovial sheaths. The tendons to the little finger continue uninterrupted in an extension of the common sheath.

Figure 4: Flexor sheaths of the human right hand

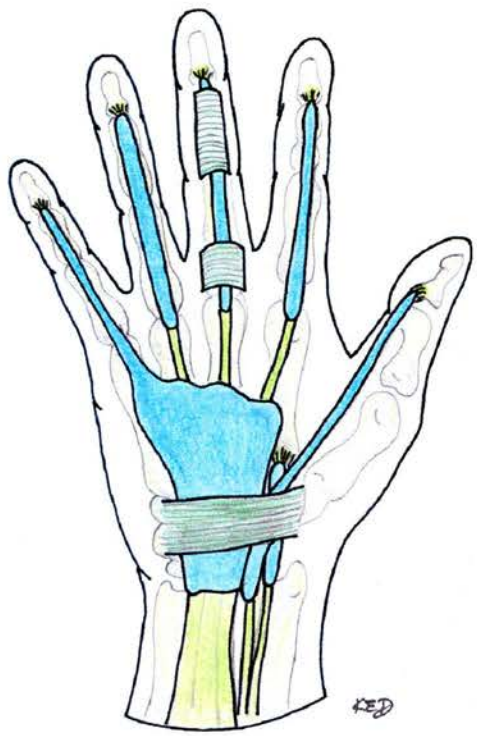

The palmar aspect of the right hand is illustrated detailing the normal anatomic configuration of flexor tendon synovial sheaths (blue).

At the level of the proximal phalanges, each of the FDS tendons divides into two slips, allowing the FDP to pass through, before reuniting for a short distance and then dividing again, into radial and ulnar slips, upon insertion into the sides of the middle phalanx of each finger. The FDP having passed between the FDS slips continues to course distally inserting into the base of the distal phalanx of each finger.

Figure 5: Anatomical course of FDS and FDP in the human finger

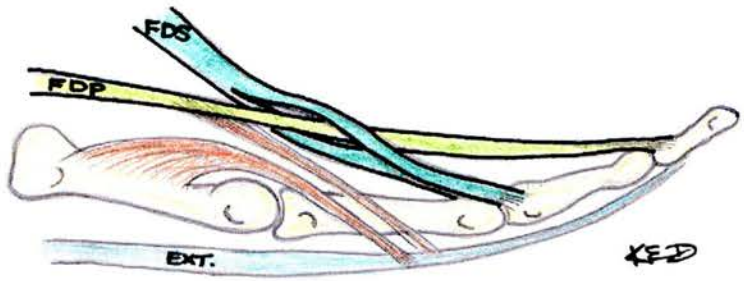

Tendon insertions in the human digit (EXT = extensor tendon)

Comparative anatomy of the ovine model

Clearly the greatest difference between the forelimb of the human and the sheep is that in the sheep the function of the forelimb is limited to that of weight-bearing without any need to perform fine motor skills. As such the process of evolution has resulted in the sheep having a hoof, composed of distal-phalanges, very large metacarpal bones (approximately equal in size to its radius and ulna) rudimentary carpal bones and a relatively short humeral bone, as illustrated below.

Figure 6: Comparative anatomy of the ovine model

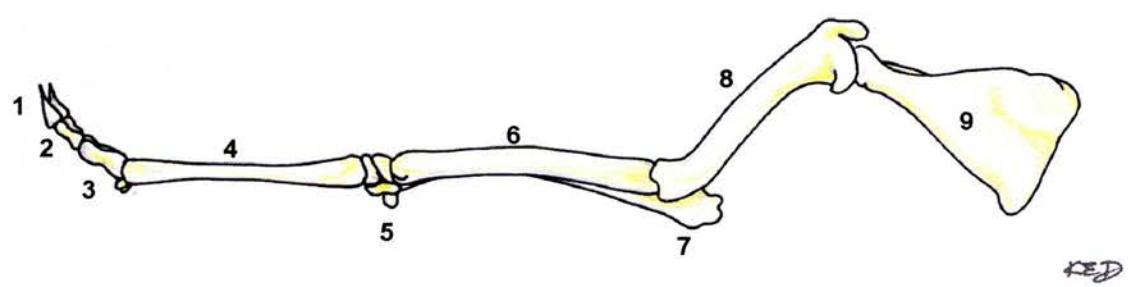

1 = distal phalanx
2 = middle phalanx
3 = proximal phalanx
4 = metacarpal bones III & IV
5 = carpal bones
6 = radius
7 = ulna (olecranon)
8 = humerus
9 = scapula

The FDS of the sheep arises from two heads; the medial epicondyle of the humerus (pars superficialis, PS) and a smaller head (pars profunda, PP) from the postero-lateral margin of the radius. The two tendon slips (FDS PS and FDS PP) unite just proximal to the level of the carpal bones, to form the common FDS tendon. As in the human case, this tendon inserts into the base of the middle phalanx.

Figure 7: FDS in the right forelimb of the sheep

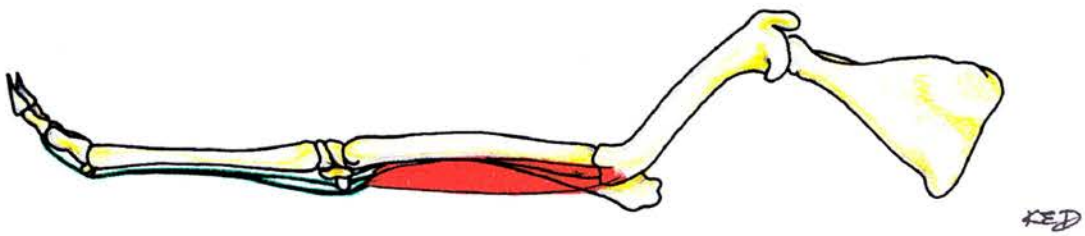

Medial view, FDS muscle bellies shown in red. The tendon slips of FDS PS (below) and FDS PP (above) are shown as single lines continuing distally to insert into the middle phalanges

The FDP arises from the lateral border of the ulna and inserts into the base of the distal phalanx/hoof. Both muscles are also supplied by branches of the median nerve and their tendons are collectively enclosed within a synovial sheath. The sizes of the FDS and FDP tendons in the adult sheep are comparable to that of the human case (see also Ovine Model, page 48).

Vascular supply of the human flexor tendons

The blood supply to the fingers runs infero-laterally to the course of the tendons. It is derived from branches of both the radial (deep palmer arch) and ulnar (superficial palmar arch) arteries which run distally along the lateral sides of the phalanges, as digital arteries. Digital nerves accompany the digital arteries to supply the skin of the

palmer aspect of the fingers as well as the distal half of the dorsal aspect of each finger. In general the ulnar nerve branches give rise to the digital nerves of one and a half fingers on the ulnar side (little finger and ulnar half of the ring finger) whilst the median nerve gives branches supplying the remaining fingers and thumb (thumb, index, middle and radial half of the ring finger).

The intrasynovial part of a flexor tendon receives a dual nutritional supply; a segmental, intrinsic supply originating from the paratenon, in common with that of all types of tendon and an additional extrinsic supply provided by the synovial sheath (see Flexor sheaths below). It has been shown that upon flexion and extension of the digit, the synovial fluid from the sheath is forced into the interstices between tendon fascicles and thus the tendon is nourished by the process of imbibition (Manske & Lesker 1985). The importance of both of these nutritional systems, perfusion and diffusion, have been demonstrated (Manske & Lesker 1982; Steinberg 1997), but there remains much debate and interest regarding the balance of the two systems in both normal and healing tendons (Jones et al. 2000).

Figure 8: Cross-sectional view of the human digit

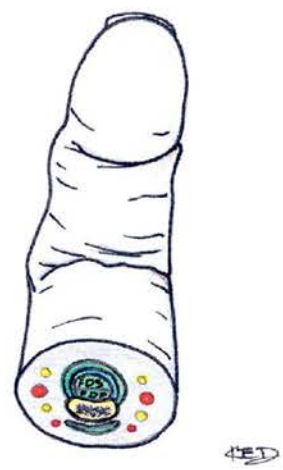

In the centre of this cross-sectional view of the finger the FDS tendon lies above the FDP. They are enclosed within the digital synovial sheath and lie adjacent to the palmar aspect of the proximal phalanx. The digital arteries are indicated in red, the digital nerves in yellow.

Flexor sheaths

Flexor sheaths may be thought of as essentially double-walled hollow tubes that are sealed at both ends (Leddy 1988). However they are in fact highly specialized structures that secrete a fluid, synovial fluid, between the layers of their walls. They provide the tendons with a source of nutrition and an environment which facilitates low friction gliding, essential for optimal digital function. The tendons appear to be invaginated into the sheath which wraps around and suspends the tendon from a fold of synovial membrane know as the mesotendon or vincula (Powers 2003). It is these vinculae which transport nerves and blood vessels to the enclosed tendons.

Figure 9: Schematic illustration of a human digital flexor sheath

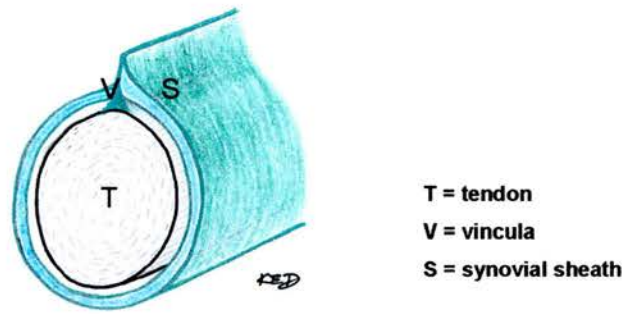

The digital sheaths also contain thickened fibrous areas know as annular (A) and cruciate (C) pulleys (Leddy 1988). These are of fundamental importance as they are responsible for retaining the position of the digital sheath and enclosed tendons (A) whilst facilitating shortening (C) during the movement of flexion.

Figure 10: Fibrous pulleys of the human digital flexor sheath

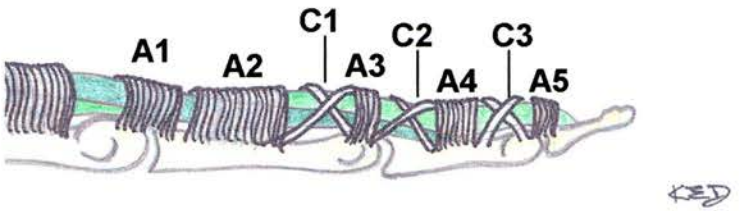

The fibrous bands of the digital sheaths commence at the level of articulation of the metacarpal and proximal phalangeal bones and end at the base of the distal phalynx.

OVERVIEW OF TENDON INJURIES

Epidemiology

The hand is one of the most commonly injured parts of the body and hand injuries have been reported to account for a quarter of all accidents (BSSH 2002) as well as being the leading occupational injury treated in the United States' hospital emergency departments (Sorock et al. 2001). Of these injuries, laceration of a flexor tendon is one the most commonly sustained (Steinberg 1997), although the exact incidence is unknown. Much research has been carried out, and is indeed continuing, to advance our understanding of the biomechanics and physiological processes of tendon repair. Despite recent advances, a great deal of debate still exists regarding the best methods of repair of tendon injuries.

Zone Classification

In order to assist classification of flexor tendon injuries and discussion of their appropriate management, the flexor tendons were historically divided into 'zones'. This was originally described by Verdan, C in 1960 (Helm 2003) but has since been modified to produce a five zone classification as illustrated below (Leddy 1988).

Figure 11: Zone classification of flexor tendons of the hand

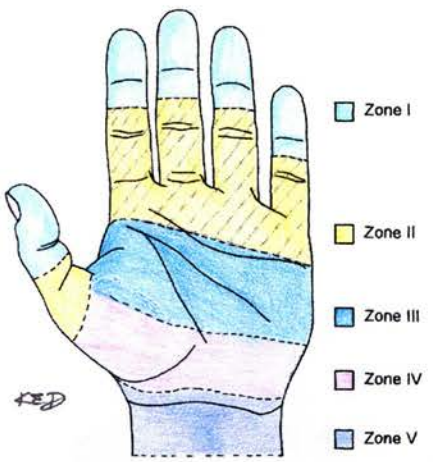

Zone two was previously termed 'no man's land' by Bunnell in 1918 (Kleinert & Pickford 1997)

Diagnosis

Not all cases of tendon injury are straightforward to diagnose. However, in clear-cut cases, examination reveals a lack of movement of the affect joint(s) distal to the level of transection. Testing for function of the superficialis tendon is performed by asking the patient to flex the affected finger whilst the examiner blocks movement of all other fingers of that hand, keeping them in extension. This normally results in flexion of the finger at the metacarpo-phalangeal joint and the proximal interphalangeal joints only.

Figure 12: Clinical examination for function of FDS tendon

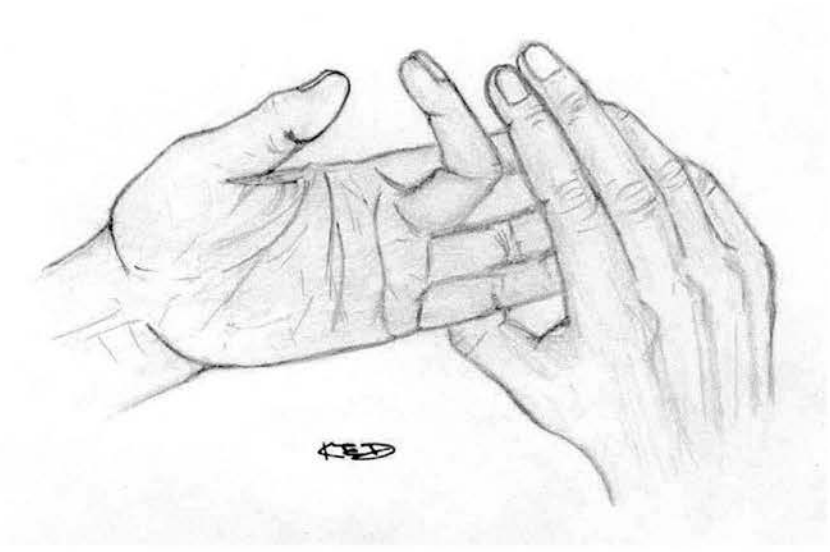

The hand on the left of the illustration is that of the patient in whom the FDS tendon is being assessed. The hand shown on the right is that of the examiner, which is shown isolating movement to only the finger under examination (left middle finger) by inactivating the profunda unit with passive extension of the remaining fingers.

To test function of the profundus tendon the patient is asked to move the affected finger whilst the examiner blocks the proximal interphalangeal joint (see illustration over page). This should result in movement of the tip of the finger provided the FDP tendon is intact.

Figure 13: Clinical examination for function of the FDP tendon

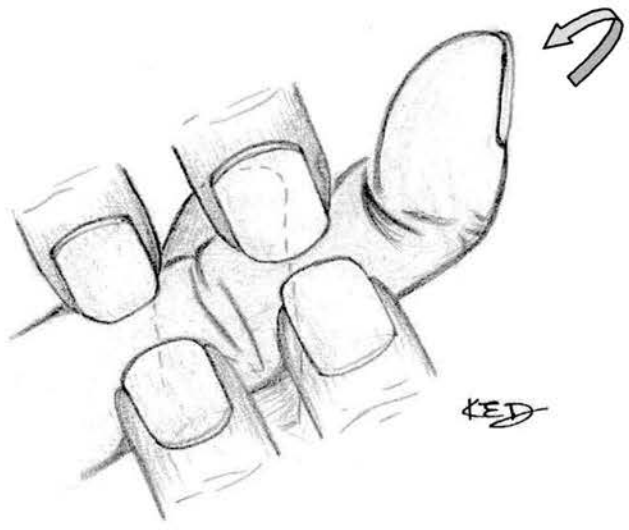

The finger being tested is shown in the middle of this illustration, the examiners four fingers and thumb (represented by the dotted line behind the joint) can be seen blocking flexion of the proximal phalangeal joint.

These tests of function are also then repeated against resistance which is provided by the examiners fingers.

Clearly these clinical tests rely on patient cooperation with the assessment, which may not be possible especially in the case of young children, confusion, hysteria etc. It should also be noted that in cases where incomplete transection has occurred movement distal to the level of injury may still be possible, though it is often associated with pain or discomfort. So in general, if there is doubt regarding tendon transection (or associated neurovascular injury) exploration of the wound is advisable.

Management

As with any injury a thorough examination should be accompanied by cleansing of any associated wounds. Initially this may consist of cleansing with an antiseptic solution such as Betadine® (a 10% povidone-iodine solution). A more thorough cleansing and debridement will most likely require some form of anaesthetic, however this should only be instilled once examination for any sensory loss has been performed. If the wound requires further exploration it is usually best performed by an experienced surgeon under the sterile conditions of theatre. A local, regional or general anaesthetic may be required depending upon the site and extent of injury sustained and the individual characteristics of the patient concerned.

Healing & Sequelae

In order to function efficiently, tendons are required to glide smoothly through very confined spaces of their sheaths and to be mechanically very strong and inextensible. To achieve this they are composed of dense bundles of collagen fibers with a relatively sparse intrinsic blood supply. After injury, two distinct mechanisms of healing have been demonstrated to be active (Beredjiklian 2003): an intrinsic pathway, where the cells for the healing response come from within the tendon and epitenon (Lundborg, Rank, & Heinau 1985; Manske et al. 1984) and an extrinsic pathway, where the cells migrate from out-with the tendon (Potenza 1969). The extrinsic pathway is activated early after the injury has occurred whereas the intrinsic mechanism is delayed by several days. However, much debate still exists regarding the balance and importance of these mechanisms. During the process of healing of tendons three distinct phases have been identified; inflammatory, fibroblastic and remodelling (Strickland 1999). The inflammatory phase occurs first in the healing period, up to around one week after injury and involves the migration of extrinsic inflammatory cells to the site of injury. The fibroblastic phase peaks around three weeks after injury at a time when proliferation of fibroblasts predominates with the laying down of collagen and revascularization of the tissue. The final phase, remodelling, occurs from about eight weeks onwards and is when the newly formed, irregularly placed, collagen fibers become organized along the axis of the tendon.

Adhesions

During the process of healing in an injured tendon, 'adhesions' are seen to develop. These can be defined as 'abnormal attachments between tissues or organs' and occur as a natural part of the fibroblastic response to injury (Jaibaji 2000). Adhesions are initially vascular structures which may provide the area of repair with essential nutrients soon after trauma has occurred. With progression of the healing process these adhesions are remodelled to greater or lesser degrees. However, all too frequently the persistence of some adhesions is sufficient to limit the excursion of the tendon upon contraction of its muscle and thus interfere with joint movement and function. Such adhesions are often referred to as restrictive adhesions

There are a number of factors believed to promote the process of adhesion formation (which one can attempt to minimize during the process of surgical repair). These tend to stimulate the extrinsic pathway of healing and the most important ones are listed below (Matthews, Richards 1976; Strickland 2000):

I. handling of tissues (minimal, gentle tissue handling is essential)

II. exposure of the inner surface of the repaired tendon (hence use of an epitenon suture to fold in the edges, whilst also greatly increasing the strength of repair)

III. presence of any foreign substance on the surface of the tendon (an argument against epitenon suture placement, or for promoting the development of different types of epitenon suture)

IV. compromise of the intrinsic blood supply (*e.g.* due to excessive suture material within the tendon; strangulation of the repair site),

V. immobilization (hence the introduction of many different regimens for mobilization, along with the requirement to maximize suture strength of the repair).

Over the years there have been a number of authors who believed that adhesions were a necessary and vital part of the tendon healing process (Leddy 1988) whilst others, such as Manske and Gelberman, believed (and have demonstrated with *in vitro* studies) that tendons possess an intrinsic potential to heal and can do so in the absence of adhesion formation (Manske et al. 1984). Thus the degree to which

adhesions should potentially be modulated has been in question, let alone any postulated methods of how this could be achieved.

However, it is now universally agreed that the persistence of restrictive adhesions is one of the most frustrating and disabling sequelae of tendon injury in the hand, especially in Zone II. Such adhesions are the basis for substantial morbidity and their consequences necessitate further operative interventions as well as prolonged periods of recuperation and hand therapy (Jaibaji 2000). They produce negative effects on both the patient and surgeon, in addition to a notable economic impact on society and as such generate much interest in the field of tendon research.

Clearly there exists a very fine balance between the stability and mobility of a repair; the amount, type and method of suture placement to provide strength at the repair site with minimal risk of interfering with the blood supply or bulk of the healed tendon and thus its ultimate strength or requirement for smooth gliding motion. As such, finding a 'solution' to this problem of restrictive adhesion formation is a rather complex matter.

Mobilization

The post-operative management of repaired flexor tendons is of critical importance to the outcome of surgical intervention. Immobilization of the repaired digit(s) was historically the preferred method of post-operative care. In 1941 Mason described the site of early tendon repair as a 'gelatinous exudate' and at that time it was believed that the repair site was not capable of withstanding externally applied forces. Recent studies have challenged this view and immobilization has since been found to be associated with problems of joint stiffness and a decrease in Ultimate Tensile Strength (UTS) in the first 5-9 days post-operatively (Boyer et al. 2001). A number of studies have demonstrated that tendons actually respond in a positive manner to increased levels of mechanical stress (Banes et al. 1995; Hannafin et al. 1995; Hannafin & Arnoczky 1994; Harwood et al. 1999). Immediate mobilization of the flexor tendon repair has now been demonstrated to reduce peritendinous adhesions and increase tensile strength, DNA content, eventual excursion, and uptake of synovial fluid (Bolitho 2001). Thus current practice has moved to the implementation of post-operative mobilization regimens. Clearly, patient cooperation and compliance with a

rehabilitation protocol is essential if optimum function is to be regained whilst maintaining a low rate of complications.

In the literature available to-date, much attention has been paid to the development of specific protocols to optimize rehabilitation. However a great degree of diversity exists between the different programmes proposed, as regards type of motion used (active or passive), type of splint used (dynamic or static) and the timing of the progressive steps through the mobilization protocol. Despite this, the aim remains constant: to allow controlled gliding of the repaired tendon relative to the sheath and surrounding tendons or tissues in order to minimize adhesion formation and to maintain capsular movements of the joints, thus avoiding the development of digital flexion contractures. Certain common principles have become considered as standard for all postoperative rehabilitation protocols (Strickland 1999) these include:

1) position at rest for wrist and metacarpo-phalangeal joints; maintained in flexion
2) position at rest for proximal and distal interphalangeal joints; maintained in extension
3) frequent application of motion (active or passive) in a structured programme of rehabilitation

All protocols are designed to guide the patient through progressively intensifying exercises of the injured tendon. However, this progressive motion must be kept within certain limits in order to avoid rupture of the repaired tendon whilst healing is taking place. Current rehabilitation protocols use both passive and active mobilisation regimens. The main argument for regimens that instigate passive motion before active is simply that passive motion results in less force being transmitted across the repaired tendon whilst it is believed to be most vulnerable to stresses of force. In a series of studies using a canine model Gelberman and colleagues showed that passive mobilization enhanced the healing process, resulting in fewer adhesions, a more rapid return of tensile strength, better nutrition and minimal repair site deformation of the tendons compared against immobilized repairs (Gelberman et al. 1982). Then a few years later, Aoki et al and Hitchcock et al published results of their series of studies on the effects of active mobilization on the tendon repair site (Aoki et al. 1997; Hitchcock et al. 1987). These two authors demonstrated that the application of active mobilization further enhanced the strength of repair and biological response to injury

to the extent that the tendons were shown to maintain their tensile strength during the early weeks of healing.

The risk with post-operative mobilization, however, is the complication of tendon rupture. Immediately after operation the degree of risk involved is clearly dependent upon the amount of force that can safely be applied across the freshly repaired tendon, which in turn is dependent upon the suture method used for repair and the condition of the injured tendon tissue. As discussed earlier, a fine balance exists between increasing the strength of the suture, modifying the method used, and potentially compromising the blood supply, nutrition or gliding characteristics of the healing tendon. Thus the amount of force applied across the repair site to allow mobilization of the tendon, without increasing the risk of rupture, must be carefully balanced.

At present the specific rehabilitation protocol used for each patient depends upon the surgeon's choice of repair method and personal preference for one protocol over another. However, irrespective of the method of rehabilitation chosen for any patient, it is essential to instigate frequent follow-up in specialized multidisciplinary hand clinics. The progress of each patient can be closely supervised, monitored and adapted to their individual needs.

In this study post-operative mobilization was active and uncontrolled. No attempt was made to immobilize the ovine limb after operation. This decision was backed by the findings of Aoki et al who demonstrated that in the canine model the UTS did not diminish in the first three weeks after operation if immediate active mobilization was allowed (Aoki et al. 1997). Also the observations of the team at the Marshall Building had an important role to play in this decision. Their experience of previous research projects where splints or plaster of paris casts had been applied to ovine limbs was that these efforts had proved futile, the splints being broken or eaten off almost immediately. Thus it was decided that, so long as the repairs did not immediately rupture, active mobilization was likely to prove beneficial rather than detrimental to the healing tendon and at the same time be the most manageable form of post-operative care.

METHODS OF REPAIR

Non operation

In the modern surgical setting non-operative treatment of tendon injuries is only rarely an option. The reason for this is the poor functional outcome and frequent complications which are likely to occur in the absence of surgical intervention. These complications include stiffness, triggering, synovial sheath entrapment and late rupture. Also there are often concomitant injuries of nerves, blood vessels, or bone, which necessitate surgical exploration and treatment. However, if a tendon was only partially ruptured - less than 60% of its cross-sectional area - then the decision not to operate could be a feasible option (McCarthy et al. 1995b). In such a scenario immediate active motion of the digit would be of critical importance in ensuring optimal functional outcome.

Surgical Indications for Primary repair

Tenorrhaphy, or primary repair, refers to surgical end-to-end repair of a divided tendon as soon as possible after injury. This can only be performed if the following criteria are met:

I. Adequate facilities and skill are available
II. There is not excessive tissue loss
III. There are no associated fractures which cannot be immobilized
IV. There is no gross contamination of the wound
V. The divided tendon ends can be approximated

Should any of the above criteria not be met, a more appropriate alternative procedure should be performed, such as delayed primary repair, tendon grafting etc.

PRINCIPLES OF REPAIR

General principles

As previously mentioned in this chapter, the principles of atraumatic tissue handling were highlighted by Bunnell as early as 1918 and are of fundamental importance when operating in the hand, especially within the confines of Zone II. Along with this, meticulous haemostasis, use of a tourniquet and, most basic of all, carefully planned positioning of the patient and ease of surgical access, should be routinely adhered to.

Aim - the ideal repair

Such a repair would allow for easy placement of suture, minimal tissue handling, a neat repair site with minimal gap (see Tensile testing and Morphology, page 43) between repaired ends and minimal bulk, yet with sufficient strength to allow early mobilization and smooth gliding of the tendon. In practice though, these requirements are not all easy to achieve!

The complexities involved in surmounting the problems inherent to achieving this aim are testament to the fact that there remains great variation in the methods of repair used in current practice despite the sheer number of publications of different suture methods, materials, adjuncts and protocols for mobilization which have been tried and researched to-date. However, despite this 'debate' on the optimal method of repair, a number of basic principles have been agreed upon by most hand surgeons (Beredjiklian 2003). These include the use of:

I. a core suture (two or more strands) with equal tension across all strands
II. an epitenon suture
III. wrist and metacarpophalangeal joints maintained in flexion at rest
IV. distal and proximal interphalangeal joints maintained in extension at rest
V. a post-operative mobilization program (passive or active)
VI. a multidisciplinary approach for review and appraisal of outcome

'GOLD STANDARD' REPAIR

It is generally accepted that the 'gold standard' method of tendon repair involves the placement of a core suture, such as the modified Kessler core suture (see Core Suture below) and a running epitenon suture (see Epitenon suture, page 33) combined with an early postoperative mobilization protocol (Strickland 1999). This is probably still the most commonly used combination for flexor tendon repair (Helm 2003). In a survey conducted by McCarthy and colleagues, 72% of 591 hand surgeons surveyed in America used the modified Kessler core suture (McCarthy et al. 1995a). This survey specifically investigated the repair technique used for partially lacerated flexor tendons as opposed to completely divided tendons but it gives a good indication of the high frequency of continued use of the modified Kessler core suture (albeit for a different type of flexor tendon injury the management of which is more controversial and will not be entered into within the scope of this research work).

Core Suture

Most hand surgeons prefer to place a grasping core suture using a synthetic braided suture (Steinberg 1997). The core sutures in use today are mostly variants of the technique originally described by Kirchmayr in 1917 (Kleinert & Pickford 1997). The modified Kessler core, illustrated over the page, uses a single strand of suture with one centrally placed knot whereas the original suture described by Kessler used two sutures with two peripherally placed knots.

Figure 14: Illustration of core suture techniques

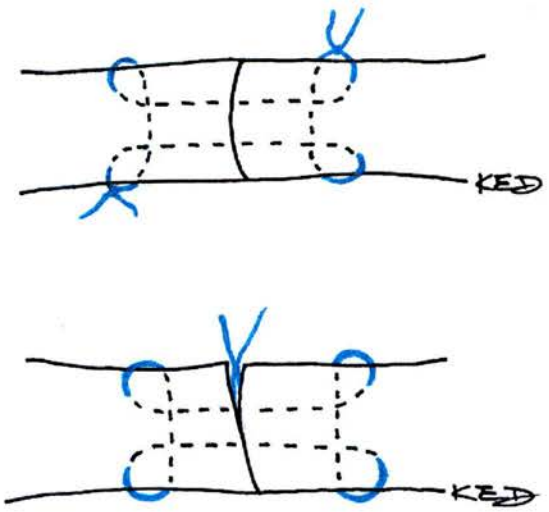

Above: Original core suture described by Kessler, placed with two strands of suture material and two peripheral knots.

Below: Modified Kessler core suture, placed with a single strand of suture and only one, buried, central knot.

In recent years a number of authors have published their research showing that the greater the number of strands that cross the repair site, the greater the strength of repair (Angeles, Heminger, & Mass 2002; Labana et al. 2001; Smith & Evans 2001; Wada et al. 2000; Wang, Xie, & Tang 2003) and some of these new methods are gaining popularity in specialist hand centres. However, the use of such multiple-strand core techniques must be balanced against the inherent increased risk of creating a bulky repair and compromising the healing process by interfering with the tendons intrinsic vascular supply owing to the amount of suture material being placed within its core.

Epitenon suture

In addition to a core suture the majority of hand surgeons today place an additional running epitenon suture around the circumference of the site of repair (Steinberg 1997). This serves to invaginate the ends of the tendon thus avoiding exposure of the inner core of the tendon and stopping the area of repair from catching on the tendon sheath (triggering), as well as exponentially increasing the strength of repair (Wade, Muir, & Hutcheon 1986). Many techniques for this have been described, the simplest being an over-and-over circumferential suture (as illustrated below) but other newer methods such as the cross-stitch circumferential suture (Silfverskiold & Andersson 1993) are also being used in clinical practice today.

Figure 15: Illustration of circumferential epitenon suture techniques

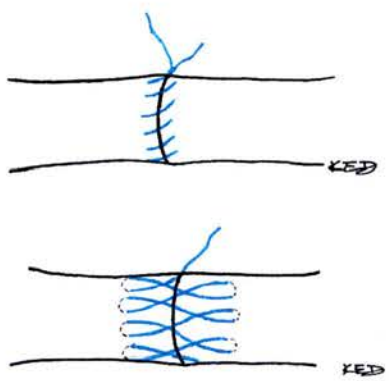

Above: Simple over-and-over circumferential suture (Strickland)

Below: cross-stitch circumferential suture (Silfverskiold)

NOVEL TECHNIQUES

Numerous different operative techniques (and programmes for postoperative mobilization) have been devised and studied in an attempt to overcome the frustrating complication of post operative restrictive adhesion formation and to improve functional outcome after flexor tendon injury. From studies carried out to-date, a fine

balance has been seen to exist between limiting the formation of adhesions and interfering negatively with the healing process of the repaired tendon. Although healing is a multifactorial process, maintenance of adequate perfusion to the lacerated and repaired tendon remains the single most important factor in obtaining good healing (Leddy 1988).

Historically, a number of blocking agents were used in an attempt to isolate the repaired tendon from the surrounding tissues. These included the use of fascia, peritoneum, tunica vaginalis, vena cava, cellophane, nylon, Teflon, polyethylene, silastic sheaths, and gelatine tubes (Meislin et al. 1990). However, these were found either to initiate foreign body reactions or to interfere with tendon nutrition and healing and thus did not prove at all beneficial. More promising studies have included the incorporation of various pharmacological or other agents around the site of repair. These have included the use of NSAID's (Riley et al. 2001) 5-fluorouracil (Cerovac et al. 2001; Khan et al. 2000) hyaluronic acid (Wiig & Abrahamsson 2000); ADCON®-TN gel (Golash et al. 2003; Mentzel et al. 2000) human-derived fibrin sealant (Jones et al. 2002). A number of membranes and diffusible barriers have also been used; condroitin sulphate-coated polyhydroxymethyl methacrylate membrane (Gudemez et al. 2002), Sterispon wrapping (Austin & Walker 1979) a mesh sleeve (Silfverskiold & Andersson 1993) expanded-polytetrafluoroethylene diffusible membrane (Hanff & Hagberg 1998), hyaluronic acid membrane (Isik et al. 1999). To-date, no single method has been entirely successful.

However, of most recent interest has been the development of biocompatible, biodegradable materials which exhibit anti-adhesiogenic effects, such as polyvinyl alcohol-hydrogel shielding (Kobayashi, Toguchida, & Oka 2001), Interceed (TC7) an absorbable barrier (Meislin et al. 1990) and Seprafilm a bioresorbable membrane (Menderes et al. 2004).

These materials, ADCON®-TN, INTERCEED(T7) and Seprafilm are all American products which have been reported by their respective authors as being successful in reducing adhesion formation in the rabbit and rat model and advocated for use in tenolysis procedures. However, concurrently in the UK the Research and Development Company Giltech Limited (see Biodegradable Glass, below) produced

an entirely different biodegradable product, an inorganic polymer - controlled release glass (CRG) which was the product of interest to be evaluated in this research project.

BIODEGRADABLE GLASS

Company Information

The Scottish Research and Development Company Giltech Limited was founded in 1984 to develop novel biomaterials for medical devices. It is based in Ayr (12 North Harbour Estate, Ayr, KA8 8AA) and has an excellent record for the application of its technologies in the medical field with successful products including the Arglaes® and Sorbisan® wound dressing ranges. One of their newer controlled release products is the innovative wrap substance – Controlled Release Glass (CRG) wrap.

CRG - product Information

This product has been established as being both biocompatible and biodegradable and was originally produced for use in the laboratory of the Peripheral Nerve Research Group in 1998 (Gilchrist et al. 1998). It was first manufactured in the form of rigid tubes and was used for repairing nerves. These tubes were impermeable and acted as reservoirs for *e.g.* growth factors. However since this time, further refinement of the characteristics and processing of CRG have led to the additional production of a wrap which has the appearance of a very fine sheet of lens or paper tissue. This has three great advantages over the rigid tubes. The wraps are pliable, can be cut to any desired size or shape and thirdly, since these sheets are made from matted strands of CRG they have the great benefit of being permeable. The wraps are composed of a combination of metal cations (Na^{+}, Ca^{++}) with phosphate and oxide anions and contain no silicon, thus upon degradation they always form into simple ionic substances which are all found normally in tissue fluid. Chemically therefore, this is an ideal substance for implantation and its role in the prevention of adhesion formation is postulated to

result from an early space-occupying effect followed by dissolution into what is effectively extracellular fluid. The rate of solution can be altered by the manufacturers simply by changing the proportions of the CRG constituents, thus tailoring degradation to the requirements of any given situation.

The original rigid tubes were shown in an ovine model successfully to support nerve regeneration and it was suggested that they may also have reduced adhesion formation although this was not formally quantified as it was not an objective of the study (Gilchrist et al. 1998).

The new fine polymer mesh wraps are seen to be pliable and easily fashioned to any desired size or shape, permeable, degrade over a defined and modifiable time into naturally occurring bodily substances and yet have a more robust structure than a gel. Therefore it was postulated that the CRG wraps may be used with anti-adhesiogenic effect in the surgical repair of tendons and the planning behind this research began.

Manufacture of CRG wraps

The flexible, biodegradable wraps are made from one or more non-woven layers of water soluble glass fibres. Upon dissolution (the rate of which is controlled by the manufacturers by varying the composition of the glass) the glass fibres release ions and ionic compounds which occur naturally in human tissue fluid, but which vary dependent upon the compounds within the glass itself.

The water soluble glass can be manufactured in various forms, dependent upon the constituents used and their relative proportions. However, each mixture of glass consists of a 'former' (usually P_2O_5), non-toxic glass 'modifiers' (including metals, lanthanoid oxides or carbonates and alkaline earth metals) and glass 'additives' (such as boron containing compounds). Thus varying amounts of the following chemicals were included into the glass mix used for this project: sodium oxide (Na_20), silver oxide (Ag_20), zinc oxide (ZnO), calcium oxide (CaO), magnesium oxide (MgO), phosphorus pentoxide (P_2O_5), iron oxide (Fe_2O_3), boric oxide (B_2O_3).

The exact chemicals and their relative proportions were carefully selected by the manufacturing company to allow accurate tailoring of dissolution rate, which was mainly determined by the ratio of glass-former to glass-modifiers.

Once the appropriate glass forming composition had been decided upon it was mixed and heated to a melting temperature of around 750-1050°C. This temperature was then slowly lowered until the working temperature (approximately 200°C less than the melting temperature) was achieved; this was the temperature at which fibre formation could begin. The molten glass was poured into a brushing with several fine holes drilled in a row along its base. These holes were initially sealed with a substance which gradually melted over the period of time required for the glass to reach its required working temperature.

Figure 16: Diagrammatic representation of equipment for production of CRG wraps

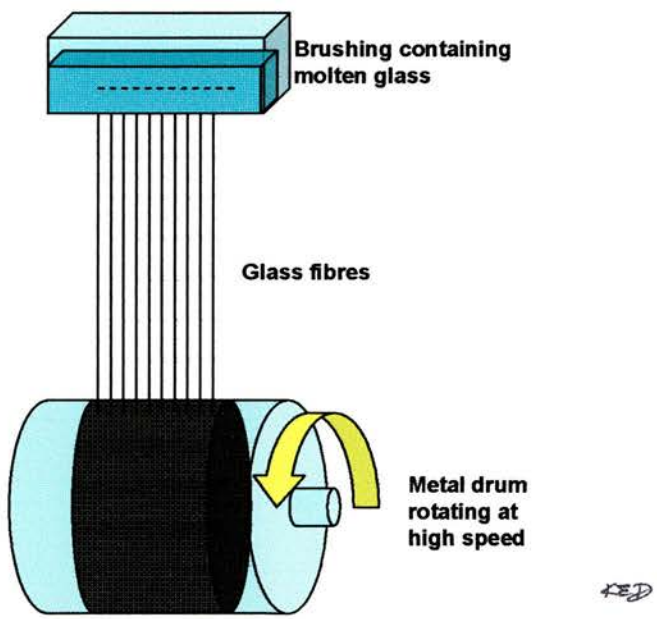

Once the sealant had melted, the molten glass ran downward through the air forming fine glass fibres, which landed and cooled on a drum that turned at high speed, winding the fibres around it. These windings of fibres were then cut perpendicular to their direction (longitudinally along the surface of the drum) and removed as a bundle of fine glass fibres. The lengths of these fibres were uniform, equal to the

circumference of the drum, and they were substantially aligned in the same direction. The bundle of fibres was then laid flat on a clear surface and one of the non-cut edges gently teased sideways away from the bundle. The fibres expanded to form a fine non-woven web and this expansion was continued until the fibres of the web were well separated. Several layers could then be overlapped to obtain the desired thickness of glass wrap. To combine layers, the first layer was placed on a non-stick backing material (siliconized sheeting) and a binding material was applied to the web. This binding material was polycaprolactone dissolved in chloroform. The additional layer of web was placed on top and a further piece of non-stick material applied before the layers were sandwiched together and pressed flat. Once the chloroform had evaporated the backing material was peeled off leaving behind a bound web of double layers of glass fibres. The wrap material was then cut to size (though it could also have been be rolled, or left in large sheets) packaged and sterilized. The sterilization process was carried out using gamma radiation as this did not degrade the wrap. The CRG wrap was then ready for experimental use.

Figure 17: CRG wrap

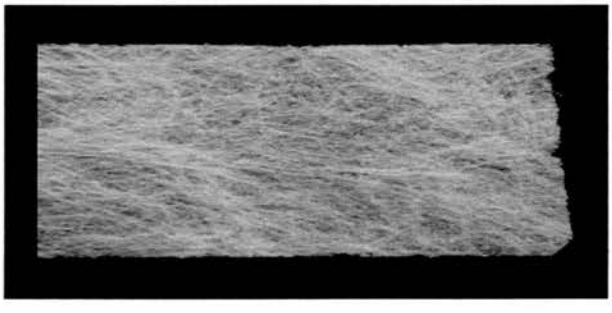

INDICATORS OF OUTCOME

The indicators of outcome chosen for this study were decided upon after extensive review of the available literature. This comprehensive review was carried out during the planning for the project and immediately revealed a problem inherent to the comparison of results of different studies: that which arises from the variation in choice of indice(s) for measuring outcome and in the methods used to gain results. Thus the indices chosen for this work were selected to provide as detailed an analysis as possible of different types of tendon repair, using a novel method of *in-vivo* assessment along with several more traditional indices of outcome.

Clearly, it is of fundamental importance to consider the original goal of any study in order to be in a position to comment upon the appropriateness of the assessments performed and conclusions drawn. In this respect the literature available to-date can be superficially subdivided into two main groups: 1) studies assessing suture material or technique and 2) those assessing the actual process of tendon healing or anatomy.

Many of the published studies have had the principal aim of assessing the performance, especially strength, of new suture materials or techniques. These have generally been performed on *ex-vivo* tissue harvested from cadavers (Angeles, Heminger, & Mass 2002; Labana et al. 2001; Wade, Muir, & Hutcheon 1986; Zobitz et al. 2001) or on *ex-vivo* animal tendons (see animal models, foot of page). The tendons were either frozen for future use (Angeles, Heminger, & Mass 2002; Aslam & Afoke 2000; Labana et al. 2001; Silfverskiold & Andersson 1993; Wada et al. 2000) or freshly divided and repaired. In these experiments the repaired tendons were immediately tested for tensile strength and function. Therefore, these studies concentrated only on the basic properties of suture material and technique, without exploring the effects that the new substances or methods had on the process of tendon healing. Thus although interesting tensile and other biomechanical profiles were described, many questions remained unanswered regarding the effects of these new methods/techniques on the process of tendon healing. Without further research into these effects, the potential application of the new methods/techniques to clinical practice may be precluded. Hence, this group of studies ought to be considered the first step in a series, and have the purpose of answering the basic question 'does this new suture material or technique work?' in terms of both ease of application and immediate resultant strength.

After this, further steps should be taken, to explore the interactions of any new material or technique in the context of tendon healing. The best approach for studying these interactions during the healing process is through the use of animal models and in vitro cellular studies. Such studies have generally involved the setting up of groups of cases which were left to heal for various time intervals after operation before being assessed. Animal models used have included the pig (Smith & Evans 2001; Wang, Xie, & Tang 2003), dog (Pruitt et al. 1996; Wada et al. 2001; Zhao et al. 2001),

sheep (Silfverskiold & Andersson 1993), fowl (Isik et al. 1999; Kobayashi, Toguchida, & Oka 2001; Tanaka et al. 1995) and rabbit (Austin & Walker 1979; Cerovac et al. 2001; Chow, Hooper, & Chan 1983; Gudemez et al. 2002; Hanff & Hagberg 1998; Jones et al. 2002; Jones et al 2000; Khan et al. 2000; Meislin et al 1990; Menderes et al. 2004; Wiig & Abrahamsson 2000).

However, as mentioned above, the series of studies published to-date have performed assessments on harvested tissue (*in-vitro*), as opposed to attempting any form of *in vivo* assessments. A wide range of cleverly constructed measuring devices, clamping mechanisms, pulley systems (with or without the inclusion of displacement or force transducers) have also been used (Gudemez et al 2002; Isik et al. 1999; Kobayashi, Toguchida, & Oka 2001), but again these assessments have been performed on *ex-vivo* tissue (see ROM, page).

In view of these observations, one of the aims of this project was to devise an animal model for the assessment of flexor tendon function *in vivo* after surgical repair and a pre-specified period of healing. At the same time, however, it was considered fundamental to include a number of standard assessments of tendon function and composition in order to provide as broad a picture as possible of the effects on healing of the surgical interventions. This would also facilitate comparison of results with those originating from other studies published to date. Three of the assessments performed in this study - tensile testing, morphology and percent composition - were chosen because they were considered to be important basic measures for assessing outcome of tendon healing. Also two *in vivo* tests, doppler flux and the novel dynamic assessments (see chapter 2, pages 74-94), were included for the first time to advance the level of understanding of tendon repair during the process of healing.

Blood Flow

Laser Doppler Blood Flowmetry (LDBF) is a minimally invasive method of assessing superficial blood flow of tissues (see Laser Doppler Blood Flowmetry, page 75). It has previously been used to assess blood flow in the achilles tendon of the rat and human (Astrom 2000; Astrom & Svensson 1991; Astrom & Westlin 1994). Aside from these applications however it is a relatively underused tool in the scientific

armamentarium available for the assessment of tendons and their process of healing. Thus this informative means of assessing blood flow was chosen to be used as the first basic indicator of outcome in this study.

Tensile testing and Morphology

These assessments can clearly only be performed on harvested tissue and not *in vivo*. Review of the literature, however, revealed a degree of variation within the methodology for these relatively basic indicators of outcome and also showed the tissue specimens to originate from two broad groups; freshly harvested and repaired tendons (cadaver/animal) or those from animal models, harvested after a spell of *in vivo* healing. Thus fundamental differences in study design make it more difficult to compare outcomes between studies.

Tensile testing

One indicator of outcome which has frequently been used, especially when comparing different suture techniques, is that of ascertaining the tensile profile of a repaired tendon. Tensile testing has generally been carried out using standard tensile test machines (see Mechanical Assessment, page 95), with particular attention being given to the ultimate tensile strength, UTS. Review of the literature revealed a number of differences within the methodology for tensile testing which must be allowed for when attempting any comparison between studies. These factors include the use of cyclic/non-cyclic tension, the rate of cross-head speed and the method of clamping the tissue sample to avoid slippage or shearing.

Some studies have also examined gap formation. This is an important concept because the development of a gap between the two ends of the repaired tendon is the precursor to eventual failure at the repair site. In the early 1980s Seradge and colleagues (Seradge 1983) illustrated this in the clinical setting by marking repaired tendons and then measuring the gap between the repaired ends. He showed that the formation of a gap between the repaired ends of tendon predicted a poor final outcome and the larger the gap, the worse the end result. Various other authors

(Silfverskiold, May, & Tornvall 1992) have set up studies to investigate whether gap size correlates with clinical outcome, and some have attempted to define the size of gap that may predict an acceptable outcome. Although there is still some debate in this area, it may be concluded from the results of all these studies that the key to achieving optimum results is to minimize any potential for gap formation. In this study, however, it was decided to concentrate only on the tensile profile obtained when the tendon was loaded to breaking strength, this value of UTS being of fundamental clinical importance.

Morphology of tendons

The morphological assessments performed to-date have ranged from the very simplistic (measuring the 'bulk' of repair by winding a thread around the circumference of a dissected repaired tendon, six times, marking it and laying it out on a ruler [Williams & Amis 1995]) to more sophisticated micro-calculations performed on histological cross-sections of removed tissue (*e.g.* Gudemez et al. 2002; Meislin et al. 1990; Tanaka et al. 1995; Wada et al 2001), and immunohistochemical studies (*e.g.* Khan et al. 2000). Since one of the aims of this study was to maintain a high level of scientific precision for all indices measured and observed, great care was taken in processing the tissue samples to enable detailed histological examinations and calculations to be performed (see Morphological Assessments, page 99).

Range of movement

As previously mentioned, a number of cleverly designed devices have been used by various authors to obtain measurements of degrees of flexion or motion of a digit with a repaired tendon enclosed. Although these have been carried out on harvested tissue, the tendons have in most instances been left in their original sheath and pulley system (Gudemez et al. 2002; Isik et al. 1999; Kobayashi, Toguchida, & Oka 2001). However in one study 'friction' was measured by pulling freshly dissected and repaired cadaver tendons through a pulley system (A2) created from the dissected

digit of one of the cadaver hands. As stated by the author, the fact that the dissected pulley was not of the same anatomical origin as that of the tendon under examination had considerable implications on the usefulness of the test (one tendon stuck firmly within the sheath) and on the results obtained (Williams & Amis 1995). However all of the above-mentioned studies have aimed toward designing a model appropriate for the assessment of movement or friction, and thus ultimately quantification of adhesions.

In-vivo tendon dynamics

This new method of assessing the outcome of healing of repaired tendons was developed in view of the perceived gap in the literature of *in vivo* indices of outcome.

Movement of a repaired tendon is clearly dependent upon the sum of two opposing forces: 1) the force applied in an attempt to move the tendon (initiated by nerve stimulation and muscular contraction) and 2) the resistance to gliding that must be overcome in order to allow movement to take place. The former is clearly limited by the breaking strength of suture material and method of repair used, whilst the latter is affected by the bulk of repair, presence of adhesions and any other limitations imposed by the anatomical surroundings of the individual healing tendon (eg as a result of concomitant injuries sustained, such as underlying bony fracture). Hence, one of the aims of this research project was to develop an *in vivo* model to assess tendon dynamics within as close as possible their normal anatomical and physiological environment, in order to expand upon the information gained through basic tensile testing and morphological analyses.

The apparatus and methodology devised for this assessment (described in In vivo dynamic assessment of tendons, page 81) allowed for detailed evaluation of the displacement, velocity and acceleration of the FDS tendons which occurred upon nerve stimulation. The specialized limb fixation apparatus (see Fixator Frame Bracket page 76) was designed in close collaboration with a colleague from the University of

Edinburgh department of Engineering, Mr Brendan Hawes. It was developed to replace the original apparatus that had been used by previous researchers in the PNRG, which had consisted of a simple pulley system and weights. In the original experiments the cord for the pulley was attached to the distal end of the limb by means of a Steinman pin driven through the hoof of the animal, the cord being looped around the pin. Weights were then hung on the end of the cord to maintain the limb in extension during muscular contraction, which was initiated by electrical stimulation of the nerves of the brachial plexus. The proximal end of the limb was kept in position by the opposing force of the operating table supports against the thorax of the animal. The major limiting factor of this setup was the lack of any specific point of limb fixation and therefore the potential for movement other than that being assessed, to cause error within the observed values. This was not an area of great concern for the previous studies, given that they had been assessing the characteristics of nerve repair which generally showed more profound changes in end muscle function than was expected to be seen after tendon injury and repair. The aim of the *in vivo* dynamic assessments was to detect potentially very small differences in musculo-tendonous function and thus modifications in the old apparatus were felt to be of critical importance. The new apparatus was developed to provide a stable frame within which the tendon and muscle of interest (FDS) could be reliably and repeatedly assessed whilst the limb remained firmly fixed; a reference point of fixation close to the origin of the FDS muscle was chosen. Initial studies were performed on ovine carcasses and carefully dissected specimens of the forelimbs, before carrying out a pilot study.

OBJECTIVES OF RESEARCH PROJECT

The objectives set out at the start of the project were as follows:

1. To establish a systematic programme of physiological and anatomical assessment of tendon function which may be applied to the experimental model
2. To use (1) to establish the properties of normal tendons at site(s) to be used in the model
3. To assess, using (1) in comparison with data obtained in (2) the effects of repairing a tendon using conventional methods *e.g.* modified Kessler suture technique.
4. To repeat (3) to assess the value of additionally repairing the epitenon
5. To consider the anti-adhesiogenic effect of a CRG wrap in the model (3)
6. To consider the anti-adhesiogenic effect of a CGR wrap in the model (4)

Aims added within the first few months of commencing the study:

7. To consider the effects of dissection only in the otherwise normal model
8. To consider the effects of dissection and CRG wrap only in the otherwise normal model
9. To consider the effects of addition of a second anti-adhesiogenic agent to the model (6)

Full details of experimental groups are given in Chapter two Protocol, page 55.

CHAPTER 2

MATERIALS AND METHODS

OVINE MODEL

The animal model chosen for this research study was the sheep (*Ovis aries*, order Ungulata) which has been used as a laboratory animal in medical research since the later years of the 19th century. This choice of model was based on a number of different factors. First, there is evidence in the literature to suggest that the ovine model is very appropriate for the study of techniques or tissue responses that one then wishes to attempt to relate to human subjects. This is because there is a closer correlation between the bone and soft tissue composition of the human body and sheep, than with other animal models commonly used in research (Martini et al. 2001). Secondly, the size and anatomical setting of the organs and tissues of the sheep make it a good model for extrapolation to the human case (Rand 2002). Of particular note, the flexor tendons in the forelimb of the adult sheep are roughly comparable in size to those of the flexor tendons of the human hand. The third consideration was the fact that the research group with which this project was affiliated, The Peripheral Nerve Research Group, had previous, very successful, experience working on the nerves in the forelimbs of sheep, with a large data-base of physiological and neuromuscular information, though they had not studied tendons before.

ETHICAL APPROVAL

The proposed plan for this experimental research project was described in detail and submitted to the Home Office for inspection. After review of its contents ethical approval and a Project Licence were granted. The appropriate Home Office Animal Handling Course was then successfully completed and a Personal Licence obtained for this work.

CHOICE OF FLEXOR TENDON

As briefly mentioned in Chapter 1, page 19, the flexor digitorum superficialis (FDS) tendon in the sheep is composed of two slips (see illustration below) enclosed in a tendon sheath, alongside the FDP tendon. Upon opening the flexor sheath, the pars superficialis is found to lie above the pars profunda, separated by only a very small amount of thin connective tissue. In the human however, this tendon is composed of a single slip only. Hence the choice of FDS tendon for this work was based primarily on the fact that it allowed the study of a tendon injury which caused minimal incapacity in the animal model whilst representing an equivalent injury of great disability in the human. The superficialis slip of the FDS tendon of the right forelimb was chosen to be divided and repaired.

Figure 18: Ovine flexor digitorum superficialis

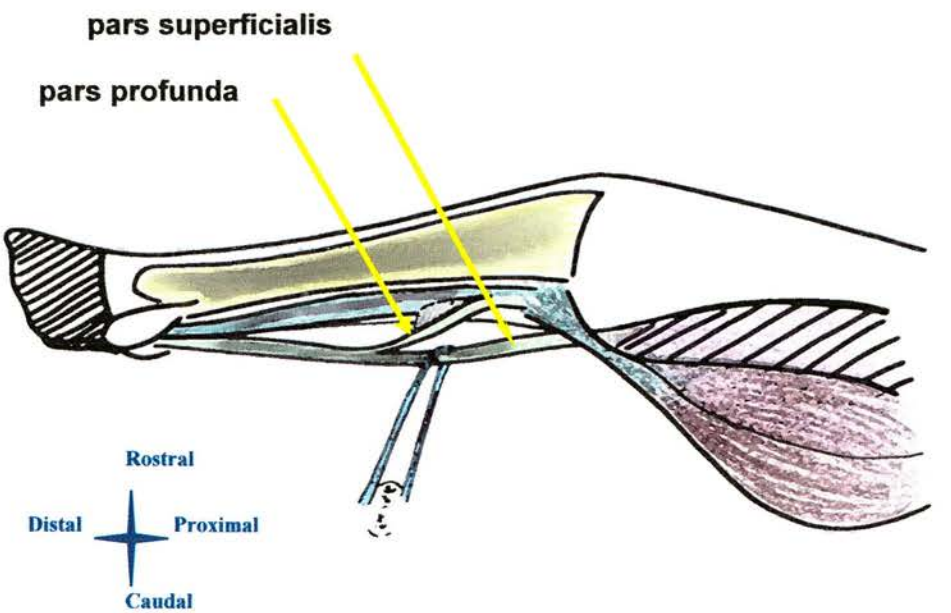

Illustration of ovine right foreleg dissection

RESEARCH PROTOCOL

The protocol devised for this study is detailed below.

Group Size

The sample size of any research project is clearly critical to the potential relevance of results gained, and conclusions drawn, at the end of the study. Home Office regulations (Home Office (H.M.S.O) 1986) and Ethical Committees demand that numbers of cases are kept to an absolute minimum and thus it is of fundamental importance to be as accurate as possible when predicting the group size required for a study.

During the planning of this research project, power calculations were performed based on data from previous ovine nerve research carried out by the Peripheral Nerve Research Group. One of these studies had involved peripheral nerve injuries in the foreleg of several groups of animals. Part of the final assessment in this study included measurement of the isometric myogram of the tetanically contracting flexor carpi radialis muscle (which lies adjacent to the FDS muscle) in each repair group and for a control group of normal animals. These measurements of tension were the closest variable available, comparable to the variables that it was proposed to measure in this new study. So values were obtained, with permission, and used to make an initial prediction of required group size. The method for calculating sample sizes was described by Kirkwood (Kirkwood 1991) as follows:

$$N > \frac{(u+v)^2\left(\sigma_1^2 + \sigma_2^2\right)}{(\mu_1 - \mu_2)^2}$$

where:

$\mu_1 - \mu_2$ is difference between means

σ_1 and σ_2, are the standard deviations

v corresponds to the desired significance level (*e.g.* if significance level is 5% $v = 1.96$)

u corresponds to the desired power (*e.g.* if power = 90% $u = 1.28$)

N is the sample size of each group

The mean values for tension from the previous research were 25.12N (normal) and 14.47N (repaired and CNTF treated) with corresponding standard deviations of 2.79N and 2.91N respectively. These were inserted into the equation above and a minimum group size of N=5.63 given. Thus if a level of resolution equivalent to this was required, groups of at least 6 animals would need to be used.

In theory therefore, group sizes of 6 animals were predicted as being adequate. However, as the proposed measurement of *in vivo* tendon displacement had never before been attempted by the group, or by any other researchers in the published literature, it was decided to carry out a small pilot study before proceeding further.

This pilot study was carried out on three cases. Clearly this was not of sufficient size for calculating any statistically significant results, but it was used to obtain example values of the measurement, in millimetres, for the displacement that would be observed during the FDS stimulation (see In vivo dynamic assessment of tendons, page 81). This information was then used to re-check the predicted group size of N=6, by performing power calculations on the observed displacement results using a computer software program Statistica (Statsoft Inc., Tulsa, USA).

The first value chosen to study in these pilot cases was that of the ratio (right divided by left) of the maximum displacement of the tendon obtained on muscular contraction (see Understanding and Processing Picoscope Data, page 90) *DmR/L*. Values obtained and the basic descriptive statistics are shown in the table overleaf:

Pilot case No.	*DmR/L*
1	0.142
2	0.227
3	0.058

Mean	0.142
SD	0.085

Inserting these values into the appropriate power analysis section of the Satistica software program a sample size of six was predicted to reach a power of 0.900. This is illustrated in the graph below:

Figure 19: Sample size calculation based on displacement results

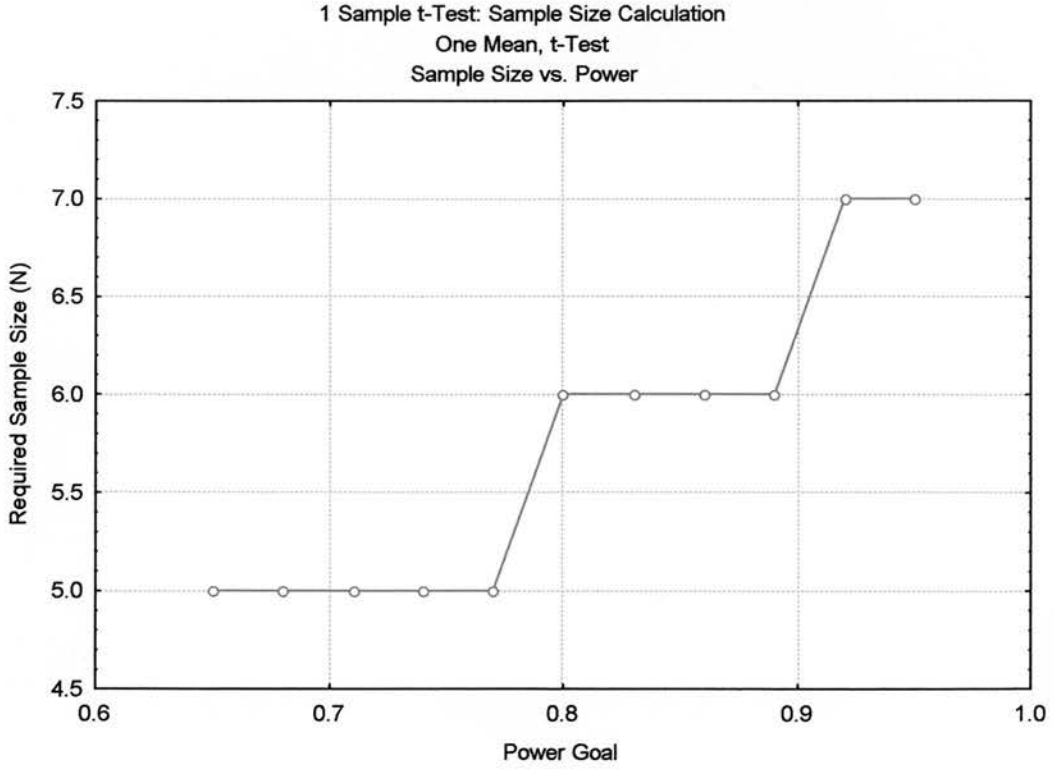

Hence this calculation suggested that a group size of six would be sufficient to yield information of statistical significance attaining a power goal of 0.900. The graph shown above also demonstrated that should an animal be lost from a group, for any unforeseen reasons, a group size of 5 should still yield results with a reasonable power goal of up to 0.78.

The tendons from the same three pilot cases then underwent assessment of breaking strength of both right and left FDS (see Mechanical Assessment, page 95). This was one of the two assessments proposed to be undertaken on only half of each group, as the tendon would be destroyed in the process and thus not suitable for proceeding to undergo histological assessment. The same statistical procedure as above was performed to calculate sample size. The results and informative power graph produced are illustrated below:

Pilot case No.	***R/LF***
1	1.038
2	0.344
3	0.772

Mean	0.718
SD	0.349

Figure 20: Sample size calculation based on tensile test results

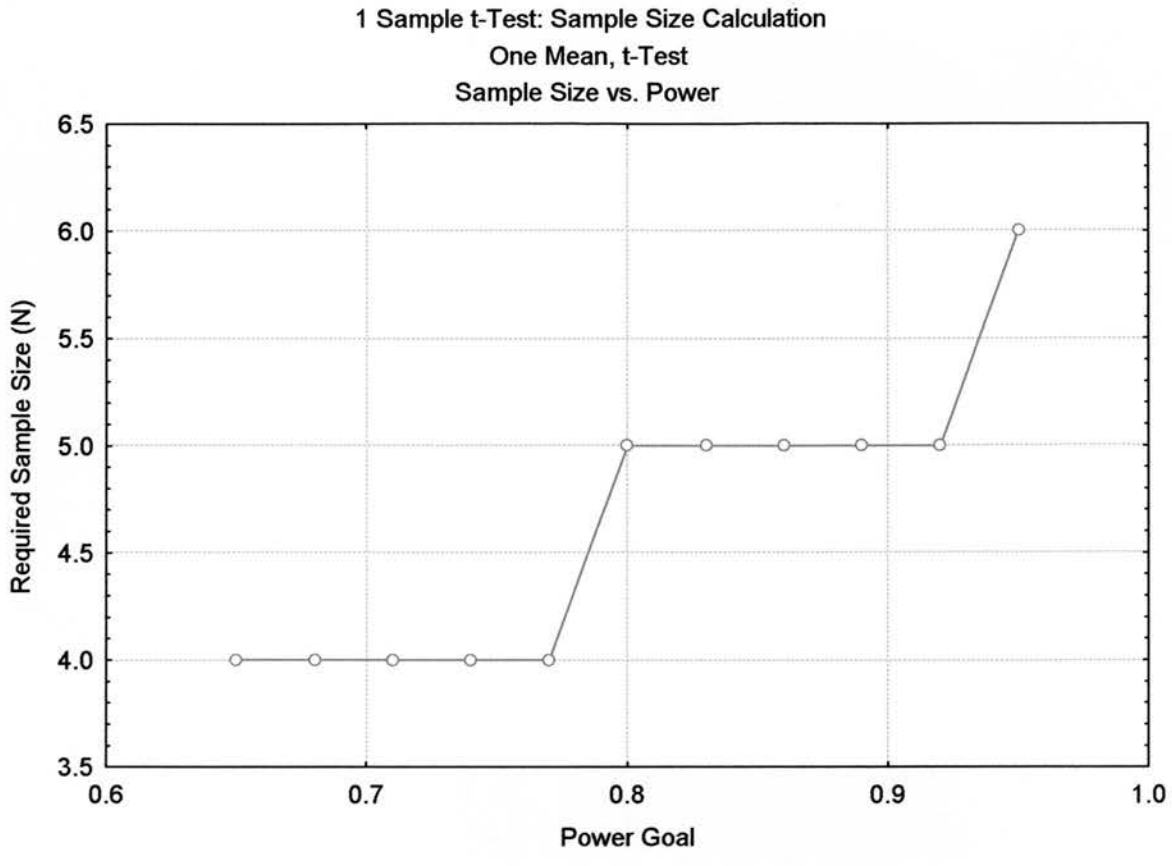

Thus analysis of the values obtained from mechanical testing of the pilot case tendons calculated that a group size of five would be sufficient to yield results with a statistical power of 0.921.

In view of these findings it was decided to proceed with groups of six cases each for the assessments of mechanical strength and histology (the tendons being destroyed during the process of these assessments). However for all other assessments, which would preceed the aforementioned tests, groups containing twelve cases would be used.

Protocol

In total twelve groups, of twelve animals each, were studied.

Group 1 was the normal control group. Groups 2-8 were the different surgical procedures being assessed.

The first five groups were chosen from the outset and a further three (groups 6, 7 &8) were added at a later stage in the research period in order to attempt to examine in greater detail some of the aspects of tendon healing. In the groups where tendon injury was simulated, complete division of the tendon (tenotomy) was carried out by performing a clean cut with a surgical blade.

Group	Experiment
1	Normal Controls
2	Tenotomy + modified Kessler repair
3	Tenotomy + modified Kessler repair + repair of epitenon
4	Tenotomy + modified Kessler repair + CRG wrap
5	Tenotomy + modified Kessler repair + repair of epitenon + CRG wrap
6	Dissection only (No tenotomy)
7	Dissection + CRG wrap (No tenotomy)
8	Tenotomy + modified Kessler repair + repair of epitenon + CRG wrap + other anti-adhesiogenic agent

Two time-cohorts of experimental animals were studied. The first was used to assess all surgical groups (2 - 8) six weeks after surgery. At this time most of the early healing process would have occurred and investigation of early scar tissue could be performed which later may be remodelled as healing progressed. In the human case this would be the time when one would aim to remove any splints and increase mobilization to within normal limits. The second time-cohort was used to assess an additional set of groups 2, 3, 4 &5, six months after initial surgery. The purpose of

this cohort was to investigate the more permanent scarring resulting from adhesion formation. The normal controls were obviously examined without any time period, thus in total twelve groups were studied.

Assessment

The objective of each of the different assessments was to determine specific characteristics of the FDS tendons which were related to function.

Each case in every group underwent *in vivo* (physiological) observations followed by harvesting of the tendon for *in vitro* (morphological or mechanical) analyses. These tests were performed for both the operated right forelimb FDS and the non-operated left forelimb FDS thus creating an individual control for each case, in order to minimize within-group variation.

In vivo assessments

The purpose of these assessments was to ascertain information regarding the function of the FDS tendons whilst they remained in their natural physiological environment, '*in situ*'. Two different assessments were performed. The first, Laser Doppler Blood Flowmetry (LDBF), was carried out to observe the superficial blood flow of the tendons near the site of surgical repair (see Laser Doppler Blood Flowmetry, page 75). The second was a novel technique which attempted to measure the displacement, velocity and acceleration of the tendons upon contraction of the FDS muscle (see In vivo dynamic assessment of tendons, page 81).

In vitro assessments

After the *in vivo* assessments had been performed, the FDS tendons were removed from the animal and subjected to one of two additional tests (*in vitro)*. One of these was a mechanical test performed in order to determine the tensile properties of the tendon (see Mechanical Assessment, page 95) whilst the other examined the morphological characteristics (see Morphological Assessments, page 99).

ANIMAL HOUSING AND RESEARCH FACILITIES

The research facilities used for this study were based at three different sites in Edinburgh. The greater part of the experimental work was carried out at the Marshall Building (see below) where all the operative procedures and *in vivo* assessments were performed. The equipment required for tissue processing, along with stationery, computer access and office accommodation was all provided by the Department of Clinical Neurosciences at the Western General Hospital, under the directorship of Professor Peter Sandercock. The tensile testing of the tendons took place in one of the laboratories of the University Department of Engineering (see Mechanical Assessment, page 95), access having been permitted by Professor Joseph McGeough and Mr Jim Hutcheson. In addition to this, library resources were accessed at the Royal College of Surgeons of Edinburgh, the Erskine Medical Library and the Western General Hospital Library.

The Marshall Building

All of the experimental procedures were carried out at the Marshall Building; an Edinburgh University part-owned research facility in Roslin. This unit was under the directorship of Mr. Dennis Doogan and had a delightful staff team comprising six members. All team members were highly experienced in the running of surgical research projects as well as in the day to day care of the animals.

Animal selection and care

In accordance with Home Office regulations, the animals bought in from commercial sources were housed in the keeping facilities of the building for at least one month prior to any surgery. This enabled the animals to acclimatize to their new environment and thus minimize any potential suffering or stress. However, approximately half of the animals in this study were born and raised on site.

A variety of different breeds of sheep was used within this study including Booroola, Blackface, Finn, and Dorset. The ages of the animals ranged between one and five

years. Both the criteria of breed and age were randomly allocated between study groups.

Each animal was thoroughly checked over by the Home Office Named Veterinarian for the Marshall Building prior to being included in the study. This check was carried out during the week before surgery and ensured that a strict level of good health was attained from the outset.

Preoperative care

The day before planned surgery, each animal was transferred to a pre-operative pen and food, but not water, was withheld for a period of at least twelve hours. From here the animal was moved into a weighing machine, just prior to induction of anaesthesia, to allow accurate calculation of the required anaesthetic dose based on the individual animal's weight. The animal was then walked through into the anaesthetic room.

Anaesthesia

The appropriate intravenous induction dose of thiopentone sodium was calculated for each animal according to dosage guidance instructions:

$$\text{Dose (mg)} = 20\text{mg kg}^{-1}$$

Each animal was held calmly, whilst one side of its neck was shaved with electrical clippers to allow clear visualization of the external jugular vein. The individualized dose of thiopentone was then injected into the external jugular vein. Within a matter of seconds the animal collapsed gently to the ground, lightly unconscious (thus breathing spontaneously) allowing transfer onto the anaesthetic trolley. Placed in the supine position, endotracheal intubation was performed, confirmed and secured in place by tying with a tape. The animal was swiftly transferred through to the operating room and the endotracheal tube attached to the ventilator. The anaesthetic machine used for all cases was a Manley Pulmovent machine. Anaesthesia was maintained with a 1:1 mixture of oxygen and nitrous oxide carrying vaporized halothane, tailored to the requirements of each animal to ensure a sufficient level of

unconsciousness and relief from pain (usually between 0.5 – 2% halothane and at a flow rate of approximately 6 l min^{-1}).

Intra-operative care

Having established anaesthesia, each animal was connected to the following non-invasive monitoring devices to allow continuous assessment of its condition throughout the operative period.

Electrocardiographic (ECG) monitoring

For each of the primary operative procedures, the front legs and one of the back legs of the animal were clipped of hair over a small area, sufficient to allow attachment of an ECG lead, which was then fixed in place with zinc oxide tape. For the secondary operative (harvesting) procedure a slight modification in lead placement was made as the animals were required to be placed in supine position rather than right lateral position (see Secondary surgical procedures, page 69) and both forelimbs were operated upon. As such, these cases required placement of the anterior limb leads onto the lateral chest wall close to the axilla of each limb. This change of position necessitated fixation of the leads by suturing to the skin. In all instances the leads were connected to a Hellige ECG monitor (Servomed) and continuous monitoring was performed until the animal had regained consciousness at the end of the procedure.

Oxygen Saturation

A pulse oximeter probe was clipped gently to the animals tongue and continuous monitoring of pulse rate and oxygen saturation was performed throughout the operative period. The monitoring device used was a Microspan 3040 Oximeter (BCI - Smiths Medical).

Temperature

A fine thermometer probe was inserted into the oropharynx of each animal allowing a continuous recording of basal temperature to be displayed on the appropriate screen of the Hellige ECG monitor.

Post-operative care

At the end of each primary surgical procedure the animal was given an individualized dose of an anti-inflammatory non-steroidal drug, flunixin meglumine (50mg per 25kg) and the first of three prophylactic doses of the antibiotic Streptopen (procaine penicillin G and dihydrostreptomycin), Pitman-Moore Ltd, UK). The animal was then allowed to recover from the anaesthetic in the operating theatre under continued non-invasive monitoring. Once lightly conscious and breathing spontaneously the animal was extubated, the monitoring devices were removed and it was then transferred to an individual recovery pen in an area adjacent to theatre.

Figure 21: Ovine recovery pens

Each animal was kept here, under close observation, until fully recovered before being moved to a larger more distant communal pen. The animals were reviewed regularly throughout each day as they continued with their normal life.

SURGICAL PROCEDURES

All surgical procedures were performed by a single surgeon, the present author, and were carried out in a strictly reproducible way.

The surgical procedures were of two distinct types. The primary procedure was to enable the different experimental groups to be set up with the animal being allowed to recover at the end. The secondary procedure was undertaken to assess the tendon at the end of the appropriate healing time, initially *in vivo* but then to proceed to non-recovery of the animal and harvesting of the tendon.

Primary Surgical Procedure

Preparation

The anaesthetized animal was positioned in the left lateral position. Padded side-supports were attached to the operating table, against the belly and back of the animal, in order to maintain this position without applying any undue pressure. The left foreleg was gently tied back, hoof against the padded support of the belly, thus providing a clear operating field for the right foreleg. An additional table support was placed under the right foreleg and the limb was clipped of its wool.

Each primary surgical procedure was then carried out under strict aseptic technique.

The right foreleg was prepped with povidone–iodine solution (Adams Healthcare) and a sterile bag tied around the hoof. Sterile drapes were placed over the operating table and animal to isolate, and leave exposed, only the right foreleg.

Incision

An approximately five centimetre curvilinear incision was made in the longitudinal axis of the postero-medial aspect of the right foreleg of the animal, running distally from the point of the ulnar styloid process. This particular site was chosen so that at the end of the procedure, once closed, the skin incision would not lie in contact with the operative site of the tendon. The subcutaneous fascia was then divided to expose

the FDS flexor tendon sheath. Throughout the surgical procedure, the operative field was kept moist by occasional gentle irrigation with normal saline solution and haemostasis was secured as necessary by the use of bipolar diathermy.

Figure 22: Foreleg incision

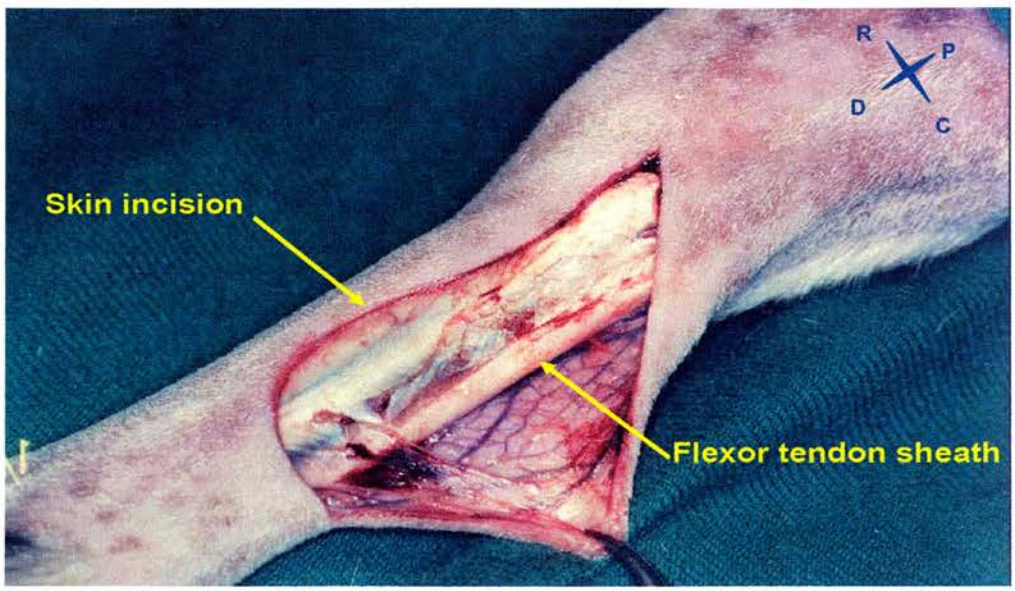

A stay suture was placed loosely in the skin flap to hold it out of the way of the operative site and the tendon sheath was incised longitudinally.

Figure 23: Incising the FDS tendon sheath

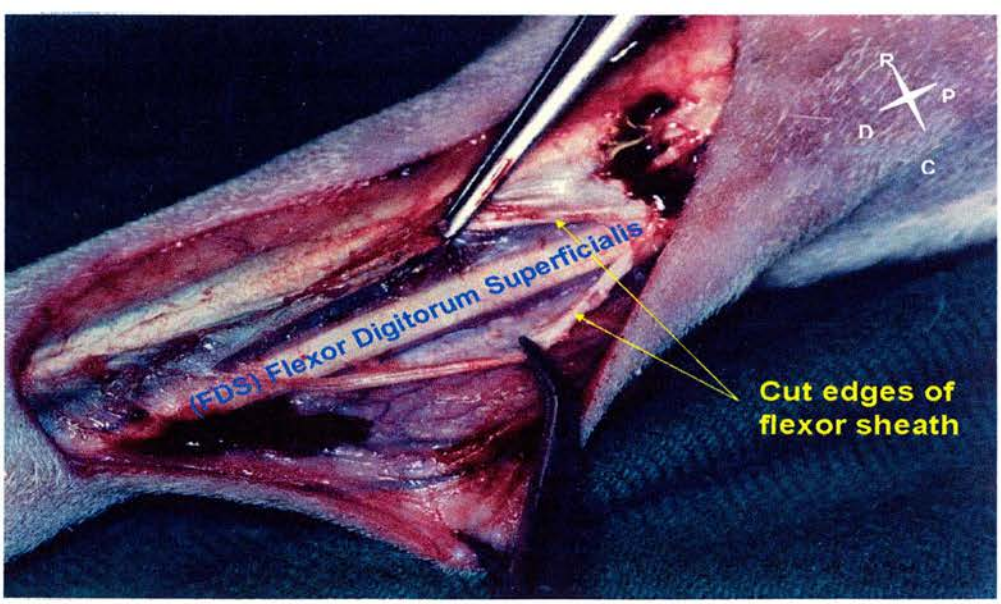

The FDS pars superficialis slip was identified and traced to its junction with the FDS pars profunda.

Figure 24: Identification of FDS tendon slips

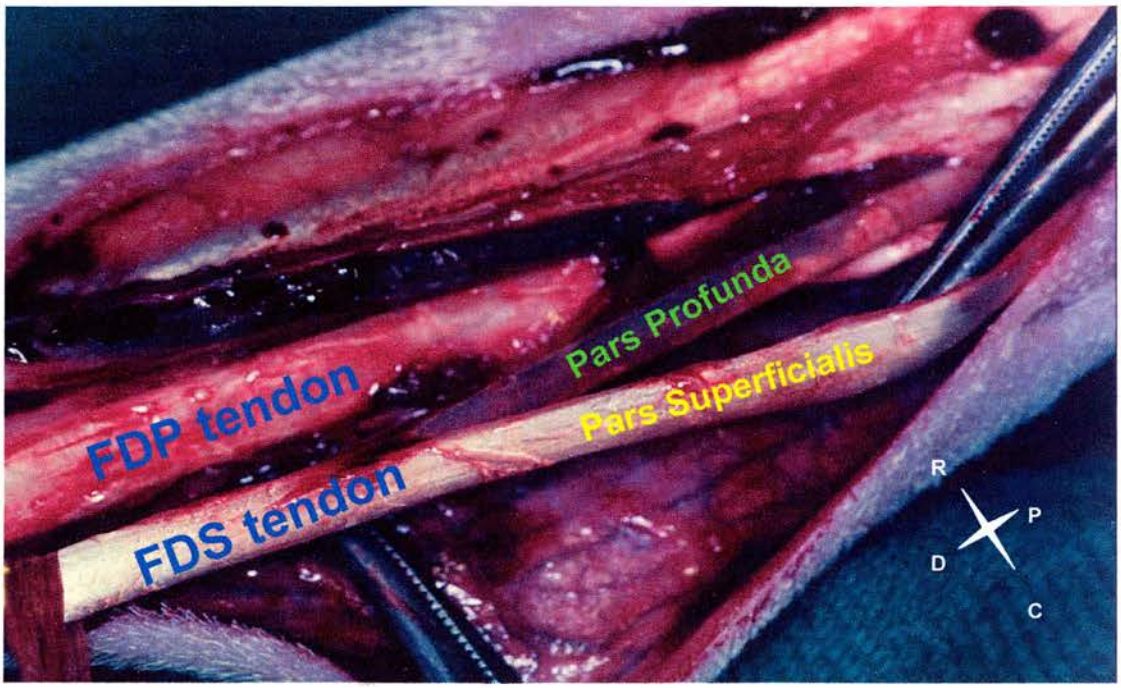

Using surgical callipers a distance of 2.5cm was measured, in a proximal direction, along the FDS pars superficialis slip from the point of tendon fusion. Here the FDS PS slip was held gently but securely with an appropriately sized Meyer's neurotome. For the first few cases a sterile 25 gauge (orange) needle was placed further proximally in transverse direction through the tendon slip to act as an anchor and limit any possible retraction after transection. However it was quickly discovered that proximal end retraction was minimal and was able to be accounted for by limb position alone, thus this step was discontinued.

The tendon was then transected cleanly with a sterile blade at the 2.5cm point held within the neurotome.

Figure 25: Tenotomy of the PS slip of the FDS tendon

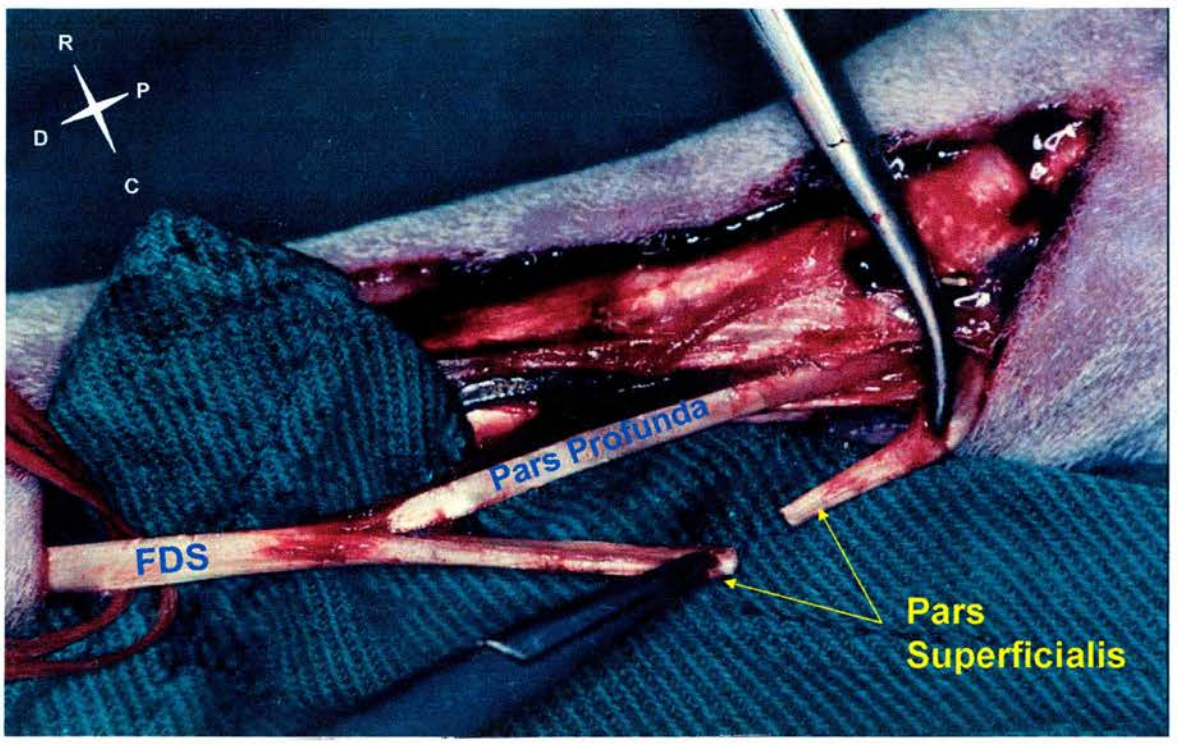

Primary repair of the tendon was carried out according to group protocol.

Methods of primary repair

In all cases a locking modified Kessler core suture (see Protocol, page 55) was placed using 4/0 Ethibond (Ethicon Ltd. UK) a braided polyester coated suture with round bodied needle.

Figure 26: Placement of core suture

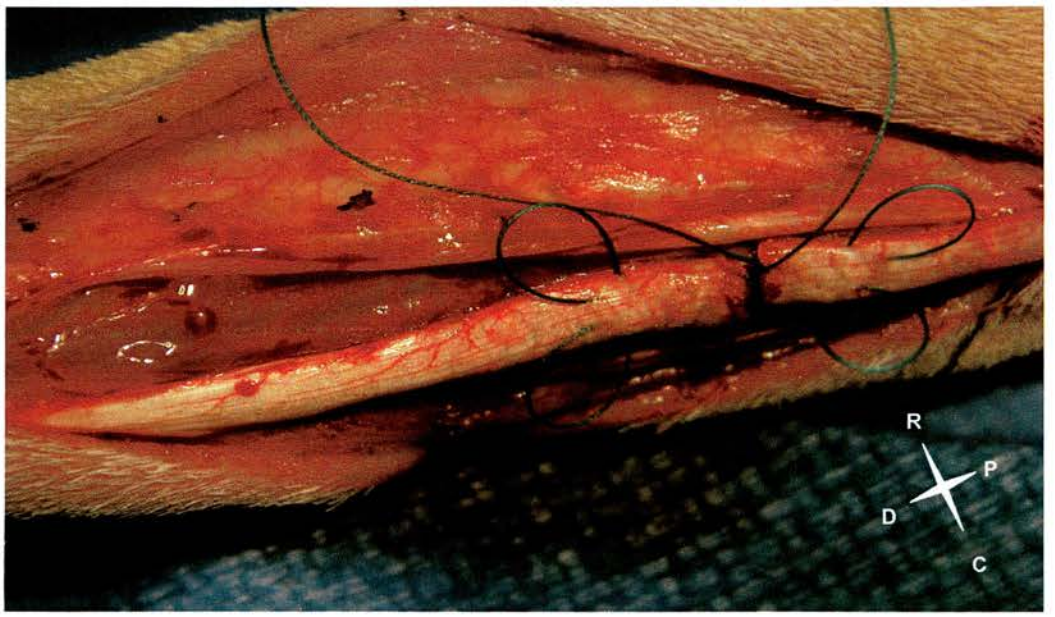

Figure 27: Securing the core suture

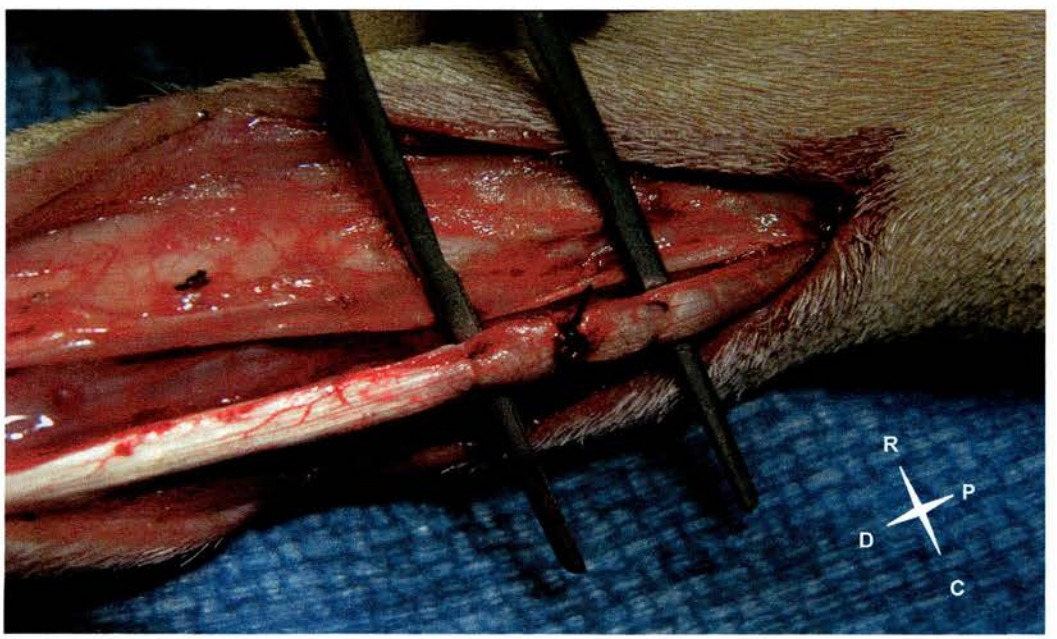

Groups 4 and 5 then had the addition of a continuous epitenon suture of 6/0 Ethibond completely burying the knot and suture ends of the Kessler core.

Figure 28: Placement of epitenon suture

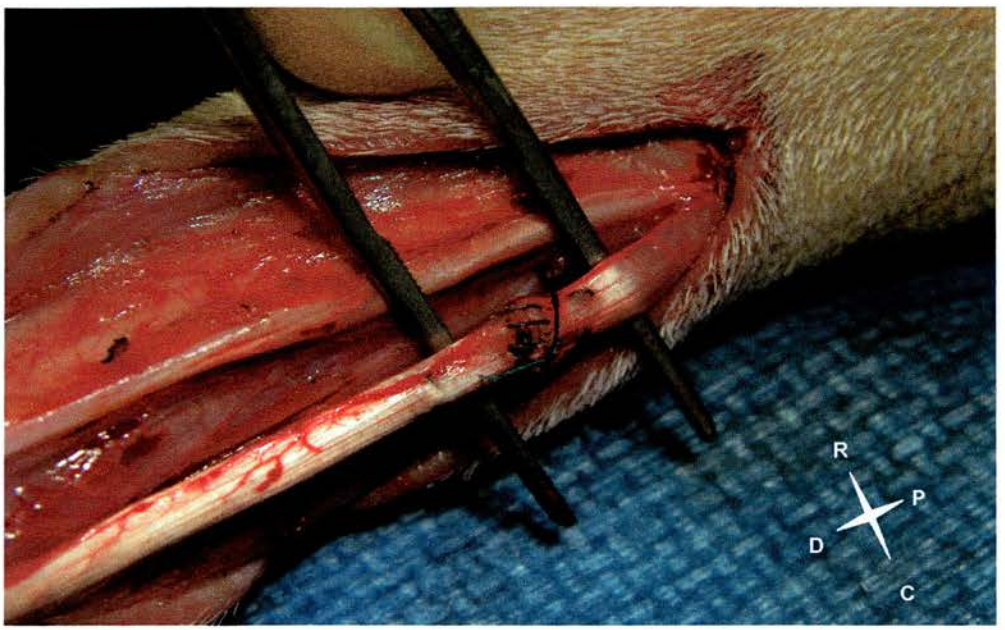

Groups 3 (Kessler core only) and 5 (Kessler core + epitenon) then had the addition of the CRG wrap. This was produced in sterile sheets from which a strip of approximately 2cm width, 6cm length was cut and placed under the area of repair.

Figure 29: Placement of CRG wrap

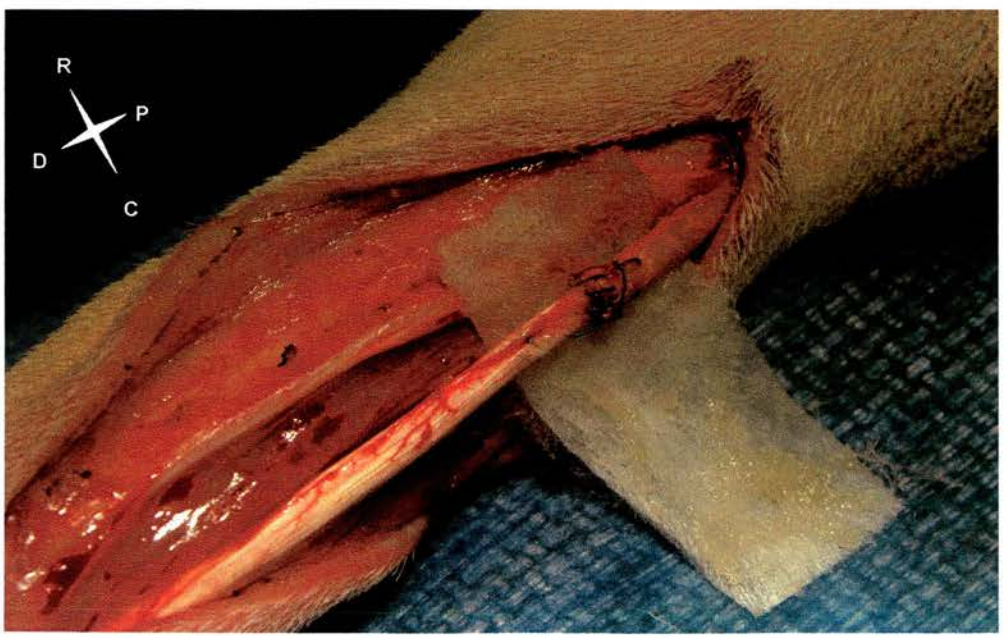

This was then folded around the repair site.

Figure 30: Folding the CRG wrap

Group 8 also had the addition of a very thin smearing of triamcinolone acetonide paste (see Triamcinolone group, page162) which was applied to the inner aspect of CRG wrap prior to being wrapped around the repair site. This can be seen on the illustration presented above. The wrap was trimmed in length and secured in place by addition of a few drops of CRG glue placed on the under-surface of the overlapping edge of wrap.

Figure 31: Securing the CRG wrap

The cut edges of the FDS sheath were brought to lie in approximation with one another over the site of repair. The stay suture was removed from the skin flap and haemostasis re-checked. The skin incision was closed with continuous suture of subcuticular 4/0 vicryl (polyglactin 910; synthetic absorbable sterile suture, Ethicon Ltd. UK).

Figure 32: Skin closure

A dressing in the form of a spray (Opsite spray; Smith and Nephew, UK) was then applied. This produced a transparent, quick-drying film that was elastic and water-resistant but permeable to moisture vapour and air. Unlike traditional bandages, which are commonly bitten off by animals, this dressing was well tolerated.

Secondary surgical procedures

For these procedures full aseptic technique was not strictly adhered to owing to the fact that the animal was not to recover. However this only eliminated the use of sterile drapes and preparative povidone-iodine solutions and allowed minimal contact between tendon and the equipment necessary for carrying out the assessments, without the need for sterilization.

Preparation

The anaesthetized animal was placed on the operating table in the supine position and all non-invasive monitoring applied. Padded side supports were attached to the table, against either side of the chest wall of the animal, in order to support the animal without applying any undue pressure. The animal was then gently rotated toward the side of the foreleg which was to be assessed first. This foreleg was clipped of its wool up to the level of the radio-ulnar joint with the humerus.

Incision

An approximately 3cm incision was made over the bony prominence of the olecranon process of the proximal ulna on the posterior aspect of the foreleg. This point was chosen as it was the area of bone closest to the origin of the FDS muscle. Using 'Synthes' orthopaedic equipment a 2.5 mm hole was drilled vertically downward through the medial surface of the bony prominence and out from the lateral aspect. This hole was then tapped using a 3mm hand tap tool and guide before insertion of a 60mm long surgical screw. The screw was driven through the bone until the two ends were protruding approximately equal distances from each surface of the olecranon.

Figure 33: Olecranon screw fixation of proximal limb

The limb and screw were then carefully manouvered into a specially designed metal frame (see Fixator Frame Apparatus, page 76) which enabled fixation and thus stabilization of the limb during the assessments of in situ blood flow and tendon displacement (see *In vivo* Physiological Assessments, page 74).

Figure 34: Proximal limb fixation

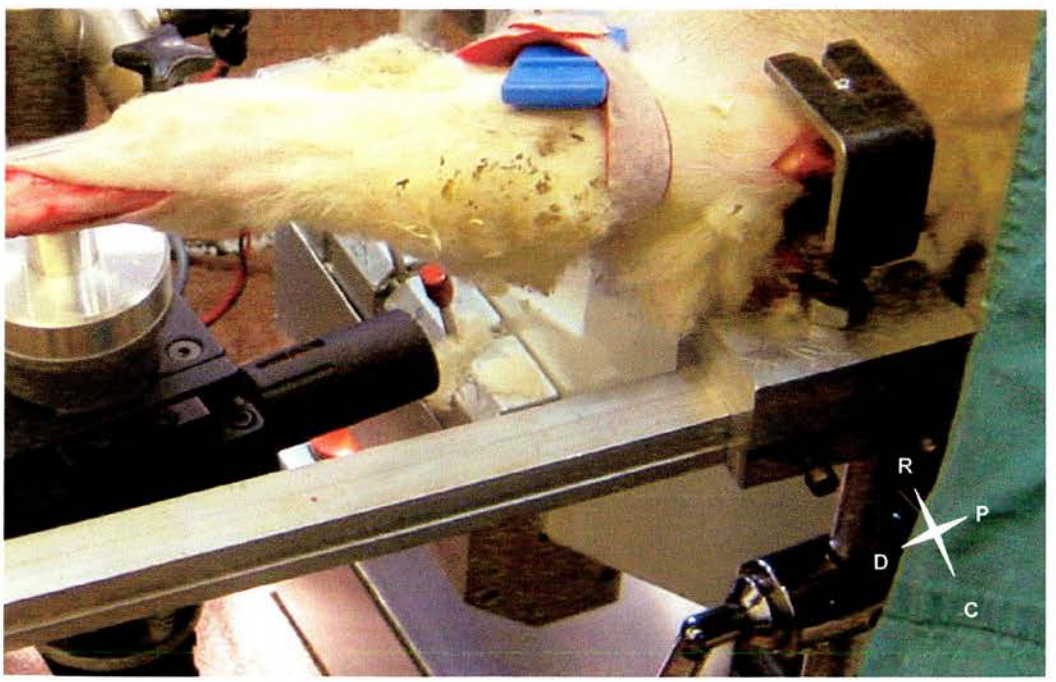

A second incision was then made close to the site of the primary intervention. However this incision was placed further posteriorly than the original incision, directly over the course of the FDS tendon. Gentle dissection was used to lift the skin flaps and expose the tendon with minimal disturbance to the surrounding tissues. No attempt was made to identify the edges of the flexor sheath, or dissect any of the tissue overlying the FDS tendon. A stay suture was then applied loosely to the edges of the skin flaps to hold them back and ensure good exposure of the surgical field.

Figure 35: Skin incision for secondary procedure

The Doppler blood flow assessment was then performed (see Laser Doppler Blood Flowmetry, page 75).

Once these data had been collected and the apparatus removed, further dissection of the FDS tendon was performed. The conjoint part of the FDS tendon was traced distally and transected over the carpal bones, close to its point of insertion. This free distal end was then tied tightly with a length of inextensible 1/0 linen (Ethicon Ltd. UK) and a short loop was made at its distal tip in order to attach it to the appropriate apparatus to allow assessment of its displacement, upon muscle contraction (see In vivo dynamic assessment of tendons, page 81).

Figure 36: Fixation of distal FDS tendon to transducer

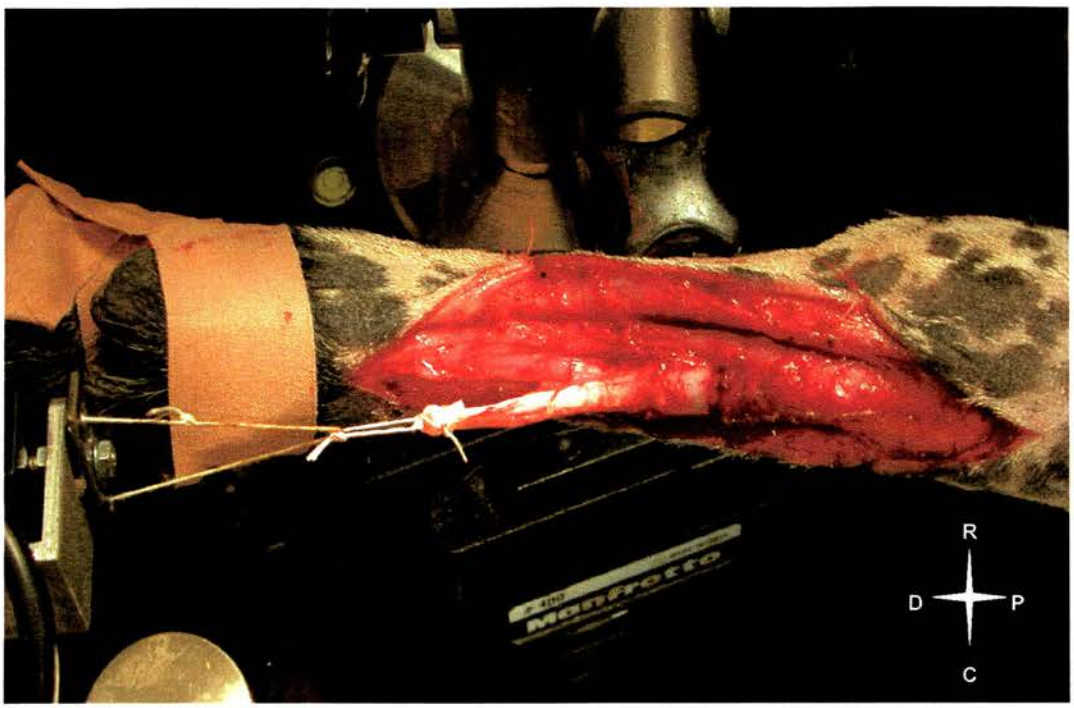

Once this second *in vivo* assessment had been carried out the tendon was dissected proximally. Great care was taken to follow the tissue planes and thus dissect out the tendon along with any/all other adherent tissues.

Figure 37: FDS tendon dissection for harvesting

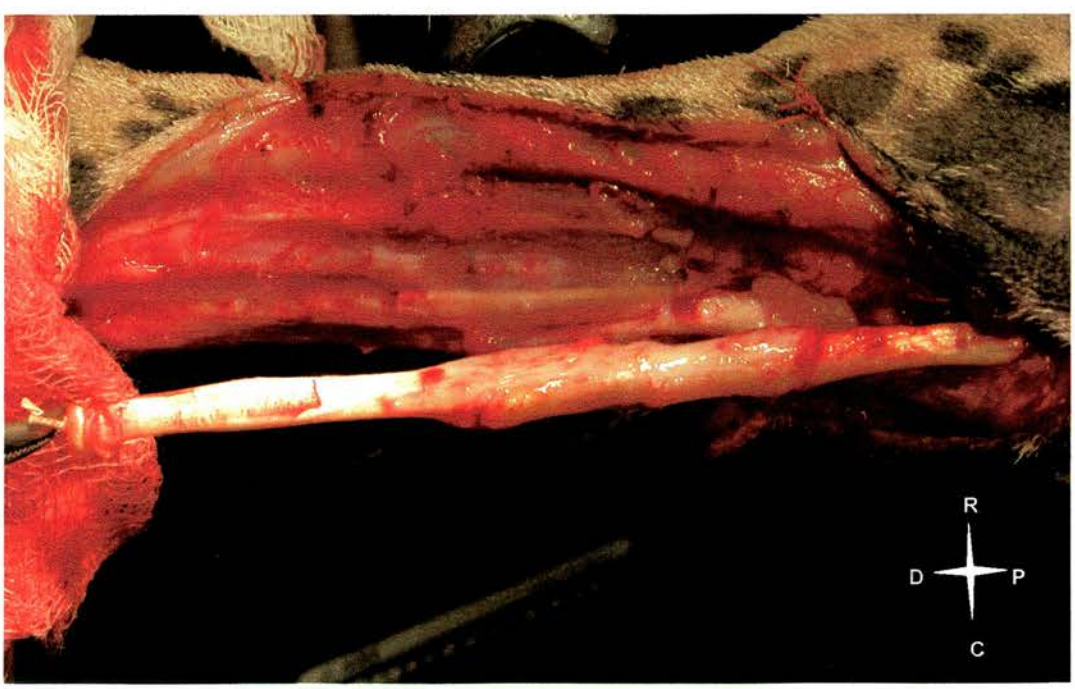

The tendon was transected proximally at the level of junction with its muscle fibers and stored appropriately according to protocol; the tendons in half of each group were cleanly cut, with a fresh blade, into short sections and immediately stored in 10% formalin solution, prior to processing for morphological analysis. The tendons comprising the remaining half were wrapped, in their entirety, in swabs soaked with Hartman's physiological salt solution ready for fresh mechanical testing later the same day.

All these procedures were then performed on the contra-lateral foreleg of each animal.

End of Secondary surgical procedure

After the assessments and harvesting of both FDS foreleg tendons and whilst the animal was still under anaesthesia a lethal dose of sodium pentobarbitone (Euthetal®; Rhone Merieux, Ireland) was administered by intrajugular injection. This was carried out in accordance with Home Office protocol, vital signs continued to be observed until they had ceased and the animal was pronounced dead.

TENDON ASSESSMENT

The aims of the various different assessments performed on the FDS tendons were to determine characteristics relating to function and morphology of the healing tendons. All aspects of the processing and analysis of the tendons were carried out by a single operator, the present author, and were performed in a strictly reproducible manner.

Facilities

The assessment and processing of the tendons took place at three different locations. The first analyses were carried out at the Marshall Building and included the two physiological tests performed during the secondary surgical procedure. Then, after harvesting of the tendons and in accordance with the project protocol, the tendons stored in formalin solution were taken to the laboratories of the Western General Hospital of Edinburgh, Department of Neurophysiology where tissue processing required for morphological analysis was carried out. The other half of each group of tendons was taken fresh from harvesting, wrapped in saline soaked swabs, to the Edinburgh University Department of Mechanical Engineering, King's Buildings, where the mechanical testing was performed.

In vivo Physiological Assessments

Two of the assessments performed on the FDS tendons were carried out with the animal under general anaesthesia. These *in vivo* assessments were Laser Doppler Blood Flowmetry (see next page) and measurement of the displacement, velocity and acceleration of FDS tendon excursion (see In vivo dynamic assessment of tendons, page 81).

Laser Doppler Blood Flowmetry

The purpose of this assessment was to quantify the superficial blood flow in the FDS tendons at sites both proximal and distal to the region of operative repair. Laser Doppler Blood Flowmetry (LDBF) provides a minimally-invasive, real-time measurement of superficial, local tissue blood flow. This was the first assessment to be performed at the time of harvesting because it was of critical importance that the FDS tendons and surrounding tissues were minimally disrupted, so that the course of superficial blood supply remained intact.

Apparatus and Principles

The apparatus used consisted of a commercially available MBF3/D Laser Doppler Blood Flow monitor manufactured by Moor instruments limited (Axminster) and a specially designed frame (see Fixator Frame Apparatus, page 76) which was attached to the operating table. This frame allowed fixation of the limb being studied, by the olecranon process of the ulna proximally and stabilization of the hoof distally, thus minimizing movement and risk of producing artifact on the recorded blood flow trace.

Laser Doppler Apparatus

The MBF3/D monitor consisted of a laser unit with the option of one or two probes and an LCD screen.

Figure 38: Laser Doppler Flowmetry Apparatus

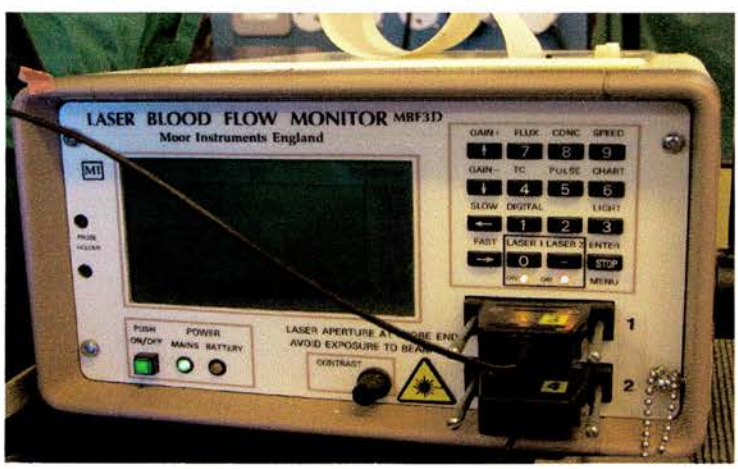

This monitor used laser radiation generated by a semiconductor laser diode which operated at a wavelength of 780 nm to 820 nm and a maximum possible power of 1.5mW. With the probes attached to the laser housing block the laser light was coupled into the optic fibers and transmitted within the fiber to the tissue being examined. The probe's aperture was only 7mm diameter and emitted a diverging beam of light with an angular spread of thirty degrees. This technique depended on the Doppler principle whereby the incident light was reflected back off the moving red blood cells in the superficial blood vessels, causing the light to undergo a Doppler frequency shift (broadening) which related to the speed of movement of the cells (Wright & Davies 1995). This backscattered light was then passed onto a photo-detector within the MBF3/D. The signal was amplified and processed by both an analogue and then digital processor and calculations displayed on the LCD screen regarding the perfusion data. Three different variables were obtained; concentration, speed and flux. However this study concentrated on the assessment of flux which is defined as the product of average speed and concentration of the moving red blood cells in the tissue sample volume. This arbitrary unit of flux is the most relevant and most widely used of these flowmetry measurements.

Fixator Frame Apparatus

The additional metal frame used for this study was designed and constructed in collaboration with colleagues in the Edinburgh University Department of Mechanical Engineering under the directorship of Professor McGeough. One of his postgraduate students, Mr. Brendan Hawes, devoted time and expertise to reviewing the old pulley and weights system of limb stabilization previously used in work carried out by the Peripheral Nerve Research Group and devising a more robust and appropriate system for this study.

The purpose of this frame was to hold the forelimb in a stable position whilst assessments of blood flow and displacement were being performed on the FDS tendon and thus minimize any artifact or erroneous results which may have derived from simultaneous movement of the limb.

Figure 39: Fixator frame apparatus

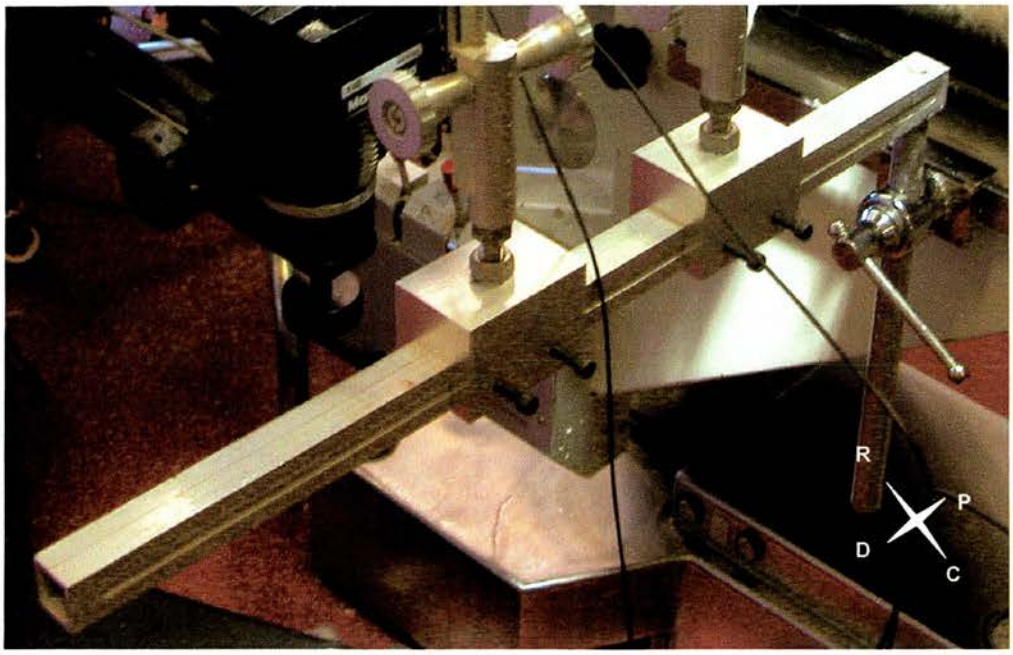

The frame consisted of a long straight rigid metal support bar which attached to the operating table using one of the standard table vices. Various other attachments could then be fitted onto this fixed support bar in order to hold the limb and appropriate pieces of apparatus in place. The most important of these was a bracket attached proximally on the support bar into which the olecranon screw was fitted.

Figure 40: Proximal limb fixator bracket

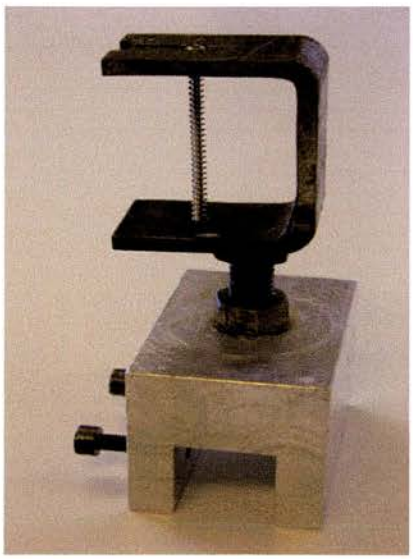

The hoof or distal end of tendon was then attached to the distal end of the bar dependent upon the assessment being carried out. When measuring blood flow the hoof was gently taped to the distal end of the support bar, but when measuring displacement the transected end of FDS tendon was tied to the displacement transducer which was in turn fixed securely to the support bar by means of a clamp. This then provided a fixed datum which incorporated the FDS muscle, its tendon slips and attachment into a stationary inertial frame of reference along the axis of the support bar.

Figure 41:Fixation of distal end of FDS tendon

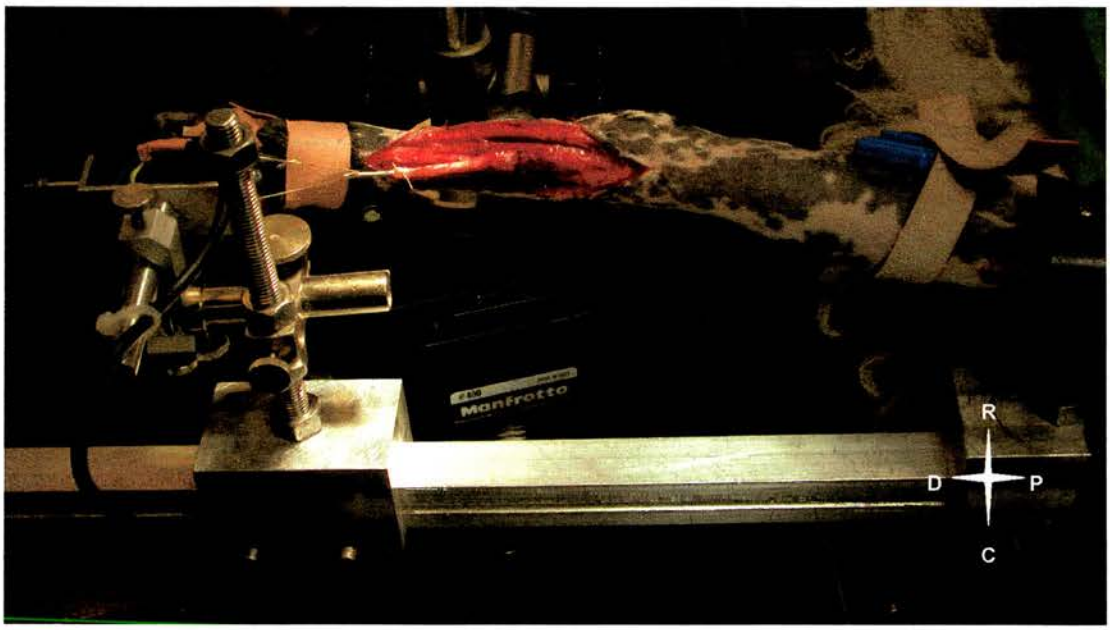

Calibration

Regular calibration of the doppler probes was performed in order to minimize any change that occurred in the probes over time. This was performed by placing each probe, in turn, into a tube of standard reference solution provided by the manufacturers. This solution used the brownian motion of polystyrene microspheres in water to produce the reference signals.

It was also important to ensure that test conditions were optimal and constant for each case in order to standardize measurements and eliminate other factors that might have influenced the blood flow. The operating and room lights were switched off to minimize ambient light. The body position of the animal was secured by appropriate cushioned table supports and the temperature monitored and maintained throughout. Both the forelimb being assessed and the doppler probes were fixed to the rigid metal support bar to minimize movement artefact.

Set up

With the animal under general anaesthesia the forelimb to be assessed was fixed at the proximal end by means of a screw placed through the olecranon process of the ulna and fixed into the bracket on the support arm. The hoof was then gently taped to the distal end of an additional support bar and the two doppler probes, mounted into sophisticated micro-manipulators which were capable of x-y-z axis adjustment with micrometer precision. These in turn were screwed into brackets which were mounted and fixed securely to the rigid metal support bar.

Figure 42: Laser Doppler Flowmetry set up

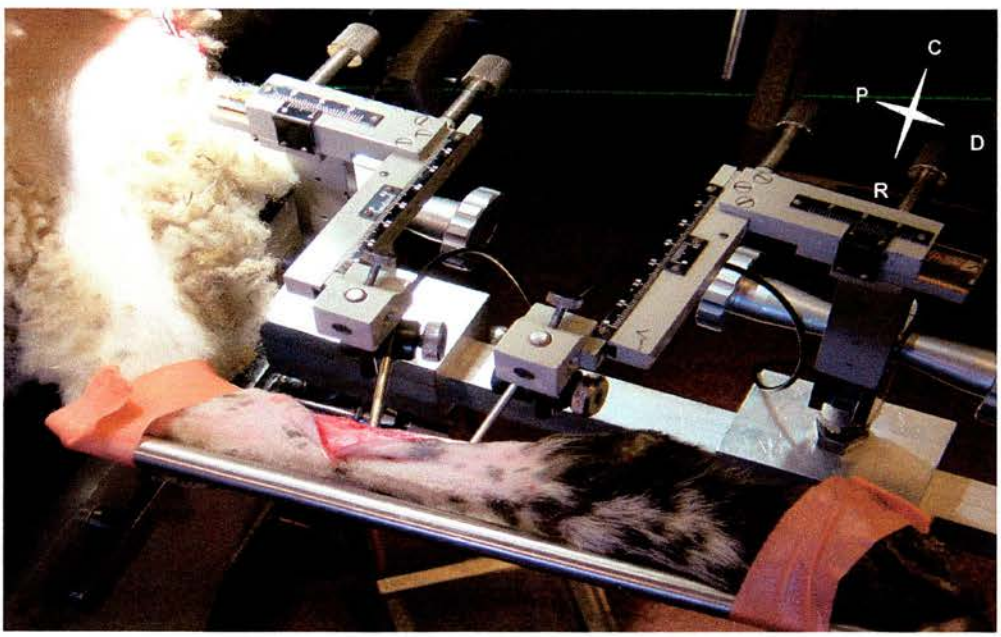

The probes were positioned over the tendon repair site, approximately 3 cm apart with the first probe placed on the surface of the tendon proximal to the site of repair and the second probe placed distally.

Figure 43: Laser Doppler probe placement

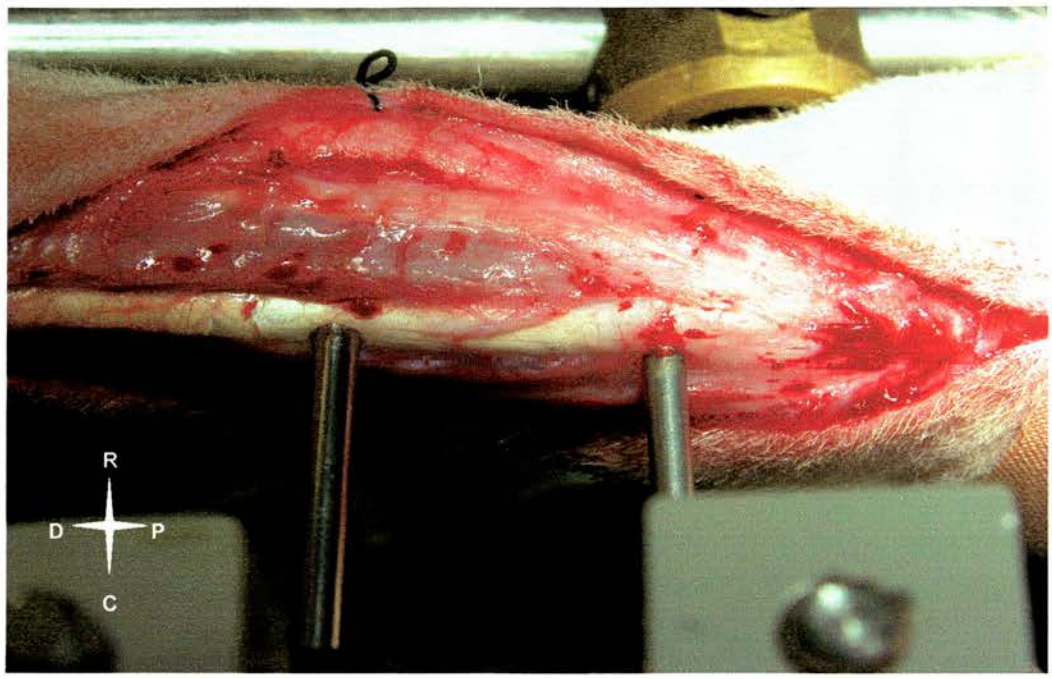

Having already checked the calibration and correct placement of the probes, the graphic display was set to run at a sampling rate of 40 Hz and a time constant of 0.5 seconds per division. Conditions for performing the assessment were re-checked, optimized and the laser beams turned on. The machine was allowed to run undisturbed for two periods, each of five minutes. The data displayed on the LCD screen were simultaneously recorded onto a laptop computer by means of the computer software provided by the manufacturer. The data were then stored in appropriately named files for later analysis.

In vivo dynamic assessment of tendons

The purpose of this novel method of assessment was to enable measurement of the displacement, velocity and acceleration of the FDS tendon upon contraction of its muscle. The theory behind this was that, if it was possibile to measure and display the displacement, velocity and acceleration of the tendon, it might then be possible to identify changes (caused by overcoming frictional forces imposed by the presence of adhesions) from the normal pattern of movement that could be attributable to the presence of varying numbers of adhesions.

Apparatus and principles

The apparatus used for this assessment was the commercially available Pico ADC 216 (see below), a displacement transducer, the metal fixator frame (see Fixator Frame Apparatus, page 76) with special bracket for the transducer and a nerve stimulator.

Personal Computer 'Oscilloscope'

The Pico ADC 216 and its oscilloscope emulating software were produced by Pico Technology Limited (www.picotech.com).

Figure 44: Pico ADC 216

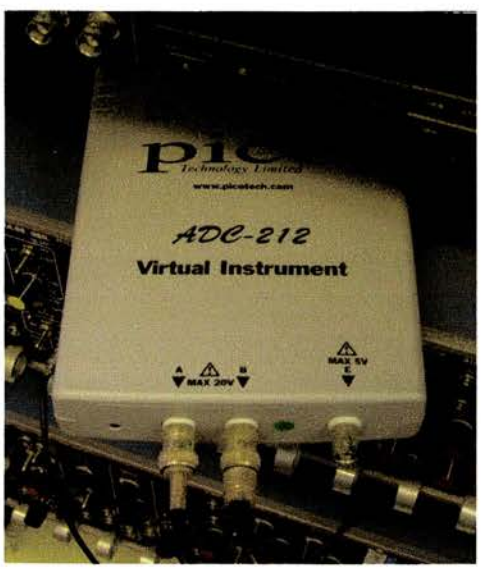

The Pico ADC 216 emulated a high resolution, high precision oscilloscope and was used to convert the output voltage of the displacement transducer (see below) from a 16 bit analogue to digital signal over the period of time taken for the FDS muscle contraction. Connected via a parallel port cable, these data were stored and displayed on the computer screen oscilloscope.

Figure 45: Computer 'oscilloscope' (Pico)

Displacement transducer

A Linear Potentiometric Displacement Transducer (LPDT), Sakae 15FLP30A, manufactured by Sakae Tsushin Kogyo Limited was chosen for this study.

Figure 46: Sakae LPDT

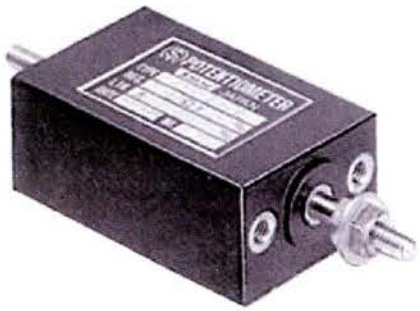

Table 1: Sakae LPDT specifications

Model Number	**15FLP30A**
Resistance Value	10kΩ
Total Resistance Tolerance	±10%
Independent Linearity Tolerance	±1.0%
Resolution	Essentially Infinite
Output Smoothness	Below 0.1% against input voltage
Contact Resistance Variation	Below 2% C.R.V.
Power Rating	0.5W
Electrical Stroke	30±0.5mm
Mechanical Stroke	30±0.5mm
Insulation Resistance	Over 1000MΩ at 1,000 V.D.C
Dielectric Strength	1 minute at 1,000 V.A.C.
Internal Spring Restoring Force	Approx. 300gf (3N)
Stopper Strength	Approx. 2kgf (20N)
Resistance Temperature Coefficient	±400p.p.m/°C
Weight	Approx. 30g

In order to accommodate attachment of the tendon to this transducer the shaft was slightly modified by the addition of a small metal plate containing two holes through which the linen tie, attached to the end of the tendon, could be secured. In so doing the shaft required to be permanently displaced by a further 13mm, making this the new point of zero displacement. The LPDT was then recalibrated (see Calibration page 88).

Figure 47: LPDT bracket attachment

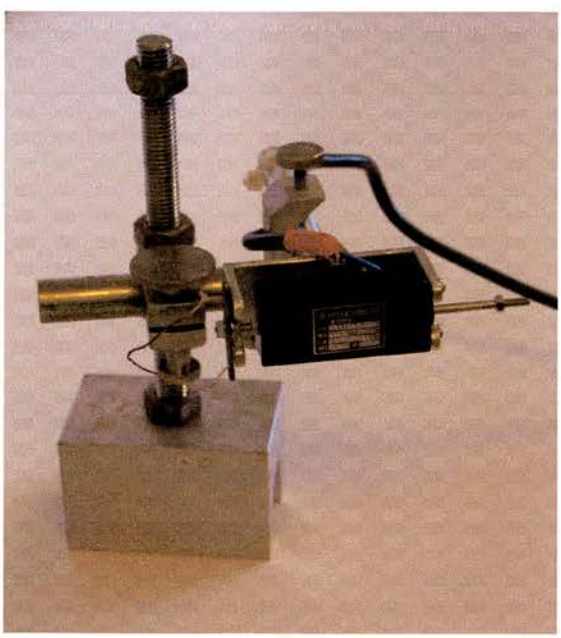

The LPDT was attached to a 10V power supply (Thurlby DC power supply) and connected to the tendon and Picoscope so that it acted as a variable potential (voltage) divider as shown below

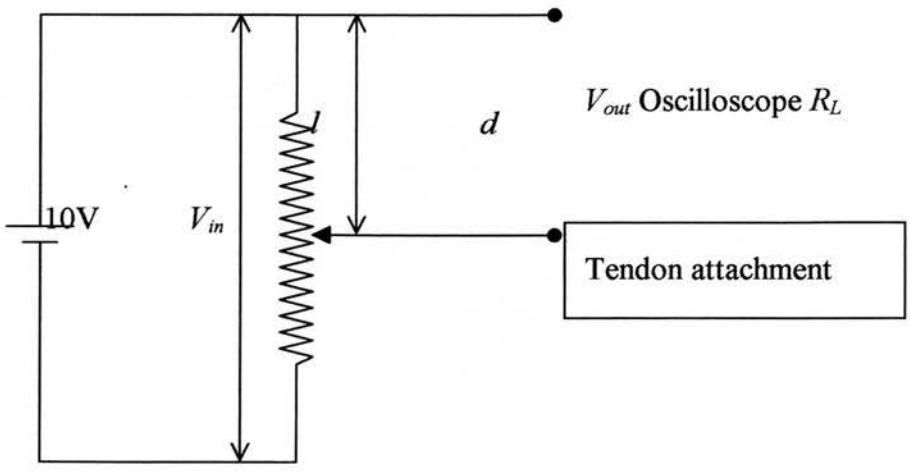

Where:

l is the electrical stroke (30mm from the LPDT specifications)

V_{in} the input voltage

d the displacement

V_{out} the output voltage

The output voltage was related to the input voltage by the linear relationship

$$V_{out} = V_{in}\frac{d}{l}$$

When the load resistance (R_L), resistance of the Picoscope channel, was taken into consideration, the equation became

$$V_{out} = V_{in}\frac{d\,R_L}{l\,R_L + d(l-d)}$$

However, the load resistance only significantly affected output voltage at small values owing to the fact that current was drawn from the circuit. As the load resistance tended toward infinity the effect became negligible as less and less current was drawn from the circuit. The load resistance for this study was the impedance of the input channel of the Pico ADC 216, which was 1 MΩ and thus was taken as being essentially infinite. Therefore the first equation above could be rearranged to make *d* the subject and thus allow calculation of displacement in Volts.

$$d = \frac{l V_{out}}{V_{in}}$$

This value was later converted into mm (see Calibration, page 88).

In the present experiment the objective was to measure the displacement of the tendon not the force of its contraction. In order to do this accurately the transducer chosen was required to have the lowest possible internal resistance, such that this could be regarded as negligible and thus not diminish the length of excursion that was observed upon isotonic contraction of the FDS muscle. This work must not be confused with the large body of previous research which has used force transducers to measure isometric tension; the way in which force transducers operate is to balance internal resistance against the force applied by the muscle (allowing only internal spring displacement to occur) and as such force transducers are required to have high internal resistance.

Fixator Frame Bracket

A lockable sliding bracket was made to attach to the support bar of the fixator frame apparatus. This bracket was designed to hold the LPDT using a micro adjustment system which enabled the LPDT to be precisely positioned and aligned distal to the FDS tendon, continuing along its natural course, prior to being secured into position along the support arm (see figures 41 and 47, pages 78 and 83 respectively). The proximal limb bracket of the support bar apparatus was used as previously described (see Secondary surgical procedures, page 69).

Nerve Stimulator Apparatus

This consisted of a mains-powered signal generator (Digitimer, model DS7) which was used to supply a pulse of current via connecting cables to nerve stimulator leads which were in turn attached to the limb of the animal. The signal generator was set to produce a single square wave pulse of current, of 200μs duration. The current and voltage could be set independently; a constant current of 30-50 mA was used which resulted in a range of -5V to 5V. The signal generator was triggered manually to deliver a single pulse of current sufficient to cause supramaximal stimulation of the FDS muscle thus causing it to contract isotonically (shortening in length) as if stimulated naturally by its own supplying nerve. The signal generator also had an output channel which used transitor-transistor logic (TTL) to allow connection to the Pico ADC unit (via input channel A) which was then triggered on the rising edge of the input voltage. During the contraction of the FDS muscle belly, the distal FDS tendons were displaced proximally pulling on the LPDT and resulting in a measurable displacement and velocity displayed and recorded on the Picoscope.

Figure 48: Nerve stimulator – displacement circuit

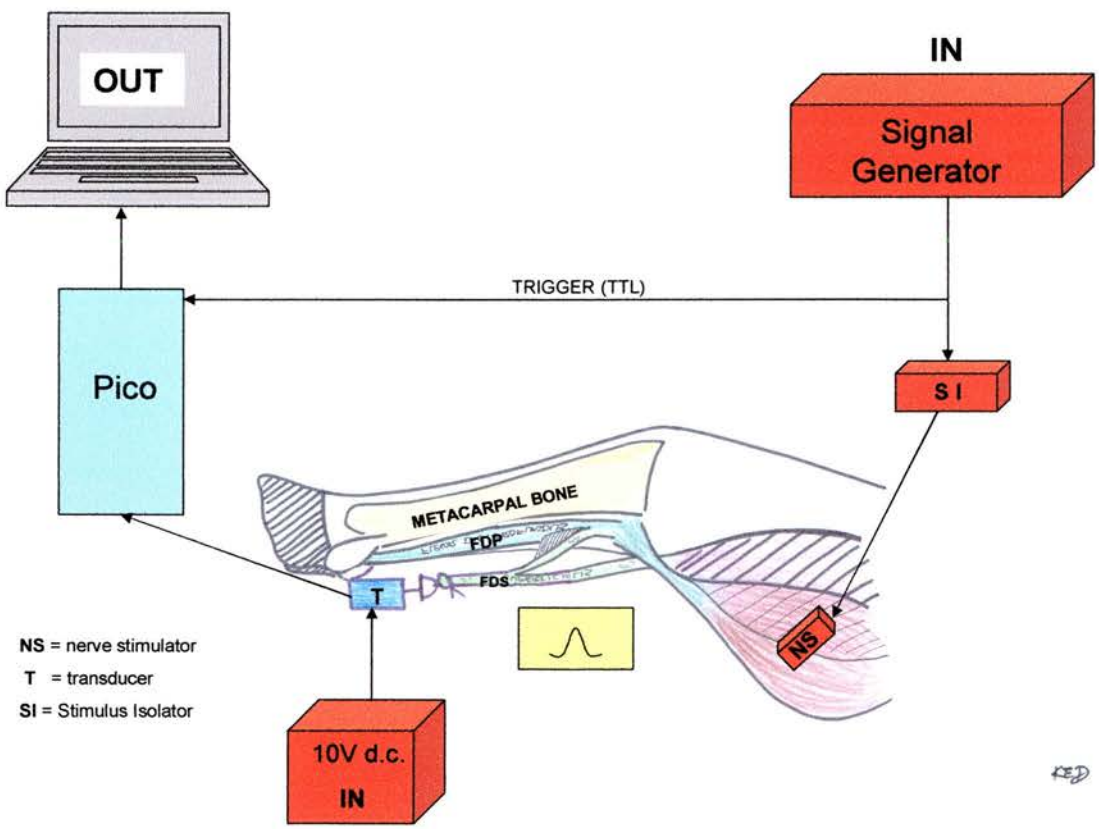

At the start of the study direct nerve stimulation was used by means of dissecting clear the proximal part of the brachial plexus of nerves high up in the forelimb of the animal. The end of the stimulator cable was attached to a tiny clamp into which the median nerve (a branch of which supplied the FDS muscle) was placed as illustrated below.

Figure 49: Direct nerve stimulation of median nerve

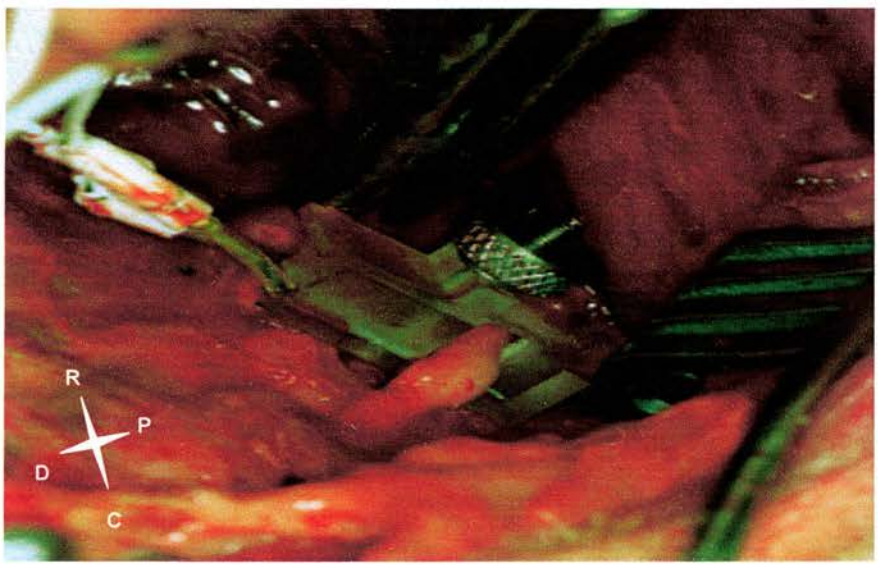

The median nerve of the ovine forelimb has been dissected clear of its surround tissue, high up in the axilla and carefully placed inside the connector end of the direct nerve stimulator cable.

However these early cases were also repeated using transcutaneous nerve stimulation. This simply involved use of two small saline soaked pads, one positive the other negative, placed a few centimeters from each other in a small blue plastic case connected to the end of the stimulator cable. The pad was placed on the shaved area of skin overlying the region of the median nerve trunk which branched to supply the FDS muscle (as previously determined by postmortem forelimb dissection) and therefore did not necessitate any tissue dissection. The two different methods of nerve stimulation resulted in excitation of muscle contraction with equivalent output results, hence the remainder of cases underwent transcutaneous nerve stimulation only.

Figure 50: Application of transcutaneous nerve stimulator pad

The blue plastic casing of the cutaneous nerve stimulator pad can be seen lying over the region of the median nerve branch to the FDS muscle. Secured in place by means of a velcro strap it contained the saline soaked conducting pads (inferiorly).

Calibration

In order to ensure that the initial tension of the tendon and muscle unit was always consistent the LPDT body was moved in a distal direction using the micro adjustment mechanism, extracting the shaft from the body until the Picoscope meter read close to 4 Volts. This corresponded to a certain displacement and load on the internal spring and therefore a resultant restoring force which provided initial tension consistent with Hooke's Law:

$$F = kd$$

Where F is the force exerted by the spring on the tendon resulting in tension, k is the spring constant (a measure of the spring's stiffness) and d is the displacement of its free end from the position of the spring in the relaxed state, the distance the shaft has been extracted from the body of the LPDT.

The output voltage signal obtained from the transducer varied in a linear relationship with the displacement of the transducer shaft and was calibrated so that the output voltage could be converted to a displacement value of millimetres by use of a simple formula. A calibration graph for this transducer was constructed, using an input voltage of 10V and with the Picoscope in DC mode. The *y* axis was the output voltages (V) recorded and these were plotted against the *x* axis of the measured length of LPDT shaft displacement in millimetres (mm).

Figure 51: LPDT calibration curve

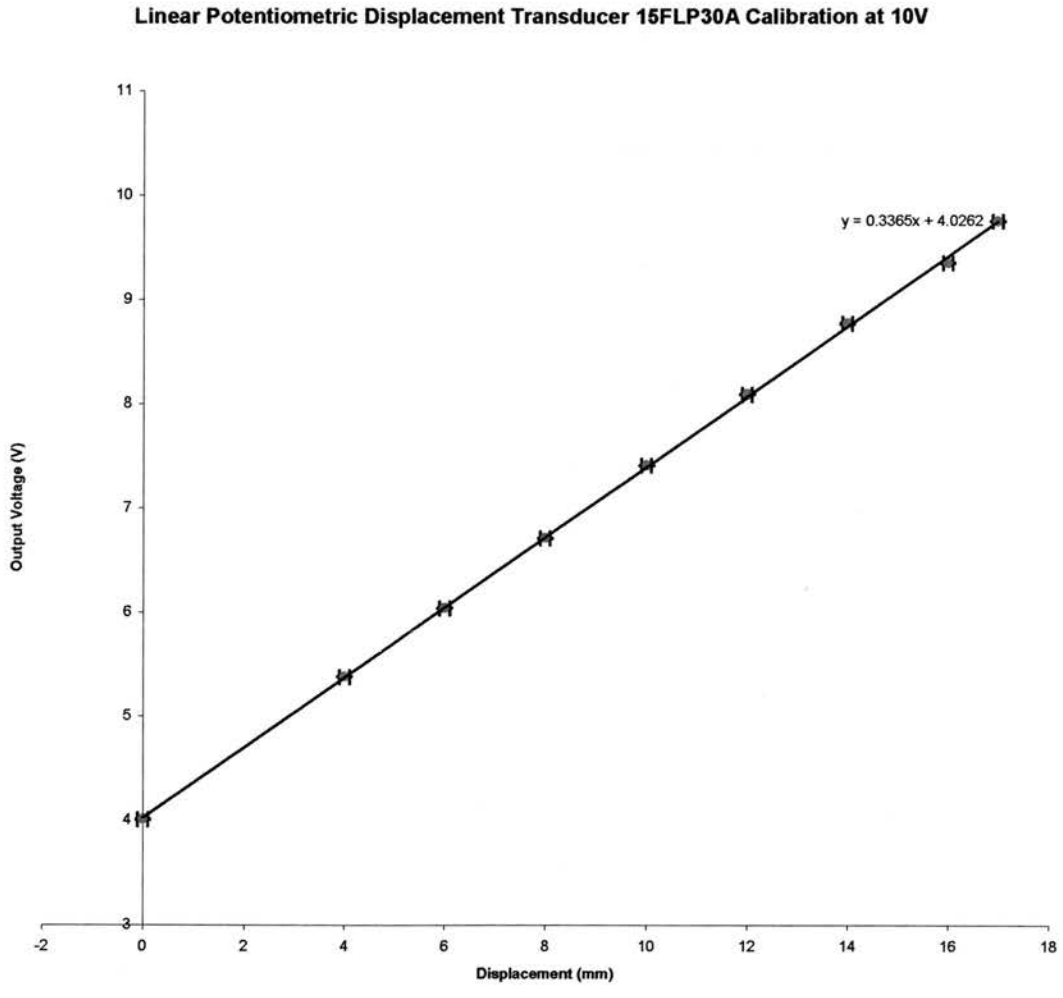

A 'best-fit' line was applied to the calibration graph from which the required conversion formula was then derived.

$$d(mm) = \frac{output(V) - c}{0.3365}$$

Where:

d is displacement

c, the constant

The constant, c was the offset potential recorded on the oscilloscope after fine adjustment of the transducer–tendon unit. It was always maintained close to 4V and was automatically recorded as the first datum point of each output trace.

Understanding and processing Picoscope Data

The output signal from the LPDT could be processed and displayed by the Picoscope in either DC or AC mode. Set to DC mode the oscilloscope display essentially provided a graph of displacement versus time (blue line in graph below). In AC mode it displayed the rate of change of DC voltage $\frac{dV}{dt}$. Since the output voltage had already been shown to have a relationship directly proportional to displacement (x), the AC mode effectively gave the instantaneous velocity $\frac{dx}{dt}$. As such, in the AC mode the oscilloscope display provided a graph of velocity versus time (red line in graph below).

Figure 52: Oscilloscope display of displacement and velocity

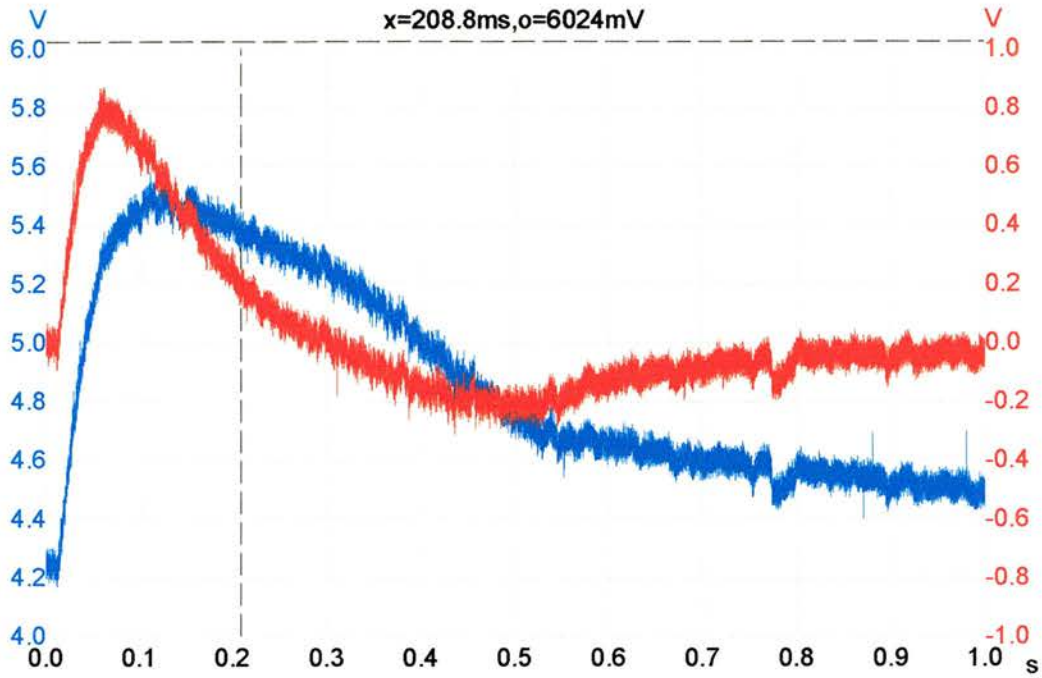

The blue line displays displacement and the red line velocity, of the FDS tendon upon nerve stimulation.

Obviously it was also possible to derive mathematically velocity from the displacement values by differentiation, or vice versa by integration. When both the channels were used simultaneously (as in the illustration above) the process of 'chopping channels' meant that fewer data points were collected from each channel. Thus the accuracy of each graph (and subsequently fitted curve) was diminished. So for this study it was decided to set the Picoscope to display the LPDT voltage output in DC mode only, thus providing a graph of displacement against time at maximum sensitivity and the velocity data were derived mathematically, as were the acceleration data.

The raw output data were stored in appropriately named files and later exported to a software program, Datafit (Oakdale Engineering) for analysis. The reason for exporting the data was threefold. The raw data recorded by Picoscope was a large series of data points but included a fair amount of background noise so by calculating

the best fitting curve it was possible to determine specific points, such as maxima and minima, more accurately. Also having fitted a curve to the data points it was then possible to obtain the equation of the curve, differentiate this and plot the resultant velocity curve, differentiate once again and plot the acceleration curve. Since both the displacement and velocity graphs shared the same time-axis they could also be overlaid and plotted using two separate vertical axes thus aiding interpretation. This was performed by further exporting the data into a software program Statistica (Statsoft Inc., Tulsa, USA).

Figure 53: Superimposition of displacement and velocity curves

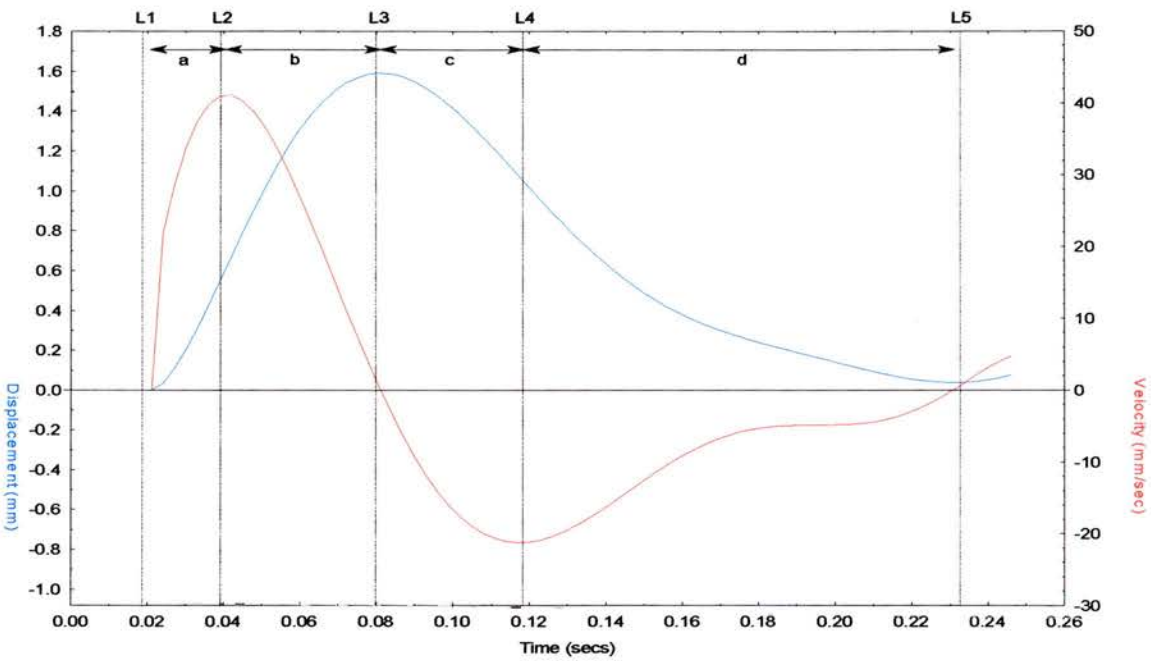

Once the graphs had been produced values were obtained for the following list of variables:

Maximum displacement (D_m) on supramaximal nerve stimulation producing isotonic twitch.

Time to achieve maximum displacement (tD_m)

Displacement at the point of half relaxation (Dhr)

Time to half relaxation ($tDhr$) after isotonic twitch.

Total twitch time (T_t)

Maximum velocity (*Vmax*)

Time to maximum velocity (*Vmax*)

Time to zero velocity (V_{zt})

Time to zero acceleration (*t0Accel*)

Set up

After the assessment of laser doppler blood flow had been completed the animal was kept under anaesthesia, in the same position, with its foreleg fixed proximally to the support bar. The tape was removed to release the hoof and the tendon was dissected distally, divided from its insertion and secured to the LPDT by a short length of 1/0 linen, Ethicon Ltd. UK.

Figure 54: Fixation of distal end FDS to LPDT

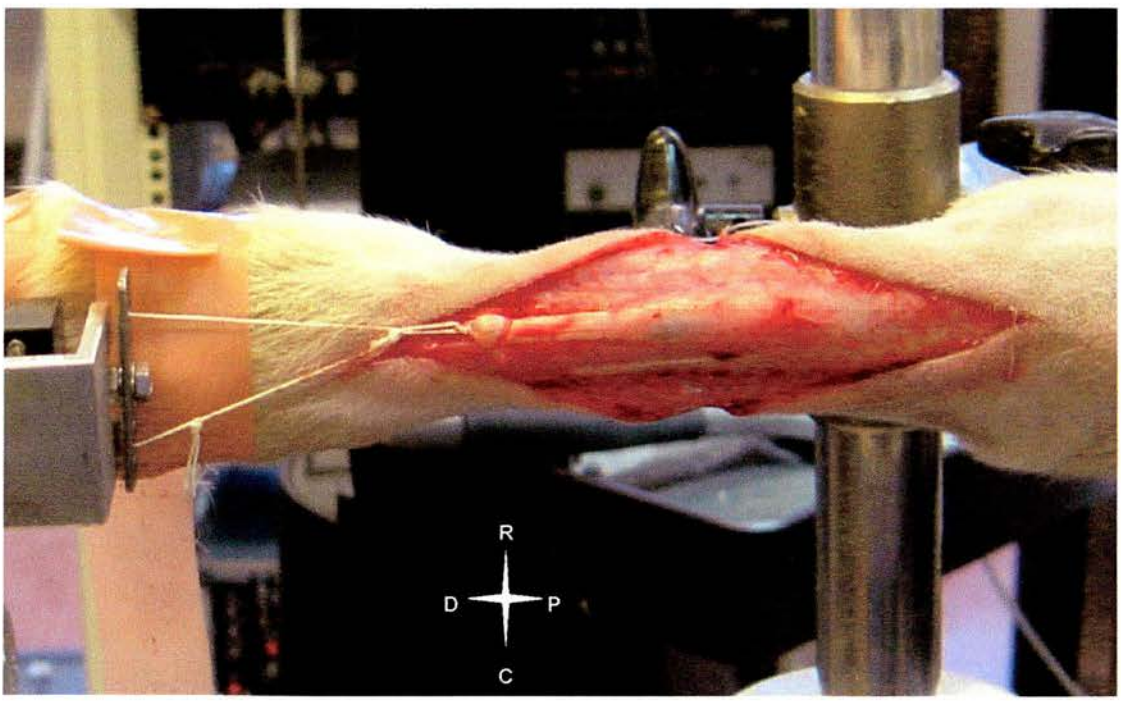

The LPDT mounted in its bracket was carefully and precisely aligned at the distal end of the FDS tendon following its natural course and secured in position on the support bar.

Figure 55: Aligning the FDS tendon and transducer

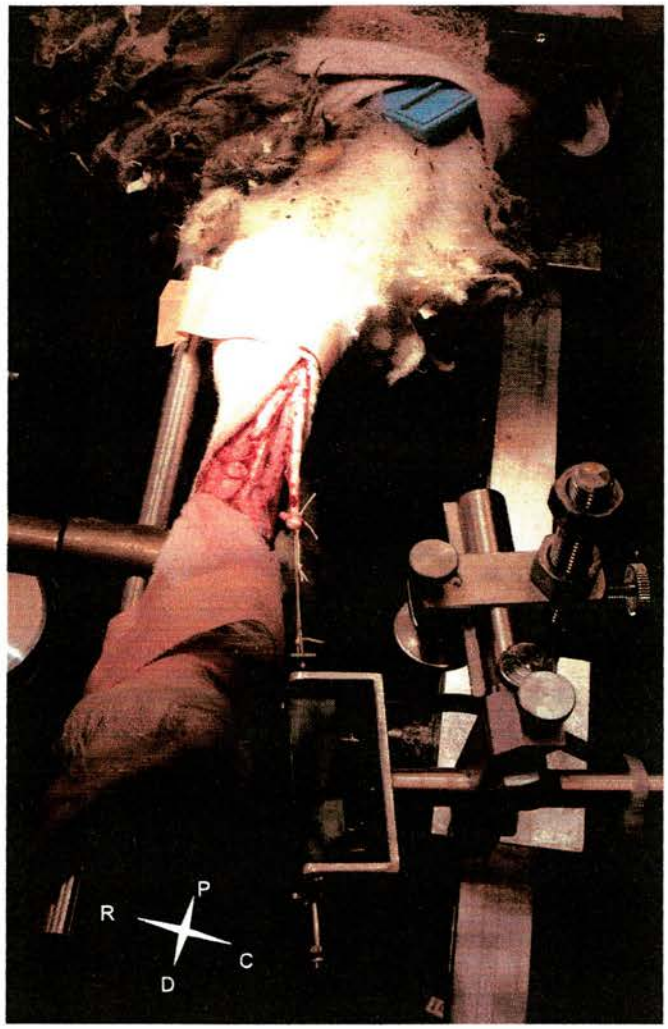

The transcutaneous nerve stimulator cable was placed on the shaved area of skin on the proximal limb and held in place by means of a Velcro strap. The Picoscope was switched on. The LPDT was adjusted to obtain a Picoscope meter reading of close to 4 Volts and the stimulator triggered to release a single pulse of current large enough to evoke FDS muscular contraction. The data were stored and the process repeated with increased current being delivered through the stimulator in order to ensure that supramaximal stimulation of the muscle had occurred.

In vitro Assessments

These were performed after the FDS tendons had been harvested and each of the two tests was carried out on only half of every group of cases; six cases per group were tested for mechanical strength whilst the remaining six were processed for histological examination.

Mechanical Assessment

As per protocol, half of the cases in each group underwent mechanical testing. Immediately after harvesting they were wrapped in swabs soaked in Hartman's physiological salt solution and sealed in individual, case-labelled, plastic packets. At the end of each day of harvesting, the fresh tendons were taken to the University Department of Mechanical Engineering at King's Buildings where access had been granted to use the Instron mechanical testing machine. Each repaired tendon and its contra-lateral normal tendon were placed in turn into the machine and a tensile test conducted.

Tensile testing principles

A tensile test is probably the most fundamental mechanical test that can be carried out on a material and demonstrates how it reacts to forces being applied in tension. The test results are displayed on a graph to produce a curve illustrating the tensile profile of the material being assessed. Although much information can be gained from these graphs, for the purposes of this study particular attention was paid to point of tendon failure. This is the point of particular interest in any tensile profile and is referred to as the 'ultimate tensile strength' (UTS) of the material being tested. It is the maximum load that the specimen sustained during the test. Obviously the UTS is of great functional importance when evaluating methods of tendon repair and it is indeed one of the measurements frequently referred to in published literature when debating the efficacy of methods of repair.

Instron Machine

The tensile test machine used for this study was the Instron 4500 model manufactured by Instron Corporation, UK. This consisted of a sample testing unit, computerized controls and a graphic display unit.

Figure 56: Instron tensile testing machine (4500)

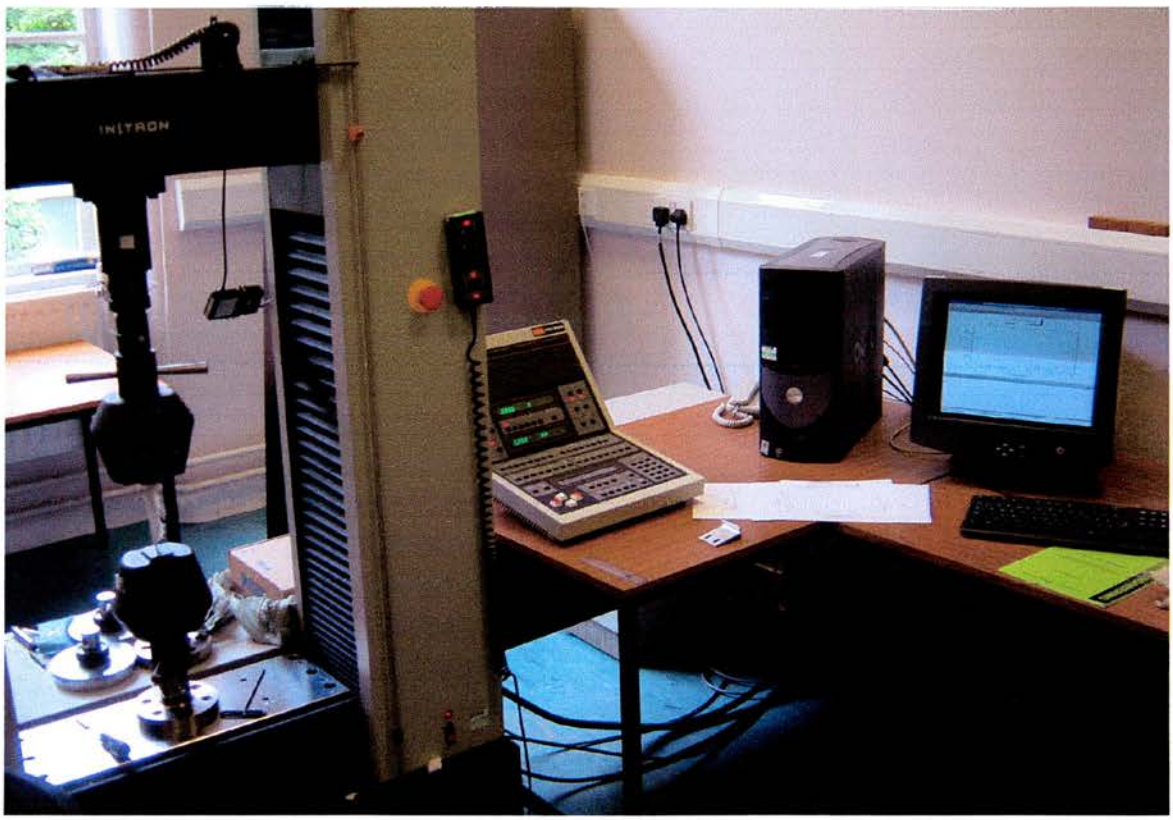

When the Instron machine was switched on an appropriate tensile test regimen required to be selected from the computer menu bar. For this study a regimen of continuous incremental loading was chosen with a crosshead speed of 20mm min^{-1} and time base of 10 points per second. The output display was selected to plot force (automatically displayed in kilograms of force, kgf) against displacement (mm). The calibration of the machine was checked before the tendon to be tested was inserted into the vice heads of the testing unit (see Instron vice modification, over page). It was important to keep the time of air exposure of the tendon to a minimum so that its characteristics were not affected by drying out. Therefore the tendon was only

removed from its saline swabs once the machine was ready for testing and the process of placing the tendon into the vice heads was performed as efficiently as possible. Once the tendon was in place the vice heads were carefully distracted until a force of 0.5kgf was observed; then the test was commenced.

Instron vice modification

Prior to commencing the study much time was spent in collaboration with colleagues of the Department of Engineering, designing appropriate vice clamps to hold the tendon ends securely during testing. This posed a difficult problem which had not been discussed in detail in the literature where tensile testing of tendons had been performed. The main problem was that of slippage of the tendon ends within the Instron vice heads. If the clamps were closed very tightly around the tendon ends then deformity and tearing at the edge of the clamp head resulted. Several different methods were considered and tried but in the end the best solution was found to be the addition of two specially designed metal T-pieces which had a hole cut in their stems.

Figure 57: T-piece insertions for Instron vice heads

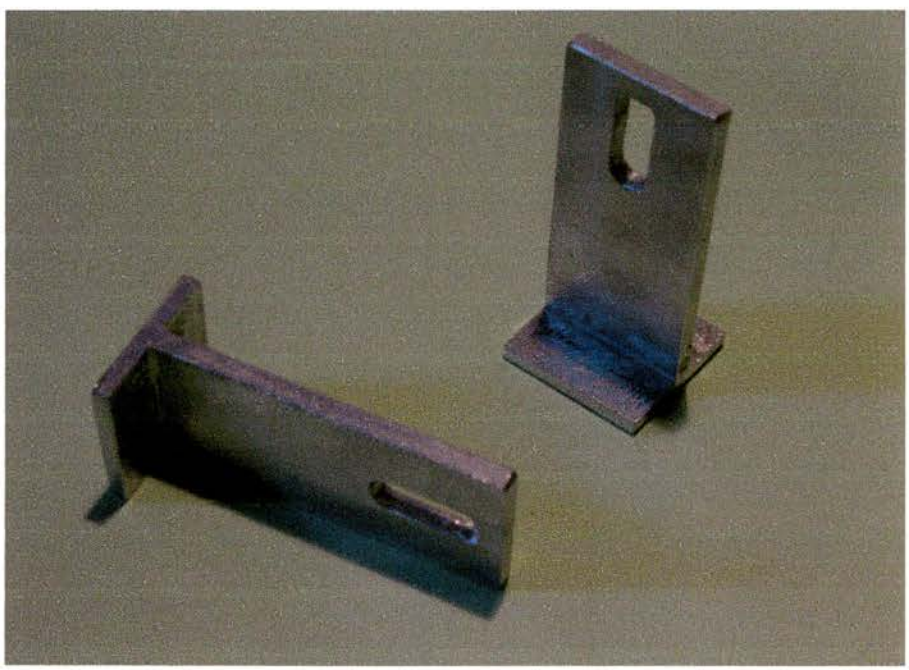

A decent length of the tendon end was placed through the hole thus creating a u-bend. Fine sandpaper was positioned on either side of this end to keep it in place and the T-piece was carefully slotted into the manufacturer's vice heads which were then closed. This was repeated for the opposite end and the tensile test then performed.

Figure 58: Securing the FDS tendon in the Instron vice heads

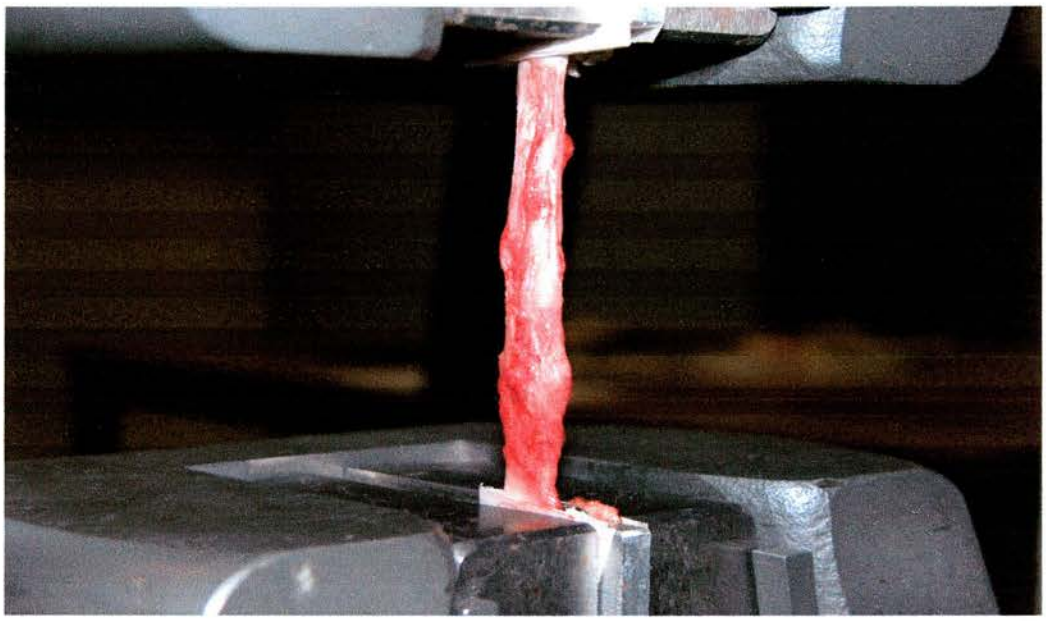

Using this method of fixation, the tendons were observed to thin out upon distraction but they did not slip. This was checked at the end of each test by observing the shape of tendon after being removed from the vice. As illustrated below, the portion of the tendon that was in the hole of the T-piece remained intact despite thinning of the distracted portion. It was also noted that even when the tendon ruptured close to one of its ends there was always a small portion of tendon free from the clamp head thus eliminating tearing by the vice edge as the mechanism of failure.

Figure 59: FDS after rupture and removal from Instron machine

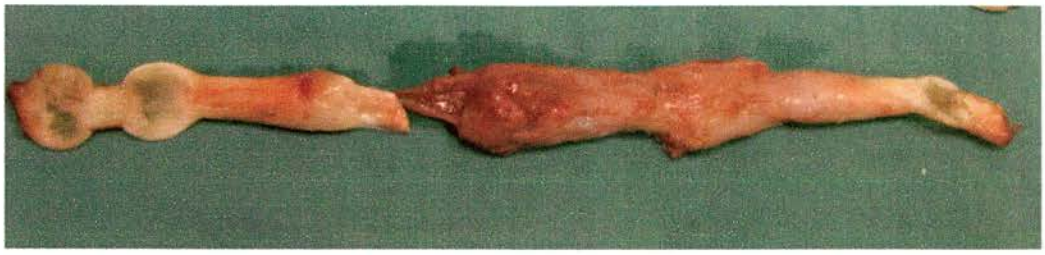

Data Manipulation

The data obtained were saved in appropriately named ASCII files and later exported to an Excel Spreadsheet (Microsoft). Illustrative graphs were produced such as the one below and the units of force could also then be converted easily from kgf to newtons by multiplying each data point by 9.80665.

Figure 60: Tensile test output graph

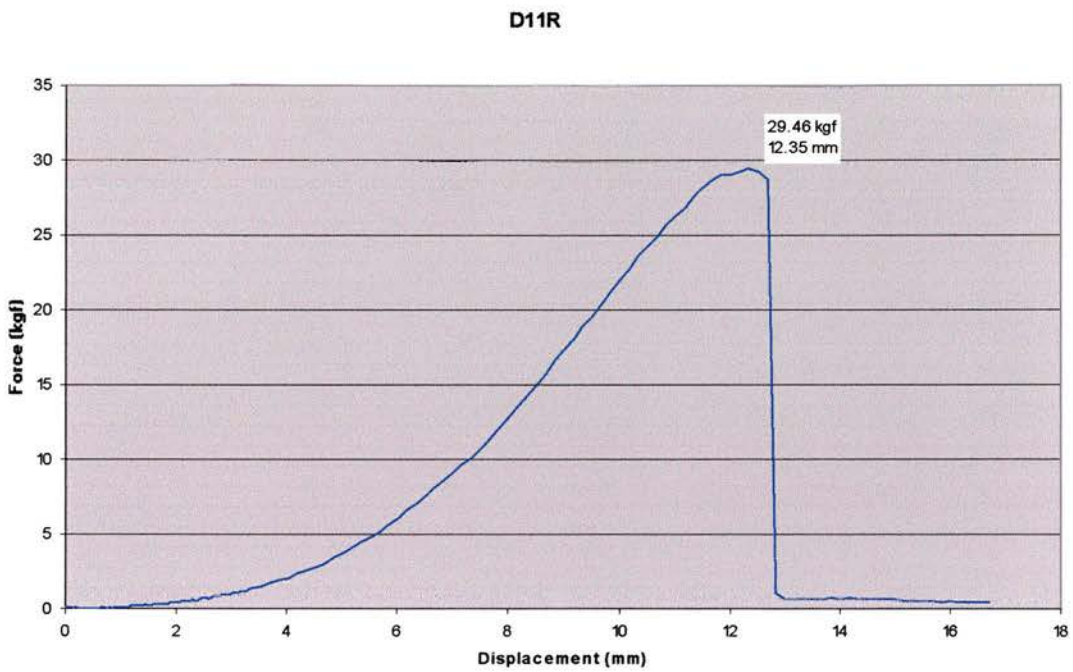

Morphological Assessments

As per protocol, the FDS tendons from half of each group of cases underwent morphological analysis. These tendons were stored individually in 10% formalin solution immediately after harvesting. This was performed in order to preserve and harden the tissue samples whilst causing minimal distortion of their physical features, chemical characteristics or staining properties. The samples were then taken to the Neurophysiology laboratories at the WGH where they were processed in preparation for analysis.

Wax Embedding

The first step in the process of preparing the samples for sectioning was to impregnate them with wax and embed them into wax blocks which could be securely held for cutting sections. The tissue impregnation with wax was performed using a Tissue-Tek VIP wax processor.

Figure 61: Wax impregnation machine (Tissue-Tek VIP)

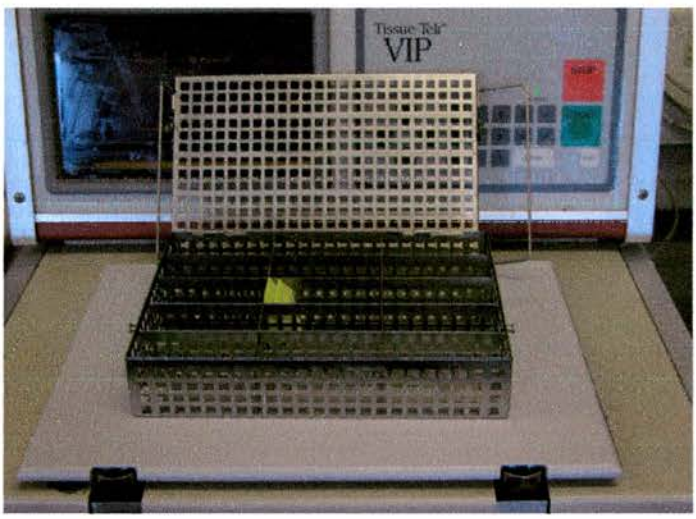

This process was carried out in batches, the stored tendon segments being removed from their formalin solution at this time. Each tendon section was checked for size and trimmed as necessary to ensure a good fit with correct orientation within the plastic embedding cassettes. To create cross sectional slides of the tendons the samples required to be orientated with the cut edges against the floor and roof of the cassette, the tendon fibers running perpendicularly. The cassettes were then clearly labelled with a lead pencil in order that the labelling would survive exposure to the processing liquids and solvents.

The plastic cases containing specimens were loaded into a specimen rack and placed into the VIP machine, the lid securely closed and an appropriate embedding program commenced. The program chosen for this study was program option 4 which bathed the samples in solutions of alcohol of increasing purity, then xylene and finally molten wax (see appendix 1). The alcohol served to dehydrate the tissue samples. The xylene acted as a link between the other two solutions as it was completely miscible with both, and the molten wax impregnated the tissues preparing them for the final stage of embedding into wax blocks. This program was left to run overnight, the entire cycle taking approximately eighteen hours to complete.

The final stage of the embedding process required the use of an embedding centre, the one used was also manufactured by Tissue-Tek.

Figure 62: Wax embedding centre

Each specimen was removed from its cassette and placed in a stainless steel cassette mould. Careful attention was once again paid to the orientation of the sample to ensure that the cut section would yield cross sectional views of the tendon. The base of the plastic cassette was then separated from its lid before being placed on top of the tissue sample. Molten wax was poured on top to fill up the steel cassette mould. This was then placed to cool on a cooling tray which was kept at a temperature of minus four degrees. Once the wax had set, the embedded sample was removed from the steel cassette ready for sectioning.

Microtome sectioning

In order to prepare appropriately fine slivers of tendon tissue for mounting onto microscope slides, a rotary microtome (Shandon AS 325) was used.

Figure 63: Microtome

This was simply a specialized knife with a mechanism for advancing the wax specimen block standard distances across it. The wax embedded sample blocks were mounted onto the vice of the microtome and a fresh blade was inserted at the beginning of each cutting session. Disposable blades were used and were frequently moved to a clean contact surface, or changed as the processing continued, to ensure clean slicing of the samples. This was especially important for the samples which contained suture material, although all samples were fairly hard and quickly blunted the blade. Unsurprisingly, a sharp blade was the key to achieving the best sections. The thickness gauge was positioned to cut slivers of just seven microns and a water-bath was filled and heated ready to receive the slivers after sectioning. This was an

important step as the cut sections were fragile and wafer thin, with occasional wrinkles which were smoothed out on contact with the warm water.

Slide mounting

The slides used for this study were commercially available Superfrost® Plus 1mm thick microscope slides (BDH Laboratory supplies, UK) which had been electrostatically charged for improved binding. The cut sections of specimen were carefully floated out of the water bath onto microscope slides before being allowed to air-dry. Since the cut sections were so thin, it was possible to cut multiple sections from each tissue sample. Two or three sections were therefore mounted on each slide and at least two slides were made per sample. The slides were then labelled in pencil.

Histological staining techniques

Before any staining could be commenced the embedding process had to be reversed to get the paraffin wax out of the tissue in order to allow the water soluble dyes to penetrate the sections. The slides were therefore run through a series of xylenes to alcohol to water to rehydrate them (see appendix 2).

General Principles

The purpose of histological staining is to make various tissue, cellular components and extrinsic matter more evident. The principle behind any histological staining technique is that the dyes, either natural or synthetic, are taken up by different cell and tissue components in a selective or preferential manner. The mechanisms involved are of two types, chemical or physical. In the chemical dye reactions, union between the dye and stained substance occurs by means of chemical bonds such as salt linkages and hydrogen bonds. These are dependent upon the acid-base characteristics of the tissues and as such staining results in fairly predictable colour patterns. The second type of staining mechanism is a physical reaction, that of absorption of the dyes. The dye may be absorbed on the surface of the structure, or precipitated within the

structure dependent upon what is favoured by the surrounding environmental factors, such as pH, temperature etc (Stainsfile 1998).

Thus staining techniques make use of a variety of dyes that have been chosen for their ability to stain different cellular components of tissues. Two different staining techniques were chosen for this study, haematoxylin and eosin (H&E) and Gomori's trichrome.

Haematoxylin and Eosin Stain

H&E is a very general histological stain and probably the most widely used of all stain varieties. It is composed of haematoxylin-metal complexes which act as a basic dye (positively charged), combined with eosin which acts as an acid dye (negatively charged). The dyes undergo chemical reactions with tissue substances, forming cellular bonds. Any substance that links with the haematoxylin dye is coloured a shade of purple, and said to be basophilic. That which links with the eosin dye is coloured a pink shade and said to be acidophilic (or eosinophilic). Thus nucleic acids in the cytoplasm and nuclei are stained blue, purple or black and the more basic proteins of the cytoplasm and extracellular tissue (collagen) are stained pink.

A complete set of slides was stained with H&E following the method described in appendix 3. This procedure was performed with care in a fume cupboard and the slides then completed by placement of a coverslip (see Applying coverslip, over page).

Figure 64: Histological staining apparatus

Gomori's Trichrome Stain

This is a variant of a group of techniques described as 'trichrome' staining. Trichrome literally means 'three coloured' but this class is in fact used to describe staining methods which use two or more acid dyes of contrasting colours (Stainsfile 1999). These dyes selectively colour different basic tissue structures and are most commonly used to demonstrate the presence of collagen. There are two main variants in this group of techniques; those which use a multi-step approach and those using a single step method. The one step methods combine all dyes and reagents into a single solution whereas the multi-step approaches apply the dyes sequentially. Compared with the Masson's multi-step approach, the Gomori's one step method had been shown to be simpler to conduct, less time-consuming, more cost effective and yet indistinguishable in end result, except for the colour of the collagen which stained blue rather than green (Tobias 1995). Thus the Gomori trichrome stain was used for this study. A complete set of slides was stained with Gomori's trichrome stain following the method described in appendix 4. This was performed with care in a fume cupboard and the slides then completed by placement of a coverslip.

Applying the coverslip

To complete the process of slide preparation a thin piece of glass was placed over the stained section on the slide. This served to protect the tissue from being scratched, provide better optical quality for viewing under the microscope and to preserve the tissue section. However, before this could be carried out the stained slide had to go through the reverse process of that performed in preparation for staining, to remove the excess water. It was therefore passed through a series of alcohols and xylenes to dehydrate it (see appendix 5). Then a coverslip was gently laid in place over a couple of drops of fixative glue. The glue used for this study was a thermoplastic substance, Meltmount™ 1.539 (Cargille Meltmount, New Jersey, USA). The number corresponded to the refractive index of the glue, which was optically similar to the classical fixative Canada Balsam (made from the resin of the balsam fir tree of North America; *Abies balsamea*) and most importantly, to the refractive index of the glass slides and cover slips.

Slide scanning

In order to perform the morphometric analysis of the prepared tissue sections it was necessary to upload specific images to the Analytical Imaging Station computer program (see AIS Morphometric Analysis below). A number of different methods could be used to perform this task. For work previously carried out by the Peripheral Nerve Research Group a specially adapted microscope had been used. This was computer assisted and took photographic images directly from the viewfinder of the microscope which were then stored as usable .tiff files. This was clearly suitable for the degree of magnification required for examining individual nerve fibers, but even under the lowest power of magnification it gave too small an image field to be of constructive use when attempting to calculate quantitative data of the entire cross section of a repaired tendon. The notion of importing several image sections and then uniting them before carrying out the analysis was considered but carried too great a risk of error from overlap of indistinct margins of the images (this function was not available in the version of AIS software used). So instead the slides were scanned using a commercially available scanner by Hewlett Packard (PrecisionScan Pro). Each slide was scanned using a resize function of 600%, thus ensuring optimal detail of the image obtained. However, it should be noted at this point that the analyses being performed were only to allow calculation of the circumference, maximum/minimum diameters, area etc and thus the image did not require to be of great cellular definition. The scanned images were stored and uploaded as .jpg (joint photographic experts group) files.

AIS Morphometric Analysis

For these morphometric assessments a commercially available computer software program, Analytical Imaging Station (Version 3.0, Revision 1.1; Imaging Research Inc.) was used. This was essentially a sophisticated computer-assisted tool for obtaining quantitative data from an image. Upon opening the program, custom settings could be selected to control for colour of the imported image (full colour was chosen), and to select which measurements were to be calculated. The measurements

of basic morphometry chosen to examine were as follows; area, perimeter, feret x, feret y and form factor. The area was derived purely from the boundary (no account being taken of any artifact within the tendon substance). The perimeter was computed as the sum of distances between the midpoints of boundary vectors. Feret x and y were the maximum diameter in the given axis, x or y respectively. The overall shape of the tendon was calculated as the form factor:

$$\text{Form Factor } F = \frac{4\alpha\pi}{p^2}$$

Where: $\pi = 3.142$, α = cross-sectional area (μm^2), p = perimeter (μ)

This essentially indicated the roundness of the tendon using a range of values from 0 to 1, where 1 equated to a perfect circle. The more convoluted (and longer) the perimeter, the less circular the target and thus the value of the form factor became closer to zero. First an image was imported (as a .jpg file) into the software program and the calibration set. This was performed by measuring a known distance from the image (the markings of a ruler placed below each slide at the time of scanning) which was calculated by the program to give a reading in pixels. Thus for the scale used, 1mm equated to 47.2 pixels. Although each slide was scanned on exactly the same scale, this calibration was checked regularly. Using the software tools provided, a mouse was used to draw precisely around the outline of the tissue section on the imported image and the appropriate areas selected to prompt calculation of the desired parameters. The software program used digital image processing to extract the selected data from the image. For example to calculate the tissue 'area' the number of pixels inside the target outline borders were counted and a conversion applied according to the calibration that had previously been set. These values were calculated for each non-operated tendon as well as every repaired tendon of each allocated case. The results were then able to be reviewed as independent values as well as the more important ratio values of right divided by left, thus as previously discussed, variation within groups was minimized.

Calculation of Percent composition

The purpose of this assessment was to quantify the percentage composition of the various tissue components of all FDS tendons at their site of repair. The tissue components studied were tendon fibre (T), suture (S), vascular (V) and 'other' (O). An LW200 universal microscope (MinServ) with graticule eye piece was used. The graticule was of the indexed-grid-square type which is most commonly used for particle counting. It had a side length of 10mm and 100 subdivisions. A magnification power of x 40 was used (objective lens x4, eyepiece x10) and each slide was initially positioned with the left hand margin of the graticule grid aligned to just within the left hand margin of the tissue sample. A count of composition was then made designating one of the aforementioned categories, T, S, V &O, to each square of the grid. In this assessment the fibrotic 'other' tissue was differentiated from the 'tendon' tissue as it stained a slightly lighter shade owing to its lack of organization. It was almost exclusively found on and around the margins of the tendons at the sites of repair. Where more than one type of tissue structure was present within the square, the category allocated accounted for that occupying the major part. This same process was repeated two more times aligning the margins to the right side and also to the bottom of graticule and tissue section. The three values were then added together and averaged to obtain the mean value used for later statistical analysis. Since some of the values were 'zero', for example amount of suture in non-operated tendons, and these values were analysed as absolute values, not as ratios (see Percent composition, page 145).

EXPERIMENTAL GROUP AND CASE NAMES

At the commencement of this research project it was decided to name each case according to the surgical experimental group to which it had been randomly allocated. However in order to keep the code names short (a limiting factor of fundamental importance when using the statistical software program which had a finite number of characters per variable and case) each experimental group was simply denoted by a single letter as shown below:

A = Kessler Core

B = Kessler core and epitenon

C = Kessler Core and wrap

D = Kessler Core, epitenon and wrap

(N = Normal control group)

In order to distinguish the different time-cohorts, individual cases in the six month groups were allocated sequential numbers (1 to 12) whilst those in the six week groups were allocated sequential letters (A to N, the letter "I" was omitted owing to the risk of confusion with the numeral 1).

E.g:

A1, A2 = Kessler Core, six month cases

AA, AB = Kessler Core, six week cases

B1, B2 = Kessler core and epitenon, six month cases

BA, BB = Kessler core and epitenon, six week cases

Further to this, for ease of interpreting results of group comparisons, the six week time-cohort groups were denoted 'early', whereas the six month time-cohort groups were denoted 'late':

AEarly, BEarly... = groups assessed at six weeks after surgery

ALate, Blate... = groups assessed at six months after surgery

Early in the course of conducting this project, three additional experimental groups were proposed and permitted to be included in the project licence. These groups were added in order to enhance the amount of information that could be gained from carrying-out this research project and they were named as follows:

S = Dissection only

W = CRG wrap only

T = D group + triamcinolone

The dissection only group (S) underwent a primary surgical procedure which involved simply dissecting down to the tendon and preparing it as if for tenotomy without performing the tenotomy or proceeding further. The skin was then closed as per protocol. The CRG wrap group (W) underwent similar preparation as described above, again without tenotomy being performed, but this time a wrap of CRG was placed around the intact tendon before the skin was closed. The final group to be added were identical to group D (Kessler core and epitenon repair + CRG wrap) but they had an additional anti-adhesiogenic substance added to the wrap; triamcinolone (see Triamcinolone group, page 162). Each of these additional groups was assessed at six weeks after operation.

A full list of the 'codes' used for case and variable identification during the recording and analysis of data in this study can be found in appendix 6. An abbreviated list of the more pertinent variables may be found on the laminated pull-out sheet at the back of this volume.

STATISTICAL ANALYSIS

The method of statistical analysis used to evaluate the data acquired during this research project was based on that which was developed by the Peripheral Nerve Research Group, Department of Clinical Neurosciences, University of Edinburgh for the appraisal of models of nerve injury and their surgical repair (Fullarton, Myles, & Glasby 2002; Fullarton 1995; Fullarton et al. 2000; Fullarton & Glasby 1997; Glasby, Fullarton, & Lawson 1997).

As previously mentioned in this chapter the data acquired from each assessment were statistically appraised in two different formats. First as raw data values, for left and right sides independently, then as the more important ratio of data (right divided by left) thus minimizing within-group variation. It was feasible to perform these two methods of analysis for all data except those of the morphological percent composition of the tendons. These results could only be evaluated as absolute values since some of the values were zero (*e.g.* amount of suture material in a non-operated tendon).

Statistical analysis was carried out as detailed below and as summarized in the flowchart of the statistical algorithm (over page).

Figure 65: Flowchart for statistical analysis of data

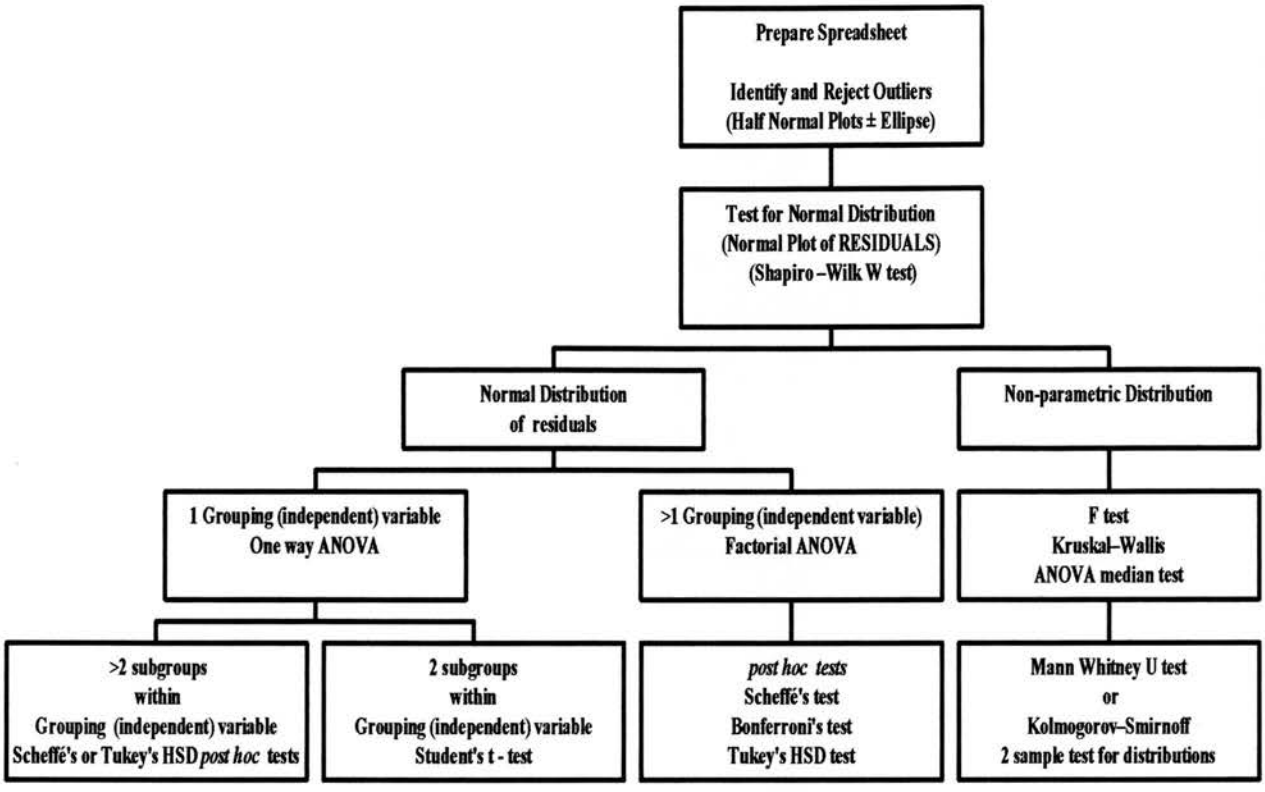

The raw data were organized into a large spreadsheet using the computer programme 'Microsoft Excel'. The far left-hand column contained a list of identification numbers of the individual experimental subjects. In a column immediately to the right of this the independent variable 'Experiment' was placed as a list in which the surgical subgroups, *i.e.* different surgical procedures, were designated. In subsequent columns to the right, each dependent variable was recorded. Once the Excel spreadsheet was complete, containing all of the morphological and physiological results, it was imported into the statistics computer programme 'Statistica' (version 6.0' — Statsoft Inc, 2300 East 14th Street, Tulsa, O.K. 71404, U.S.A.). This programme offered an extensive range of statistical analyses and graph-plotting options.

Outliers

The data were then reviewed so that outlying data-points could be identified and rejected. This was accomplished by plotting *'half-normal' probability plots* in which the selected variable was plotted in a scatter plot against the values 'expected from the normal distribution with the same mean and variance' for each column of data.

Figure 66: Half-normal probability plot

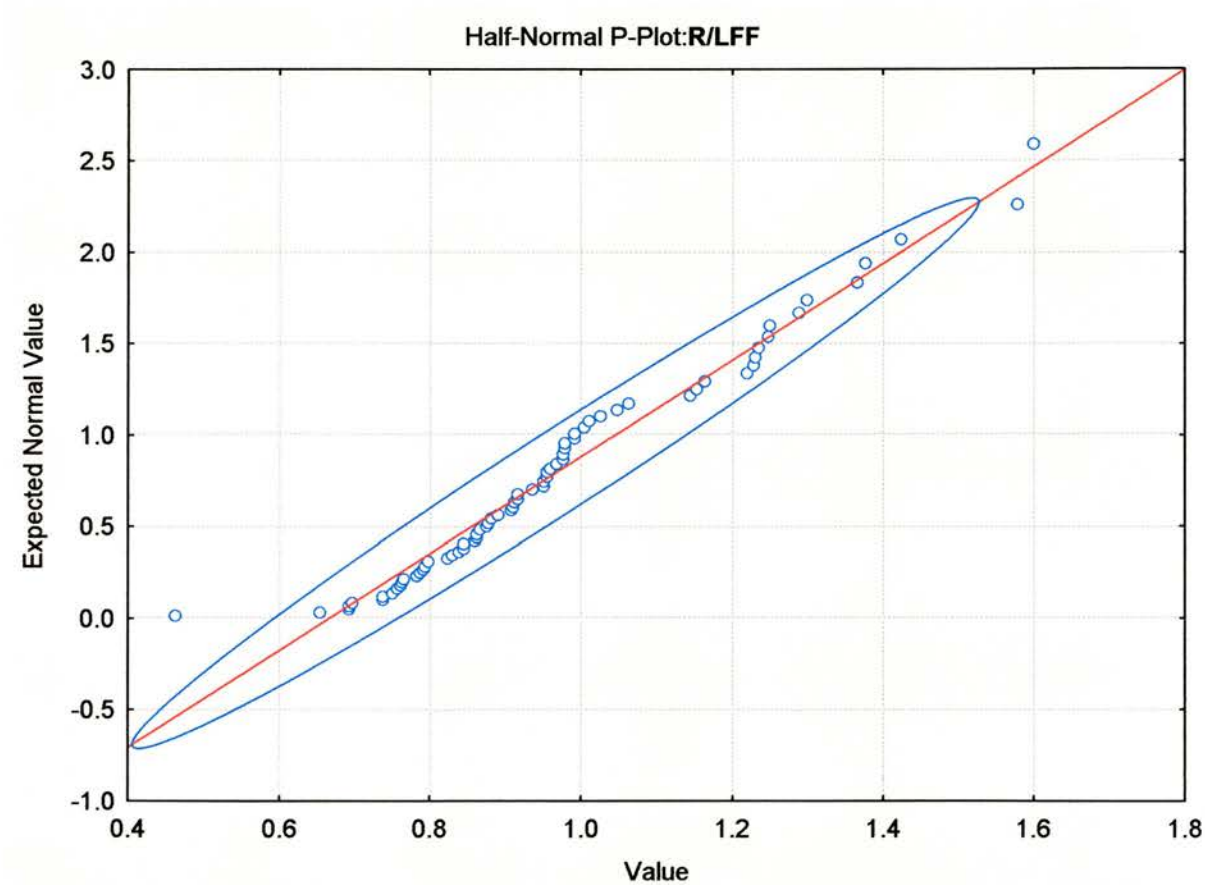

The *half-normal probability plots* were constructed in the same way as the standard *normal probability plot* (see below), except that only the positive half of the normal curve was considered. Consequently, only positive normal values were plotted on the *Y-axis*. An ellipse was then drawn on each plot to represent the 95% confidence intervals for the distribution. The points lying outside this ellipse were considered to be outliers and were rejected from the study.

After this process, the resulting spreadsheet was saved and termed 'weeded data'. This became the fundamental spreadsheet upon which all the statistical analyses of results were based.

Residuals

Residuals may be defined as the deviations of the observed values of the dependent variable from the predicted values, given the current model (Statistica electronic manual: www.statsoft.com). A residual must be differentiated from a statistical error with which it is commonly confused. A measurement error (misnomer) is the amount by which an observation differs from the expected value based on the whole population from which the statistical unit was randomly chosen. The expected value is the average for the entire population and is thus typically unobservable. On the other hand a residual is an observable *estimate* of the unobservable error. To calculate a residual the *sample* average is used to estimate the population average.

Having rejected the outliers from the spreadsheet, each of the columns of data was used to determine the residuals of that variable and the residuals were then re-plotted as *normal probability plots*. This was performed in order to determine whether or not the data fitted a *normal distribution*. It was better to use residuals rather than the data themselves as occasionally the distribution of a set of data points is not normal when the distribution of residuals is and it is this that matters. With this approach the need to use the less sensitive non-parametric tests was minimized.

Figure 67: Graph of data points for variable VmR/L

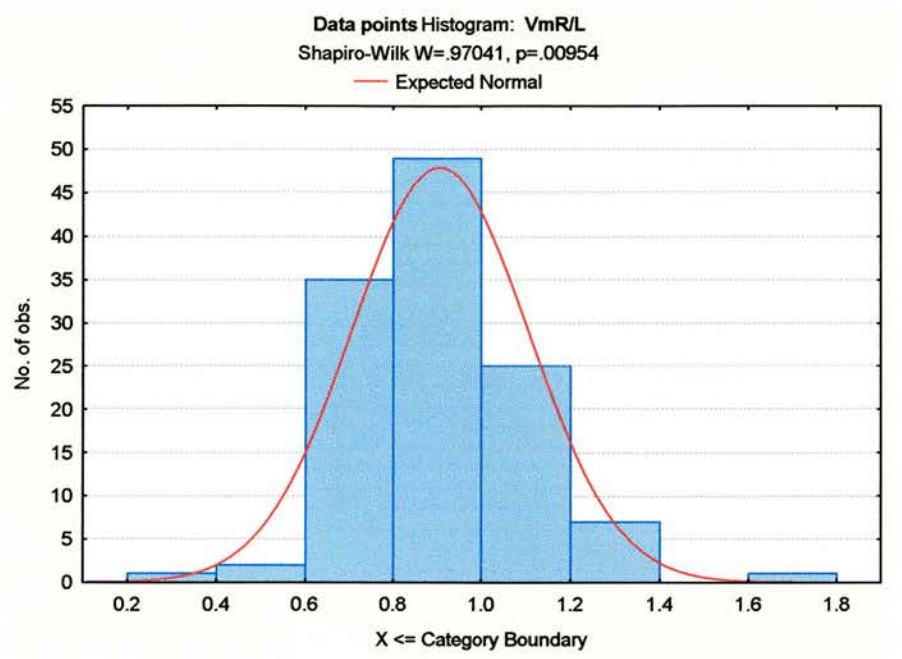

Plot of the data values obtained for the above variable, showing a significant p value – non-parametric distribution of data

Figure 68: Graph of residuals for variable VmR/L

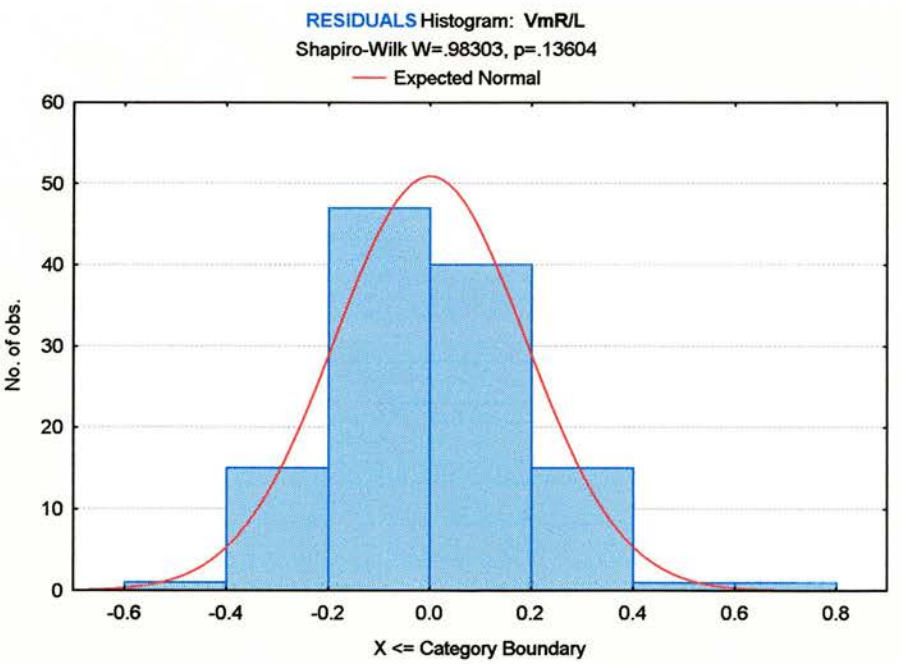

Plot of the residuals obtained for the same variable above, showing a normal distribution of data

The standard *normal probability plot* was constructed as follows. First, the residual values for each variable were rank ordered. From these ranks, *Z values* (i.e., standardized values of the normal distribution) were computed based on the assumption that the data came from a normal distribution. These *Z values* were plotted on the y-axis in the plot. If the residual values of the variable under consideration (plotted on the x-axis) were normally distributed, then all values would fall onto a straight line in the plot. If the values were not normally distributed, they would deviate from the line.

Figure 69: Normal probability plot

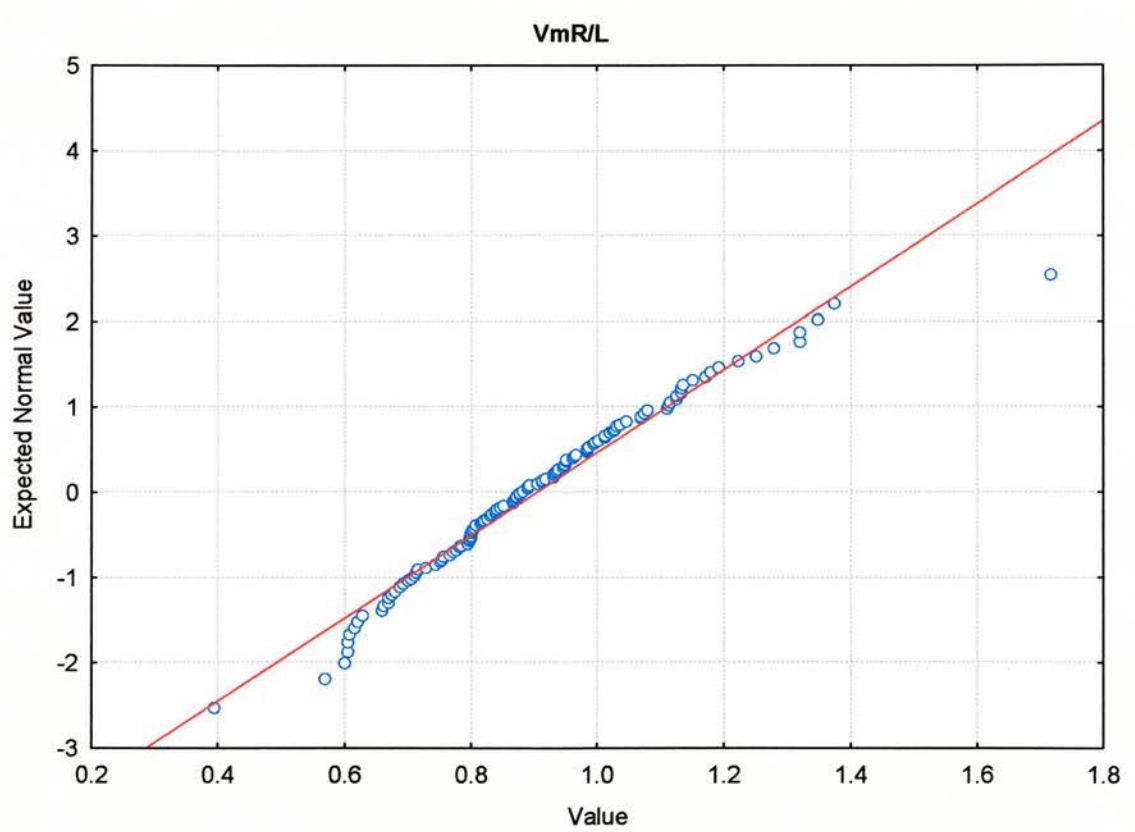

The blue circles represent the residual values for the variable VmR/L. The red line represents the expected normal value for data obtained from a population with normal distribution. The blue 'line' created by the circles is essentially straight and thus these residual values are likely to have a normal distribution; the fit of the curve is tested below.

The fit of the computed line to the scatter of the raw data was tested by the programme using the *Shapiro–Wilk W test.*

Figure 70: Graph of Shapiro-wilk W test for variable VmR/L

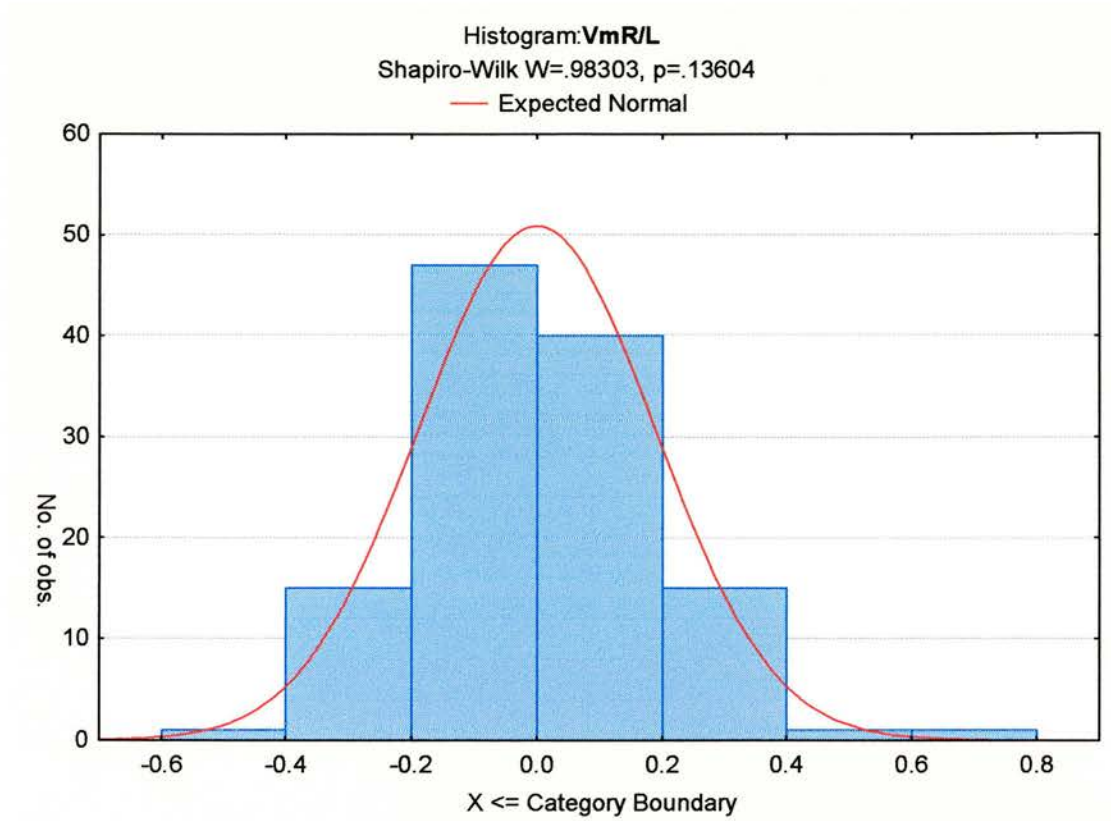

The Shapiro-Wilk W test for this variable, VmR, showed the residual values of the observed data to have came from the same population as the computer generated 'expected' values, and thus be normally distributed; $p>0.05$

If the *W statistic,* so produced was significant, then the hypothesis that the respective distribution was normal had to be rejected. The *Shapiro-Wilk W test* was the preferred test of normality because of its good power properties as compared to a wide range of alternative tests (Shapiro, Wilk, & Chen, 1968). At this point the columns of dependent variable data in the spreadsheet that were not normally distributed were converted to a red fount for easy identification.

Identifying differences

The next two stages in statistical testing were directed at identifying the presence of differences (variants of the *F test* or non-parametric equivalent) and identifying where those differences lay (variants of *Student's t test* or non-parametric equivalent). Different algorithms had to be adopted for normally and non-parametrically distributed data.

Parametric data

For normally distributed data, the *F test* was applied in the form of *one way* ANOVA. The independent variable with its subgroups was the 'grouping' or 'factor' in the ANOVA calculation and the dependent variables were the columns of weeded data. From the ANOVA, 'p' values for statistical differences were identified.

Table 2: Analysis of variance

	Analysis of Variance (Tendon Results - ratios on small groups) Marked effects are significant at p < .05000							
Variable	SS Effect	df Effect	MS Effect	SS Error	df Error	MS Error	F	p
R/LF	3.459913	7	0.494273	7.739856	58	0.133446	3.703926	0.002241

In order to find where differences lay it was necessary to perform *post hoc* tests which compared the means of the independent groups of data. The theoretical basis for this was *Student's t test* which compared the means of two independent samples. This test asked the question: 'What is the probability that the two samples (represented by their means) were drawn from the same population?'. Rather than actively testing for 'significant differences' it tests for probability of likeness. ANOVA therefore computed the probability that the independent samples came from the same population, disclosing multiple differences where present. If repeated t tests were to be performed on a single cohort of data, there would be an increased likelihood of Type I error in the analysis. Type I error is the acquisition of 'false positives'. Thus when there were

more than 2 subgroups within the independent variable, the more conservative *Scheffé test* was used. This was a variant of the *t test* specifically designed for use in order to reduce the probability of type 1 error in the situation of analysis of variance where multiple groups were being considered.

Table 3: Scheffé test - Analysis of variance for multiple groups

	Scheffe Test; Variable: R/LF Marked differences are significant at p < 0.05											
EXP	{1} M=.98782	{2} M=1.1590	{3} M=1.1252	{4} M=.26902	{5} M=1.2193	{6} M=1.1583	{7} M=1.1578	{8} M=1.0379	{9} M=.33733	{10} M=.34429	{11} M=.40359	{12} M=.31721
N {1}		0.954104	0.991758	0.000002	0.778399	0.980741	0.981165	1.000000	0.000006	0.000008	0.000074	0.000003
S {2}	0.954104		1.000000	0.000000	0.999998	1.000000	1.000000	0.997237	0.000000	0.000000	0.000000	0.000000
W {3}	0.991758	1.000000		0.000000	0.999837	1.000000	1.000000	0.999875	0.000000	0.000000	0.000000	0.000000
T {4}	0.000002	0.000000	0.000000		0.000000	0.000000	0.000000	0.000000	0.999994	0.999983	0.995403	1.000000
ALate {5}	0.778399	0.999998	0.999837	0.000000		0.999999	0.999999	0.950532	0.000000	0.000000	0.000000	0.000000
BLate {6}	0.980741	1.000000	1.000000	0.000000	0.999999		1.000000	0.999056	0.000000	0.000000	0.000002	0.000000
CLate {7}	0.981165	1.000000	1.000000	0.000000	0.999999	1.000000		0.999090	0.000000	0.000000	0.000002	0.000000
DLate {8}	1.000000	0.997237	0.999875	0.000000	0.950532	0.999056	0.999090		0.000001	0.000001	0.000011	0.000000
AEarly {9}	0.000006	0.000000	0.000000	0.999994	0.000000	0.000000	0.000000	0.000001		1.000000	0.999992	1.000000
BEarly {10}	0.000008	0.000000	0.000000	0.999983	0.000000	0.000000	0.000000	0.000001	1.000000		0.999998	1.000000
CEarly {11}	0.000074	0.000000	0.000000	0.995403	0.000000	0.000002	0.000002	0.000011	0.999992	0.999998		0.999888
DEarly {12}	0.000003	0.000000	0.000000	1.000000	0.000000	0.000000	0.000000	0.000000	1.000000	1.000000	0.999888	

Table showing results of Scheffé test for the ratio of data for the variable of Force. The subgroups from the same distribution are shown in black whilst those with significantly different distributions are shown in red.

Non-parametric data

For data which were not parametrically (normally) distributed, statistical analysis based upon the ranking of data had to be used. There is a variety of tests equivalent to the more sensitive parametric tests used above but for this study the *Kruskal-Wallis test* was chosen. This is a non-parametric alternative to one-way (between-groups) ANOVA. It was used to compare two or more samples, and tested the null hypothesis that the different samples in the comparison were drawn from the same distribution or from distributions with the same median. Thus, the interpretation of the *Kruskal-Wallis test* was similar to that of the parametric one-way ANOVA, except that it was based on ranks rather than means.

Table 4: Kruskal-Wallis AVOVA by ranks

Depend.: tDmR/L	Code	Valid N	Sum of Ranks
N	101	12	391.0
S	102	11	441.0
W	103	12	675.0
T	112	10	565.5
ALate	113	11	819.0
BLate	114	10	721.5
CLate	115	10	782.5
DLate	116	12	776.0
AEarly	117	6	542.5
BEarly	119	6	368.0
CEarly	120	12	765.5
DEarly	121	12	902.5

Kruskal-Wallis ANOVA by ranks; tDmR/L

Independent grouping variable = experiment

Kruskal-Wallis test H (11, N=124) =22.27731, p=.0223

The results of Kruskal-Wallis test for the ratio of data for variable tDm (time to maximum displacement) revealed that there were differences in distribution between subgroups ($p<0.05$).

For testing where the differences lay the *Mann-Whitney U test* was used. This test assumed that the variable under consideration had been measured on at least an ordinal (rank order) scale. The interpretation of the test was essentially identical to the interpretation of the result of a t-test for independent samples, except that the *U test* was computed from rank sums rather than means. The *U test* is the most powerful (or sensitive) nonparametric alternative to the t-test for independent samples; in some instances it may offer even greater power to reject the null hypothesis than the t-test. Therefore each variable shown by the *Kruskal-Wallis test* to have $p<0.05$ was examined in detail by the *Mann-Whitney U test*; each experimental subgroup was tested independently against all other subgroups within that variable, in order to identify where differences lay.

Table 5: Mann-Whitney U test

variable	Mann-Whitney U Test (Tendon Results - ratios) By variable EXP Marked tests are significant at p <.05000									
	Rank Sum N	Rank Sum S	U	Z	p-level	Z adjusted	p-level	Valid N N	Valid N S	2*1sided exact p
R/LF1	111.0000	189.0000	33.00000	-2.25167	0.024344	-2.25167	0.024344	12	12	0.024184
tDmR/L	135.0000	141.0000	57.00000	-0.55391	0.579640	-0.55391	0.579640	12	11	0.607524

Table of results of Mann-Whitney U test, showing results of comparison of the normal subgroup (N) with the dissection only subgroup (S). Variable R/LF1 has a p value in red ($p<0.05$) and therefore this test has revealed significant differences in distribution between these two subgroups, N & S.

STATISTICAL POWER

The power of a statistical test is an extremely important concept and is defined as: 'The probability of rejecting a false statistical null hypothesis'. Calculation of statistical power is of fundamental importance both in pre-determining the size of samples before undertaking any experiments (see Group size page 50) and at the end of analyzing results, in assessing the sensitivity of the analyses that were used. Failing to reject a false null hypothesis (false negative) is referred to as Type II error and the probability of detecting such an error is defined as:

$$p\ (\text{Type II}) = \beta$$

Hence the power of a test may be expressed as $1-\beta$. The higher the value of the power, the less likely a risk of type II error occurring and therefore the power of a test should ideally be around 0.9.

The power calculations for this project were performed using the comprehensive '*Power Analysis*' module of the software program 'Statistica'. The calculations made for sample size have been described in full on page 50 (Group Size) whilst the power calculations for each of the analyses used for each dependent variable may be found at the end of the results section (Power Analysis, page 148).

CHAPTER 3

RESULTS

GENERAL FINDINGS

One hundred and forty-four animals were included in this project, equally distributed among 12 study groups (n=12). A total of six deaths occurred (see below), with two cases being replaced. Thus the final number of cases available for analysis at the end of the study was one hundred and forty.

Deaths

There were 6 deaths, 4.2% of cases.

Four deaths (2.8%) were unrelated to surgery, as confirmed by post-mortem examination. Two of these cases died early in the study period and were therefore able to be replaced (5th case of group ALate and 4th case of group CLate).

Two further deaths (1.4%) occurred in the triamcinolone (T) group. These deaths were related to surgery. The animals developed early wound infection, which rapidly led to wound dehiscence (both at 9 days after primary surgery, see page 162). Thus, in accordance with Home Office regulations and the project protocol, these animals were painlessly killed by lethal injection of barbiturate.

Figure 71: Wound dehiscence

Wound dehiscence at post-operative day 9 in the right forelimb of the first case from the triamcinolone group. The divided ends of the FDS tendon (arrows) protrude from the centre of the wound.

Complications

These are summarized in table 6, below.

Table 6: Complications

Group	Seroma	Infection	Dehiscence	Death	Other
AEarly	0	0	0	0	0
BEarly	0	0	0	0	0
CEarly	1	0	0	0	0
Dearly	0	0	0	0	0
ALate	1	0	0	2 (1 replaced)	1 x scrotal hernia
BLate	1	0	0	2 (1 replaced)	1 x scrotal hernia
CLate	0	0	0	0	1x Crohn's disease
DLate	1	0	0	0	0

Group	Seroma	Infection	Dehiscence	Death	Other
N	0	0	0	0	0
S	0	0	0	0	0
W	0	0	0	0	0
T	12	6	2	2	0

The most common post-operative complication observed in this research project was a wound seroma (n=16, 11.4%). In the cases undergoing tendon repair without triamcinolone, the incidence of this complication was very low (n=4, 2.9%), the seromas were small, resolved rapidly and spontaneously, and did not cause lameness in any of the cases. However this was not so for the triamcinolone (T) repair group. All cases in this group developed a wound seroma within a couple of days after surgery. Six cases (50%) then developed wound infection and in two of these cases (18%) the infection rapidly caused wound dehiscence, which required euthanasia of the affected animals. The remaining ten cases responded well to antibiotic treatment (Streptapen for one week) and daily changes of a pressure dressing.

Figure 72: wound seroma

Wound seroma at post-operative day 3 in a case from the triamcinolone group.

Figure 73: Pressure dressing

Pressure dressing as applied to the operated limb of each case in the triamcinolone group, after development of seroma.

The data acquired from each of the assessments were statistically appraised as both absolute values and, more importantly, 'ratio data' (in order to minimize within-group variation – see Statistical analysis, page 111). All results presented in this chapter are derived from analysis of the ratio data, except for the percent composition of the tendons, which were evaluated as absolute values.

BLOOD FLOW

The data resulting from this assessment of blood flow can be found in appendix 7.

All the abbreviations used for the recorded variables may be reviewed by referring to the pull-out sheet at the end of this volume.

General observations

The typical appearance of intact and operated tendons, after the skin had been incised, is shown in figures 74 - 76.

Figure 74: Intact FDS tendon prepared for the assessment of blood flow

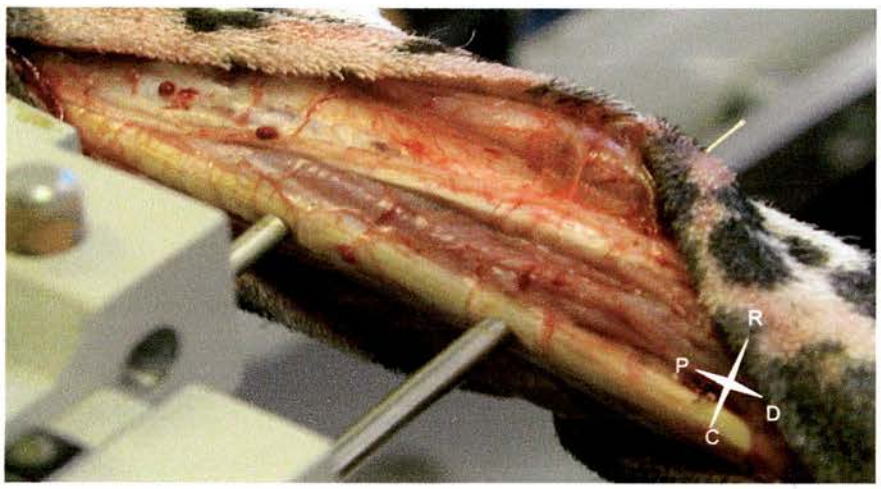

This shows a non-operated left FDS tendon during the assessment of blood flow. The surrounding connective tissue is very thin and minimal in quantity.

Figure 75: Right FDS tendon (six weeks) prepared for the assessment of blood flow

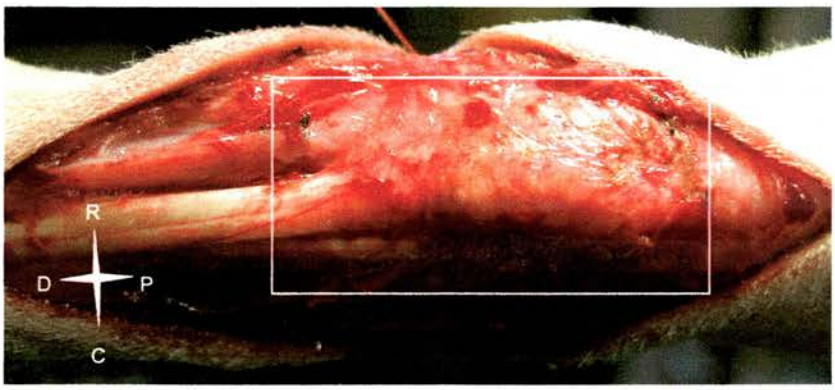

This repaired FDS tendon is from the group BEarly. The site of repair (inside rectangle) appears widened and covered with thickened connective tissue.

Figure 76: Right FDS tendon (six months) prepared for the assessment of blood flow

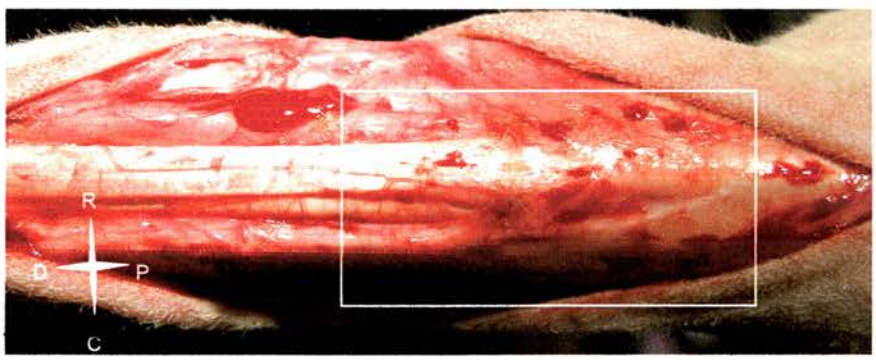

Repaired FDS tendon from the group (DLate). The site of repair (inside rectangle) appears to be covered by a thin amount of connective tissue with little evidence of any increase in superficial vascularity.

Three examples of typical flowmetry traces recorded during the assessment of blood flow are shown below.

Figure 77: RBC flux in a non-operated FDS tendon

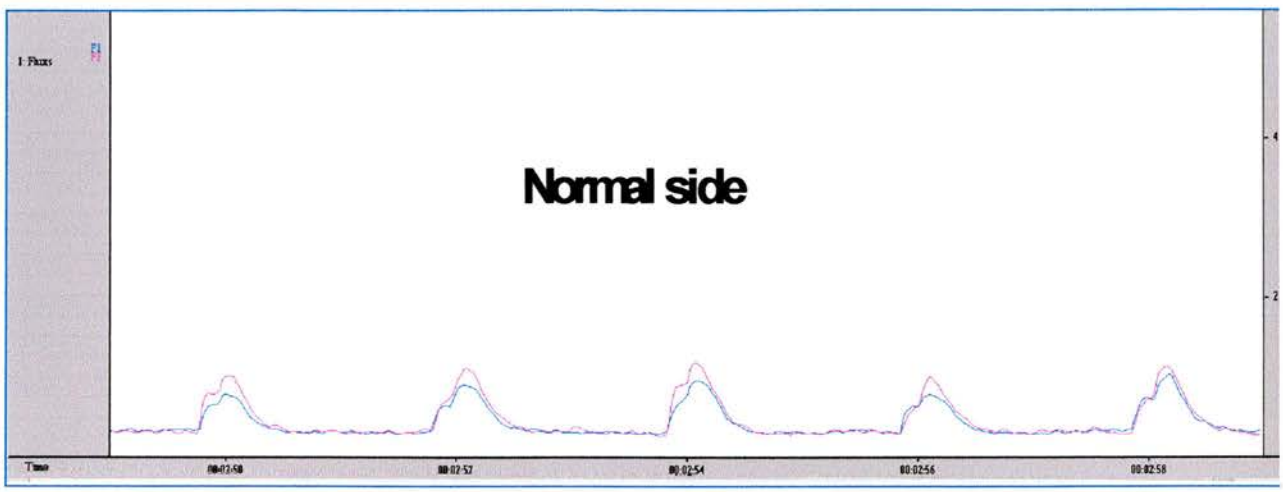

This trace shows the RBC flux obtained from a non-operated FDS tendon. The blue line represents flux from the proximal probe and the red line, the distal probe. In this case the probes record similar levels of flux.

Figure 78: RBC flux in a core only repair assessed at six weeks

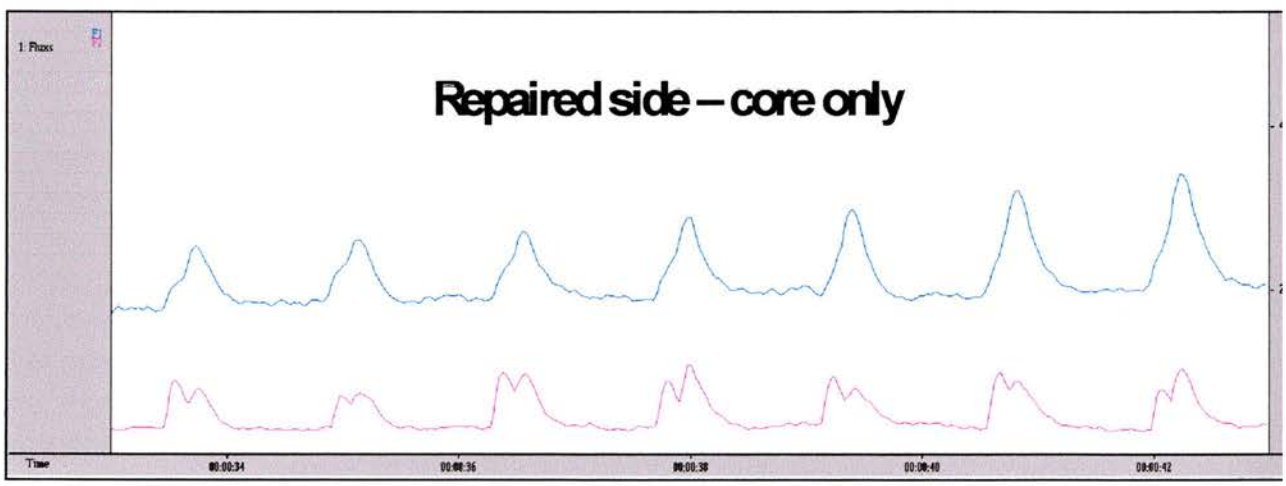

This trace shows RBC flux recorded from the repaired FDS of a case from group AEarly. The proximal probe (blue line) registers higher levels of flux than the distal probe (red line).

Figure 79: RBC flux in a repaired FDS assessed at six months

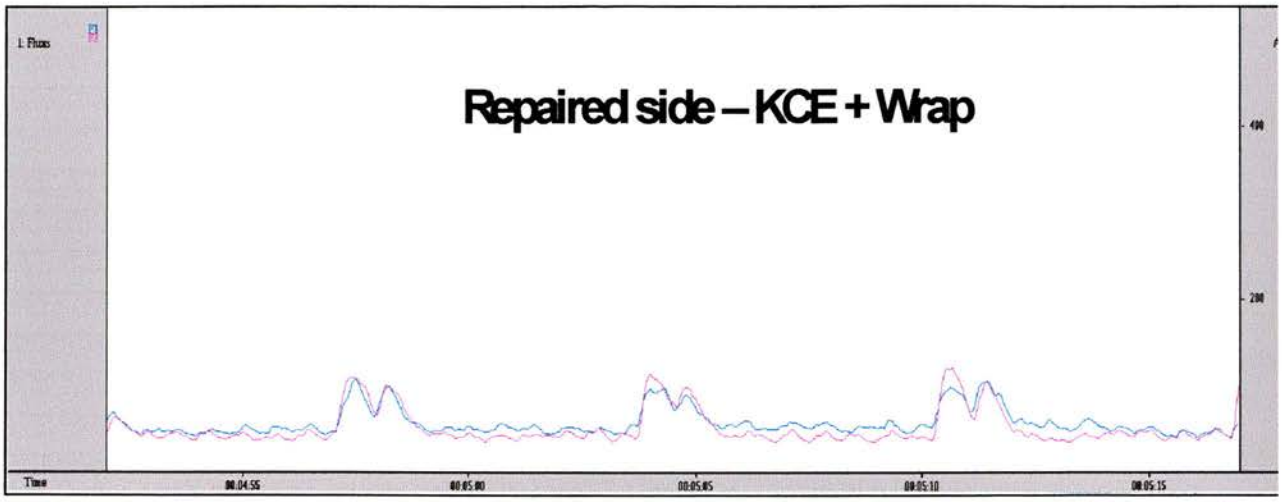

This trace shows RBC flux recorded from the repaired FDS of a case from the group DLate. Flux levels from both probes are similar.

There were significant differences between groups for two of the variables, characterizing blood flow, R/LF1 and R/LF1-F2, as detailed below.

R/LF1

This variable was the ratio of right (repaired) divided by left (non-operated) values for proximal Doppler flux.

Figure 80: Proximal doppler blood flow

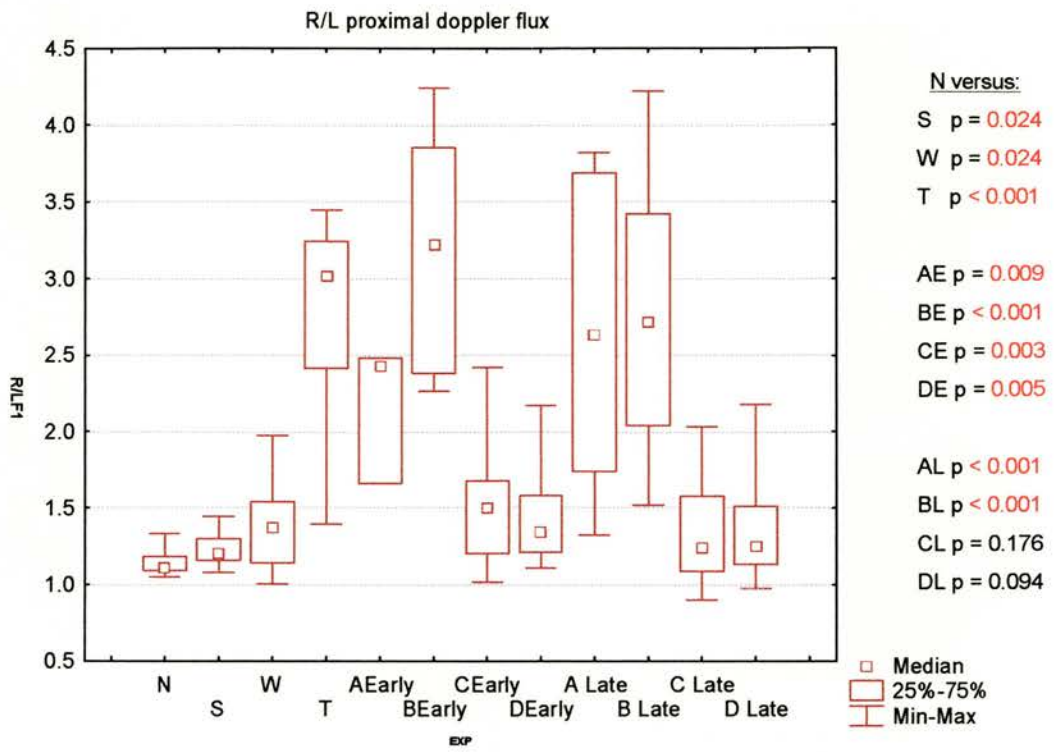

At six weeks after tendon repair proximal flux values (just proximal to the site of repair) were significantly elevated in all groups compared to the normal group. However, comparison between these groups showed that the repairs performed incorporating the CRG wrap (W, CEarly and DEarly) showed significantly less pronounced elevation of flux levels, when compared to those repairs without CRG.

At six months after repair, the two groups incorporating the CGR wrap (CLate and DLate) showed no difference in proximal flux levels when compared against the normal control group. The remaining two groups, without wrap, showed significantly elevated levels of flux compared to the normal group.

R/LF1-F2

This variable was the ratio of the difference in flux values recorded, at the site of repair (F1) and after the site of repair (F2).

Figure 81: Differential blood flow

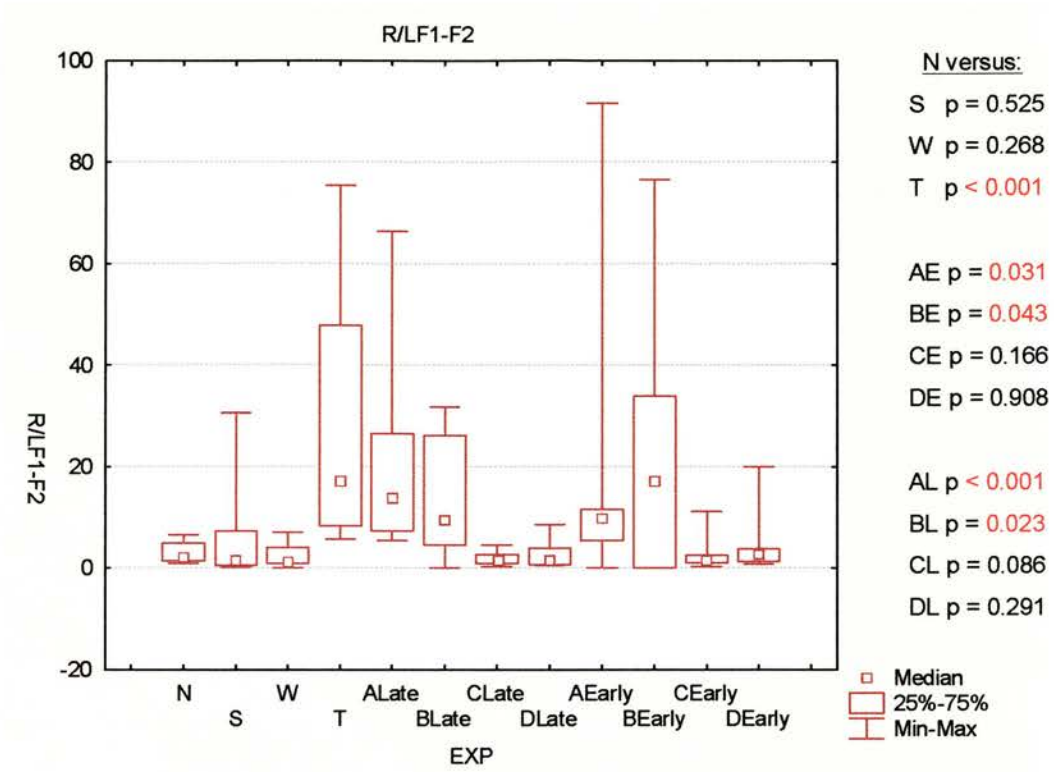

At both six weeks and six months after surgery, significantly elevated (differential) flux levels were seen for all the groups repaired without using the CRG wrap (AEarly, BEarly, ALate, BLate) and for the group with triamcinolone (T), $p<0.05$.

At both six weeks and six months after surgery, all groups that incorporated CRG wrap (CLate, DLate, CEarly, DEarly, W) and the dissection only group (S) showed no difference in differential flux levels when compared to the normal control group.

No significant differences were found for the remaining variables recorded during the assessment of blood flow.

Thus in this study, inclusion of CRG wrap at the time of tendon repair correlated with either a less pronounced elevation of flux levels or no difference at all in flux levels compared to the normal group.

IN-VIVO TENDON DYNAMICS

The data resulting from the assessments of displacement, velocity and acceleration can be found in appendix 8.

The abbreviations used for the recorded variables may be reviewed by referring to the pull-out sheet at the end of this volume.

General observations

A typical example of a graph obtained for the variable displacement is shown below. Example graphs calculated for velocity and acceleration are also shown.

Figure 82: Datafit plot of displacement

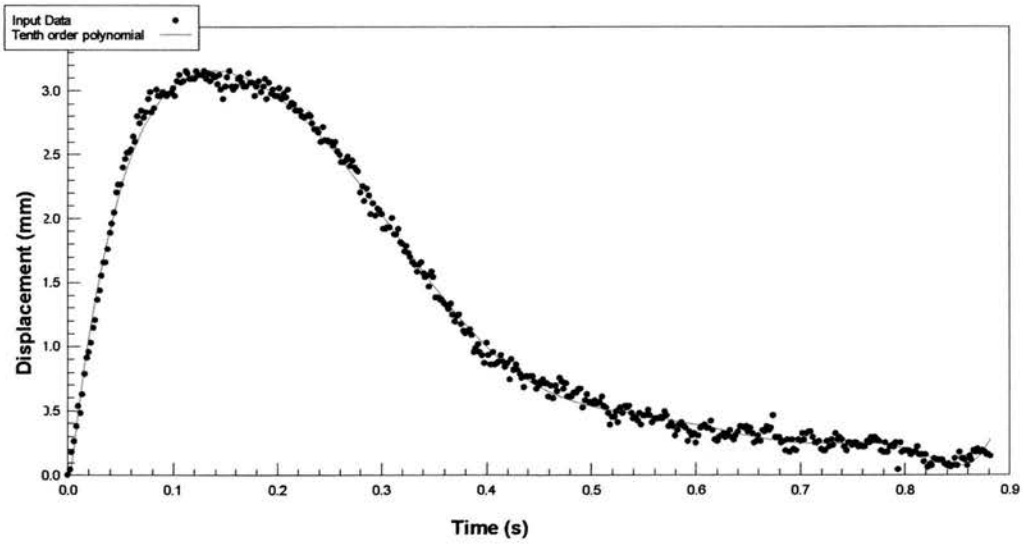

This graph shows displacement (mm) on the y-axis against time (s) on the x-axis, during FDS muscular contraction, for a non-operated tendon, group N.

Figure 83: Datafit plot of velocity

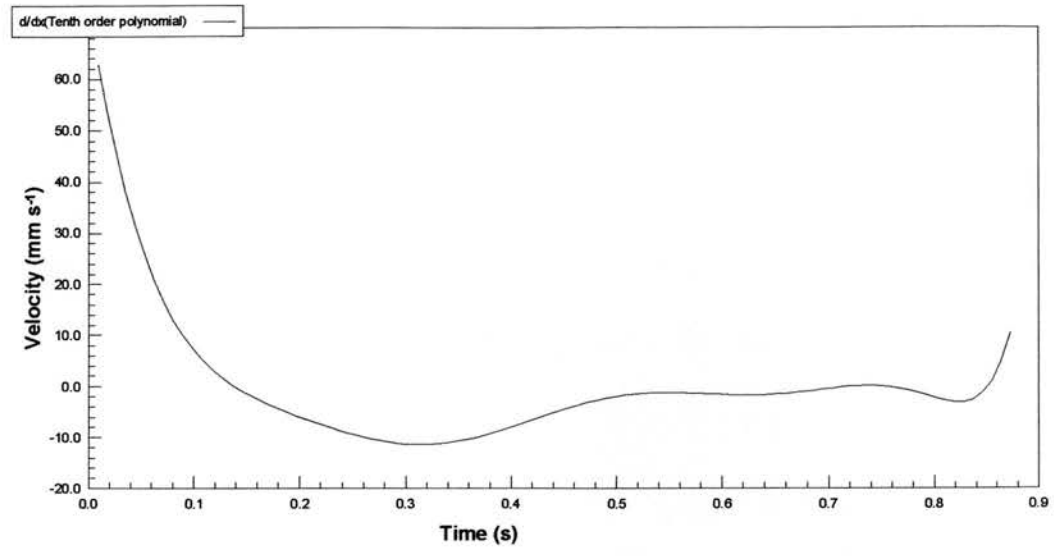

This velocity versus time curve was obtained by differentiating the values recorded for displacement in the case illustrated above.

Figure 84: Datafit plot of acceleration

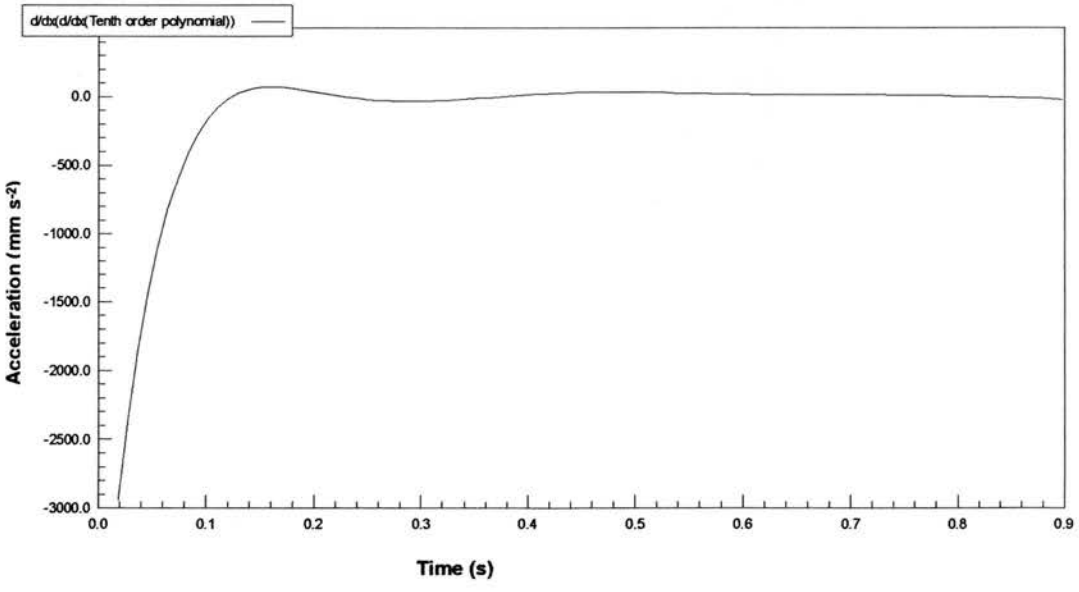

This acceleration curve was obtained by differentiating the values obtained for the velocity curve (which in turn were obtained by differentiating the data recorded from the original displacement of the FDS tendon).

Two variables characterizing the *in vivo* dynamic assessments showed significant differences between experimental groups; tDmR/L (time to maximum displacement) p=0.022 and t0AccelR/L (time to zero acceleration) p=0.017.

R/L tDm

This was the ratio of right divided by left values for the time taken by the tendons to reach maximal displacement after transcutaneous nerve stimulation.

Figure 85: Time taken to achieve maximum displacement

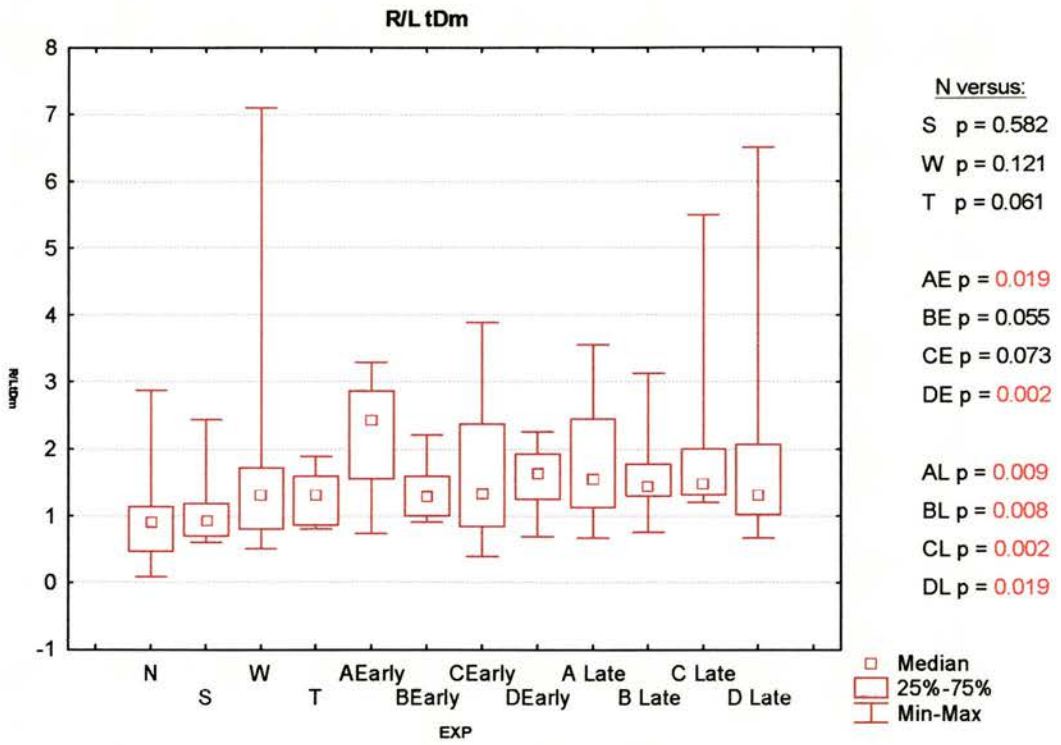

The significant differences between subgroups were as follows:

The normal control group showed a significantly shorter time to maximum displacement from all Late groups (ALate, BLate, CLate, DLate) and two of the Early groups (AEarly, DEarly).

The dissection only group (S) showed a significantly shorter time to maximum displacement from ALate p=0.042, BLate p=0.035, CLate p=0.009 and AEarly p=0.027.

No differences were seen between groups with respect to either the time of assessment, or the method of surgical repair performed.

No pattern of clinical relevance was discernable from these results.

R/L t0Accel

This variable was the time taken for the tendon to return to zero acceleration after nerve stimulation.

Figure 86: Time taken to return to zero acceleration

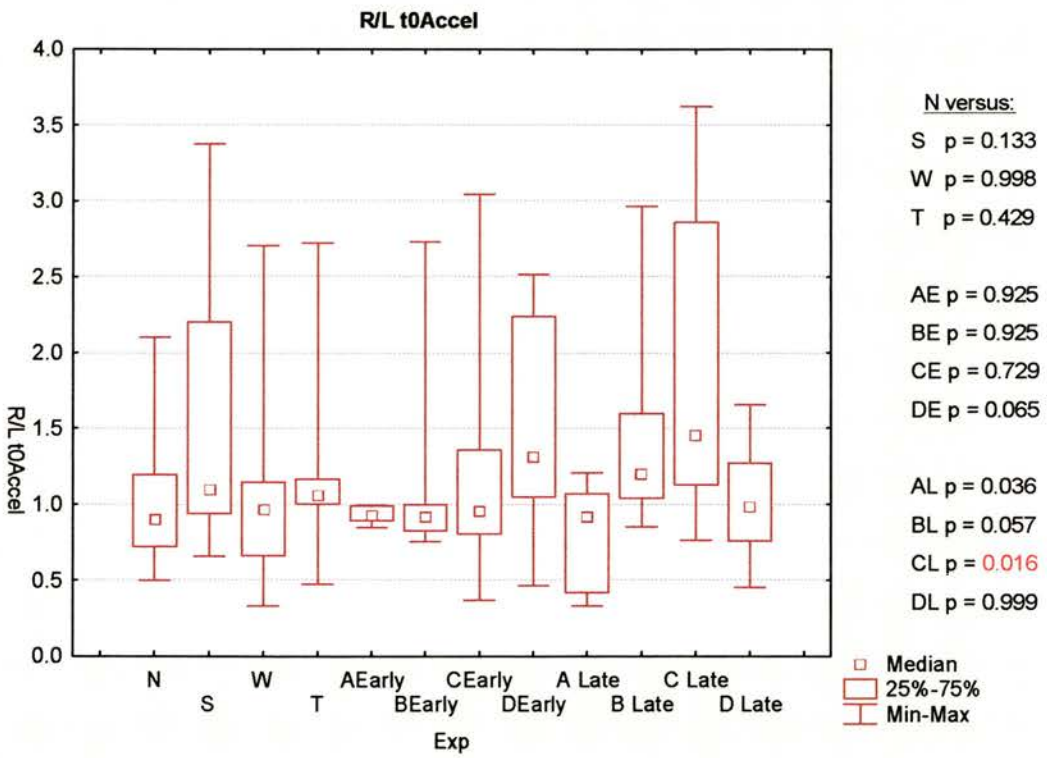

The normal control group was significantly different from only the CLate group and the dissection only group, S, from ALate (p=0.036). The wrap only group, W was different from CLate (p=0.023). ALate group was different from BLate (p=0.005), CLate (p=0.002), DEarly (p=0.007). BLate group different from AEarly (p=0.011). CLate group different from DLate (p=0.027), AEarly (p=0.012), DEarly (p=0.025).

No clear pattern of clinical interest could be established from these findings.

TENSILE STRENGTH ASSESSMENT

The data set resulting from the tensile assessments can be found in appendix 9.

The abbreviations used for the recorded variables may be reviewed by referring to the pull-out sheet at the end of this volume.

General observations

Below are photographic examples of the typical appearance of tendon rupture observed on reaching maximum tensile strength at the conclusion of the tensile test.

Figure 87: FDS tendon rupture at UTS

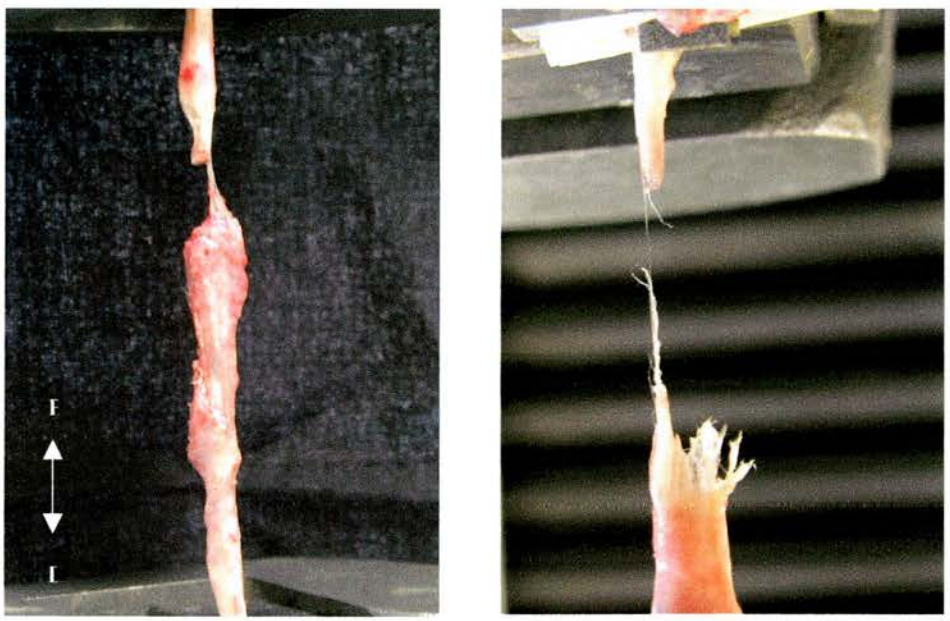

Left: Repaired FDS tendon assessed at six weeks, failure occurring at the site of repair.

Right: Repaired FDS tendon assessed at six months, rupture occurring near the proximal end of the specimen.

The six week tendon repair groups consistently failed at the site of repair when the maximal tensile strength was reached.

Figure 88: Ultimate failure of FDS tendons at their sites of repair

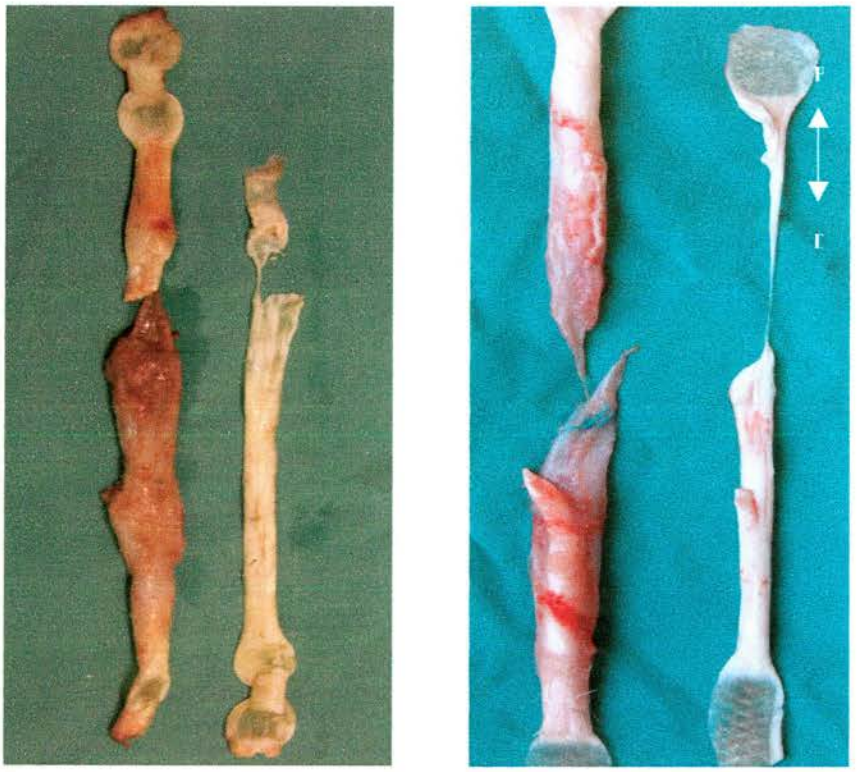

FDS tendons from two cases examined at six weeks after repair. The repaired tendons lie to the left of their respective control (non-operated left FDS tendon). Both repaired tendons failed at their site of repair on reaching ultimate tensile strength. The non-operated controls failed at the proximal end of the FDS tendon slip.

However, by six months after repair the tendons broke at the proximal end of the specimen, the single tendon slip of FDS tendon, which was the thinnest part of the repaired tendon.

Figure 89: Appearance of FDS tendons after tensile testing

A repaired FDS tendon (below) is shown with its respective non-operated control (above) after having been assessed for UTS, six months after surgical repair. Both tendons ruptured near to the proximal end of the specimens.

A typical example of the graphic output obtained during a tensile test is shown below.

Figure 90: Tensile profile

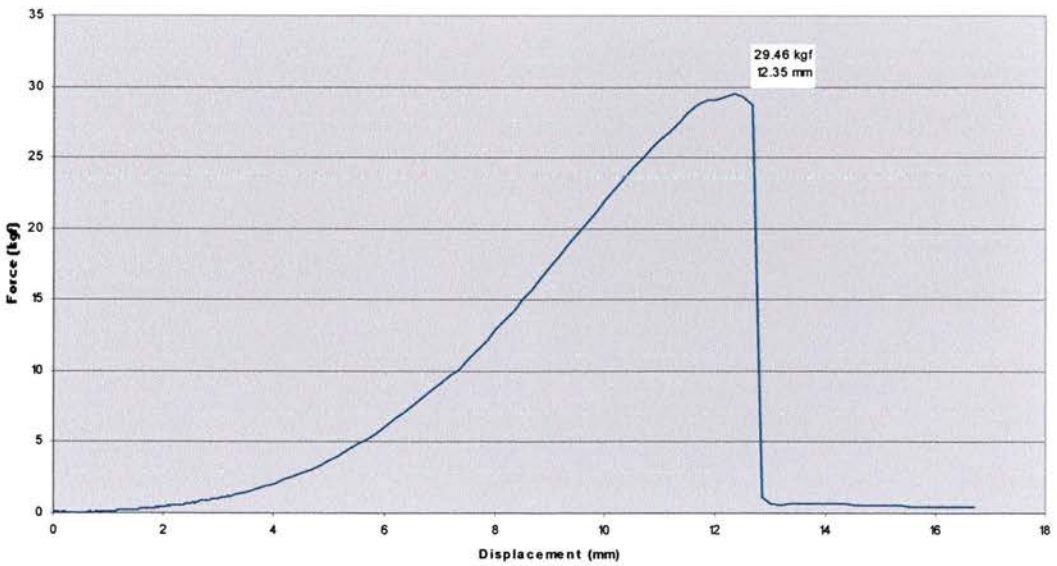

Output graph from Instron 4500, obtained at the end of the tensile test for the repaired FDS tendon from group DLate. Ultimate tensile strength reached was 29.46 kgf (288.90 N) at 12.35 mm of distraction.

There were significant differences between groups for one of the variables recorded from the tensile profile, R/LF $p<0.001$.

R/LF

This was the ratio of right divided by left breaking force values for the tendons placed in the Instron tensile testing machine.

Figure 91: Ultimate Tensile Strength (UTS)

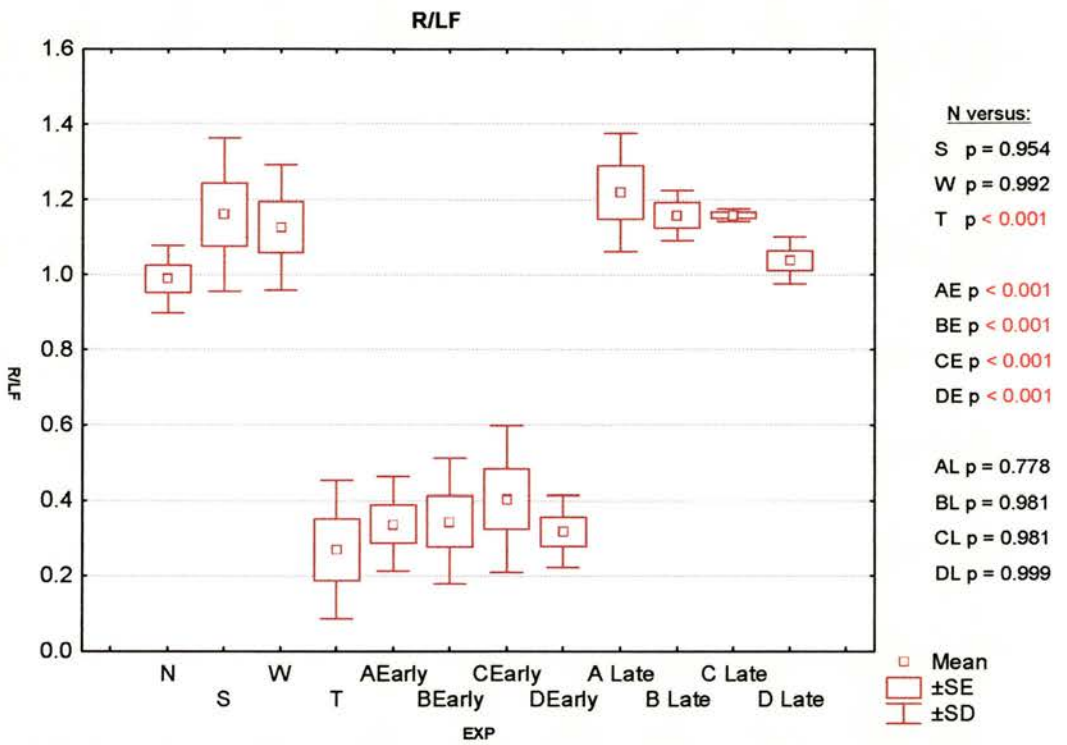

There was a significant reduction in breaking strength between the normal control group (N) and all the groups at six weeks which had been surgically divided and repaired (T, AEarly, BEarly, CEarly, Dearly) each with $p<0.001$.

No significant differences were found between the normal control group and any of the late repairs (ALate, BLate, CLate, DLate) or the dissection only (S) or wrap only groups (W).

No significant differences in breaking strength were found between the subgroups for method of repair when examined at either six weeks or six months after operation.

Thus in this study, incorporation of CRG wrap at the time of tendon repair did not interfere with the breaking strength of the healing tendons when examined at either six weeks or six months after surgery.

MORPHOLOGICAL ASSESSMENTS

The data set resulting from these assessments can be found in appendices 10 (AIS data) and 11 (percent composition data).

The abbreviations used for the recorded variables may be reviewed by referring to the pull-out sheet at the end of this volume.

AIS calculations

General observations

Two typical examples of the outcome of sectioning and staining the tendons for microscopic examination are shown below.

Figure 92: H&E stained FDS cross-section

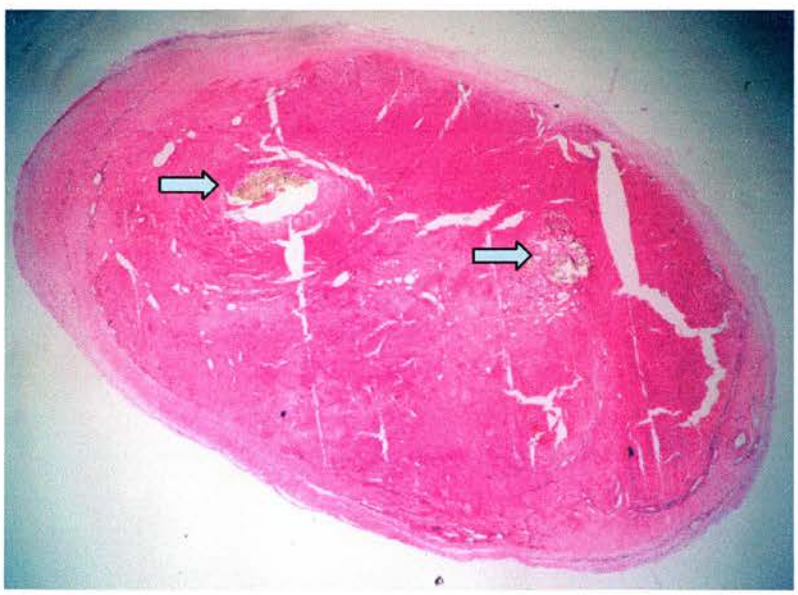

Cross-sectional view through the repair site of a tendon from the group AEarly (H&E x10). The two strands of suture material (arrows) are seen traversing the core (Kessler suture).

Figure 93: Gomori stain of repaired FDS tendon

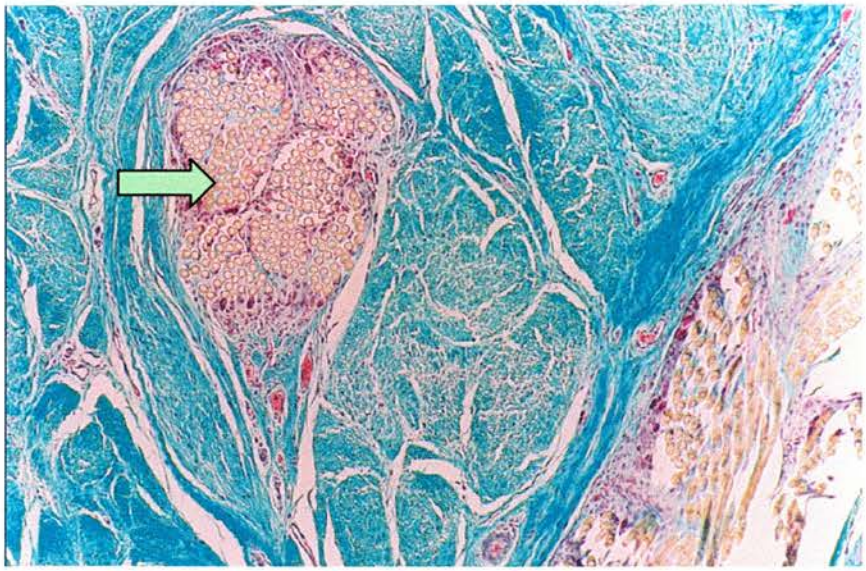

Multiple fibrous strands of core suture material (arrow) set amidst bundles of collagen fibres in a repaired FDS tendon assessed six weeks after surgery (Gomori stain x 40).

Figure 94: Gomori stained perimeter of FDS pars superficialis

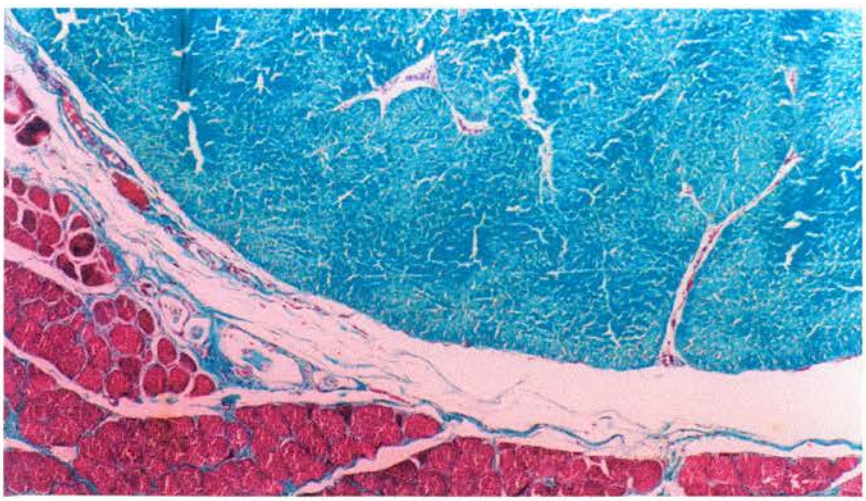

This slide demonstrates the clarity of tissue discrimination using the Gomori stain technique; the junction between the pars superficialis tendon slip (blue) and a few muscular fibres (red) joining it to the pars profunda slip underneath (x100).

Two of the variables characterising tendon morphology showed significant differences between groups and are detailed below.

R/LA

This was the right divided by left ratio values calculated for the area of the tendons examined in cross-section.

Figure 95: Cross-sectional area

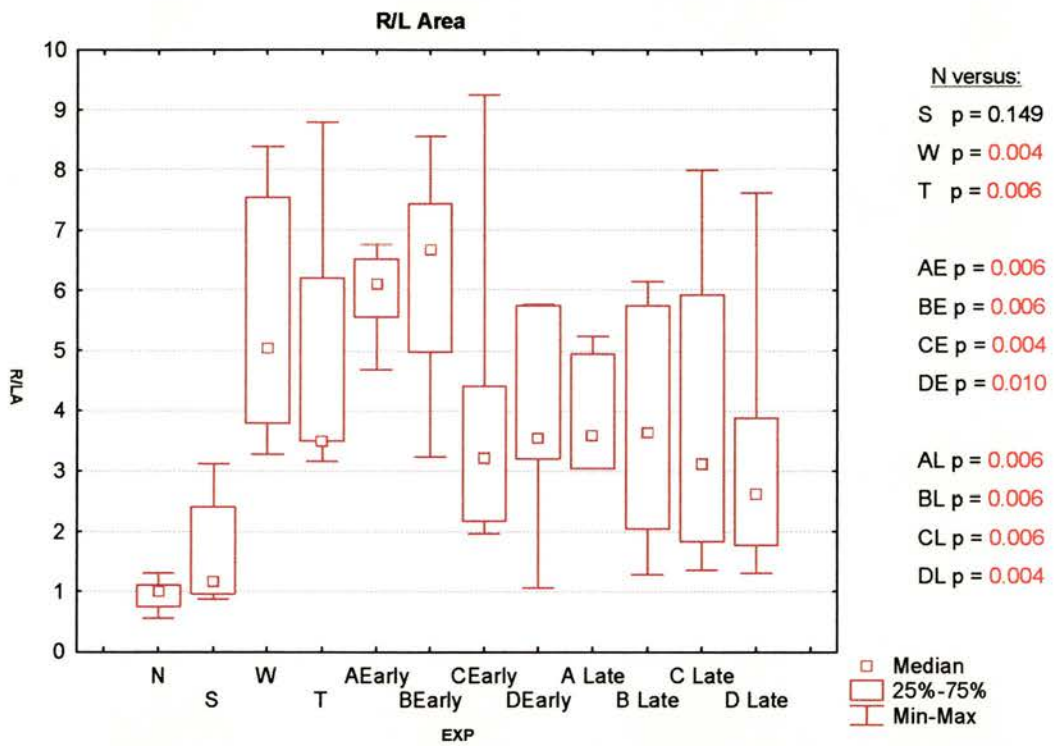

All groups, except the dissection only group S, showed a significant increase in ratio of tendon area after operation, when compared with the normal control group. Comparison between subgroups of methods of repair showed only that ALate had significantly smaller cross-sectional area than AEarly (p=0.028).

No differences were found between the different methods of operation performed, apart from the dissection only group which showed a significantly less pronounced increase in cross-sectional area than that observed from the other operative groups.

No significant differences were found with regard to the time of examination of the cases.

R/LXF

This was the right divided by left ratio values for X feret of each case examined histologically.

The X feret is defined as the maximum distance of the horizontal axis of each histological section and was calculated using the AIS software package (see AIS Morphometric Analysis, page 106).

Figure 96: maximum horizontal axis of FDS cross-section

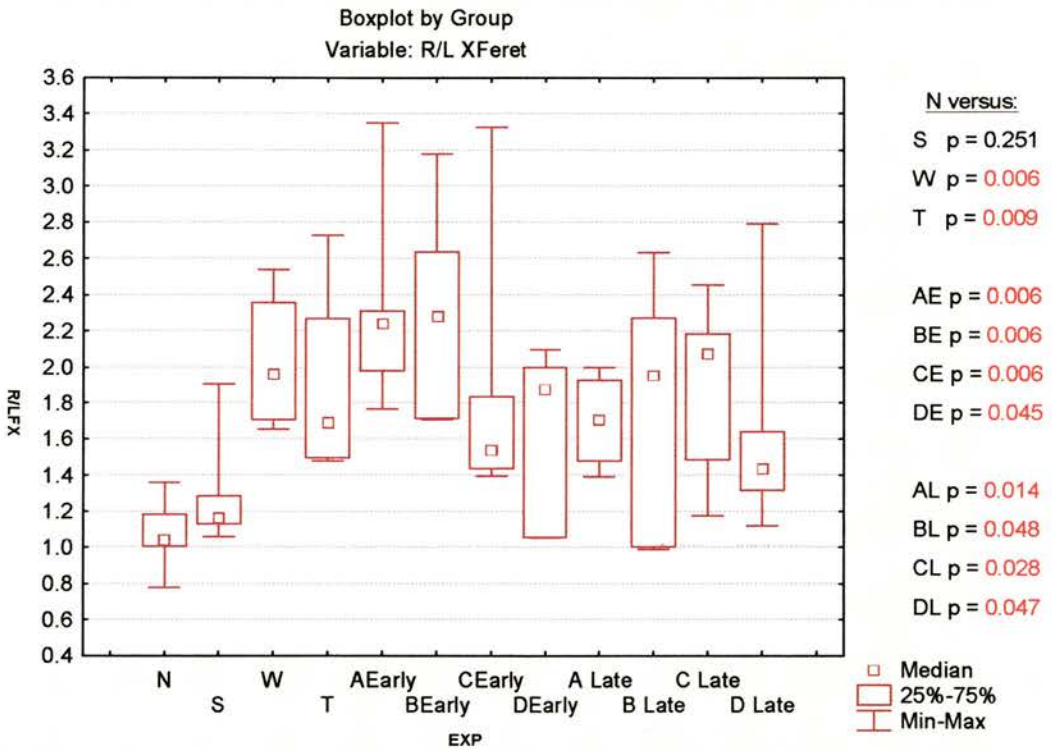

All groups, except the dissection only group (S), showed a significant increase in X-feret ratio when compared to the normal control group.

Therefore in this study, the groups which had CRG wrap added to the tendons at the time of repair, did not show any difference in 'bulk' of repair from those without the wrap.

Percent composition

Analysis of the absolute values obtained from the right tendons were considered for the variables characterizing tissue composition of the tendons (see Calculation of Percent composition, page 108). These were compared against the control group of (non-operated right) tendons.

There were significant differences between groups for two of the variables of composition, RS $p= 0.004$ and RO $p<0.001$, as detailed below.

RS

This variable was the percent composition of suture material present in the histological sections of the right tendons.

Figure 97: Suture material in FDS cross-sections

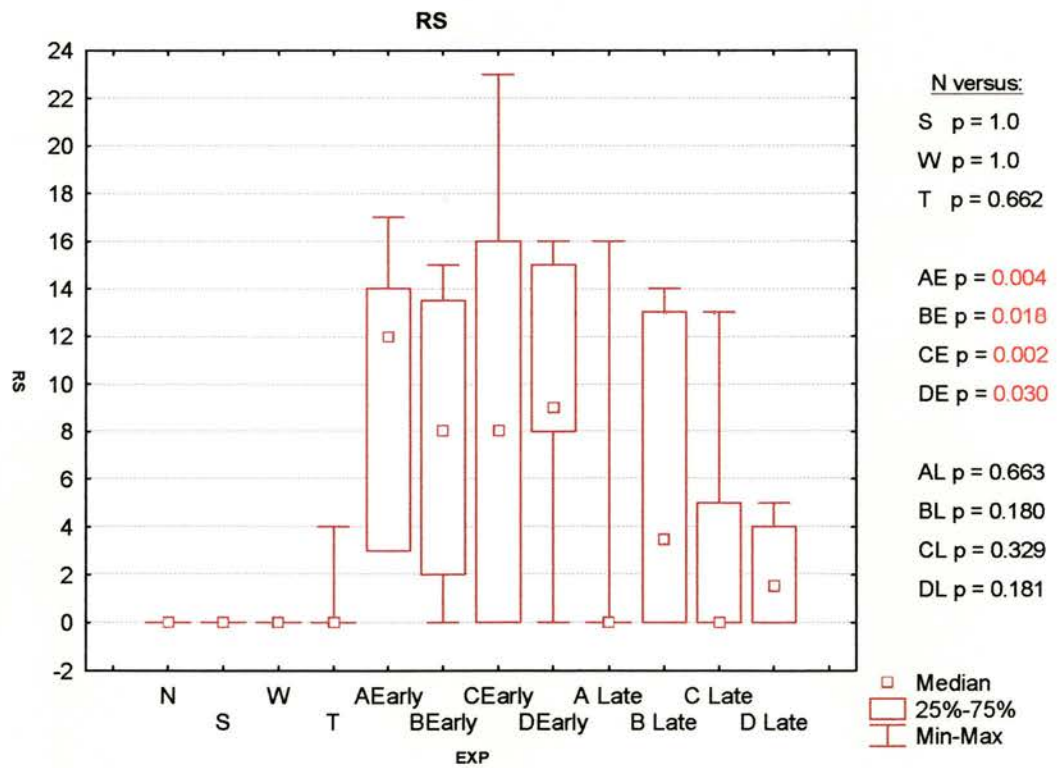

Significant differences were found between the amount of suture material present in the control group and all the early tendon repairs (AEarly, BEarly, CEarly, DEarly) but not with the late repairs.

No significant differences were found between the subgroups of method of repair at either of the time periods.

RO

This variable was the percent composition, of 'other' tissue present on morphological examination of the composition of the right tendons. This referred to the fibrous/connective tissue present at the site of repair.

Figure 98: Fibrous tissue in FDS cross-sections

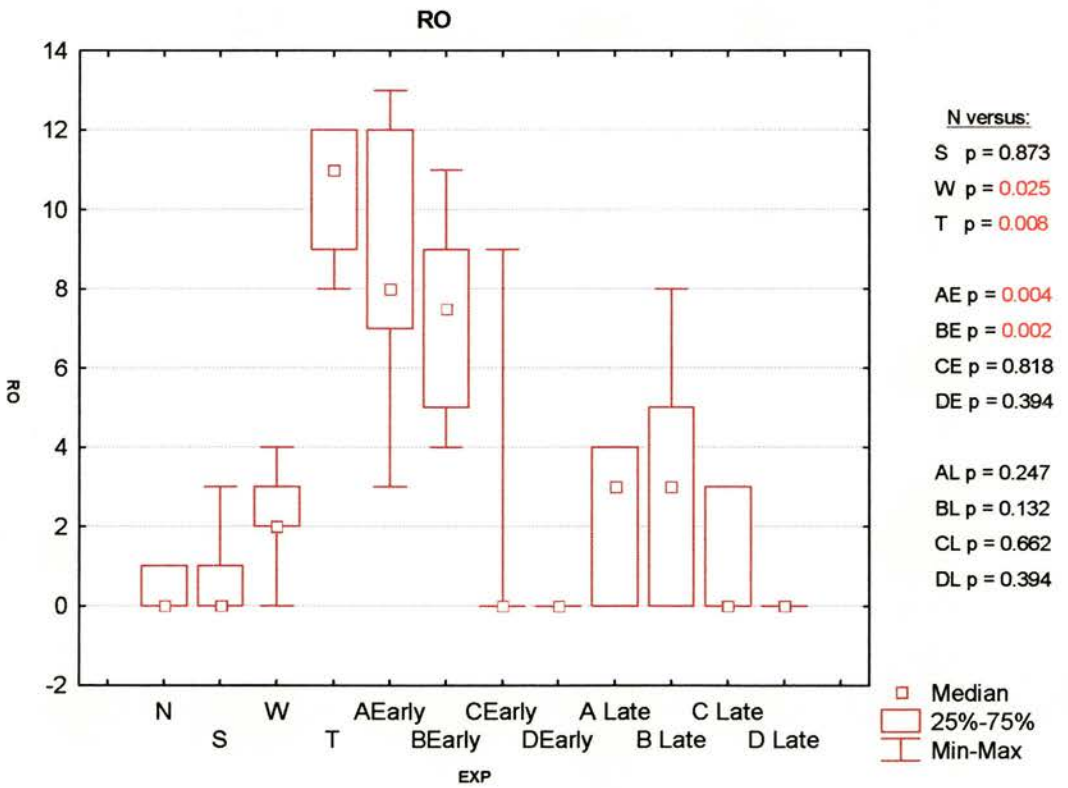

When compared to the normal group, significant increases in fibrous tissue were seen in the wrap only (W), triamcinolone (T), AEarly and BEarly groups.

At six weeks after repair comparison between groups showed that the two groups without CRG wrap in the repair process (AEarly and BEarly) and the triamcinolone group (T) had significantly increased amounts of fibrous tissue compared to the other groups.

At six months after repair comparison between groups showed the two groups of repairs without CRG (ALate and BLate) to have significantly increased amounts of fibrous tissue when compared to DLate ($p=0.036$ and $p=0.022$ respectively).

Thus in this study, incorporation of CRG wrap at the time of repairing the tendons was not found to alter significantly the amount of suture material remaining when examined at six weeks or six months after operation. However, the repairs performed with CRG wrap did result in a lesser percentage of fibrous tissue at the site of repair.

POWER ANALYSIS

Power studies were undertaken, as the final part of the analysis of results, to test the sensitivity of the analyses used for each variable and thus the 'probability of rejecting a false statistical null hypothesis' (see Group Size, page 50).

This process was performed for each dependent variable, using the 'power analysis' module of the Statistica software program.

A descriptive statistics summary was created for each dependent variable in order to obtain the values of the means for each group and the standard deviation of all groups. These values were then used to complete the power analysis calculations. The power and a graph of power against 'n' (pages 148-151), were then computed.

The results of the power analyses are summarized over the page:

Table 7: Results of power analysis

Dept. variable	Power	number per group (n)
R/LF1	**1.000**	**12**
R/LF2	0.940	12
R/LF1-2	**1.000**	**12**
DmR/L	0.527	12
tDmR/L	0.707	12
DhrR/L	0.445	12
tDhrR/L	0.619	12
tTTR/L	0.493	12
VmR/L	0.688	12
tVmR/L	0.421	12
t0AccelR/L	**0.906**	**12**
R/LF	**0.999**	**6**
R/LD	0.441	6
R/LA	**0.953**	**6**
R/LP	0.974	6
R/LL	0.948	6
R/LXF	**0.891**	**6**
R/LYF	0.848	6

Dept.variable	Power	Group N
R/LFF	0.553	6
RT	0.999	6
RV	0.999	6
RS	0.927	6
RO	0.999	6

The variables shown in red represent those for which significant differences were found between groups.

It can be seen from the table above that for every dependent variable (apart from tDmR/L) that showed significant differences between its groups, the analyses performed had very high power values. As such the probability of type II error was minimal. The variable tDmR/L had a power value of only 0.707, however despite the number of cases in this study statistically significant differences were found between groups for this variable. Thus where a statistically significant result was found, the group sizes predicted at the outset of this study have been demonstrated, retrospectively, to have been of an appropriate size to detect reasonable departures from the null hypothesis.

The power graphs for these variables are printed on the next couple of pages.

Figure 99: Power calculation graphs

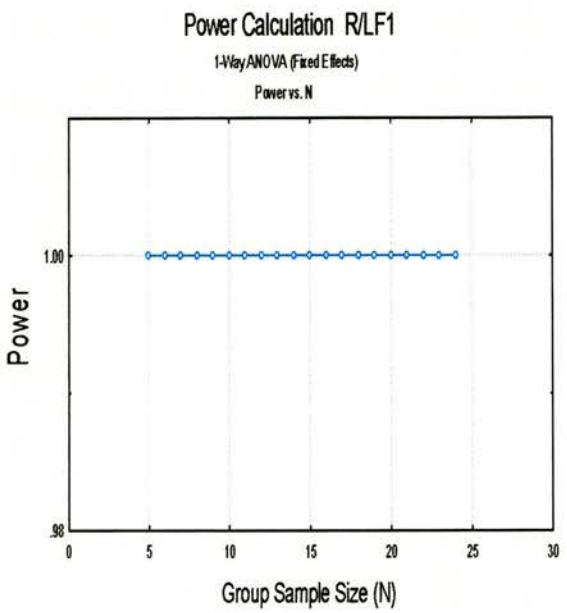

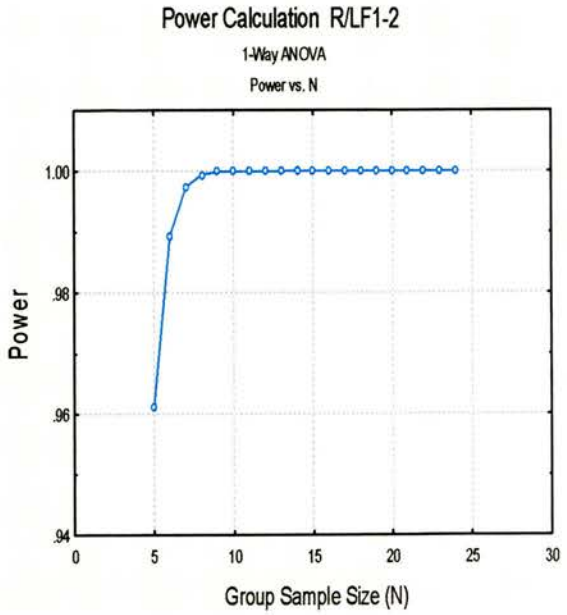

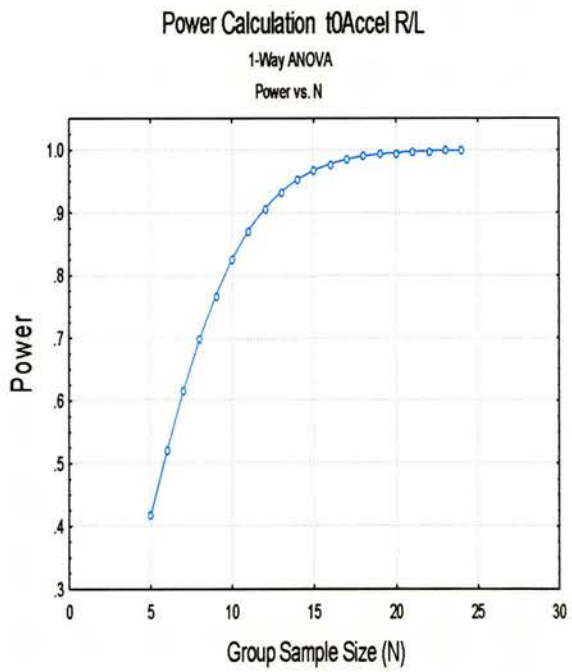

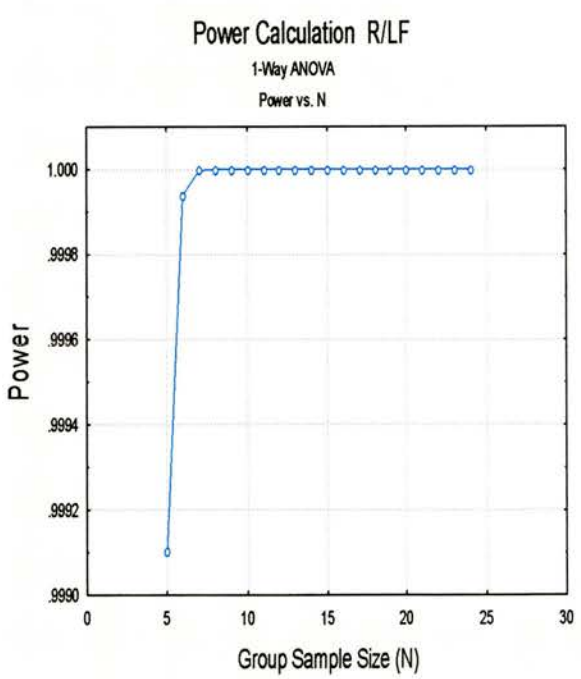

Figure 100: Power calculation graphs (continued)

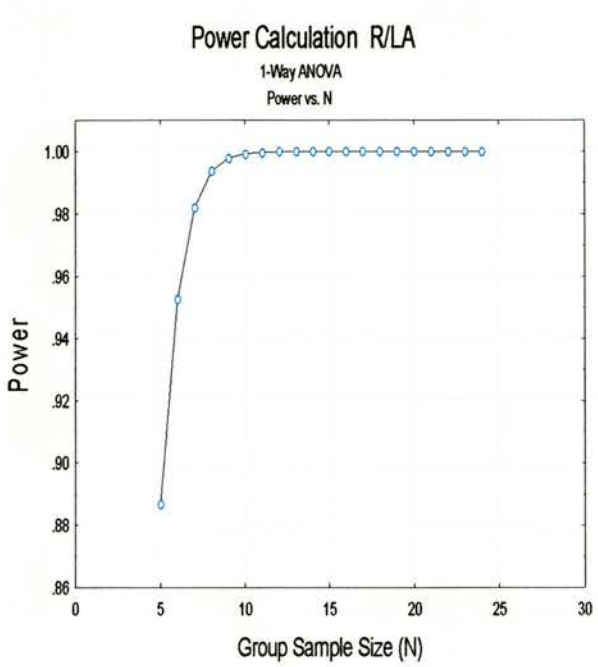

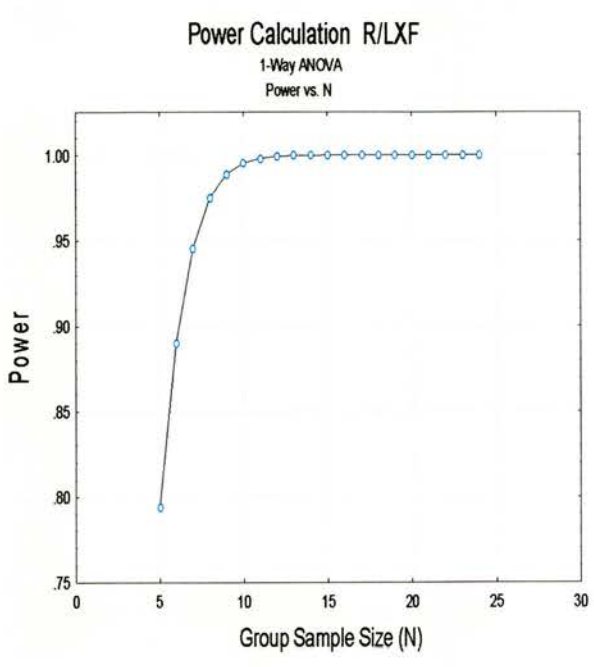

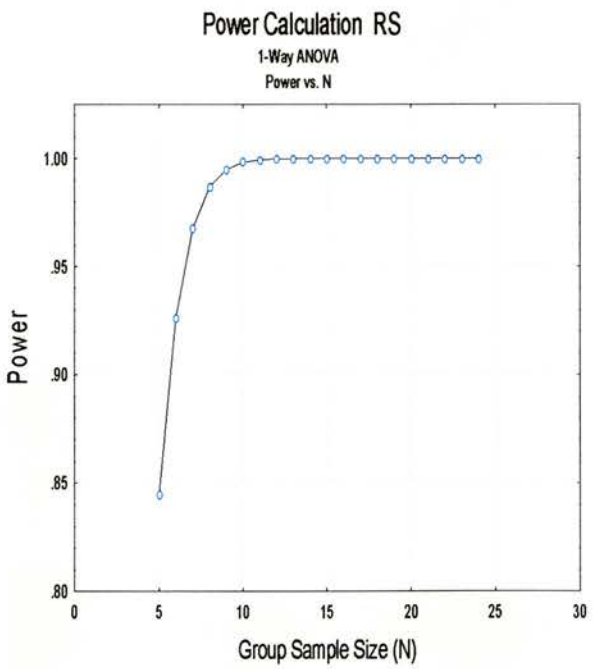

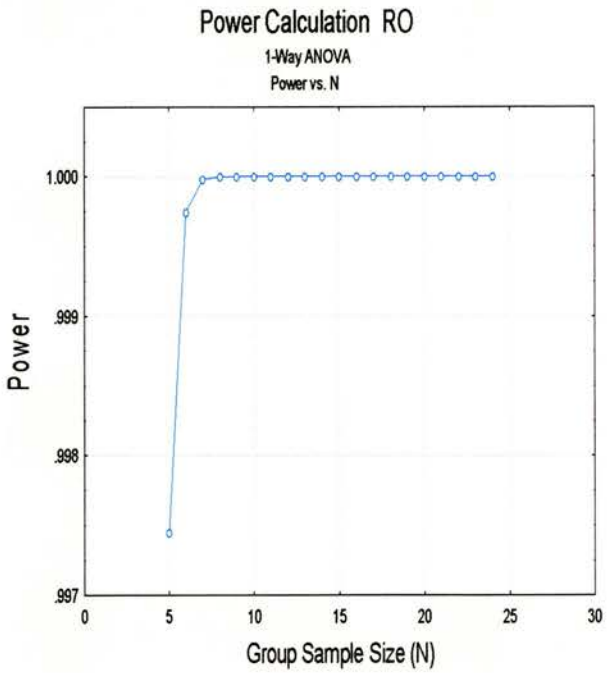

Figure 101: Power calculation graph for tDmR/L

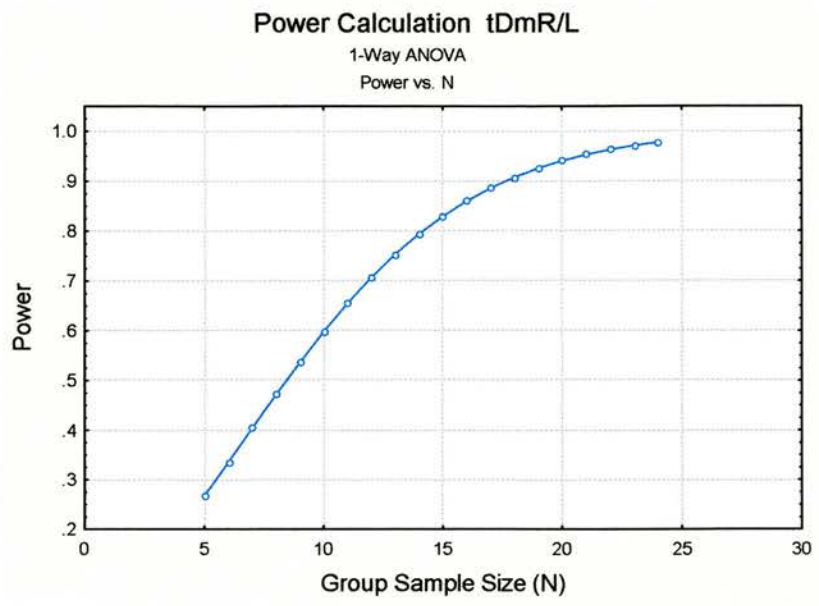

In a few instances, however, where no statistically significant result was detected the power value was observed to be low (see summary table 7, page 148). The possibility of type II error was therefore much greater. An example of this is the dependent variable DhrR/L which had a power of only 0.4453 (N=12). The power analysis graph is shown below:

Figure 102: Power calculation graph for DhrR/L

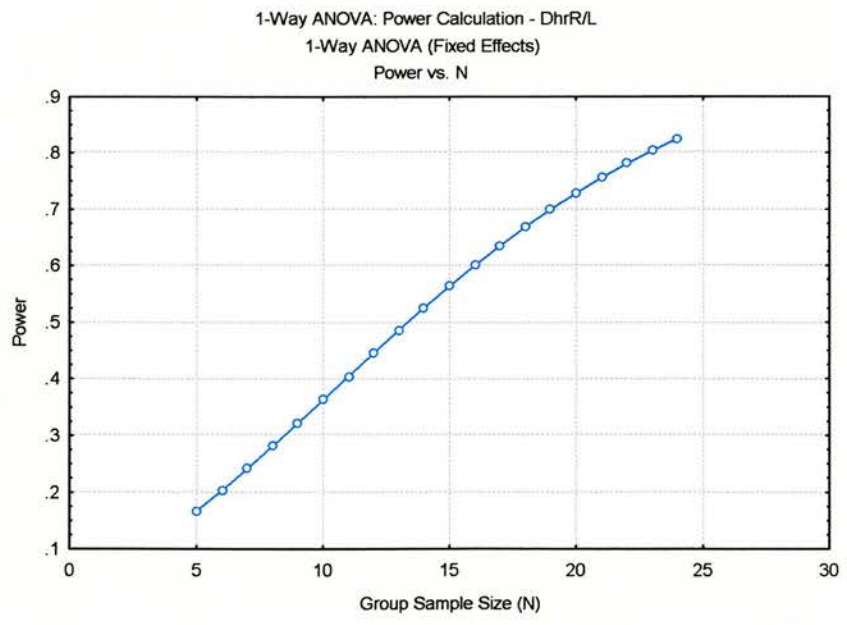

Thus retrospectively, it was shown that the sample size for this test was too small to provide reliable answers to the questions it was investigating. Of particular importance were the low values of power for the analyses performed on the variables from the *in vivo* dynamic assessments, *e.g.* DmR/L and VmR/L with power values of 0.527 and 0.688 respectively. The implications of this are discussed in detail in Discussion Chapter 4 (see In vivo tendon dynamics, page 159).

CHAPTER 4

DISCUSSION

This project was designed to assess the effects of several different surgical techniques and a new product, CRG wrap, on the process of flexor tendon healing. The hypothesis set out to be tested stated that 'the addition of a potentially anti-adhesiogenic agent to the process of tendon repair would result in no difference in musculoskeletal function or tendon characteristics after recovery'.

BLOOD FLOW

The first assessment to be performed was the *in vivo* assessment of superficial blood flow by laser doppler flowmetry. This proved simple to perform, was reproducible and the results were striking. When compared to the normal group, all operative groups except for the two groups examined at six months that incorporated CRG wrap (CLate and DLate), showed a significant increase in superficial blood flow over the site of repair; this equated to elevated levels of proximal doppler flux being recorded.

At six weeks after repair, although flux levels were elevated in all groups when compared to the normal group, comparison between groups showed that the repairs performed with CRG wrap (W, CEarly and DEarly) had significantly less pronounced elevation of flux compared to the other six week repair groups (without the wrap). No significant differences were found between these three surgical methods of repair which incorporated the CRG wrap (W, CEarly, DEarly).

By six months after operation, the two groups which had incorporated CRG wrap at the time of repair (CLate and DLate) showed no significant differences from the normal group proximal flux levels, or from any of the other groups repaired with

CRG wrap. Thus it appeared to be the inclusion of CRG wrap, as opposed to the surgical method used, which accounted for this 'down regulation' of flux levels.

Another important finding was that no significant differences were detected for flux levels measured at the second doppler probe, placed distal to the site of repair (R/LF2). This implied that neither the type of surgical repair performed, nor the addition of CRG wrap had interfered with superficial blood flow beyond the site of repair. Thus the integrity of distal tissues had not been compromised by any of the methods of repair used.

Therefore in this study, surgical intervention was seen to cause an elevation in flux levels at the site of tendon repair, when compared with the normal group. This increase in superficial blood flow was most likely due to an 'overgrowth' of superficial blood vessels as part of the natural healing process. However, the incorporation of CRG wrap into any of the surgical repair groups was seen to diminish the healing response by decreasing this extrinsic vascular proliferation over the site of repair. However, this did not interfere with the superficial blood flow beyond the site of repair or with the strength of the repaired tendons (see below).

TENSILE TESTING, MORPHOLOGY AND PERCENT COMPOSITION

Tensile testing

When assessed at six weeks after repair all groups in which the tendon had been surgically divided, then repaired (AEarly, BEarly, CEarly, DEarly), broke at an UTS bearing a lesser load than their respective non-operated left side, and lesser load than the normal group. However, by six months after repair all groups showed no difference in UTS when compared to the normal group. Another interesting finding was that at six months after repair, many of the operated tendons had an UTS greater than their respective non-operated side (R/LF ratio value > 1). The results obtained from these tensile assessments are of interest as absolute data values as well as in their ratio form. This is because consideration of the absolute values allows the results to

be interpreted in terms of newtons achieved at UTS. Hence, a summary graph of the mean UTS and 95% confidence intervals is shown below.

Figure 103: UTS values for right and non-operated tendons

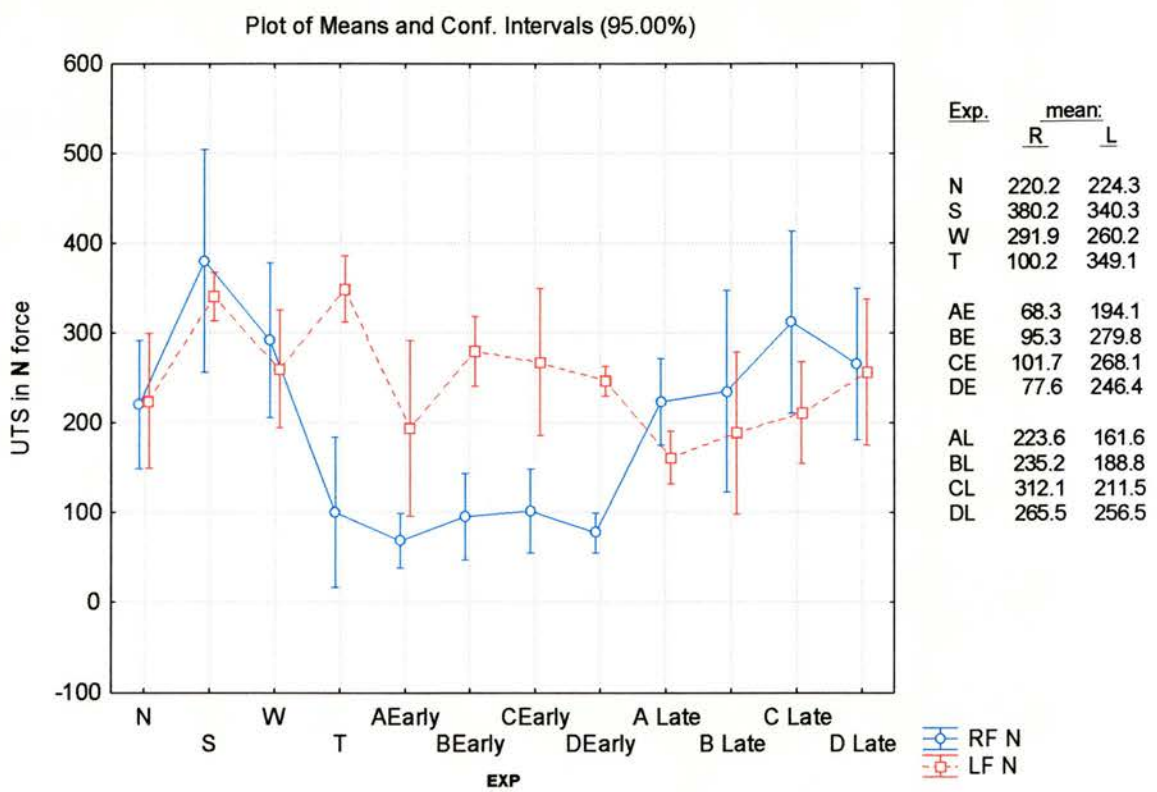

Exp.	mean: R	L
N	220.2	224.3
S	380.2	340.3
W	291.9	260.2
T	100.2	349.1
AE	68.3	194.1
BE	95.3	279.8
CE	101.7	268.1
DE	77.6	246.4
AL	223.6	161.6
BL	235.2	188.8
CL	312.1	211.5
DL	265.5	256.5

The all groups mean for repaired FDS UTS (T, A-DEarly, A-DLate) was 164.4N. The mean UTS of the normal group right FDS tendons was 220.2N and that for the left (non-operated) sides of all groups was 248.4N. When assessed at six weeks the UTS means of the early repair groups were significantly lower than the normal control group mean, as would be expected given that the assessments were carried out at an early stage in the process of healing of the tendons. When assessed at six months after operation, no significant differences from the UTS of the normal control group were found. No differences were found between groups with respect to the method of surgical repair performed, when examined at either six weeks or six months after repair.

In the human it is not known exactly how much force a repaired tendon must withstand during the process of healing (Labana et al. 2001): clearly it is a dynamic process which is affected by the individual circumstances of each case. However, in 1992 Schuind et al. performed investigations on patients undergoing surgery for carpal tunnel syndrome, in which the forces occurring in the flexor tendons were measured during various different movements of the wrist and digits. He and his colleagues concluded that tendon forces reaching 8.9N occurred during passive mobilization of the fingers and forces of up to 34.4 N occurred during unrestricted active mobilization of the fingers (Schuind et al. 1992). Another reference figure which has been calculated with respect to digital forces is that which is apparently required to produce active tendon excursion in a repaired tendon of a traumatized finger; 22 N (Strickland 1999). Obviously the results from this research are based on an ovine model and thus the relevance of these findings to humans must be made with caution. However, when examined at six weeks after repair, there was no evidence of rupture at the repair site (other than in the triamcinolone group, see page 162), the mean UTS of the repaired tendons (T, A-DEarly) was 88.6N and there were no significant differences found between groups. This amount of force is well above the range of forces described by Schuind et al and Strickland. Although it is not yet know what range of force is involved in the ovine model during the process of healing, it is reasonable to assume that forces between 8-34N could have been exerted. However even if lesser magnitudes of force were involved in the ovine model during the period of healing the results obtained in this study still allow useful information to be gained and potentially extrapolated to the process of healing of human flexor tendons.

Thus it can be concluded that the addition of CGR wrap to either method of tendon repair performed in this study did not impair the strength of healing tendons when assessed at either six weeks or six months after surgical repair.

Bulk of repaired tendon

Results of the morphological assessments showed that after any surgical intervention (other than dissection only, group S) examination of the site of repair revealed an increase in bulk of the tendon (cross-sectional area [R/LA] and maximum horizontal axis [R/LX Feret]). The only significant difference between groups was found

between ALate and AEarly; Kessler core repairs at six weeks and six months respectively, with the dimensions measured at the site of repair being significantly greater when assessed at six weeks. Therefore it can be concluded that the incorporation of CRG wrap into the process of tendon repair in this project, did not significantly alter the bulk of the resultant repaired tendons. Thus the gliding characteristics of the FDS within the confined space of its sheath should not be restricted by the addition of CRG wrap, though clearly further work would be required to confirm this.

Tissue composition of the tendons

When examined at six weeks after operation, the two groups of tendons which incorporated the CRG wrap in the repair method (CEarly and DEarly) revealed less fibrous and connective tissue at the site of repair, compared with the other groups. These two groups, CEarly and DEarly, showed no difference from the normal group. But when examined at six months after repair, all experimental groups showed no difference from the normal group. Thus it may be postulated that, in this study, addition of CRG wrap at the time of tendon repair resulted in a 'down-regulating' effect on the early fibroblastic response during the process of healing. This occurred without interfering with the amount of fibrous tissue present at the later stage of healing (assessed at six months). It is of critical importance, however, that this finding is considered in conjunction with the results of the tensile strength assessments. Together these assessments demonstrate that the lesser percent of fibrous tissue present at six weeks after tendon repair, was not associated with any loss of strength of the tendons; no significant differences were found.

It was also revealed that more suture material was present at the earlier time of examination, six weeks, than at the later stage of six months. With regard to method of repair, comparison between groups showed no differences in amount of suture material present. Importantly the presence of CRG wrap was not found to significantly alter the amount of suture material remaining when the tendons were examined at either six weeks or at six months after repair.

IN VIVO TENDON DYNAMICS

Results of the displacement and velocity assessments did not reveal any discernable pattern of differences between groups for any of the variables recorded. Despite all care having been taken in the planning and development of this method for assessment of the tendons, the power studies performed at the end of the analysis of results (see Power Analysis, page 147) showed that the group size predicted at the outset was too small to detect reliably differences for these two indices of outcome: displacement and velocity. It must therefore be concluded that although these groups appeared to have been drawn from the same population, the number of cases per group was not sufficient to allow the null hypothesis to be accepted without risk of type II error: accepting a false null hypothesis. Indeed undetected differences may have been present but missed by too small a sample size.

There are two possible solutions that could be used to address this problem, one retrospective the other prospective. Retrospectively the group sizes could have been increased. However in the absence of supporting data from the pilot study this was not known to be a future problem. In fact had there been evidence for this at the outset of the project, ethical approval would have had to have been obtained for larger group sizes and this may have proved problematic given the case numbers desired by the power calculations (~25 cases). The second solution would be to proceed with further research to address the best method of increasing the sensitivity of these new assessments aiming to heighten the sensitivity of the apparatus to detect greater differences between cases. This would best be achieved in collaboration, once again, with colleagues from the Department of Engineering. Indeed if a different animal model were found to demonstrate tendon excursion greater than the 3-5mm of the ovine model FDS, and thus closer to human digital excursion, the apparatus in its current form may indeed prove to be suitably sensitive for use.

The third indicator of outcome considered during the *in vivo* dynamic assessments was the variable acceleration. The time taken to reach zero acceleration was used as the principle variable for comparison between cases and groups. The aim was to detect any prolongation of, or hindrance to, motion of the tendon which could potentially be caused by the presence of and stretching or breaking down of

adhesions. The power calculation for this variable had a high value, 0.906 but the between group differences did not show any discernable pattern of clinical interest. However, results from a few recordings of acceleration which extended beyond the point of interest for this project (time to zero acceleration) showed interesting graph patterns: the repaired tendons were generally seen to have an oscillating plateau phase whilst their non-operated counterparts had a flatter plateau phase (see below). Although this could be due to re-entry of the stimulus, these few results suggested that the later plateau phase (not investigated in this study) may hold information relevant to the assessment of adhesions and thus further studies are warranted to concentrate on investigating this plateau phase too.

Figure 104: Acceleration graph of a non-operated FDS tendon

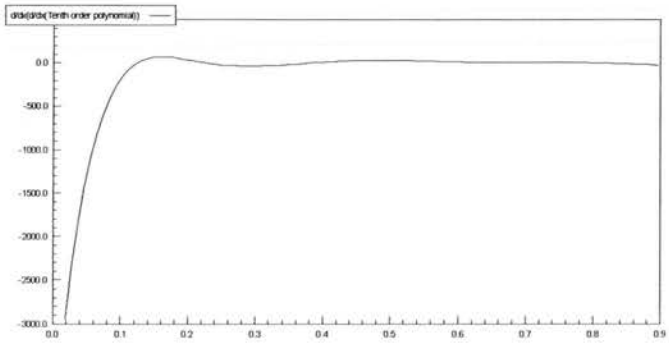

This acceleration curve from a non-operated FDS tendon shows a rapid smooth deceleration phase followed by a fairly straight plateau phase after having reached zero acceleration.

Figure 105: Acceleration graph of an FDS tendon assessed at six weeks

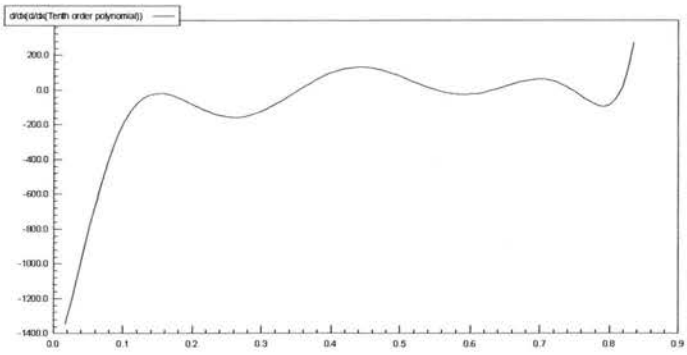

This acceleration curve from a repaired FDS tendon examined after six weeks of healing (group A) shows a rapid smooth deceleration phase to zero acceleration, followed by an oscillating plateau phase.

CRG WRAP GROUP

At the time of harvesting the tendons, gross inspection of the wrap-only group revealed a most unexpected finding; five (41.6%) of the tendons had healed in such a way as to have a large fibrous mound of tissue over the area of repair. This was out of keeping with all other groups in which the wrap had been used.

Figure 106: Appearance of W3, six weeks after primary surgery

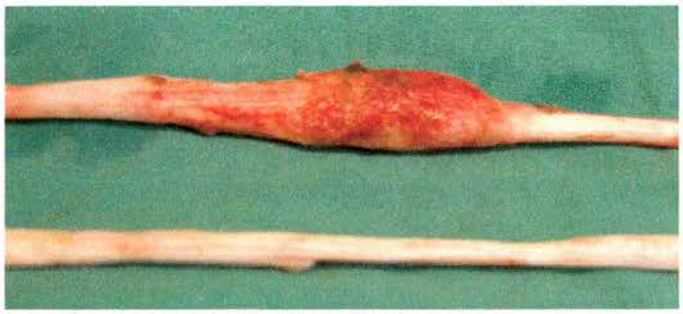

A right FDS tendon (above), from group W had CRG wrap added in the absence of any surgical insult to the tendon. Six weeks after operation the site where the wrap was added is enlarged, with respect to the remainder of the tendon its non-operated FDS (below).

The remaining seven (58.3%) tendons had healed with very little evidence of any increased bulk.

Figure 107: Appearance of W5, six weeks after primary surgery

This right FDS tendon (above), also from group W, had CRG wrap added in the absence of any surgical/traumatic insult to the tendon. However, six weeks after operation the site where the wrap was added appears only very slightly enlarged with respect to the remainder of this tendon or to its non-operated left FDS (below).

This finding was also reflected in the results obtained for the percentage of 'other' tissue present (see RO page, 146) and R/LA, R/LFX, R/LF, where resultant values reflected the inclusion of some tendons with increased bulk. Interestingly there was not much change in the range of superficial doppler flux levels, with the range of values being greater than that for the dissection-only group, but in keeping with the other groups of repairs that had been repaired incorporating the CRG wrap.

The conclusion drawn from this observation was that in the absence of any insult or injury to the tendon itself, the healing process was not initiated in the same way as after tendon injury. Instead a foreign body type reaction had occurred, creating excessive bulk around the intact tendon. Clearly given the confines of flexor tendons in zone II this finding was a very important cautionary discovery, albeit isolated to the situation of non-traumatized flexor tendons.

TRIAMCINOLONE GROUP

The right FDS tendons of the cases in this experimental group were repaired using the full surgical repair technique, Kessler core and epitenon sutures plus the CRG wrap, and the addition of an anti-inflamatory steroid agent, triamcinolone acetonide 0.1% (Adcortyl in Orobase®, Squibb). This group of animals was added to the project after becoming aware of the results of studies carried out by Mr J Yates and colleagues in Sheffield using triamcinolone paste as an antiadhesiogenic adjunct during surgery to the lingual nerve. It was postulated that the addition of this paste to the CRG wrap, at the time of surgical repair of the tendon, may further enhance the already noted anti-adhesiogenic properties of the CRG wraps in this project. Previous work published by Yuzawa in 1985 had also shown triamcinolone to have an adhesion-preventing action, when applied to a scarred tendon and its gliding floor, but the effective dose of this drug was shown to have very narrow limits (Yuzawa 1985). Thus, a preliminary step was taken in this project to see if any encouraging results might be obtained.

Unfortunately, this was not the case. The twelve repairs performed far worse than imagined, resulting in the only two cases of wound dehiscence with tendon repair rupture (nine days after surgery) and subsequent euthanasia of these two cases. The remaining ten cases all developed early wound seromas, with 'stretching' of the repair observed in six animals (66.6%) at the time of final harvesting. In these cases the tendons were found to be intact but with a thin elongated fibrous section at the site of repair with loose or irregular pieces of suture material visible on this elongated surface. The assumption made was that these cases had undergone at least partial rupture of the repair at some stage during the healing process.

Statistical analysis of results from tensile testing of these tendons showed that the addition of this agent rendered them significantly weaker than their individual control and all other groups of repair method (R/LF $p<0.001$). It was therefore concluded that triamcinolone interfered with the healing process of the tendons. In fact, shortly after the conclusion of the experiments for this project, Wong et al reported that the addition of triamcinolone acetonide to cell cultures of human tenocytes led to suppressed human tenocyte cellular activity and reduced collagen production (Wong et al. 2004).

In conclusion, it was clear that the use of even a thin film of triamcinolone paste proved inappropriate in this experimental setting of primary tendon repair. However, it can be speculated that without injury to the tendon, e.g. in the setting of secondary tenolysis procedures, the inhibitory effect on collagen production and subsequent likely limitation of the fibrous reaction conferred by the triamcinolone-impregnated wrap, could be harnessed for patients' benefit, to counter foreign-body type reactions. Further research would be needed explore this possibility in appropriately designed animal studies prior to considering its application to the clinical setting.

CONCLUSIONS

The results of this research project showed the following important clinical findings regarding the use of CRG wrap for the repair of divided tendons, in the ovine model:

The proliferative vascular response to injury was found to be diminished toward 'normal' range at six weeks after repair and within 'normal' range by six months, in all groups where repair had been performed with the addition of CRG wrap. This effect was achieved without incurring any differences in superficial blood flow beyond the site of repair and without any impairment to the strength of the healing tendons. Also, when assessed at six weeks after repair, the groups which had been repaired with the addition of CRG wrap showed a significant reduction in the amount fibrous tissue present at the repair site. This occurred without any other differences in morphological features of the healing tendons being evident at either of the times of assessment. As such the hypothesis as set out to be tested, must be rejected.

The author concludes that the use of CRG wrap may prove beneficial in the treatment of flexor tendon injuries, by limiting early adhesion formation during the time when the site of repair is most vulnerable to the forces applied across it, especially in instances where patient cooperation with rehabilitation is anticipated to be low.

Unfortunately in this study no patterns of significant difference were found in the displacement, velocity or acceleration characteristics of the *in vivo* tendon assessments. As such it has not yet been possible to correlate the diminished vascular response with any quantification of presence or absence of adhesions, by this novel technique. However, it remains likely that this reduction in superficial vascular response minimizes the potential for adhesion formation between the healing tendon and its surrounding structures. Thus further work remains to be carried out as a follow on from this exciting study.

It has indeed proved difficult to compare results of this work with studies available to-date. This is partly owing to the variation in methods and indices of outcome used by different studies (as previously discussed) but more importantly, because this work was set up to establish a new large animal model for *in vivo* assessment of tendons, thus by its very nature there are no previous studies with which to compare results. Thus for the *in vivo* dynamic testing of tendons, no comparable studies are available. The assessment of blood flow using LDBF after a period of healing, again found no previous comparable data in the literature. The results of morphological investigations ought to be interpreted in the context of the study in which they were performed since they only truly relate to the exact methods chosen for a particular study, complementing the other chosen indices of outcome. Hence comparison between studies such as these is rarely beneficial. For the assessment of tensile strength, consideration has been given to the findings of previous studies though it is emphasized again that any comparison made between studies which use different methodology, must be made with caution.

However, the author believes that through this research an important step has been made with regard to the scientific methods used in the continuing quest relating to the characteristics of tendons and their process of healing. By the introduction of this new composite approach to the evaluation of tendons it is hoped that, despite the current decline in incidence of large animal studies (a fact which the author acknowledges) the techniques described herein may be developed further and modified as necessary to contribute toward the continued development and enhancement of research into the healing of injured tendons.

BIBLIOGRAPHY

Angeles, J. G., Heminger, H., & Mass, D. P. 2002, "Comparative biomechanical performances of 4-strand core suture repairs for zone II flexor tendon lacerations", *J.Hand Surg.[Am.]*, vol. 27A, pp. 508-517.

Aoki, M., Manske, P. R., Pruitt, D. L., Kubota, H., & Larson, B. J. 1995, "Canine cadaveric study of flexor tendon repair using tendon splint: tensile strength and the work of flexion", *Nippon Seikeigeka Gakkai Zasshi*, vol. 69, no. 5, pp. 332-341.

Aoki, M., Kubota, H., Pruitt, D. L., & Manske, P. R. 1997, "Biomechanical and histological characteristics of canine flexor tendon repair using early postoperative mobilization.", *J.Hand Surg.[Am.]*, vol. 22, no. 1, pp. 107-114.

Aslam, A. & Afoke, A. 2000, "A new core suture technique for flexor tendon repair: biomechanical analysis of tensile strength and gap formation", *J.Hand Surg.[Br.]*, vol. 25, no. 4, pp. 390-392.

Astrom, M. 2000, "Laser Doppler flowmetry in the assessment of tendon blood flow", *Scand.J.Med.Sci.Sports*, vol. 10, no. 6, pp. 365-367.

Astrom, M. & Svensson, H. 1991, "Tendon blood flow assessed by laser Doppler flowmetry", *Scand.J.Plast.Reconstr.Surg.Hand Surg.*, vol. 25, no. 3, pp. 213-215.

Astrom, M. & Westlin, N. 1994, "Blood flow in the human Achilles tendon assessed by laser Doppler flowmetry", *J.Orthop.Res.*, vol. 12, no. 2, pp. 246-252.

Austin, R. T. & Walker, F. 1979, "Flexor tendon healing and adhesion formation after Sterispon wrapping: a study in the rabbit", *Injury*, vol. 10, no. 3, pp. 211-216.

Banes, A. J., Tsuzaki, M., Hu, P., Brigman, B., Brown, T., Almekinders, L., Lawrence, W. T., & Fischer, T. 1995, "PDGF-BB, IGF-I and mechanical load stimulate DNA synthesis in avian tendon fibroblasts in vitro", *J.Biomech.*, vol. 28, no. 12, pp. 1505-1513.

Beredjiklian, P. K. 2003, "Biologic Aspects of Flexor Tendon Laceration and Repair", *J.Bone Joint Surg.Am.* no. 85, pp. 539-550.

Bolitho, D. G. Hand, Tendon lacerations: flexors. Sudeckum, A.E. eMedicine. 2001. Ref Type: Electronic Citation <http://www.emedicine.com/Plastic/topic331.htm>, accessed 12-7-2003

Boyer, M. I., Gelberman, R. H., Burns, M. E., Dinopoulos, H., Hofem, R., & Silva, M. J. 2001, "Intrasynovial Flexor Tendon Repair", *J.Bone Joint Surg.Am.*, vol. 83-A, no. 6, pp. 891-899.

BSSH. Hand Surgery - An emerging speciality. BHHS 2002. Ref Type: Electronic Citation <http://www.bssh.ac.uk>, accessed 6-8-2002.

Cerovac, S., Afoke, A., Akali, A., & McGrouther, D. A. 2001, "Early breaking strength of repaired flexor tendon treated with 5- fluorouracil", *J.Hand Surg.[Br.]*, vol. 26, no. 3, pp. 220-223.

Chow, S. P., Hooper, G., & Chan, C. W. 1983, "The healing of freeze-dried rabbit flexor tendon in a synovial fluid environment", *Hand*, vol. 15, no. 2, pp. 136-142.

Fullarton, A., Myles, L., & Glasby, M. A. 2002, "Assessment of the method and timing of repair of a brachial plexus traction injury in an animal model for obstetric brachial plexus palsy.", *Journal of Hand Surgery (Br)*, vol. 27, no. 1, pp. 13-19.

Fullarton, A. C. 1995, *An Investigation into the Recovery of Function after Different Types of Injury and Repair of Peripheral Nerve - A Comparison between Non-diabetic and STZ Diabetic Rats*, Ph.D. Thesis, University of Edinburgh.

Fullarton, A. C. & Glasby, M. 1997, "An evaluation of different methods of peripheral nerve repair in the normal and diabetic rat.", *Journal of Hand Surgery*, vol. 22B, no. 4, pp. 486-491.

Fullarton, A. C., Lenihan, D. V., Myles, L. M., & Glasby, M. 2000, "Obstetric brachial plexus palsy: a large animal model for traction injury and its repair. Part I Age of the recipient.", *Journal of Hand Surgery*, vol. 25B, no. 1, pp. 52-57.

Gelberman, R. H., Woo, S. L., Lothringer, K., Akeson, W. H., & Amiel, D. 1982, "Effects of early intermittent passive mobilization on healing canine flexor tendons", *J.Hand Surg.[Am.]*, vol. 7, no. 2, pp. 170-175.

Gilchrist, T., Glasby, M. A., Healy, D. M., Kelly, G., Lenihan, D. V., McDowall, K. L., Miller, I. A., & Myles, L. M. 1998, "In vitro nerve repair--in vivo. The reconstruction of peripheral nerves by entubulation with biodegradeable glass tubes--a preliminary report", *Br.J.Plast.Surg.*, vol. 51, no. 3, pp. 231-237.

Glasby, M., Fullarton, A. C., & Lawson, G. M. 1997, "Immediate and delayed nerve repair using freeze-thawed muscle autografts in complex nerve injuries. Cavitation, fibrosis and haematoma.", *Journal of Hand Surgery*, vol. 22B, no. 4, pp. 479-485.

Golash, A., Kay, A., Warner, J. G., Peck, F., Watson, J. S., & Lees, V. C. 2003, "Efficacy of ADCON-T/N after primary flexor tendon repair in zone II: a controlled clinical trial", *J.Hand Surg.[Br.]*, vol. 28B, no. 2, pp. 113-115.

Gudemez, E., Eksioglu, F., Korkusuz, P., Asan, E., Gursel, I., & Hasirci, V. 2002, "Chondroitin sulfate-coated polyhydroxyethyl methacrylate membrane prevents adhesion in full-thickness tendon tears of rabbits", *J.Hand Surg.[Am.]*, vol. 27, no. 2, pp. 293-306.

Hanff, G. & Hagberg, L. 1998, "Prevention of restrictive adhesions with expanded polytetrafluoroethylene diffusible membrane following flexor tendon repair: an experimental study in rabbits", *J.Hand Surg.[Am.]*, vol. 23, no. 4, pp. 658-664.

Hannafin, J. A. & Arnoczky, S. P. 1994, "Effect of cyclic and static tensile loading on water content and solute diffusion in canine flexor tendons: an in vitro study", *J.Orthop.Res.*, vol. 12, no. 3, pp. 350-356.

Hannafin, J. A., Arnoczky, S. P., Hoonjan, A., & Torzilli, P. 1995, "Effect of stress deprivation and cyclic tensile loading on the material and morphologic properties of canine flexor digitorum profundus tendon: an in vitro study", *J.Orthop.Res.*, vol. 13, no. 6, p. 907.

Harwood, F. L., Goomer, R. S., Gelberman, R. H., Silva, M. J., & Amiel, D. 1999, "Regulation alpha(v)beta3 and alpha5beta1 integrin receptors by basic fibroblast growth factor and platelet-derived growth factor-BB in intrasynovial flexor tendon cells.", *Wound Repair Regen.*, vol. 7, pp. 381-388.

Helm, R. H. 2003, "The management of flexor tendon injuries in zone II", *Current Orthopaedics* no. 16, pp. 434-441.

Hitchcock, T. F., Light, T. R., Bunch, W. H., Knight, G. W., Sartori, M. J., Patwardhan, A. G., & Hollyfield, R. L. 1987, "The effect of immediate constrained digital motion on the strength of flexor tendon repairs in chickens", *J.Hand Surg.[Am.]*, vol. 12, no. 4, pp. 590-595.

Home Office (H.M.S.O.). Animals (Scientific Procedures) Act 1986; Code of practice for the housing and care of animals used in scientific procedures. Eliz II 1986 C.14 Section 21. 1986.

Isik, S., Ozturk, S., Gurses, S., Yetmez, M., Guler, M., Selmanpakoglu, N., & Gunham, O. 1999, "Prevention of restrictive adhesions in primary tendon repair by HA-membrane experimental research in chickens", *Br.J.Plast.Surg.*, vol. 52, pp. 373-379.

Jaibaji, M. 2000, "Advances in the biology of zone II flexor tendon healing and adhesion formation", *Ann.Plast.Surg.*, vol. 45, no. 1, pp. 83-92.

Jones, M. E., Burnett, S., Southgate, A., Sibbons, P., Grobbelaar, A. O., & Green, C. J. 2002, "The role of human-derived fibrin sealant in the reduction of postoperative flexor tendon adhesion formation in rabbits", *J.Hand Surg.[Br.]*, vol. 27B, no. 3, pp. 278-282.

Jones, M. E., Ladhani, K., Mudera, V., Grobbelaar, A. O., McGrouther, D. A., & Sanders, R. 2000, "Flexor tendon blood vessels", *J.Hand Surg.[Br.]*, vol. 25, no. 6, pp. 552-559.

Khan, U., Kakar, S., Akali, A., Bentley, G., & McGrouther, D. A. 2000, "Modulation of the formation of adhesions during the healing of injured tendons", *J.Bone Joint Surg.Br.*, vol. 82, no. 7, pp. 1054-1058.

Kirkwood, B. R. 1991, "Comparison of several means- analysis of variance," in *Essentials of Medical Statistics*, B. R. Kirkwood, ed., Blackwell Scientific Publications, Oxford, pp. 46-55.

Kleinert, H. E. & Pickford, M. A. 1997, "David R Boyd lecture in trauma care and emergency medical systems: Upper extremity injuries-past, present and future", *Journal of Emergency Medicine*, vol. 15, no. 5, pp. 709-719.

Kleinert, H. E., Spokevicius, S., & Papas, N. H. 1995, "History of flexor tendon repair", *J.Hand Surg.[Am.]*, vol. 20(A), p. S44-S52.

Kobayashi, M., Toguchida, J., & Oka, M. 2001, "Development of polyvinyl alcohol-hydrogel (PVA-H) shields with a high water content for tendon injury repair", *J.Hand Surg.[Br.]*, vol. 26B, no. 5, pp. 436-440.

Labana, N., Messer, T., Lautenschlager, E., Nagda, S., & Nagle, D. 2001, "A biomechanical analysis of the modified Tsuge suture technique for repair of flexor tendon lacerations", *J.Hand Surg.[Br.]*, vol. 26, no. 4, pp. 297-300.

Leddy, J. P. 1988, "Flexor Tendons - Acute Injuries," in *Operative Hand Surgery*, 2nd edn, vol. 3 D. P. Green, ed., Churchill Livingstone, New York, pp. 1935-1968.

Lundborg, G., Rank, F., & Heinau, B. 1985, "Intrinsic tendon healing. A new experimental model", *Scand.J.Plast.Reconstr.Surg.*, vol. 19, no. 2, pp. 113-117.

Manske, P. R., Gelberman, R. H., Vande Berg, J. S., & Lesker, P. A. 1984, "Intrinsic flexor-tendon repair. A morphological study in vitro", *J.Bone Joint Surg.Am.*, vol. 66, no. 3, pp. 385-396.

Manske, P. R. & Lesker, P. A. 1982, "Nutrient pathways of flexor tendons in primates", *J.Hand Surg.[Am.]*, vol. 7, no. 5, pp. 436-444.

Manske, P. R. & Lesker, P. A. 1985, "Flexor tendon nutrition", *Hand Clin.*, vol. 1, no. 1, pp. 13-24.

Martini, L., Fini, M., Giavaresi, G., & Giardino, R. 2001, "Sheep model in orthopedic research: a literature review. [Review] [62 refs]", *Comparative Medicine*, vol. 51, no. 4, pp. 292-299.

Matthews, P. & Richards, H. 1976, "Factors in the adherence of flexor tendon after repair: an experimental study in the rabbit", *J.Bone Joint Surg.Br.*, vol. 58, no. 2, pp. 230-236.

McCarthy, D. M., Boardman, N. D., III, Tramaglini, D. M., Sotereanos, D. G., & Herndon, J. H. 1995a, "Clinical management of partially lacerated digital flexor tendons: a survey [corrected] of hand surgeons", *J.Hand Surg.[Am.]*, vol. 20, no. 2, pp. 273-275.

McCarthy, D. M., Tramaglini, D. M., Chan, S. S., Schmidt, C. C., Sotereanos, D. G., & Herndon, J. H. 1995b, "Effect of partial laceration on the structural properties of the canine FDP tendon: an in vitro study", *J.Hand Surg.[Am.]*, vol. 20, no. 5, pp. 795-800.

Meislin, R. J., Wiseman, D. M., Alexander, H., Cunningham, T., Linsky, C., Carlstedt, C., Pitman, M., & Casar, R. 1990, "A biomechanical study of tendon adhesion reduction using a biodegradable barrier in a rabbit model", *J.Appl.Biomater.*, vol. 1, no. 1, pp. 13-19.

Menderes, A., Mola, F., Tayfyr, V., Vayvada, H., & BarutcuA 2004, "Prevention of Periteninous Adhesions Following Flexor Tendon Injury With Seprafilm", *Ann.Plast.Surg.*, vol. 53, no. 6, pp. 560-564.

Mentzel, M., Hoss, H., Keppler, P., Ebinger, T., Kinzl, L., & Wachter, N. J. 2000, "The effectiveness of ADCON-T/N, a new anti-adhesion barrier gel, in fresh divisions of the flexor tendons in Zone II", *J.Hand Surg.[Br.]*, vol. 25, no. 6, pp. 590-592.

Newmeyer, W. L. 2003, "Sterling Bunnell, MD: The Founding Father", *J.Hand Surg.[Am.]*, vol. 28A, no. 1, pp. 161-164.

Pearcy, L. T. Galen: A Biographical Sketch. A.S.U courses website 2004. Ref Type: Electronic Citation, accessed 12-4-2005 < http://courses.ed.asu.edu/horan/ced522readings/galen/dreams/galenbio.htm>

Potenza, A. D. 1969, "Mechanisms of healing of digital flexor tendons", *Hand* no. 1, pp. 40-41.

Powers, P. Upper extremity fascial compartments. Fonda, B. University of Vermont College of Medicine, Computer Assisted Teaching System . 2003. Ref Type: Electronic Citation, accessed 8-12-2003 < http://cats.med.uvm.edu/cats_teachingmod/gross_anatomy/upper_extremity/pages/fascia.html>

Pruitt, D. L., Tanaka, H., Aoki, M., & Manske, P. R. 1996, "Cyclic stress testing after in vivo healing of canine flexor tendon lacerations", *J.Hand Surg.[Am.]*, vol. 21, no. 6, pp. 974-977.

Rand, M. S. Farm animals as models for biomechanical research. Biothechnology Lecture notes . 2002. Ref Type: Electronic Citation, accessed 19-11-2002 < http://www.ahsc.arizona.edu/uac/notes/classes/farmmodels/farmanim_as_biomodels02.html>

Riley, G. P., Cox, M., Harrall, R. L., Clements, S., & Hazleman, B. L. 2001, "Inhibition of tendon cell proliferation and matrix glycosaminoglycan synthesis by non-steroidal anti-inflammatory drugs in vitro", *J.Hand Surg.[Br.]*, vol. 26, no. 3, pp. 224-228.

Schuind, F., Garcia-Elias, M., Cooney, W. P. 3., & An, K. N. 1992, "Flexor tendon forces: in vivo measurements", *J.Hand Surg.[Am.]*, vol. 17, no. 2, pp. 291-298.

Seiler, J. G. & Fogle, E. F. 2004, "Flexor Tendon Injuries of the Hand," in *Orthopedic Care Textbook.* Electronic Citation, accessed 9-2-2005 < http://www.orthotextbook.net/view/templates/Chapter_Entry.asp?sectionid=andsectionname=&chapterid=hnijtnfla>

Seradge, H. 1983, "Elongation of the repair configuration following flexor tendon repair", *J.Hand Surg.[Am.]*, vol. 8, no. 2, pp. 182-185.

Shapiro, S. S., Wilk, M. B., & Chen, H. J. (1968). A comparative study of various tests of normality. *Journal of the American Statistical Association, 63*, 1343-1372.

Silfverskiold, K. L. & Andersson, C. H. 1993, "Two new methods of tendon repair: an in vitro evaluation of tensile strength and gap formation", *J.Hand Surg.[Am.]*, vol. 18, no. 1, pp. 58-65.

Silfverskiold, K. L., May, E. J., & Tornvall, A. H. 1992, "Gap formation during controlled motion after flexor tendon repair in zone-II - A prospective clinical study", *J.Hand Surg.[Am.]*, vol. 17A, no. 3, pp. 539-546.

Smith, A. M. & Evans, D. M. 2001, "Biomechanical assessment of a new type of flexor tendon repair", *J.Hand Surg.[Br.]*, vol. 26, no. 3, pp. 217-219.

Sorock, G. S., Lombardi, D. A., Courtney, T. K., Cotnam, J. P., & Mittleman, M. A. 2001, "Epidemiology of occupational acute traumatic hand injuries: a literature review", *Safety Science* no. 38, pp. 241-256.

Stainsfile. Stain Theory - Principles and aids to staining. Stainsfile . 1998. Ref Type: Electronic Citation , accessed 14-5-2002 <http://stainsfile.info/StainsFile/stain/conektv/Stain theory.htm>

Stainsfile. What is a trichrome. Stainsfile . 1-6-1999. Ref Type: Electronic Citation, accessed 14-5-2002. <http://stainsfile.info/ StainsFile/stain/conektv/What_is_trichrome.htm>

Steinberg, D. R. 1997, "Flexor tendon laceration in the hand", *University of Pennsylvania Orthopedic journal*, vol. 10, pp. 5-11.

Strickland, J. W. 1999, "Flexor Tendons - Acute injuries," in *Green's operative hand surgery*, D. P. Green, R. N. Hotchkiss, & W. C. Pederson, eds., Churchill Livingstone, New York, pp. 1851-1897.

Strickland, J. W. 2000, "Development of flexor tendon surgery: twenty-five years of progress", *J.Hand Surg.[Am.]*, vol. 25, no. 2, pp. 214-235.

Tanaka, H., Manske, P. R., Pruitt, D. L., & Larson, B. J. 1995, "Effect of cyclic tension on lacerated flexor tendons in vitro", *J.Hand Surg.[Am.]*, vol. 20, no. 3, pp. 467-473.

Tobias, V. A. 1995, "Tehcnical Note: A cost-effective Masson's Trichrome Stain", *HistoLogic*, vol. 25, p. 10.

Wada, A., Kubota, H., Hatanaka, H., Hotokezaka, S., Miura, H., & Iwamoto, Y. 2000, "The mechanical properties of locking and grasping suture loop configurations in four-strand core suture techniques", *J.Hand Surg.[Br.]*, vol. 25, no. 6, pp. 548-551.

Wada, A., Kubota, H., Miyanishi, K., Hatanaka, H., Miura, H., & Iwamoto, Y. 2001, "Comparison of postoperative early active mobilization and immobilization in vivo utilising a four-strand flexor tendon repair", *J.Hand Surg.[Br.]*, vol. 26, no. 4, pp. 301-306.

Wade, P. J., Muir, I. F., & Hutcheon, L. L. 1986, "Primary flexor tendon repair: the mechanical limitations of the modified Kessler technique", *J.Hand Surg.[Br.]*, vol. 11, no. 1, pp. 71-76.

Wang, B., Xie, R. G., & Tang, J. B. 2003, "Biomechanical analysis of a modification of Tang method of tendon repair", *J.Hand Surg.[Br.]*, vol. 28B, no. 4, pp. 347-350.

Wiig, M. & Abrahamsson, S. O. 2000, "Hyaluronic acid modulates cell proliferation unequally in intrasynovial and extrasynovial rabbit tendons in vitro", *J.Hand Surg.[Br.]*, vol. 25, no. 2, pp. 183-187.

Williams, R. J. & Amis, A. A. 1995, "A new type of flexor tendon repair. Biomechanical evaluation by cyclic loading, ultimate strength and assessment of pulley friction in vitro", *J.Hand Surg.[Br.]*, vol. 20, no. 5, pp. 578-583.

Wright, M. O. & Davies, A. H. 1995, "The investigation of the peripheral circulation," in *Applied physiology for surgery and critical care*, M. A. Glasby & C. L.-H. Huang, eds., Buttler and Heinemann, Oxford, pp. 694-695.

Wong, M. W. N., Tang, Y. N., Fu, S. C., Lee, K. M., & Chan, K. M. Triamcinolone supresses human tenocyte cellular activity and collagen synthesis. Clin.Orthop. 421, 277-281. 2004.

Yuzawa, K. 1985, "Experimental studies on the healing and restoration of gliding function of the injured digital flexor tendon.", *Nippon Seikeigeka Gakki Zasshi*, vol. 59, no. 12, pp. 1107-18.

Zhao, C., Amadio, P. C., Zobitz, M. E., & An, K. N. 2001, "Gliding characteristics of tendon repair in canine flexor digitorum profundus tendons", *J.Orthop.Res.*, vol. 19, no. 4, pp. 580-586.

Zobitz, M. E., Zhao, C., Erhard, L., Amadio, P. C., & An, K. N. 2001, "Tensile properties of suture methods for repair of partially lacerated human flexor tendon in vitro", *J.Hand Surg.[Am.]*, vol. 26, no. 5, pp. 821-827.

APPENDIX 1

WAX IMPREGNATION OF TISSUES - TISSUE-TEK PROGRAMME 4

	SOLUTION	CONC.	HR: MIN	SET TEMP	P/V	AGITATION
1	Alcohol	70%	1:00	40°	Off	On
2	Alcohol	80%	1:00	40°	Off	On
3	Alcohol	90%	1:00	40°	Off	On
4	Alcohol	95%	1:00	40°	Off	On
5	Alcohol	100%	1:00	45°	On	On
6	Alcohol	100%	1:00	45°	On	On
7	Alcohol	100%	1:00	45°	On	On
8	Xylene	100%	1:00	45°	On	On
9	Xylene	100%	1:00	50°	On	On
10	Xylene	100%	0:00	50°	On	On
11	V.I.P. Paraffin	-	1:00	60°	On	On
12	V.I.P. Paraffin	-	1:00	60°	On	On
13	V.I.P. Paraffin	-	1:00	60°	On	On
14	V.I.P. Paraffin	-	0:00	60°	On	On

APPENDIX 2

STEPS FOR REMOVING WAX FROM A SECTION

'REHYDRATING' OR 'TAKING TO WATER'

No.	Solution	Time
1	Xylene I	5 minutes
2	Xylene II	5 minutes
3	Absolute Alcohol	5 minutes
4	96% Alcohol	5 minutes
5	70% Alcohol	5 minutes
6	Running tap water	5 minutes

After performing the above steps, the histological section is ready for commencing the staining schedule of choice.

APPENDIX 3

HAEMATOXYLIN AND EOSIN STAIN

Summary

Mayer's hematoxylin is used because it eliminates the necessity for differentiation and bluing of the section. It can be considered a progressive stain which produces a stained section with clearly defined nuclei while the background is completely colorless. The biggest objection to Mayer's hematoxylin as used in the past, has been that stained slides often fade after 1 to 3 years. This problem can be eliminated, however, when the slides are washed, after the hematoxylin, in running water for a minimum of 20 minutes. This method gives consistent results even when more than one person stains sections from the same block. Also, slides may be left in the hematoxylin for hours with-out overstaining.

Fixation - Any well fixed tissue.

Technique

Suitable for paraffin, celloidin, or frozen sections

Solutions

- Mayer's Hematoxylin
- Eosin Solutions
- Gram's or Lugol's Iodine

Staining Procedure

1. Remove paraffin and hydrate to water
2. Place slide rack in Mayer's hematoxylin for 15 minutes
3. Wash in running tap water for 20 minutes
4. Counterstain with eosin from 15 seconds to 2 minutes depending on the age of the eosin, and the depth of the counterstain desired. For even staining results dip slides several times before allowing them to set in the eosin for the desired time
5. Dehydrate and clear in xylene (as per protocol in Appendix 5)

Results

Nuclei - blue - with some metachromasia
Cytoplasm - various shades of pink-identifying different tissue components

APPENDIX 4

GOMORI'S ONE-STEP TRICHROME STAIN

Purpose

To identify collagenous connective tissue fibers, or to differentiate between collagen and smooth muscle fibers

Principle

In the one-step trichrome procedure, a plasma stain (chromotrope 2R) and a connective tissue fiber stain (fast green FCF, light green, or aniline blue) are combined in a solution of phosphotungstic acid to which glacial acetic acid has been added. Phosphotungstic acid favors the red staining of muscle and cytoplasm. The tungstate ion is specifically taken up by collagen, and the connective tissue fiber stain is subsequently bound to this complex, coloring the collagen green or blue, depending on the counterstain used.

Fixative

Any well-fixed tissue may be used.
Bouin's solution is used as a mordant to intensify the color reactions.

Equipment

- 56 to 58 °C oven
- Coplin jars
- Erlenmeyer flasks
- graduated cylinders
- pipettes.
-

Technique

Cut paraffin sections at 4 to 5 µm.
Mix reagents as per instructions on the following two pages

Reagents

Bouin's Solution

Picric acid, saturated aqueous solution .... 75.0 mL

Formaldehyde, 37% to 40% ..... 25.0 mL

Glacial acetic acid ..... 5.0 mL

Weigert's Iron Hematoxylin

working Solution = mix equal parts of solutions A and B.

Solution A

Hematoxylin..... 10.0 g

Alcohol, 95% ..... 1,000.0 mL

Solution B

Distilled water ..... 475.0 mL

Hydrochloric acid, concentrated ..... 5.0 mL

Ferric chloride, 29% solution ..... 20.0 mL

0.5% Acetic Acid Solution

Glacial acetic acid ..... 0.5 mL

Distilled water ..... 99.5 mL

Gomori's Trichrome Stain (Store this solution in the refrigerator)

Chromotrope 2R (Baker No. 5-F703) . . . . . 0.6 g

Fast green FCF, light green or aniline blue ..... 0.3 g

Phosphotungstic acid ..... 0.8 g

Glacial acetic acid . . . . . 1.0 mL

Distilled water ..... 100.0 mL

Procedure

1. Remove paraffin from sections and hydrate to distilled water.
2. Rinse well in distilled water.
3. Mordant sections in Bouin's solution for I hour at 56 °C.
4. Remove slides from the oven, allow to cool and wash in running water until the yellow color disappears.
5. Rinse in distilled water.
6. Stain sections in Weigert's hematoxylin for 10 minutes.
7. Wash in running water for 10 minutes.
8. Stain sections for 15 to 20 minutes in Gomori's trichrome stain.
9. Differentiate for 2 minutes in 0.5% acetic acid.
10. Dehydrate, clear, and mount with synthetic resin.

Results

Nuclei..... black
Cytoplasm, keratin, muscle fibers ..... red
Collagen and mucus ..... green or blue

APPENDIX 5

STEPS FOR DEHYDRATING A SECTION AFTER STAINING

'DEHYDRATING' OR 'TAKING TO XYLENE'

The steps below should be performed after completion of the chosen staining schedule

No.	Solution	Method/Time
1	70% Alcohol	Agitate rack, 4/6 seconds
2	96% Alcohol	Agitate rack, 10/20 seconds
3	Absolute Alcohol	Agitate, 30 seconds
4	Xylene I	-
5	Xylene II	-

Allow to air dry

After performing the above steps, the histological sections are ready for application of a coverslip.

APPENDIX 6

STATISTICA CODES

Group & Case Identification

GROUP	PRIMARY PROCEDURE	CASE IDENTIFICATION
AEarly	= KC repair at 6 Weeks	**L**etter (AA – AM)
BEarly	= KCE repair 6 Weeks	**L**etter (BA – BM)
CEarly	= KCW repair 6 Weeks	**L**etter (CA – CM)
DEarly	= KCEW repair 6 Weeks	**L**etter (DA – DM)
ALate	= KC repair at 6 Months	**N**umber (A1 – A12)
BLate	= KCE repair 6 Months	**N**umber (B1 – B12)
CLate	= KCW repair 6 Months	**N**umber (C1 – C12)
DLate	= KCEW repair 6 Months	**N**umber (D1 – D12)
N	= **N**ormal	(N1 – N12)
S	= Dissection only	(S1 – S12)
W	= **W**rap only	(W1 – W12)
T	= KCEW repair + **T**riamcinolone	(T1 – T12)

Variables

Doppler

RF1	= **R**ight **F**lux 1	(flux units)[1]
RF2	= **R**ight **F**lux 2	
LF1	= **L**eft **F**lux 1	
LF2	= **L**eft **F**lux 2	
RF1-F2	= **R**ight **F**lux 1- **F**lux 2	
LF1-F2	= **L**eft **F**lux 1- **F**lux 2	
R/LF1	= **R**ight / **L**eft **F**lux 1	
R/LF2	= **R**ight / **L**eft **F**lux 2	
R/LF1-2	= **R**ight / **L**eft **F**lux 1- Flux 2	
L/RF1	= **L**eft / **R**ight **F**lux 1	
L/RF2	= **L**eft / **R**ight **F**lux 2	
L/RF1-2	= **L**eft / **R**ight **F**lux 1- Flux 2	

[1]Flux units are related to the product of average speed and concentration of moving red blood cells in the tissue sample volume

In vivo tendon dynamics

DmR	= **m**aximum **D**isplacement, **R**ight	(mm)
tDmR	= time to **m**aximum **D**isplacement, **R**ight	(s)
DmL	= **m**aximum **D**isplacement, **L**eft	(mm)
tDmL	= time to **m**aximum **D**isplacement, **L**eft	(s)
DhrR	= **D**isplacement at **h**alf **r**elaxation, **R**ight	(mm)
tDhrR	= time to **D**isplacement at **h**alf **r**elaxation, **R**ight	(s)
DhrL	= **D**isplacement at **h**alf **r**elaxation, **L**eft	(mm)
tDhrL	= time to **D**isplacement at **h**alf **r**elaxation, **L**eft	(s)
tTTR	= time for **T**otal **T**witch, **R**ight	(s)
tTTL	= time for **T**otal **T**witch, **L**eft	(s)
VmR	= **m**aximum **V**elocity, **R**ight	(mms^{-1})
tVmR	= time to **m**aximum **V**elocity, **R**ight	(s)
VmL	= **m**aximum **V**elocity, **L**eft	(mms^{-1})
tVmL	= time to **m**aximum **V**elocity, **L**eft	(s)
DmR-L	= **m**aximum **D**isplacement, **R**ight – **L**eft	(mm)
DmR/L	= **m**aximum **D**isplacement, **R**ight / **L**eft	(mm)
DmL-R	= **m**aximum **D**isplacement, **L**eft – **R**ight	(mm)
DmL/R	= **m**aximum **D**isplacement, **L**eft / **R**ight	(mm)
tDmR-L	= time to **m**aximum **D**isplacement, **R**ight – **L**eft	(s)
tDmR/L	= time to **m**aximum **D**isplacement, **R**ight / **L**eft	(s)
tDmL-R	= time to **m**aximum **D**isplacement, **L**eft – **R**ight	(s)
tDmL/R	= time to **m**aximum **D**isplacement, **L**eft / **R**ight	(s)
DhrR-L	= **D**isplacement at **h**alf **r**elaxation, **R**ight – **L**eft	(mm)
DhrR/L	= **D**isplacement at **h**alf **r**elaxation, **R**ight / **L**eft	(mm)
DhrL-R	= **D**isplacement at **h**alf **r**elaxation, **L**eft – **R**ight	(mm)
DhrL/R	= **D**isplacement at **h**alf **r**elaxation, **L**eft / **R**ight	(mm)
tDhrR-L	= time to **D**isplacement at **h**alf **r**elaxation, **R**ight – **L**eft	(s)
tDhrR/L	= time to **D**isplacement at **h**alf **r**elaxation, **R**ight / **L**eft	(s)
tDhrL-R	= time to **D**isplacement at **h**alf **r**elaxation, **L**eft – **R**ight	(s)
tDhrL/R	= time to **D**isplacement at **h**alf **r**elaxation, **L**eft / **R**ight	(s)
tTTR-L	= time for **T**otal **T**witch, **R**ight – **L**eft	(s)
tTTR/L	= time for **T**otal **T**witch, **R**ight / **L**eft	(s)
tTTL-R	= time for **T**otal **T**witch, **L**eft – **R**ight	(s)
tTTL/R	= time for **T**otal **T**witch, **L**eft / **R**ight	(s)
VmR-L	= **m**aximum **V**elocity, **R**ight – **L**eft	(mms^{-1})
VmR/L	= **m**aximum **V**elocity, **R**ight / **L**eft	(mms^{-1})

VmL-R	= **m**aximum **V**elocity, **L**eft – **R**ight	(mms^{-1})
VmL/R	= **m**aximum **V**elocity, **L**eft / **R**ight	(mms^{-1})
tVmR-L	= **t**ime to **m**aximum **V**elocity, **R**ight – **L**eft	(s)
tVmR/L	= **t**ime to **m**aximum **V**elocity, **R**ight / **L**eft	(s)
tVmL-R	= **t**ime to **m**aximum **V**elocity, **L**eft – **R**ight	(s)
tVmL/R	= **t**ime to **m**aximum **V**elocity, **L**eft / **R**ight	(s)
t0Accel R	= time to zero **A**cceleration, **R**ight	(s)
t0Accel L	= time to zero **A**cceleration, **L**eft	(s)
t0Accel R/L	= time to zero **A**cceleration, **R**ight/**L**eft	(s)

Instron

RF	= **R**ight, maximum **F**orce	(N)
RD	= **R**ight, maximum **D**isplacement	(mm)
LF	= **L**eft, maximum **F**orce	(N)
LD	= **L**eft, maximum **D**isplacement	
R/LF	= maximum **F**orce, **R**ight / **L**eft	(N)
R/LD	= maximum **D**isplacement, **R**ight / **L**eft	(mm)

Histological

RA	=**R**ight **A**rea	(mm^2)
LA	=**L**eft **A**rea	(mm^2)
R/LA	=**R**ight/**L**eft **A**rea	(mm^2)
RP	=**R**ight **P**erimeter	(mm)
LP	=**L**eft **P**erimeter	(mm)
R/LP	=**R**ight/**L**eft **P**erimeter	(mm)
RL	=**R**ight **L**ength	(mm)
LL	=**L**eft **L**ength	(mm)
R/LL	=**R**ight/**L**eft **L**ength	(mm)
RXF	=**R**ight **XF**eret[2]	(mm)
LXF	=**L**eft **XF**eret	(mm)
R/LXF	=**R**ight/**L**eft **XF**eret	(mm)

[2] Feret = the maximum distance of the X (horizontal) or Y (vertical) axis

RYF	=**R**ight **YF**eret	(mm)
LYF	=**L**eft **YF**eret	(mm)
R/LYF	=**R**ight/**L**eft **YF**eret	(mm)
RFF	=**R**ight **F**orm **F**actor[3]	
LFF	=**L**eft **F**orm **F**actor	
R/LFF	=**R**ight/**L**eft **F**orm **F**actor	
RT	=**R**ight **T**endon fibres	
LT	=**L**eft **T**endon fibres	
RV	=**R**ight blood **V**essels	
LV	=**L**eft blood **V**essels	
RS	=**R**ight **S**uture material	
LS	=**L**eft **S**uture material	
RO	=**R**ight **O**ther/fibrous substance	
LO	=**L**eft **O**ther/fibrous substance	

[3] Form factor is a standard estimate of the circularity that relates perimeter length to area on a scale of 0 to 1, with 1 being a perfect circle. (see Chapter 2, page 108).

APPENDIX 7

DOPPLER RESULTS – 6 MONTHS (A)

CASE	PROBE	MEAN	STD	MIN	MAX	MEDIAN
A1 R	F1	102.7	50.5	57.8	321.4	79.2
	F2	18.7	13.5	5.1	78.0	12.7
L	F1	36.1	18.2	15.9	102.8	29.9
	F2	32.2	20.9	10.9	125.5	24.3
A2 R	F1	158.1	36.1	102.5	343.2	149.6
	F2	46.2	36.1	15.7	215.7	30.5
L	F1	50.1	22.9	30.4	170.1	41.2
	F2	40.0	13.8	25.7	98.0	35.0
A3 R	F1	56.0	25.8	28.0	155.7	45.9
	F2	36.4	33.8	8.2	170.8	18.8
L	F1	42.4	29.5	17.6	196.4	29.8
	F2	39.7	21.5	20.0	130.8	30.9
A4 R	F1	Died				
	F2					
L	F1					
	F2					
A5 R	F1	104.8	60.7	45.7	523.8	89.2
	F2	71.6	42.5	24.8	249.1	57.5
L	F1	52.2	28.0	23.4	176.9	41.0
	F2	51.7	18.6	26.7	125.2	45.9
A6 R	F1	212.6	99.8	102.0	719.8	186.3
	F2	149.8	77.4	40.5	546.2	142.9
L	F1	38.2	21.4	14.0	114.4	30.8
	F2	26.4	17.7	8.2	111.5	20.2

DOPPLER RESULTS – 6 MONTHS

CASE	PROBE	MEAN	STD	MIN	MAX	MEDIAN
A7 R	F1	123.2	25.6	85.4	228.8	114.1
	F2	37.6	17.2	18.9	117.1	29.9
L	F1	32.4	19.9	11.6	242.9	25.0
	F2	31.8	20.0	9.5	193.0	24.3
A8 R	F1	126.8	30.7	82.2	265.7	115.3
	F2	37.9	17.2	18.3	123.4	30.1
L	F1	33.2	16.4	16.2	107.1	27.6
	F2	32.9	29.0	12.3	190.2	21.6
A9 R	F1	85.0	26.1	50.8	186.3	74.8
	F2	33.0	22.6	12.2	142.7	23.2
L	F1	55.4	30.0	26.7	176.8	42.0
	F2	47.8	21.7	23.6	136.5	38.4
A10 R	F1	89.6	31.1	46.0	282.3	71.7
	F2	26.6	19.2	11.4	103.7	21.1
L	F1	24.3	12.1	8.7	91.7	20.7
	F2	19.8	11.5	4.4	80.0	16.6
A11 R	F1	54.6	56.6	11.7	503.1	32.6
	F2	21.9	21.8	4.5	140.5	13.1
L	F1	30.2	19.7	10.9	139.4	22.0
	F2	31.4	19.8	12.0	135.9	23.9
A12 R	F1	112.5	27.6	61.2	276.5	107.5
	F2	38.1	15.7	13.6	124.3	33.8
L	F1	43.6	19.1	23.0	154.9	36.7
	F2	46.4	19.4	24.4	165.0	40.6

DOPPLER RESULTS – 6 MONTHS (B)

CASE	PROBE	MEAN	STD	MIN	MAX	MEDIAN
B1 R	F1	169.1	53.3	83.7	287.3	163.8
	F2	89.1	57.4	26.8	174.7	80.6
L	F1	91.9	44.6	27.0	159.5	75.5
	F2	89.3	25.8	36.1	166.5	84.7
B2 R	F1	154.9	16.5	107.4	306.4	154.6
	F2	38.5	30.3	12.1	295.4	26.9
L	F1	58.0	23.9	20.0	162.5	52.3
	F2	45.7	29.6	12.5	185.5	33.1
B3 R	F1	147.4	37.2	78.9	313.8	135.7
	F2	38.9	33.3	11.9	350.5	24.7
L	F1	41.2	18.7	21.2	121.2	33.4
	F2	26.2	20.4	7.8	116.2	16.9
B4 R	F1	205.0	46.4	108.3	643.8	195.3
	F2	49.7	29.1	24.3	265.2	37.2
L	F1	48.6	21.1	22.8	180.8	43.1
	F2	36.9	16.7	14.8	101.4	32.0
B5 R	F1	80.9	29.7	37.3	264.8	74.3
	F2	47.3	22.9	21.4	177.7	39.5
L	F1	53.2	25.8	22.7	229.5	46.4
	F2	35.2	23.4	11.0	165.3	26.7
B6 R	F1	183.6	26.5	134.4	396.9	176.9
	F2	42.2	26.1	14.3	165.5	32.0
L	F1	58.5	28.9	22.3	171.3	47.8
	F2	50.4	33.8	18.2	227.7	35.7

DOPPLER RESULTS – 6 MONTHS

CASE	PROBE	MEAN	STD	MIN	MAX	MEDIAN
B7 R	F1	155.5	67.8	65.2	734.4	138.7
	F2	62.3	49.0	16.3	487.4	45.2
L	F1	77.4	55.9	19.2	332.8	54.2
	F2	61.9	37.4	20.1	241.3	46.7
B8 R	F1	142.2	40.4	67.5	387.1	138.2
	F2	40.4	27.9	13.8	234.9	30.2
L	F1	38.2	30.0	12.2	237.2	27.5
	F2	34.3	26.2	10.0	183.2	24.3
B9 R	F1	133.0	28.3	0.0	272.5	127.9
	F2	34.6	21.2	0.0	146.1	26.0
L	F1	48.2	34.6	14.9	222.3	32.2
	F2	45.1	25.5	17.4	149.5	35.0
B10 R	F1	118.5	39.3	42.3	296.9	111.4
	F2	115.4	39.1	62.1	285.8	102.9
L	F1	57.4	18.3	0.0	133.8	54.4
	F2	56.7	27.1	0.0	324.4	52.5
B11 R	F1	107.6	27.4	60.2	496.9	102.5
	F2	45.2	27.1	17.8	267.6	33.7
L	F1	32.8	12.7	15.2	98.0	28.8
	F2	30.1	13.0	13.9	100.4	25.9
B12 R	F1	117.7	25.6	78.0	368.6	111.0
	F2	34.3	21.1	15.3	260.1	26.0
L	F1	46.3	19.0	19.2	129.3	40.4
	F2	43.0	24.0	17.4	159.2	33.5

DOPPLER RESULTS – 6 MONTHS (C)

CASE	PROBE	MEAN	STD	MIN	MAX	MEDIAN
C1 R	F1	33.6	14.8	17.0	71.0	28.5
	F2	28.4	15.4	13.0	74.0	23.1
L	F1	37.4	12.2	20.0	71.0	35.2
	F2	31.2	9.3	19.0	61.0	30.3
C2 R	F1	40.5	11.3	26.0	68.0	38.0
	F2	31.2	10.9	14.0	55.0	29.0
L	F1	32.8	6.3	24.0	51.0	31.0
	F2	30.7	10.3	21.0	60.0	26.5
C3 R	F1	47.2	11.1	28.0	78.0	46.0
	F2	43.6	12.9	28.0	86.0	39.0
L	F1	36.4	13.4	19.0	68.0	33.4
	F2	31.1	10.9	17.0	61.0	28.0
C4 R	F1	35.9	7.7	26.0	55.0	34.0
	F2	28.1	11.5	16.0	50.0	22.0
L	F1	35.5	9.2	20.0	52.0	37.0
	F2	29.4	10.3	17.0	50.0	27.0
C5 R	F1	Died				
	F2					
L	F1					
	F2					
C6 R	F1	34.7	4.7	25.0	44.0	33.5
	F2	22.7	7.1	17.0	44.0	20.0
L	F1	27.9	7.3	19.0	46.0	25.5
	F2	23.8	12.5	10.0	49.0	20.0

DOPPLER RESULTS – 6 MONTHS

CASE	PROBE	MEAN	STD	MIN	MAX	MEDIAN
C7 R	F1	78.2	48.6	24.8	401.5	55.9
	F2	67.7	34.4	21.7	241.3	55.3
L	F1	71.0	16.4	38.2	205.4	57.8
	F2	50.6	12.5	29.1	129.1	46.9
C8 R	F1	95.8	33.0	59.9	252.8	80.7
	F2	92.0	36.0	54.3	241.3	75.1
L	F1	88.2	28.6	44.2	227.9	78.1
	F2	83.7	33.0	43.5	272.6	70.5
C9 R	F1	108.1	40.9	60.0	345.4	94.6
	F2	104.1	27.7	70.2	244.5	94.5
L	F1	53.2	32.9	17,2	204.2	36.8
	F2	51.4	29.6	18.1	194.9	36.5
C10 R	F1	42.2	19.6	16.8	233.8	36.8
	F2	32.0	14.7	11.7	160.3	27.2
L	F1	26.8	12.2	10.1	87.0	22.4
	F2	22.8	11.3	9.2	83.2	18.1
C11 R	F1	50.7	25.5	23.9	157.5	39.7
	F2	48.7	18.2	24.1	136.8	42.2
L	F1	34.9	17.9	15.5	137.1	28.5
	F2	27.0	11.8	12.5	106.7	23.2
C12 R	F1	41.4	17.7	23.2	141.8	35.2
	F2	32.4	12.8	10.2	147.0	19.6
L	F1	23.7	12.9	10.2	147.0	19.6
	F2	18.3	17.1	2.8	167.1	12.7

DOPPLER RESULTS – 6 MONTHS (D)

CASE	PROBE	MEAN	STD	MIN	MAX	MEDIAN
D1 R	F1	48.4	9.8	29.0	71.0	48.0
	F2	44.9	11.2	31.0	75.0	41.0
L	F1	36.4	7.8	22.0	58.0	38.0
	F2	29.8	7.5	20.0	50.0	28.5
D2 R	F1	49.9	12.8	30.0	71.0	49.0
	F2	48.6	10.4	28.0	78.0	48.0
L	F1	51.3	24.0	29.2	98.7	45.9
	F2	50.7	24.0	23.4	125.0	40.6
D3 R	F1	45.9	10.6	32.0	79.0	43.0
	F2	41.4	11.38	25.0	69.6	39.0
L	F1	38.7	13.1	18.0	72.0	35.5
	F2	36.3	11.6	20.0	67.0	33.0
D4 R	F1	35.9	10.3	21.0	102.3	53.0
	F2	34.7	13.1	19.0	76.0	31.7
L	F1	28.1	6.11	19.3	42.0	27.5
	F2	26.5	7.4	15.0	42.0	26.0
D5 R	F1	52.2	19.2	21.0	102.3	53.0
	F2	30.9	11.2	13.0	65.0	30.2
L	F1	30.1	7.43	18.0	46.0	31.0
	F2	27.0	7.39	18.0	50.0	26.0
D6 R	F1	38.2	5.4	25.0	50.0	39.0
	F2	32.4	6.2	24.0	49.0	30.5
L	F1	35.6	5.5	23.0	45.0	35.0
	F2	26.7	6.6	19.0	40.0	23.0

DOPPLER RESULTS – 6 MONTHS

CASE	PROBE	MEAN	STD	MIN	MAX	MEDIAN
D7 R	F1	87.8	49.1	35.1	257.1	65.3
	F2	69.9	31.1	32.5	176.7	54.8
L	F1	86.8	44.4	32.6	246.5	66.3
	F2	57.3	17.9	30.1	137.2	50.6
D8 R	F1	118.3	41.4	68.2	709.3	106.4
	F2	108.3	32.6	68.1	579.8	101.1
L	F1	99.3	61.7	30.7	335.8	63.9
	F2	77.8	39.1	35.7	231.8	57.8
D9 R	F1	69.4	20.0	39.5	163.7	62.5
	F2	61.1	25.9	27.1	172.6	52.0
L	F1	50.6	8.0	42.4	69.1	48.0
	F2	42.1	5.0	32.8	50.4	41.4
D10 R	F1	92.5	12.2	72.0	138.4	89.9
	F2	83.1	14.7	54.4	131.8	80.6
L	F1	42.5	18.2	18.2	118.7	34.9
	F2	41.4	12.3	22.7	101.3	37.5
D11 R	F1	50.1	34.8	9.2	222.5	40.4
	F2	33.6	27.7	5.8	194.2	20.5
L	F1	30.3	12.0	11.7	82.6	26.4
	F2	26.0	14.1	8.4	104.7	20.4
D12 R	F1	50.9	14.8	27.0	117.5	46.2
	F2	45.9	23.8	16.8	162.4	34.3
L	F1	42.0	19.7	0.0	156.6	34.8
	F2	33.3	14.4	0.0	110.8	28.9

DOPPLER RESULTS – 6 WEEKS (A)

CASE	PROBE	MEAN	STD	MIN	MAX	MEDIAN
AG R	F1	147.3	81.6	40.0	565.8	134.1
	F2	28.2	18.4	10.1	225.5	23.5
L	F1	23.5	18.9	5.7	187.4	14.0
	F2	22.2	14.5	8.1	140.4	18.3
AH R	F1	90.1	19.6	47.3	173.9	85.3
	F2	64.1	16.6	28.8	141.8	62.1
L	F1	37.2	19.0	11.1	314.4	32.4
	F2	34.5	18.4	12.1	218.8	29.8
AJ R	F1	111.3	31.9	24.0	290.8	103.8
	F2	50.9	38.6	20.2	275.7	24.7
L	F1	67.0	39.8	23.9	278.7	49.4
	F2	61.0	29.5	25.4	203.4	48.8
AK R	F1	114.7	16.8	79.8	233.2	111.6
	F2	28.2	12.6	36.3	42.7	37.1
L	F1	23.6	15.6	6.3	129.8	19.0
	F2	16.1	9.9	4.8	82.2	12.8
AL R	F1	89.1	39.1	32.7	217.6	81.1
	F2	57.9	19.5	25.2	150.9	53.2
L	F1	35.9	28.2	11.6	266.9	24.0
	F2	30.0	20.3	11.5	173.9	22.2
AM R	F1	219.1	62.3	107.3	427.0	209.0
	F2	25.1	13.1	7.1	121.1	21.5
L	F1	28.2	19.6	11.5	199.6	22.3
	F2	21.5	10.7	10.9	144.6	18.0

DOPPLER RESULTS – 6 WEEKS (B)

CASE	PROBE	MEAN	STD	MIN	MAX	MEDIAN
BG R	F1	166.1	35.8	55.7	252.8	166.9
	F2	54.2	25.4	23.2	257.9	47.2
L	F1	45.7	24.0	16.4	253.6	37.3
	F2	42.4	22.8	15.9	231.2	34.9
BH R	F1	115.2	18.8	79.0	266.1	111.8
	F2	34.9	25.0	12.9	199.2	25.4
L	F1	29.9	23.0	8.3	298.0	21.6
	F2	22.9	19.5	5.7	289.2	16.4
BJ R	F1	187.2	17.7	144.6	424.1	185.2
	F2	72.3	42.4	26.0	726.6	60.2
L	F1	78.7	39.7	27.9	404.9	66.9
	F2	77.2	36.2	18.9	370.6	68.5
BK R	F1	178.5	34.6	101.0	442.5	174.8
	F2	38.9	19.6	18.8	322.7	32.0
L	F1	42.1	28.5	17.7	636.4	37.1
	F2	40.4	37.9	15.6	796.8	31.4
BL R	F1	214.8	40.8	145.0	808.4	202.5
	F2	64.5	31.0	30.8	357.7	54.9
L	F1	76.3	29.5	28.8	265.3	70.1
	F2	69.7	29.7	28.5	326.2	61.7
BM R	F1	126.6	15.8	84.9	210.5	125.1
	F2	50.8	27.4	17.0	237.7	43.1
L	F1	55.9	49.7	16.2	888.6	41.5
	F2	52.6	40.8	21.4	882.0	41.7

DOPPLER RESULTS – 6 WEEKS (C)

CASE	PROBE	MEAN	STD	MIN	MAX	MEDIAN
CA R	F1	29.4	23.4	4.6	130.0	17.1
	F2	21.6	13.4	7.5	257.6	15.8
L	F1	19.4	13.3	4.6	116.5	14.9
	F2	18.7	11.7	6.3	88.2	14.5
CB R	F1	63.6	19.5	32.0	132.9	56.3
	F2	31.9	22.2	8.1	119.1	20.8
L	F1	42.6	22.8	15.7	495.9	37.3
	F2	31.6	19.2	9.9	423.2	27.1
CC R	F1	58.4	16.2	26.4	116.9	57.8
	F2	43.6	23.6	16.6	163.7	32.9
L	F1	57.6	40.3	19.3	852.7	46.7
	F2	47.2	30.6	14.8	342.6	35.7
CD R	F1	42.5	14.2	20.1	140.3	37.9
	F2	32.6	11.6	16.2	104.0	28.3
L	F1	26.6	13.5	10.9	147.7	21.3
	F2	19.7	10.8	7.5	86.2	15.5
CE R	F1	49.7	13.4	24.1	118.5	46.2
	F2	44.3	12.7	21.0	99.0	40.7
L	F1	28.3	13.5	7.4	143.8	24.1
	F2	26.9	14.7	8.3	182.0	21.1
CF R	F1	52.4	15.2	27.4	146.7	48.0
	F2	55.8	26.1	8.6	183.4	52.3
L	F1	23.1	19.6	3.8	117.7	14.8
	F2	19.0	15.6	1.9	101.9	12.5

DOPPLER RESULTS – 6 WEEKS

CASE	PROBE	MEAN	STD	MIN	MAX	MEDIAN
CG R	F1	59.8	24.5	19.0	309.0	55.7
	F2	57.4	30.0	14.8	281.4	49.2
L	F1	29.7	13.5	23.8	126.1	47.0
	F2	48.5	16.0	20.1	158.6	45.2
CH R	F1	56.8	41.9	15.1	335.5	36.2
	F2	55.2	23.2	18.8	203.4	48.9
L	F1	47.4	18.3	20.9	122.5	41.2
	F2	42.1	23.2	15.1	128.2	31.5
CJ R	F1	51.6	30.0	17.5	201.6	38.0
	F2	50.2	36.5	14.7	194.1	32.6
L	F1	46.8	28.0	14.5	189.5	36.2
	F2	45.6	30.4	13.8	188.0	32.6
CK R	F1	53.9	36.7	17.2	539.0	39.4
	F2	50.1	28.1	13.7	352.1	39.9
L	F1	38.3	19.9	17.1	143.7	31.6
	F2	33.1	17.2	15.6	141.2	27.3
CL R	F1	48.6	37.5	9.8	341.7	31.2
	F2	41.7	34.4	7.5	267.0	25.2
L	F1	26.4	28.0	4.5	413.1	17.2
	F2	22.2	20.6	3.4	190.9	14.4
CM R	F1	64.2	25.8	33.4	213.7	54.3
	F2	55.4	20.7	27.7	177.1	48.0
L	F1	41.3	26.2	12.8	188.3	28.5
	F2	36.2	19.0	13.0	160.3	26.7

DOPPLER RESULTS – 6 WEEKS (D)

CASE	PROBE	MEAN	STD	MIN	MAX	MEDIAN
DA R	F1	64.9	50.6	17.1	349.9	42.8
	F2	49.9	24.2	20.7	192.2	39.6
L	F1	46.0	17.3	23.1	164.9	38.4
	F2	41.0	61.5	5.2	879.2	22.8
DB R	F1	49.2	30.9	13.5	203.4	34.7
	F2	45.4	18.4	21.6	139.9	38.3
L	F1	22.7	17.6	4.0	128.9	14.9
	F2	21.6	11.4	7.7	79.0	17.8
DC R	F1	50.9	27.1	13.8	209.1	42.7
	F2	43.4	20.1	13.2	179.1	37.4
L	F1	30.8	22.4	5.5	123.2	20.8
	F2	21.4	18.4	5.7	100.4	12.2
DD R	F1	41.0	24.4	13.2	165.6	31.8
	F2	27.0	17.2	7.5	107.8	20.4
L	F1	27.2	12.6	10.4	73.9	22.5
	F2	26.5	20.4	3.9	101.5	16.5
DE R	F1	38.4	22.1	12.4	144.1	29.6
	F2	28.3	19.8	6.4	137.1	19.2
L	F1	29.5	20.6	8.5	120.3	20.8
	F2	20.2	17.7	5.6	95.5	11.6
DF R	F1	56.1	37.3	15.7	217.5	38.9
	F2	41.9	30.6	13.5	198.9	30.6
L	F1	40.6	29.8	16.9	158.2	31.5
	F2	39.4	24.2	14.7	145.9	26.9

DOPPLER RESULTS – 6 WEEKS

CASE	PROBE	MEAN	STD	MIN	MAX	MEDIAN
DG R	F1	73.5	19.3	33.4	162.0	72.4
	F2	63.9	24.7	29.4	200.1	55.0
L	F1	66.4	26.6	31.7	267.7	56.2
	F2	62.2	23.5	27.1	300.6	54.6
DH R	F1	55.1	43.2	12.7	392.2	37.4
	F2	49.7	38.8	12.4	470.6	34.5
L	F1	47.4	48.9	10.2	850.4	30.5
	F2	44.9	24.2	13.0	504.0	41.0
DJ R	F1	51.9	23.0	23.2	213.8	44.9
	F2	39.7	17.3	15.4	141.8	35.2
L	F1	41.2	22.1	18.0	377.3	34.5
	F2	38.1	33.8	11.6	630.1	28.3
DK R	F1	65.5	48.9	20.5	462.0	54.8
	F2	59.3	21.3	26.2	317.5	56.9
L	F1	52.1	27.8	27.3	225.6	41.2
	F2	47.5	19.8	28.0	151.2	39.7
DL R	F1	59.3	85.4	6.0	644.3	27.6
	F2	46.9	11.4	22.6	111.6	44.8
L	F1	51.7	29.0	13.5	185.0	40.4
	F2	39.4	20.7	15.8	143.0	32.0
DM R	F1	45.6	14.4	25.4	127.6	40.5
	F2	38.1	19.7	16.2	129.6	29.8
L	F1	26.1	21.9	4.1	125.6	14.5
	F2	23.8	11.4	9.7	68.6	18.5

DOPPLER RESULTS – 6 WEEKS (N)

CASE	PROBE	MEAN	STD	MIN	MAX	MEDIAN
N1 R	F1	29.5	19.7	9.2	212.7	22.7
	F2	26.9	16.9	9.6	187.4	21.2
L	F1	24.7	13.6	8.4	194.3	20.4
	F2	24.2	15.7	9.4	295.6	19.2
N2 R	F1	46.1	21.5	16.2	183.3	38.2
	F2	42.4	19.1	13.8	128.1	35.8
L	F1	42.2	18.7	19.5	127.0	36.6
	F2	40.2	22.8	14.3	163.2	32.4
N3 R	F1	68.2	21.1	33.7	310.8	65.1
	F2	59.2	27.5	18.6	409.8	55.0
L	F1	61.2	26.1	23.1	441.0	59.2
	F2	56.8	26.2	18.8	451.1	52.5
N4 R	F1	61.4	28.8	20.2	228.6	51.2
	F2	54.5	22.5	7.6	147.4	47.1
L	F1	51.5	18.7	28.7	189.3	45.8
	F2	48.4	27.9	17.2	366.3	40.9
N5 R	F1	54.2	31.4	16.8	220.7	43.0
	F2	39.2	17.9	16.0	170.1	33.5
L	F1	51.8	49.7	13.1	379.3	35.3
	F2	42.7	21.3	19.0	182.4	33.7
N6 R	F1	78.4	110.6	23.5	919.2	53.8
	F2	71.2	91.3	19.4	949.7	52.5
L	F1	72.0	57.3	15.5	385.8	44.1
	F2	70.9	53.1	26.3	593.3	50.2

DOPPLER RESULTS – 6 WEEKS

CASE	PROBE	MEAN	STD	MIN	MAX	MEDIAN
N7 R	F1	56.1	23.0	29.7	251.5	46.5
	F2	44.9	27.8	16.3	303.3	36.2
L	F1	48.8	15.7	28.1	131.0	42.8
	F2	46.3	18.8	19.8	151.6	40.6
N8 R	F1	86.1	44.2	34.5	434.5	72.0
	F2	76.3	26.2	40.1	250.8	66.2
L	F1	64.7	19.7	38.7	180.8	57.2
	F2	53.2	22.6	22.5	199.3	44.2
N9 R	F1	66.2	21.7	33.9	280.7	61.6
	F2	61.1	29.2	22.8	367.7	51.5
L	F1	61.7	40.8	18.2	272.8	46.6
	F2	62.7	46.3	18.2	588.9	46.7
N10 R	F1	65.5	34.4	22.9	488.8	56.5
	F2	60.4	23.2	26.1	412.4	55.5
L	F1	59.2	35.1	23.3	259.2	46.8
	F2	54.7	22.1	26.6	199.2	48.2
N11 R	F1	80.0	31.8	45.5	352.8	68.8
	F2	69.4	28.3	37.0	316.8	58.8
L	F1	73.2	35.7	37.1	484.3	62.6
	F2	70.1	41.4	30.5	585.1	55.4
N12 R	F1	55.0	28.1	13.8	172.8	50.9
	F2	48.6	27.5	19.8	204.5	37.6
L	F1	47.0	19.5	21.9	168.2	41.1
	F2	40.2	19.5	19.4	157.1	33.4

DOPPLER RESULTS – 6 WEEKS (W)

CASE	PROBE	MEAN	STD	MIN	MAX	MEDIAN
W1 R	F1	59.1	38.7	14.0	314.2	49.3
	F2	55.5	40.4	13.8	382.1	39.8
L	F1	44.3	30.2	13.8	455.6	33.7
	F2	41.2	43.9	5.3	721.3	26.6
W2 R	F1	98.6	36.1	36.0	360.7	90.1
	F2	91.0	35.4	33.5	324.2	79.6
L	F1	86.0	45.6	35.5	504.7	70.3
	F2	81.5	37.2	33.5	485.6	69.4
W3 R	F1	71.8	47.7	16.4	532.4	52.2
	F2	67.1	47.1	16.3	504.5	49.0
L	F1	50.9	19.5	28.7	243.8	44.4
	F2	46.0	23.0	19.0	331.5	38.2
W4 R	F1	87.0	50.4	31.2	280.6	62.0
	F2	74.8	35.7	32.5	224.6	57.4
L	F1	80.5	37.7	36.6	219.8	61.6
	F2	67.2	36.1	20.7	206.5	48.6
W5 R	F1	88.2	45.0	26.9	270.1	74.1
	F2	73.6	36.9	23.2	236.4	59.8
L	F1	71.8	40.9	0.0	219.9	52.2
	F2	68.1	34.6	0.0	211.8	54.6
W6 R	F1	81.9	25.9	21.1	468.7	62.2
	F2	56.0	25.9	21.1	100.0	47.4
L	F1	44.1	27.2	7.9	247.7	36.5
	F2	37.9	31.2	3.5	365.1	27.5

DOPPLER RESULTS – 6 WEEKS

CASE	PROBE	MEAN	STD	MIN	MAX	MEDIAN
W7 R	F1	76.8	29.7	0.0	233.7	68.5
	F2	57.1	23.7	0.0	192.2	47.4
L	F1	53.9	24.0	23.0	167.4	44.4
	F2	45.4	17.6	10.6	129.7	39.3
W8 R	F1	53.2	52.9	0.0	523.6	31.0
	F2	52.7	39.4	0.0	420.4	34.8
L	F1	53.0	20.6	24.8	212.8	44.8
	F2	43.0	16.3	19.6	125.7	37.0
W9 R	F1	61.6	33.6	16.8	333.1	49.2
	F2	60.2	25.6	15.5	236.2	54.0
L	F1	54.5	23.0	21.0	148.8	45.8
	F2	52.4	10.5	17.9	136.7	42.9
W10 R	F1	73.1	26.0	25.3	187.5	65.2
	F2	54.7	27.8	22.5	230.7	43.6
L	F1	49.0	19.1	27.4	147.2	42.9
	F2	48.9	28.5	17.5	203.6	38.8
W11 R	F1	83.4	31.6	31.7	208.6	82.2
	F2	56.8	25.5	13.9	157.2	50.6
L	F1	42.3	26.6	12.9	166.5	32.8
	F2	38.5	19.2	11.3	127.4	32.4
W12 R	F1	84.0	21.0	48.6	180.7	79.8
	F2	73.3	28.7	32.8	284.8	65.6
L	F1	53.0	29.4	12.0	200.1	43.5
	F2	43.6	25.2	10.0	158.9	34.3

DOPPLER RESULTS – 6 WEEKS (S)

CASE	PROBE	MEAN	STD	MIN	MAX	MEDIAN
S1 R	F1	75.9	29.3	36.4	280.7	66.4
	F2	61.5	30.2	22.1	200.5	49.3
L	F1	64.3	31.5	23.2	224.2	52.0
	F2	57.4	21.5	26.3	163.6	49.8
S2 R	F1	84.1	27.5	40.8	287.4	76.7
	F2	57.9	33.1	16.4	260.5	44.6
L	F1	71.7	31.4	31.7	190.8	58.3
	F2	70.7	35.2	28.4	224.7	55.1
S3 R	F1	83.4	31.0	41.8	204.7	73.6
	F2	72.8	44.1	18.0	217.6	55.8
L	F1	57.8	38.6	14.6	218.6	38.2
	F2	51.6	28.7	15.1	176.1	37.6
S4 R	F1	64.0	31.6	22.9	176.8	49.7
	F2	52.5	21.6	21.0	146.0	43.8
L	F1	56.2	25.6	21.2	311.8	48.3
	F2	49.0	18.8	16.6	188.7	43.9
S5 R	F1	68.1	34.4	0.0	252.8	56.8
	F2	51.9	35.0	0.0	304.0	50.1
L	F1	53.5	24.9	12.4	152.0	45.3
	F2	52.2	25.1	16.4	154.8	44.4
S6 R	F1	60.9	27.8	18.5	220.4	53.1
	F2	47.1	29.8	6.8	462.4	38.9
L	F1	56.4	24.1	16.9	148.2	47.4
	F2	55.0	22.9	20.5	135.8	47.3

DOPPLER RESULTS – 6 WEEKS

CASE	PROBE	MEAN	STD	MIN	MAX	MEDIAN
S7 R	F1	39.7	33.1	0.0	138.5	26.4
	F2	36.1	30.6	0.0	149.2	143.5
L	F1	33.4	23.8	4.2	186.4	26.5
	F2	27.3	18.0	4.6	142.4	22.7
S8 R	F1	97.2	54.6	24.9	412.2	87.7
	F2	83.3	38.0	19.2	265.9	80.9
L	F1	73.8	34.6	22.2	200.0	62.5
	F2	62.0	21.7	23.9	166.6	56.0
S9 R	F1	79.5	24.2	38.1	163.7	77.2
	F2	75.8	25.9	29.7	168.0	76.2
L	F1	56.4	27.3	20.5	306.7	46.7
	F2	49.0	35.8	15.3	457.0	36.8
S10 R	F1	64.7	17.2	27.2	151.5	62.3
	F2	63.5	21.1	31.7	159.2	57.9
L	F1	53.0	33.8	17.0	204.7	41.4
	F2	50.7	27.6	16.5	162.9	39.2
S11 R	F1	82.5	16.2	56.6	176.1	77.9
	F2	76.4	10.5	55.7	180.1	74.0
L	F1	64.6	23.2	31.8	206.5	56.9
	F2	64.4	22.7	25.2	178.3	100.5
S12 R	F1	86.3	57.1	21.1	445.5	81.3
	F2	85.8	44.4	29.3	406.8	79.5
L	F1	76.9	9.6	56.6	121.3	74.3
	F2	72.2	15.9	47.6	172.9	67.1

DOPPLER RESULTS – 6 WEEKS (T)

CASE	PROBE	MEAN	STD	MIN	MAX	MEDIAN
T1 R	F1	Died				
	F2					
L	F1					
	F2					
T2 R	F1	Died				
	F2					
L	F1					
	F2					
T3 R	F1	82.1	29.8	38.6	181.2	69.1
	F2	44.6	30.3	12.7	161.2	30.0
L	F1	59.0	10.7	27.8	85.4	58.8
	F2	54.5	19.4	19.3	317.5	50.4
T4 R	F1	88.5	16.9	46.5	169.0	87.1
	F2	34.8	15.7	10.3	109.9	87.1
L	F1	43.4	16.2	19.4	171.9	30.9
	F2	40.8	16.4	18.8	191.6	36.2
T5 R	F1	116.8	49.6	26.9	375.0	100.9
	F2	45.1	25.2	9.7	907.0	36.6
L	F1	35.5	13.7	15.8	145.0	31.9
	F2	34.0	9.0	19.8	95.5	31.9
T6 R	F1	125.1	18.7	95.6	658.3	122.0
	F2	34.7	17.1	13.2	459.1	31.2
L	F1	23.4	12.5	9.0	186.2	18.9
	F2	22.2	15.0	8.4	222.5	16.3

Doppler Results – 6 Weeks

Case	Probe	Mean	Std	Min	Max	Median
T7 R	F1	80.8	40.5	42.7	583.2	69.5
	F2	60.3	37.2	15.1	627.8	52.8
L	F1	32.5	24.8	9.3	368.1	21.2
	F2	32.5	33.0	8.2	473.7	22.2
T8 R	F1	81.2	64.0	34.0	536.5	63.6
	F2	31.3	74.6	1.9	726.9	9.9
L	F1	26.9	25.5	7.0	453.5	21.5
	F2	23.3	28.9	5.5	436.4	16.1
T9 R	F1	66.8	24.7	41.3	573.9	60.9
	F2	34.5	41.3	9.2	873.6	24.0
L	F1	20.6	12.5	8.1	199.3	17.5
	F2	17.8	11.4	6.3	188.3	14.4
T10 R	F1	75.8	18.4	26.5	248.0	72.5
	F2	24.2	11.3	9.3	150.9	20.4
L	F1	14.3	13.6	9.0	186.2	19.3
	F2	23.4	16.6	7.3	222.5	16.5
T11 R	F1	112.3	76.9	15.6	609.8	84.7
	F2	85.0	42.3	26.3	573.7	75.0
L	F1	32.6	15.8	12.2	122.3	26.8
	F2	28.0	14.0	10.4	121.5	22.8
T12 R	F1	132.4	26.1	38.5	232.5	132.5
	F2	74.9	21.9	35.4	205.6	67.0
L	F1	46.9	33.4	11.6	183.4	31.6
	F2	36.5	26.6	8.3	157.0	23.1

APPENDIX 8

PICO RESULTS – 6 MONTHS

CASE	D max	D ½ rel		V max	V zero	V min	
	mm			mms^{-1}			
	time	time	Tt	time	time	time	t0Accel
	s			s			s
A1 R	5.34	2.67	0.82	127.04	0.00	-15.68	
	0.09	0.38	0.71	0.009	0.13	0.36	0.3585
L	5.87	2.93	0.71	135.27	0.79	-19.02	
	0.08	0.37	0.76	0.01	0.11	0.37	0.3699
A2 R	4.76	2.38	0.88	117.79	1.32	-12.57	
	0.10	0.44	0.79	0.009	0.11	0.39	0.1424
L	4.86	2.43	0.55	130.12	0.11	-13.79	
	0.15	0.39	0.80	0.009	0.13	0.33	0.3304
A3 R	4.91	2.46	1.12	111.45	0.34	-12.52	
	0.32	0.55	0.90	0.009	0.10	0.48	0.1324
L	5.01	2.56	0.35	125.34	-2.06	-11.83	
	0.09	0.32	0.77	0.009	0.09	0.14	0.1509
A4 R	Died						
L							
A5 R	3.63	1.82	0.21	63.09	0.58	-10.23	
	0.19	0.47	1.10	0.016	0.45	0.46	0.4716
L	3.63	1.82	0.13	72.72	0.50	-8.38	
	0.09	0.43	0.90	0.014	0.13	0.43	0.4412
A6 R	3.50	1.75	0.36	112.76	0.47	-12.85	
	0.15	0.38	0.79	0.009	0.08	0.34	0.0996
L	4.55	2.28	0.78	114.24	0.48	-15.47	
	0.18	0.35	0.78	0.009	0.15	0.30	0.3043

PICO RESULTS – 6 MONTHS

CASE	D max (mm)	D ½ rel (mm)		V max (mms^{-1})	V zero (mms^{-1})	V min (mms^{-1})	
	time (s)	time (s)	T t	time (s)	time (s)	time (s)	t0Accel (s)
A7 R	3.07	1.53	0.56	80.63	0.88	-10.88	
	0.33	0.49	0.72	0.007	0.11	0.44	0.1544
L	3.12	1.56	0.51	71.10	0.27	-11.80	
	0.26	0.46	0.60	0.006	0.10	0.43	0.1281
A8 R	3.83	1.92	0.45	126.16	0.57	-16.90	
	0.16	0.31	0.50	0.005	0.14	0.30	0.3039
L	4.70	2.35	0.02	143.76	-0.93	-18.45	
	0.09	0.29	0.69	0.008	0.09	0.29	0.2814
A9 R	3.13	1.57	0.13	96.02	0.32	-13.79	
	0.23	0.36	0.79	0.009	0.09	0.34	0.1018
L	3.14	1.57	0.17	105.10	0.53	-9.80	
	0.08	0.28	0.61	0.008	0.07	0.31	0.1117
A10 R	3.57	1.79	0.45	76.18	0.46	-10.49	
	0.39	0.61	0.95	0.009	0.19	0.58	0.2143
L	3.88	1.94	0.54	80.20	-0.46	-7.26	
	0.16	0.61	0.93	0.009	0.14	0.61	0.2189
A11 R	4.21	2.15	0.79	57.7	0.98	-10.6	
	0.37	0.62	0.89	0.009	0.14	0.58	0.1711
L	2.77	1.39	0.33	61.89	0.004	-6.03	
	0.24	0.48	0.89	0.009	0.22	0.41	0.4099
A12 R	3.00	1.50	0.51	62.73	0.06	-11.3	
	0.27	0.42	0.84	0.009	0.24	0.39	0.1312
L	4.05	2.03	0.40	100.91	0.29	-11.07	
	0.19	0.43	0.86	0.009	0.17	0.38	0.3663

PICO RESULTS – 6 MONTHS

CASE	D max (mm)	D ½ rel		V max (mms^{-1})	V zero	V min	
	time (s)	time (s)	Tt	time (s)	time (s)	time (s)	t0Accel (s)
B1 R	5.23	2.62	0.59	121.47	0.37	-12.46	
	0.12	0.37	0.86	0.009	0.09	0.16	0.1693
L	3.35	1.77	0.19	88.39	0.29	-6.52	
	0.09	0.42	0.96	0.009	0.09	0.14	0.1386
B2 R	1.61	0.81	-0.99	33.7	0.24	-8.5	
	0.25	0.39	0.92	0.009	0.10	0.40	0.1164
L	2.34	1.17	-0.69	55.7	-0.82	-8.06	
	0.08	0.33	0.80	0.009	0.09	0.35	0.1369
B3 R	3.86	1.93	0.45	104.98	0.11	-8.95	
	0.22	0.46	0.88	0.009	0.09	0.39	0.1082
L	3.49	1.75	0.29	79.48	0.17	-13.34	
	0.02	0.25	0.72	0.009	0.04	0.07	0.0722
B4 R	3.83	1.92	0.35	101.6	0.13	-10.07	
	0.17	0.40	0.89	0.009	0.19	0.35	0.1394
L	3.27	1.64	0.12	88.3	-0.91	-9.7	
	0.01	0.36	0.81	0.009	0.09	0.36	0.1195
B5 R	5.17	2.59	1.57	67.22	0.25	-14.63	
	0.13	0.59	0.99	0.019	0.12	0.18	0.1796
L	4.31	2.16	0.75	94.79	1.02	-9.69	
	0.10	0.35	0.61	0.009	0.09	0.36	0.1793
B6 R	3.08	1.54	0.20	83.09	1.30	-8.68	
	0.09	0.29	0.73	0.009	0.08	0.28	0.1689
L	4.76	2.38	0.31	104.5	0.67	-9.58	
	0.12	0.39	0.86	0.009	0.11	0.41	0.1892

PICO RESULTS – 6 MONTHS

CASE	D max	D ½ rel		V max	V zero	V min	
	mm			mms^{-1}			
	s			s			s
	time	time	Tt	time	time	time	t0Accel
B7 R	3.64	1.82	0.38	88.89	0.12	-10.96	
	0.13	0.36	0.88	0.01	0.13	0.35	0.3507
L	3.86	1.93	0.09	101.44	-1.00	-11.25	
	0.09	0.29	0.74	0.01	0.10	0.28	0.2705
B8 R	4.10	2.05	0.42	98.24	0.70	-12.96	
	0.16	0.42	0.84	0.009	0.13	0.41	0.1452
L	4.65	2.33	0.31	122.43	0.65	-21.24	
	0.09	0.34	0.74	0.008	0.09	0.34	0.1306
B9 R	3.83	1.92	0.19	93.80	0.30	-14.8	
	0.17	0.32	0.69	0.009	0.12	0.31	0.3098
L	4.50	2.75	0.20	108.08	0.70	-19.27	
	0.10	0.21	0.61	0.008	0.09	0.18	0.1835
B10 R	3.62	1.81	0.22	95.17	0.05	-11.6	
	0.14	0.38	0.82	0.009	0.16	0.35	0.3506
L	3.50	1.75	0.17	69.33	0.37	-15.24	
	0.14	0.36	0.67	0.008	0.18	0.34	0.3275
B11 R	4.09	2.05	0.59	96.68	0.63	-13.64	
	0.19	0.40	0.78	0.008	0.14	0.36	0.3648
L	4.44	2.22	0.32	121.38	0.02	-15.6	
	0.09	0.42	0.85	0.009	0.11	0.39	0.1439
B12 R	1.95	0.98	0.09	54.29	0.02	-8.32	
	0.23	0.36	0.72	0.008	0.18	0.33	0.1236
L	2.51	1.26	0.22	31.6	0.13	-8.20	
	0.16	0.43	0.78	0.004	0.16	0.40	0.0417

PICO RESULTS – 6 MONTHS

CASE	D max time (mm s)	D ½ rel time (mm s)	Tt	V max time (mms^{-1} s)	V zero time (mms^{-1} s)	V min time (mms^{-1} s)	t0Accel (s)
C1 R	2.95	1.48	0.03	42.71	0.25	-8.67	
	0.22	0.46	1.19	0.02	0.20	0.44	0.4357
L	3.11	1.56	0.13	30.75	0.14	-5.86	
	0.04	0.63	1.40	0.02	0.28	0.57	0.5730
C2 R	3.02	1.51	0.15	32.20	0.20	-8.33	
	0.23	0.42	1.33	0.02	0.19	0.34	0.3397
L	4.09	2.05	0.32	36.93	0.40	-12.61	
	0.19	0.39	0.86	0.03	0.19	0.31	0.1187
C3 R	3.02	1.56	0.12	40.85	0.40	-8.2	
	0.19	0.41	1.12	0.02	0.17	0.32	0.3201
L	4.16	2.08	0.15	66.39	0.25	-10.72	
	0.14	0.36	0.90	0.02	0.13	0.32	0.2843
C4 R	2.66	1.33	0.42	39.24	0.22	-5.14	
	0.30	0.55	1.37	0.02	0.22	0.50	0.4978
L	2.76	1.38	0.03	40.77	0.31	-8.55	
	0.25	0.44	1.20	0.02	0.18	0.41	0.4255
C5 R	Died						
L							
C6 R	2.63	1.32	0.10	39.09	0.15	-5.89	
	0.34	0.62	1.42	0.02	0.32	0.54	0.3389
L	2.84	1.42	0.16	36.39	0.42	-7.16	
	0.22	0.53	1.19	0.02	0.23	0.48	0.1582

PICO RESULTS – 6 MONTHS

CASE	D max (mm)	D ½ rel (s)		V max (mms^{-1})	V zero (s)	V min (s)	
	time	time	Tt	time	time	time	t0Accel
C7 R	3.53	1.77	0.51	72.93	0.17	-13.46	
	0.25	0.38	0.74	0.007	0.23	0.36	0.1800
L	3.26	1.63	0.30	83.61	0.34	-12.62	
	0.19	0.56	0.68	0.009	0.16	0.35	0.1203
C8 R	4.28	2.14	0.52	74.22	0.70	-17.49	
	0.13	0.36	0.68	0.008	0,12	0.35	0.5714
L	3.25	1.63	0.10	68.78	0.43	-17.72	
	0.08	0.22	0.47	0.008	0.09	0.18	0.1579
C9 R	3.85	1.93	0.10	75.30	0.37	-16.31	
	0.28	0.49	0.77	0.009	0.13	0.47	0.4622
L	4.92	2.46	1.28	84.47	0.20	-13.50	
	0.20	0.64	0.81	0.008	0.88	0.14	0.1496
C10 R	5.02	2.15	0.13	11.37	0.80	-15.02	
	0.15	0.21	0.39	0.007	0.12	0.20	0.2046
L	3.76	1.88	0.26	86.01	0.10	-13.67	
	0.09	0.27	0.68	0.008	0.88	0.14	0.1408
C11 R	4.09	2.05	0.75	77.59	0.80	-15.02	
	0.18	0.45	0.63	0.006	0.45	0.41	0.1621
L	4.26	2.13	0.84	93.11	0.20	-8.05	
	0.09	0.60	0.94	0.009	0.13	0.50	0.1734
C12 R	3.34	1.67	0.29	77.96	0.30	-7.80	
	0.18	0.52	0.96	0.009	0.12	0.46	0.1689
L	3.99	2.00	0.38	96.78	0.36	-12.63	
	0.09	0.27	0.55	0.007	0.09	0.14	0.1389

PICO RESULTS – 6 MONTHS

CASE	D max	D ½ rel		V max	V zero	V min	
	mm			mms^{-1}			s
	s			s			
	time	time	Tt	time	time	time	t0Accel
D1 R	2.12	1.06	0.32	35.96	0.05	-3.79	
	0.13	0.56	1.60	0.02	0.14	0.51	0.5244
L	3.05	1.53	0.12	46.83	0.60	-6.9	
	0.02	0.54	1.07	0.02	0.19	0.49	0.5097
D2 R	2.98	1.49	0.14	80.06	0.01	-14.22	
	0.23	0.35	0.69	0.009	0.10	0.35	0.1069
L	3.39	1.70	0.57	81.31	0.30	-7.89	
	0.29	0.56	0.90	0.009	0.12	0.49	0.1295
D3 R	3.12	1.56	0.01	32.43	0.22	-11.23	
	0.18	0.36	0.73	0.02	0.18	0.32	0.2985
L	4.88	2.44	0.47	72.49	0.10	-8.59	
	0.14	0.51	1.05	0.02	0.12	0.52	0.2412
D4 R	3.34	1.67	0.13	56.29	0.50	-9.19	
	0.08	0.36	0.77	0.02	0.11	0.22	0.2242
L	4.17	2.09	0.21	67.06	0.50	-9.06	
	0.12	0.43	0.97	0.02	0.15	0.28	0.3038
D5 R	3.53	1.77	0.74	44.41	0.13	-6.45	
	0.36	0.61	0.14	0.02	0.24	0.55	0.5741
L	3.76	1.88	0.19	44.66	0.16	-11.78	
	0.27	0.44	0.79	0.02	0.22	0.43	0.4268
D6 R	4.86	2.43	0.25	79.47	0.97	-11.71	
	0.19	0.43	0.89	0.02	0.15	0.37	0.3682
L	4.38	2.19	0.59	71.59	0.35	-9.80	
	0.12	0.41	0.88	0.02	0.12	0.22	0.2230

PICO RESULTS – 6 MONTHS

CASE	D max time (mm/s)	D ½ rel time (mm/s)	Tt (s)	V max time (mms^{-1}/s)	V zero time (mms^{-1}/s)	V min time (mms^{-1}/s)	t0Accel (s)
D7 R	4.37	2.18	0.29	117.5	0.40	-15.56	
	0.15	0.33	0.76	0.009	0.13	0.32	0.3178
L	4.38	2.19	0.56	114.67	0.15	-12.10	
	0.11	0.41	0.71	0.007	0.10	0.35	0.3439
D8 R	3.71	1.86	0.41	70.71	0.11	-14.75	
	0.23	0.38	0.76	0.009	0.14	0.37	0.3677
L	3.67	1.84	0.29	104.86	0.05	-14.48	
	0.09	0.33	0.82	0.009	0.13	0.29	0.2841
D9 R	3.93	1.97	0.18	59.71	0.23	-12.52	
	0.11	0.37	0.77	0.02	0.12	0.39	0.1622
L	4.16	2.18	0.58	58.87	0.50	-12.66	
	0.11	0.38	0.69	0.02	0.13	0.36	0.3588
D10 R	3.44	1.72	0.36	73.97	0.50	-11.86	
	0.25	0.44	0.80	0.009	0.12	0.41	0.1467
L	3.39	1.70	0.65	90.62	0.02	-10.09	
	0.09	0.37	0.72	0.009	0.37	0.72	0.3075
D11 R	3.80	1.90	0.58	75.94	0.08	-7.42	
	0.20	0.60	0.94	0.009	0.13	0.50	0.1519
L	3.28	1.64	0.27	62.10	0.49	-11.90	
	0.16	0.49	0.76	0.009	0.18	0.46	0.1965
D12 R	3.74	1.87	0.67	74.71	0.04	-8.31	
	0.22	0.65	0.97	0.009	0.15	0.60	0.1897
L	4.06	2.03	1.30	58.44	0.30	-7.54	
	0.21	0.66	0.84	0.02	0.15	0.62	0.1654

PICO RESULTS – 6 WEEKS

CASE	D max time (mm/s)	D ½ rel time (mm/s)	Tt	V max time (mms^{-1}/s)	V zero time (mms^{-1}/s)	V min time (mms^{-1}/s)	t0Accel (s)
AG R	3.45	1.73	0.06	75.76	0.38	-16.43	
	0.23	0.39	0.71	0.008	0.12	0.37	0.1332
L	3.37	1.69	0.32	78.65	0.88	-10.90	
	0.09	0.44	0.69	0.007	0.09	0.37	0.1347
AH R	3.39	1.70	0.34	85.31	0.10	-11.28	
	0.23	0.47	0.79	0.009	0.24	0.45	0.1480
L	3.70	1.85	0.25	89.62	0.48	-11.76	
	0.07	0.44	0.83	0.009	0.12	0.42	0.1597
AJ R	3.22	1.61	0.67	85.88	0.36	-10.14	
	0.40	0.58	0.89	0.009	0.10	0.52	0.1287
L	4.39	2.19	0.29	107.41	0.41	-16.58	
	0.14	0.45	0.83	0.01	0.11	0.42	0.1308
AK R	4.26	2.13	0.17	117.85	0.18	-19.79	
	0.16	0.37	0.66	0.009	0.10	0.36	0.1206
L	4.25	2.13	0.28	115.34	0.95	-12.13	
	0.07	0.43	0.77	0.008	0.10	0.38	0.1357
AL R	4.64	2.32	0.24	122.57	0.15	-17.52	
	0.14	0.36	0.64	0.008	0.93	0.35	0.1339
L	6.04	3.02	0.47	152.59	0.94	-17.48	
	0.09	0.32	0.80	0.009	0.09	0.15	0.1461
AM R	3.58	1.79	0.25	73.21	0.19	-16.81	
	0.14	0.38	0.61	0.008	0.22	0.35	0.1309
L	3.61	1.81	0.13	76.85	0.45	-17.02	
	0.19	0.37	0.68	0.009	0.20	0.35	0.1549

PICO RESULTS – 6 WEEKS

CASE	D max time (mm/s)	D ½ rel time (mm/s)	Tt	V max time (mms^{-1}/s)	V zero time (mms^{-1}/s)	V min time (mms^{-1}/s)	t0Accel (s)
BG R	4.51	2.26	0.49	117.88	0.61	-21.13	
	0.22	0.37	0.60	0.007	0.09	0.34	0.1099
L	3.85	1.93	0.45	100.02	0.10	-13.40	
	0.10	0.41	0.72	0.008	0.11	0.38	0.1335
BH R	3.19	1.60	0.02	47.99	0.73	-15.80	
	0.19	0.43	0.68	0.004	0.11	0.40	0.1651
L	4.59	2.29	0.78	71.64	0.17	-12.64	
	0.12	0.51	0.79	0.003	0.13	0.43	0.1654
BJ R	2.83	1.42	0.17	84.42	0.07	-11.28	
	0.09	0.41	0.64	0.008	0.09	0.38	0.1166
L	3.51	1.76	0.79	100.33	0.84	-7.77	
	0.07	0.36	0.79	0.009	0.09	0.31	0.1548
BK R	6.35	3.18	0.33	140.22	1.20	-21.76	
	0.09	0.34	0.70	0.009	0.11	0.36	0.1364
L	6.39	3.19	0.39	179.29	1.10	-18.29	
	0.09	0.36	0.68	0.008	0.09	0.36	0.1335
BL R	3.15	1.58	0.54	83.10	0.42	-11.74	
	0.27	0.45	0.67	0.007	0.10	0.42	0.1291
L	3.53	1.77	0.29	98.24	0.59	-18.42	
	0.30	0.43	0.71	0.008	0.12	0.42	0.1356
BM R	3.05	1.53	0.26	91.71	0.14	-10.26	
	0.38	0.57	0.80	0.008	0.09	0.54	0.1179
L	3.58	1.79	0.29	94.79	0.58	-17.15	
	0.29	0.43	0.63	0.008	0.10	0.43	0.1335

PICO RESULTS – 6 WEEKS

CASE	D max time (mm/s)	D ½ rel time (mm/s)	Tt	V max time (mms^{-1}/s)	V zero time (mms^{-1}/s)	V min time (mms^{-1}/s)	t0Accel (s)
CA R	3.77	1.89	-0.03	36.93	0.90	-9.94	
	0.35	0.51	1.19	0.02	0.24	0.48	0.4800
L	3.67	1.84	0.07	54.35	0.80	-10.17	
	0.09	0.41	0.92	0.02	0.17	0.32	0.3055
CB R	3.79	1.90	-0.02	41.98	0.39	-9.82	
	0.33	0.49	1.18	0.02	0.22	0.47	0.4552
L	3.64	1.82	0.77	73.61	0.05	-8.96	
	0.38	0.57	1.19	0.02	0.15	0.48	0.1495
CC R	2.48	1.24	0.26	41.29	0.25	-5.99	
	0.29	0.49	0.95	0.02	0.25	0.46	0.4947
L	3.92	1.96	0.74	56.63	0.35	-8.96	
	0.18	0.61	1.07	0.02	0.29	0.55	0.5526
CD R	2.26	1.13	0.13	34.31	0.45	-5.16	
	0.38	0.61	1.16	0.17	0.21	0.56	0.2108
L	3.21	1.61	0.64	51.33	0.01	-8.10	
	0.98	0.56	0.89	0.01	0.19	0.50	0.2378
CE R	4.46	2.23	0.86	88.51	0.46	-11.09	
	0.27	0.49	0.95	0.01	0.22	0.42	0.4105
L	4.15	2.75	0.61	79.34	0.53	-10.76	
	0.33	0.49	1.14	0.02	0.15	0.50	0.1777
CF R	1.36	0.68	0.06	22.74	0.18	-4.14	
	0.41	0.58	0.92	0.01	0.14	0.56	0.1837
L	2.08	1.04	0.15	37.64	0.04	-4.83	
	0.28	0.54	1.09	0.02	0.11	0.48	0.1616

PICO RESULTS – 6 WEEKS

CASE	D max time (mm/s)	D ½ rel time (mm/s)	Tt	V max time (mms^{-1}/s)	V zero time (mms^{-1}/s)	V min time (mms^{-1}/s)	t0Accel (s)
CG R	3.03	1.52	0.15	46.67	0.73	-15.67	
	0.37	0.46	0.69	0.03	0.09	0.42	0.2665
L	5.50	2.75	0.64	67.42	0.50	-18.44	
	0.20	0.36	0.68	0.02	0.10	0.31	0.3601
CH R	4.63	2.32	0.23	94.08	0.12	-20.83	
	0.26	0.42	0.74	0.009	0.12	0.41	0.1458
L	3.60	1.80	0.16	99.33	0.009	-10.52	
	0.09	0.43	0.77	0.009	0.11	0.40	0.1437
CJ R	3.51	1.76	0.26	89.79	-0.73	-17.81	
	0.16	0.26	0.56	0.009	0.14	0.25	0.2567
L	4.15	2.08	0.78	111.23	0.42	-14.41	
	0.17	0.35	0.68	0.009	0.15	0.30	0.2999
CK R	3.42	1.71	0.07	81.59	0.65	-17.81	
	0.12	0.25	0.61	0.009	0.11	0.24	0.2395
L	3.17	1.59	0.32	65.14	0.12	-11.01	
	0.10	0.34	0.65	0.009	0.15	0.36	0.3047
CL R	2.93	1.47	0.45	65.27	0.24	-8.60	
	0.31	0.49	0.84	0.009	0.10	0.44	0.1333
L	4.01	2.01	0.20	84.10	0.59	-15.81	
	0.09	0.37	0.65	0.009	0.15	0.36	0.3617
CM R	2.54	1.27	0.01	63.54	0.78	-11.59	
	0.13	0.26	0.60	0.009	0.11	0.31	0.2327
L	3.12	1.56	0.19	79.76	0.60	-14.72	
	0.17	0.30	0.64	0.009	0.16	0.28	0.2843

PICO RESULTS – 6 WEEKS

CASE	D max time (mm/s)	D ½ rel time (mm/s)	Tt	V max time (mms^{-1}/s)	V zero time (mms^{-1}/s)	V min time (mms^{-1}/s)	t0Accel (s)
DA R	2.74	1.37	0.22	37.03	0.42	-6.44	
	0.25	0.47	0.77	0.02	0.19	0.43	0.4491
L	3.14	1.57	0.09	40.34	0.09	-8.08	
	0.18	0.46	0.83	0.02	0.18	0.46	0.4400
DB R	2.41	1.21	0.17	39.38	0.14	-6.68	
	0.31	0.50	0.99	0.02	0.20	0.46	0.4609
L	2.71	1.36	0.19	51.99	0.18	-7.57	
	0.28	0.48	0.99	0.02	0.15	0.44	0.1830
DC R	2.21	1.11	0.32	23.46	0.18	-4.73	
	0.49	0.77	1.03	0.02	0.23	0.66	0.2416
L	3.40	1.70	0.47	65.36	0.12	-9.68	
	0.30	0.52	0.99	0.01	0.13	0.47	0.1484
DD R	3.09	1.55	0.22	51.64	0.03	-10.09	
	0.31	0.47	0.74	0.02	0.26	0.45	0.4360
L	3.98	1.99	0.61	69.43	0.33	-7.21	
	0.30	0.67	1.08	0.02	0.29	0.52	0.1995
DE R	3.08	1.54	1.09	51.44	0.16	-5.40	
	0.31	0.69	0.93	0.01	0.24	0.51	0.5196
L	3.09	1.05	0.46	49.88	0.01	-5.84	
	0.18	0.80	1.12	0.01	0.18	0.64	0.2241
DF R	3.38	1.69	0.80	48.24	0.46	-7.26	
	0.28	0.47	0.88	0.02	0.17	0.42	0.4200
L	3.58	1.79	0.33	67.63	0.24	-7.60	
	0.19	0.46	1.02	0.02	0.14	0.38	0.3706

PICO RESULTS – 6 WEEKS

CASE	D max	D ½ rel		V max	V zero	V min	
	mm	mm		mms^{-1}	mms^{-1}	mms^{-1}	
	s	s		s	s	s	s
	time	time	Tt	time	time	time	t0Accel
DG R	3.44	1.72	0.16	103.80	0.35	-15.89	
	0.20	0.32	0.75	0.009	0.17	0.30	0.1000
L	5.15	2.58	0.52	121.82	-1.20	-12.97	
	0.09	0.39	0.76	0.008	0.97	0.39	0.1377
DH R	4.42	2.21	0.26	107.93	1.00	-19.48	
	0.31	0.44	0.82	0.009	0.09	0.42	0.1322
L	4.57	2.29	0.65	104.17	0.60	-20.16	
	0.19	0.31	0.54	0.009	0.16	0.29	0.2856
DJ R	3.67	1.83	0.15	59.02	0.86	-11.66	
	0.19	0.44	0.78	0.009	0.13	0.43	0.1893
L	4.75	2.38	0.33	124.05	0.65	-21.58	
	0.09	0.35	0.64	0.008	0.09	0.35	0.1271
DK R	4.48	2.24	0.22	129.22	0.22	-16.77	
	0.11	0.35	0.66	0.009	0.09	0.35	0.1394
L	4.70	2.35	0.20	138.76	0.50	-15.14	
	0.16	0.39	0.77	0.01	0.09	0.35	0.1308
DL R	2.67	1.34	0.13	50.98	0.35	-12.09	
	0.18	0.32	0.60	0.007	0.14	0.31	0.2997
L	2.68	1.34	0.20	77.47	0.33	-10.90	
	0.08	0.37	0.63	0.009	0.13	0.34	0.1306
DM R	2.83	1.42	0.26	72.38	0.008	-11.93	
	0.29	0.41	0.75	0.008	0.09	0.39	0.2997
L	4.31	2.16	0.12	87.04	0.42	-20.64	
	0.17	0.28	0.69	0.009	0.15	0.28	0.2661

PICO RESULTS – 6 WEEKS

CASE	D max time (mm s)	D ½ rel time (mm s)	Tt	V max time (mms^{-1} s)	V zero time (mms^{-1} s)	V min time (mms^{-1} s)	t0Accel (s)
N1 R	3.15	1.58	0.26	63.00	0.64	-11.41	
	0.11	0.33	0.66	0.009	0.13	0.31	0.3117
L	4.07	2.04	1.26	89.89	0.37	-12.03	
	0.13	0.42	0.67	0.009	0.45	0.36	0.3510
N2 R	3.12	1.56	0.68	79.71	0.13	-9.65	
	0.15	0.38	0.76	0.009	0.17	0.31	0.3050
L	3.24	1.62	0.23	66.88	0.71	-15.44	
	0.15	0.26	0.57	0.009	0.13	0.24	0.2337
N3 R	2.83	1.42	0.69	69.19	0.22	-8.64	
	0.22	0.50	0.79	0.009	0.10	0.43	0.1230
L	3.32	1.66	0.73	68.32	0.59	-10.29	
	0.35	0.55	0.82	0.009	0.15	0.49	0.1850
N4 R	2.40	1.20	0.06	74.26	0.52	-9.10	
	0.07	0.31	0.46	0.009	0.07	0.35	0.1150
L	2.89	1.45	0.62	79.69	0.70	-8.97	
	0.22	0.42	0.77	0.01	0.10	0.37	0.1100
N5 R	3.77	1.89	0.18	121.37	0.22	-11.69	
	0.07	0.31	0.65	0.009	0.08	0.32	0.1221
L	3.73	1.87	0.22	113.47	0.51	-11.42	
	0.82	0.32	0.72	0.009	0.91	0.34	0.1372
N6 R	3.03	1.52	0.11	104.48	0.55	-14.41	
	0.11	0.23	0.57	0.006	0.09	0.21	0.2102
L	2.95	1.48	0.30	77.44	0.51	-11.30	
	0.18	0.36	0.78	0.01	0.19	0.32	0.1003

PICO RESULTS – 6 WEEKS

CASE	D max	D ½ rel		V max	V zero	V min	
	mm			mms^{-1}			
	s			s			s
	time	time	Tt	time	time	time	t0Accel
N7 R	3.54	1.78	0.20	105.55	0.29	-9.48	
	0.80	0.35	0.76	0.009	0.08	0.34	0.1289
L	4.11	2.06	0.84	118.68	0.80	-8.04	
	0.84	0.39	0.76	0.009	0.08	0.13	0.1204
N8 R	3.37	1.69	0.32	81.65	0.49	-12.01	
	0.19	0.38	0.78	0.009	0.13	0.37	0.1587
L	3.19	1.96	0.27	81.81	0.20	-13.44	
	0.59	0.39	0.75	0.009	0.12	0.37	0.1812
N9 R	4.21	2.11	0.74	81.06	0.50	-22.99	
	0.11	0.21	0.43	0.009	0.09	0.16	0.1680
L	3.33	1.12	0.13	58.48	0.95	-11.29	
	0.09	0.32	0.55	0.007	0.08	0.25	0.2559
N10 R	3.08	1.54	0.41	95.46	0.38	-7.79	
	0.21	0.44	0.72	0.008	0.20	0.36	0.0929
L	2.77	1.39	0.39	84.20	0.05	-8.70	
	0.02	0.41	0.69	0.01	0.10	0.36	0.1208
N11 R	4.47	2.24	0.71	128.45	0.15	-11.66	
	0.86	0.51	0.78	0.009	0.10	0.46	0.1282
L	3.76	1.88	0.27	97.22	0.98	-10.72	
	0.30	0.51	0.87	0.009	0.10	0.48	0.1424
N12 R	3.33	1.67	0.18	95.32	0.02	-12.01	
	0.17	0.36	0.68	0.01	0.10	0.34	0.1410
L	4.14	2.07	0.33	134.96	0.30	-15.51	
	0.13	0.33	0.57	0.007	0.11	0.29	0.2837

PICO RESULTS – 6 WEEKS

CASE	D max	D ½ rel		V max	V zero	V min	
	mm	mm		mms^{-1}	mms^{-1}	mms^{-1}	
	s	s		s	s	s	s
	time	time	Tt	time	time	time	t0Accel
W1 R	2.38	1.19	0.34	59.03	0.46	-9.42	
	0.28	0.39	0.65	0.008	0.11	0.37	0.1212
L	3.29	1.65	0.16	98.54	0.26	-13.27	
	0.17	0.34	0.66	0.008	0.11	0.33	0.1273
W2 R	3.02	1.51	0.22	77.95	0.78	-9.25	
	0.08	0.43	0.75	0.009	0.10	0.42	0.1326
L	3.82	1.91	0.56	95.20	0.08	-9.01	
	0.10	0.49	0.83	0.009	0.11	0.44	0.1471
W3 R	3.50	1.75	0.26	101.34	0.63	-12.98	
	0.17	0.42	0.74	0.009	0.09	0.38	0.1093
L	4.79	2.40	1.15	122.86	0.46	-7.60	
	0.13	0.49	0.81	0.009	0.12	0.34	0.3372
W4 R	3.11	1.51	0.51	84.38	0.22	-8.67	
	0.29	0.56	0.87	0.009	0.12	0.50	0.1358
L	4.79	2.40	1.15	122.86	0.46	-7.60	
	0.13	0.49	0.84	0.009	0.12	0.34	0.3103
W5 R	3.95	1.98	0.23	121.19	0.57	-12.04	
	0.18	0.40	0.76	0.009	0.09	0.34	0.1129
L	4.225	2.13	0.45	107.53	0.08	-15.69	
	0.19	0.39	0.71	0.009	0.19	0.36	0.1287
W6 R	3.15	1.76	0.28	102.68	0.61	-11.16	
	0.16	0.36	0.71	0.008	0.15	0.29	0.1233
L	4.02	2.01	0.31	125.10	0.60	-12.43	
	0.09	0.35	0.64	0.007	0.09	0.31	0.1266

PICO RESULTS – 6 WEEKS

CASE	D max (mm)	D ½ rel		V max (mms^{-1})	V zero	V min	
	time (s)	time (s)	Tt	time (s)	time (s)	time (s)	t0Accel (s)
W7 R	4.02	2.01	0.31	130.51	0.07	-12.18	
	0.09	3.50	0.64	0.007	0.08	0.30	0.1332
L	5.10	2.55	0.16	139.46	0.73	-19.17	
	0.18	0.35	0.76	0.009	0.12	0.35	0.3359
W8 R	3.79	1.89	0.38	103.75	0.51	-10.19	
	0.11	0.44	0.82	0.009	0.10	0.42	0.1373
L	3.85	1.98	0.73	99.13	0.28	-9.95	
	0.19	0.44	0.67	0.007	0.20	0.34	0.1167
W9 R	3.48	1.74	0.19	111.45	0.09	-13.52	
	0.17	0.34	0.70	0.008	0.18	0.30	0.1142
L	3.64	1.82	0.41	108.41	0.15	-12.06	
	0.13	0.35	0.78	0.009	0.15	0.30	0.1116
W10 R	3.21	1.61	0.17	78.84	0.60	-9.26	
	0.17	0.39	0.78	0.009	0.12	0.37	0.3593
L	3.42	1.71	0.23	110.17	0.50	-11.89	
	0.13	0.31	0.60	0.009	0.09	0.29	0.1329
W11 R	2.66	1.33	0.13	79.24	0.29	-9.49	
	0.08	0.35	0.73	0.008	0.12	0.31	0.3020
L	4.01	2.01	0.28	69.81	0.39	-14.57	
	0.10	0.32	0.74	0.008	0.12	0.26	0.2726
W12 R	2.48	1.24	0.04	68.52	0.07	-12.59	
	0.78	0.26	0.37	0.009	0.98	0.25	0.2558
L	3.41	1.71	0.31	87.23	0.19	-9.69	
	0.11	0.39	0.75	0.009	0.11	0.36	0.1626

PICO RESULTS – 6 WEEKS

CASE	D max time (mm s)	D ½ rel time (mm s)	Tt	V max time (mms^{-1} s)	V zero time (mms^{-1} s)	V min time (mms^{-1} s)	t0Accel (s)
S1 R	2.54	1.27	0.23	79.25	0.87	-8.70	
	0.07	0.44	0.82	0.009	0.07	0.38	0.1093
L	3.61	1.81	0.35	105.29	0.49	-10.79	
	0.10	0.36	0.61	0.009	0.09	0.33	0.1455
S2 R	4.05	2.03	0.21	93.95	0.06	-13.71	
	0.29	0.46	0.83	0.01	0.10	0.43	0.1310
L	4.39	2.19	0.48	117.59	0.49	-12.53	
	0.12	0.39	0.69	0.007	0.09	0.35	0.1441
S3 R	3.55	1.78	0.30	102.97	0.001	-10.69	
	0.09	0.39	0.82	0.009	0.11	0.35	0.3461
L	3.93	1.72	0.23	112.83	0.39	-10.90	
	0.15	0.41	0.86	0.009	0.09	0.34	0.1482
S4 R	3.58	1.79	0.20	87.37	0.58	-11.34	
	0.18	0.41	0.78	0.009	0.15	0.39	0.3617
L	3.82	1.91	0.26	113.03	0.08	-13.19	
	0.22	0.41	0.81	0.009	0.09	0.37	0.1071
S5 R	4.62	2.31	0.25	101.86	0.63	-15.28	
	0.08	0.33	0.69	0.008	0.11	0.32	0.3310
L	4.69	2.35	0.22	115.42	0.22	-14.75	
	0.12	0.39	0.80	0.009	0.14	0.36	0.3506
S6 R	3.44	1.72	0.12	91.11	0.08	-13.09	
	0.17	0.35	0.67	0.009	0.17	0.33	0.3167
L	3.82	1.96	0.20	137.78	0.87	-11.59	
	0.07	0.30	0.61	0.007	0.07	0.28	0.1420

PICO RESULTS – 6 WEEKS

CASE	D max time (mm/s)	D ½ rel time (mm/s)	Tt	V max time (mms^{-1}/s)	V zero time (mms^{-1}/s)	V min time (mms^{-1}/s)	t0Accel (s)
S7 R	3.59	1.80	0.31	47.51	0.45	-15.54	
	0.22	0.38	0.65	0.01	0.14	0.33	0.3467
L	3.73	1.81	0.41	59.44	0.68	-14.73	
	0.02	0.37	0.73	0.008	0.17	0.34	0.3427
S8 R	3.63	1.82	0.23	106.52	0.70	-8.42	
	0.11	0.37	0.74	0.008	0.98	0.35	0.1710
L	3.89	1.95	0.44	94.51	0.48	-9.12	
	0.12	0.39	0.79	0.009	0.11	0.35	0.1638
S9 R	3.35	1.68	0.25	84.13	0.09	-10.87	
	0.17	0.38	0.74	0.009	0.14	0.35	0.3514
L	3.77	1.89	0.32	85.46	0.42	-12.49	
	0.15	0.35	0.70	0.009	0.16	0.30	0.2948
S10 R	3.45	1.73	0.20	88.67	0.94	-9.59	
	0.11	0.37	0.73	0.008	0.11	0.31	0.2106
L	4.22	2.11	0.52	90.03	0.60	-11.43	
	0.15	3.56	0.70	0.009	0.13	0.33	0.3214
S11 R	4.11	2.06	0.36	119.06	0.36	-11.95	
	0.15	0.37	0.73	0.008	0.11	0.31	0.3054
L	4.54	2.27	0.41	118.81	0.61	-13.67	
	0.16	0.39	0.79	0.01	0.12	0.35	0.1408
S12 R	3.33	1.67	0.03	64.71	0.86	-13.98	
	0.13	0.28	0.60	0.008	0.11	0.29	0.2870
L	4.28	2.14	0.18	102.87	0.44	-17.30	
	0.11	0.28	0.58	0.008	0.11	0.25	0.2519

PICO RESULTS – 6 WEEKS

CASE	D max	D ½ rel		V max	V zero	V min	
	mm			mms^{-1}			
	time	time	Tt	time	time	time	t0Accel
	s			s			s
T1 R	Died						
L							
T2 R	Died						
L							
T3 R	3.44	1.72	0.38	78.41	0.24	-9.56	
	0.16	0.38	0.82	0.009	0.15	0.32	0.3260
L	4.14	2.07	0.25	104.31	0.45	-18.93	
	0.19	0.31	0.62	0.009	0.15	0.29	0.2806
T4 R	4.80	2.40	0.83	112.65	0.15	-16.58	
	0.19	0.38	0.77	0.009	0.18	0.34	0.3304
L	5.40	2.70	0.26	129.69	0.67	-19.73	
	0.22	0.42	0.76	0.009	0.22	0.39	0.1442
T5 R	4.32	2.16	0.23	79.95	0.33	-22.41	
	0.17	0.32	0.60	0.01	0.07	0.27	0.1298
L	5.31	2.66	0.52	159.42	0.28	-16.19	
	0.09	0.38	0.68	0.008	0.09	0.34	0.1299
T6 R	5.38	2.69	0.26	129.69	0.68	-19.63	
	0.22	0.42	0.76	0.009	0.21	0.40	0.1731
L	5.53	2.77	0.36	136.79	0.59	-19.38	
	0.17	0.41	0.69	0.009	0.13	0.39	0.1662

PICO RESULTS – 6 WEEKS

CASE	D max	D ½ rel		V max	V zero	V min	
	mm			mms^{-1}			s
	s			s			
	time	time	Tt	time	time	time	t0Accel
T7 R	4.22	2.11	0.32	53.94	0.74	-20.48	
	0.17	0.32	0.57	0.01	0.15	0.32	0.3167
L	4.36	2.18	0.49	136.49	0.24	-16.82	
	0.13	0.31	0.62	0.008	0.12	0.27	0.1165
T8 R	4.53	2.27	0.39	136.00	0.77	-16.31	
	0.08	0.39	0.65	0.009	0.08	0.33	0.1665
L	5.11	2.56	0.38	127.25	0.98	-16.46	
	0.10	0.32	0.57	0.009	0.09	0.35	0.1445
T9 R	3.49	1.75	0.25	92.34	0.41	-12.04	
	0.27	0.44	0.80	0.009	0.09	0.39	0.1357
L	3.71	1.86	0.23	78.84	0.67	-18.54	
	0.17	0.39	0.66	0.009	0.13	0.38	0.1294
T10 R	4.18	2.09	0.28	104.89	0.28	-20.79	
	0.21	0.34	0.60	0.009	0.19	0.33	0.1233
L	4.56	2.29	0.51	124.99	0.56	-14.37	
	0.21	0.42	0.70	0.007	0.09	0.34	0.1164
T11 R	3.40	1.70	0.43	87.41	0.64	-10.67	
	0.24	0.46	0.85	0.009	0.96	0.41	0.2659
L	4.04	2.02	0.20	78.47	0.23	-17.87	
	0.15	0.29	0.51	0.009	0.15	0.28	0.1245
T12 R	3.60	1.80	0.22	62.89	0.93	-15.13	
	0.28	0.42	0.71	0.009	0.13	0.41	0.3183
L	4.29	2.15	0.27	103.51	0.28	-16.80	
	0.19	0.34	0.66	0.009	0.16	0.32	0.1506

APPENDIX 9

INSTRON RESULTS – 6 MONTHS (A)

	kgf	mm
CASE	Force (UTS)	Displacement
A1 R	24.60	15.56
L	19.12	13.17
A2 R	19.61	9.62
L	18.74	14.22
A3 R	22.95	9.75
L	17.44	11.46
A6 R	16.91	10.85
L	15.30	4.02
A10 R	29.96	12.29
L	11.47	7.61
A12 R	23.48	9.69
L	16.9	14.98

INSTRON RESULTS – 6 MONTHS (B)

	kgf	mm
CASE	Force (UTS)	Displacement
B2 R	17.77	10.91
L	16.09	9.27
B5 R	13.34	15.89
L	11.27	17.43
B6 R	21.61	18.46
L	17.42	11.86
B7 R	16.00	12.05
L	11.04	10.47
B11 R	38.98	12.65
L	26.90	7.82
B12 R	36.22	11.65
L	32.79	11.15

INSTRON RESULTS – 6 MONTHS (C)

	kgf	mm
CASE	Force (UTS)	Displacement
C1 R	29.69	12.11
L	26.02	12.57
C4 R	19.85	13.56
L	16.81	15.11
C6 R	21.58	16.79
L	18.69	8.15
C10 R	43.82	6.63
L	19.06	10.65
C11 R	35.44	13.35
L	30.69	6.65
C12 R	40.58	8.49
L	18.15	13.17

INSTRON RESULTS – 6 MONTHS (D)

	kgf	mm
CASE	Force (UTS)	Displacement
D1 R	18.22	10.93
L	17.97	16.09
D2 R	20.93	10.99
L	18.91	15.42
D6 R	22.33	14.69
L	20.94	16.01
D10 R	35.44	11.50
L	33.57	6.23
D11 R	27.23	8.93
L	29.46	12.35
D12 R	38.27	9.32
L	36.10	7.13

INSTRON RESULTS – 6 WEEKS (A)

CASE	kgf Force (UTS)	mm Displacement
AG R	6.25	11.43
L	38.42	7.52
AH R	12.84	13.21
L	29.89	7.39
AJ R	5.27	8.62
L	26.86	7.20
AK R	7.01	13.66
L	16.28	7.66
AL R	4.94	8.33
L	13.47	4.80
AM R	5.46	6.22
L	12.46	14.04

INSTRON RESULTS – 6 WEEKS (B)

	kgf	mm
CASE	Force (UTS)	Displacement
BG R	12.42	13.99
L	31.30	11.19
BH R	4.99	6.74
L	30.81	8.76
BJ R	9.95	6.80
L	31.98	8.46
BK R	17.39	12.18
L	27.80	6.65
BL R	8.13	9.97
L	21.87	7.01
BM R	5.44	17.06
L	27.40	9.36

INSTRON RESULTS – 6 WEEKS (C)

	kgf	mm
CASE	Force (UTS)	Displacement
CB R	11.56	3.88
L	22.98	5.30
CC R	13.34	3.61
L	18.97	6.57
CD R	6.77	6.64
L	19.38	7.37
CG R	17.52	9.15
L	37.81	9.97
CH R	6.65	6.72
L	31.22	9.79
CJ R	6.38	13.67
L	33.65	7.36

INSTRON RESULTS – 6 WEEKS (D)

CASE	kgf Force (UTS)	mm Displacement
DB R	7.94	10.42
L	26.91	5.66
DC R	5.58	6.58
L	25.46	10.43
DF R	5.94	5.32
L	23.13	13.63
DG R	7.15	7.85
L	26.74	5.98
DH R	9.84	7.35
L	25.09	8.59
DJ R	11.05	9.19
L	23.38	4.04

INSTRON RESULTS – 6 WEEKS (N)

	kgf	mm
CASE	Force (UTS)	Displacement
N4 R	12.56	4.72
L	12.59	5.12
N6 R	25.94	8.11
L	31.13	7.49
N7 R	24.65	8.21
L	25.41	9.32
N8 R	14.85	7.04
L	15.09	4.79
N9 R	28.63	8.56
L	26.00	9.53
N10 R	28.12	5.99
L	27.07	5.89

INSTRON RESULTS – 6 WEEKS (S)

CASE	kgf Force (UTS)	mm Displacement
S1 R	43.26	10.19
L	31.47	10.23
S2 R	45.01	9.16
L	37.20	8.09
S3 R	27.35	9.54
L	34.15	14.47
S4 R	45.28	9.19
L	34.38	9.88
S5 R	39.55	12.26
L	36.30	7.81
S6 R	44.92	8.79
L	38.66	9.56

INSTRON RESULTS – 6 WEEKS (W)

	kgf	mm
CASE	Force (UTS)	Displacement
W4 R	20.36	8.11
L	18.62	6.70
W5 R	44.66	10.97
L	34.48	9.79
W6 R	24.10	8.78
L	23.30	7.42
W7 R	27.99	8.65
L	24.57	9.26
W8 R	29.77	7.70
L	34.14	12.04
W9 R	31.70	15.28
L	24.07	6.32

INSTRON RESULTS – 6 WEEKS (T)

CASE	kgf Force (UTS)	mm Displacement
T1 R	Died	
L		
T3 R	7.03	12.18
L	37.30	7.28
T4 R	20.85	12.23
L	39.36	8.66
T6 R	6.74	8.78
L	34.43	8.68
T7 R	3.41	8.15
L	57.99	11.38
T8 R	13.05	15.43
L	35.05	7.17

APPENDIX 10

MORPHOMETRIC AIS DATA – 6 MONTHS

CASE NO		IOD HUE	IOD INTESNS	AREA mm^2	PERIM mm	LENGTH mm	FERET X mm	FERET Y mm	FORM FACTOR
A4	L	Died							
	R								
A5	L	178.82	0.485	3.218	7.673	3.276	1.886	2.903	0.687
	R	183.88	0.553	11.529	15.862	6.450	3.771	5.890	0.576
A7	L	183.80	0.513	6.333	10.608	4.395	3.326	3.475	0.707
	R	182.50	0.532	19.263	18.589	7.764	5.191	6.038	0.701
A8	L	184.79	0.445	5.180	8.915	3.459	2.924	2.564	0.819
	R	181.56	0.481	15.754	16.914	6.912	4.068	6.038	0.692
A9	L	173.68	0.449	3.675	8.027	3.326	1.674	3.178	0.717
	R	182.46	0.524	18.142	20.028	7.746	5.911	5.466	0.568
A11	L	179.76	0.538	4.790	9.067	3.692	3.072	2.669	0.732
	R	184.78	0.475	25.113	19.336	6.917	5.699	5.657	0.844

CASE NO		IOD HUE	IOD INTESNS	AREA mm^2	PERIM mm	LENGTH mm	FERET X mm	FERET Y mm	FORM FACTOR
B1	L	175.97	0.550	7.720	11.637	4.662	2.606	4.470	0.716
	R	184.64	0.513	18.549	19.633	6.878	5.148	5.424	0.605
B3	L	183.81	0.487	4.637	8.793	3.549	3.136	2.373	0.754
	R	182.63	0.505	26.630	23.757	7.967	7.119	6.038	0.593
B4	L	174.66	0.523	5.800	9.359	3.647	3.263	2.373	0.832
	R	183.71	0.483	11.890	15.363	5.856	3.220	5.720	0.633
B8	L	176.67	0.494	3.350	7.094	2.850	2.246	2.119	0.836
	R	180.39	0.570	20.575	18.958	7.090	5.911	5.890	0.719
B9	L	189.00	0.447	4.249	8.020	3.103	2.564	2.352	0.830
	R	181.33	0.464	20.756	19.454	7.625	4.936	6.038	0.689
B10	L	179.91	0.495	8.991	11.767	4.556	4.004	3.369	0.816
	R	182.19	0.535	11.515	16.480	5,654	4.025	5.487	0.533

MORPHOMETRIC AIS DATA – 6 MONTHS

CASE NO		IOD HUE	IOD INTESNS	AREA mm^2	PERIM mm	LENGTH mm	FERET X mm	FERET Y mm	FORM FACTOR
C2	L	183.04	0.459	2.468	7.538	2.892	2.881	1.589	0.767
	R	190.11	0.485	10.560	22.032	7.717	5.975	6.038	0.532
C3	L	177.46	0.457	5.788	11.181	4.367	2.203	4.216	0.582
	R	191.88	0.593	18.004	17.790	7.045	4.809	5.975	0.715
C5	L	Died							
	R								
C7	L	171.09	0.585	2.418	6.187	2.198	2.013	1.864	0.794
	R	179.78	0.503	19.334	17.093	6.439	4.936	5.911	0.832
C8	L	175.74	0.482	4.938	8.560	3.200	2.839	2.485	0.847
	R	184.47	0.495	9.032	13.257	4.744	4.216	3.559	0.646
C9	L	178.25	0.486	6.880	9.899	3.492	2.966	3.008	0.882
	R	206.67	0.496	9.319	11.915	4.197	3.475	3.623	0.825

CASE NO		IOD HUE	IOD INTESNS	AREA mm^2	PERIM mm	LENGTH mm	FERET X mm	FERET Y mm	FORM FACTOR
D3	L	179.72	0.473	5.231	8.514	2.910	2.627	2.733	0.907
	R	183.10	0.461	20.253	20.300	7.735	7.331	5.148	0.618
D4	L	181.91	0.507	3.778	8.776	3.337	2.754	2.458	0.616
	R	184.04	0.478	28.789	25.323	9.866	9.301	5.996	0.564
D5	L	178.20	0.445	3.372	8.625	3.294	2.436	2.606	0.570
	R	185.87	0.533	8.655	14.259	5.040	3.157	4.597	0.535
D7	L	178.33	0.537	4.538	8.625	3.371	2.818	2.627	0.767
	R	182.81	0.535	8.655	14.259	5.040	3.157	4.597	0.535
D8	L	185.13	0.454	5.049	10.451	3.998	2.013	3.983	0.581
	R	180.54	0.530	8.965	12.463	5.065	3.305	4.640	0.725
D9	L	171.51	0.507	4.668	8.618	3.427	2.521	2.860	0.790
	R	182.83	0.556	6.091	14.477	5.061	3.602	4.492	0.365

MORPHOMETRIC AIS DATA – 6 WEEKS

CASE NO	IOD HUE	IOD INTESNS	AREA mm^2	PERIM mm	LENGTH mm	FERET X mm	FERET Y mm	FORM FACTOR
AA L	193.21	0.440	5.152	9.248	3.739	2.924	2.754	0.757
R	198.71	0.509	24.130	20.263	7.353	5.784	5.614	0.739
AB L	178.52	0.502	3.106	7.805	2.934	2.479	1.949	0.641
R	194.68	0.547	32.215	27.054	9.642	8.305	6.038	0.553
AC L	176.23	0.494	3.675	9.547	4.197	2.797	3.411	0.507
R	187.01	0.545	22.443	18.652	7.129	4.936	5.551	0.811
AD L	182.65	0.505	4.084	8.218	3.090	2.585	2.458	0.760
R	183.39	0.511	27.603	21.902	8.273	5.763	6.038	0.723
AE L	175.97	0.511	4.803	9.306	3.379	3.199	2.288	0.697
R	185.58	0.553	26.660	21.809	8.132	7.394	5.212	0.704
AF L	175.09	0.516	4.813	9.217	3.542	3.072	2.585	0.712
R	182.99	0.561	31.358	23.213	8.421	6.928	5.953	0.731

CASE NO	IOD HUE	IOD INTESNS	AREA mm^2	PERIM mm	LENGTH mm	FERET X mm	FERET Y mm	FORM FACTOR
BA L	174.85	0.568	2.950	6.873	2.482	2.373	1.970	0.785
R	182.76	0.598	9.535	12.905	5.093	4.068	3.941	0.719
BB L	180.15	0.521	3.689	8.445	3.674	3.347	2.055	0.650
R	197.63	0.505	18.366	10.063	6.432	5.720	5.254	0.537
BC L	181.47	0.470	3.911	8.863	3.470	2.987	2.691	0.626
R	205.24	0.568	26.096	22.831	7.290	6.716	6.038	0.629
BD L	176.55	0.562	3.806	8.208	3.239	3.199	1.589	0.710
R	195.42	0.496	32.579	26.936	8.269	7.394	6.038	0.564
BE L	178.22	0.567	4.538	9.053	3.802	3.072	2.712	0.696
R	199.26	0.421	33.764	26.402	8.165	8.093	6.038	0.609
BF L	181.23	0.498	3.671	8.231	3.387	2.267	2.966	0.681
R	200.31	0.532	34.019	22.076	7.230	7.203	6.038	0.877

MORPHOMETRIC AIS DATA – 6 WEEKS

CASE NO		IOD HUE	IOD INTESNS	AREA mm^2	PERIM mm	LENGTH mm	FERET X mm	FERET Y mm	FORM FACTOR
CA	L	183.73	0.399	4.307	8.330	3.319	2.818	2.479	0.780
	R	193.03	0.495	18.983	18.543	7.137	4.216	6.038	0.694
CE	L	179.27	0.517	3.360	7.340	2.830	2.436	2.097	0.792
	R	202.79	0.454	31.070	23.841	8.758	8.093	5.953	0.687
CF	L	185.48	0.423	7.581	13.545	4.899	4.025	3.898	0.519
	R	189.98	0.477	25.855	21.330	7.616	5.614	6.038	0.714
CK	L	178.85	0.463	5.184	8.624	3.243	2.775	2.585	0.876
	R	188.58	0.604	15.576	17.082	6.870	3.983	6.038	0.671
CL	L	178.75	0.510	6.911	9.761	3.454	3.157	2.966	0.911
	R	184.20	0.479	14.991	16.138	6.251	5.784	3.729	0.723
CM	L	180.33	0.473	5.622	8.792	3.230	2.797	2.648	0.914
	R	185.90	0.515	11.048	12.647	4.656	4.364	3.390	0.868

CASE NO		IOD HUE	IOD INTESNS	AREA mm^2	PERIM mm	LENGTH mm	FERET X mm	FERET Y mm	FORM FACTOR
DA	L	176.22	0.584	5.070	8.641	3.210	2.797	2.691	0.853
	R	209.56	0.553	29.236	23.455	7.521	5.869	6.038	0.668
DD	L	189.39	0.423	9.790	13.613	5.512	3.898	4.809	0.664
	R	193.93	0.503	31.302	21.765	7.868	7.500	4.894	0.830
DE	L	195.24	0.536	4.596	10.492	3.918	3.750	2.288	0.525
	R	185.58	0.538	15.316	15.241	5.740	3.941	5.455	0.829
DK	L	165.41	0.549	3.414	8.012	3.345	2.839	2.267	0.688
	R	191.22	0.539	19.610	16.848	5.719	5.678	5.106	0.868
DL	L	177.61	0.512	4.299	7.725	2.997	2.648	2.034	0.890
	R	189.86	0.591	15.830	17.394	7.041	4.809	6.038	0.657
DM	L	175.04	0.549	4.393	8.059	3.179	2.775	2.228	0.850
	R	172.82	0.600	4.676	8.490	3.217	2.924	2.225	0.815

MORPHOMETRIC AIS DATA – 6 WEEKS

CASE NO	IOD HUE	IOD INTESNS	AREA mm^2	PERIM mm	LENGTH mm	FERET X mm	FERET Y mm	FORM FACTOR
N1 L	180.49	0.547	4.591	8.118	2.919	2.754	2.479	0.875
R	178.88	0.519	5.050	8.607	3.237	2.140	3.199	0.857
N2 L	179.65	0.505	5.740	9.188	3.400	3.136	2.797	0.855
R	177.76	0.474	5.330	9.446	3.912	3.157	2.966	0.751
N3 L	182.61	0.605	5.024	8.674	3.323	2.797	2.606	0.839
R	182.10	0.544	5.346	9.152	3.501	3.305	2.311	0.802
N5 L	179.55	0.568	3.578	8.488	3.598	2.246	3.136	0.624
R	177.38	0.498	4.648	8.105	3.075	3.051	2.076	0.889
N11 L	174.12	0.589	3.215	7.900	3.270	2.203	2.903	0.647
R	174.83	0.554	2.391	6.142	2.517	2.288	1.631	0.796
N12 L	175.60	0.545	6.554	10.500	4.246	4.131	2.267	0.747
R	178.5	0.523	3.623	8.602	3.564	2.267	3.220	0.615

CASE NO	IOD HUE	IOD INTESNS	AREA mm^2	PERIM mm	LENGTH mm	FERET X mm	FERET Y mm	FORM FACTOR
W1 L	181.67	0.536	2.439	6.934	2.893	2.436	1.907	0.637
R	185.72	0.545	7.981	12.757	4.699	4.025	3.305	0.616
W2 L	174.21	0.585	2.612	7.867	3.568	2.331	2.797	0.530
R	183.65	0.559	15.992	17.533	6.167	5.9111	4.301	0.654
W3 L	177.41	0.517	3.455	7.614	2.997	2.903	1.716	0.749
R	187.87	0.513	29.007	22.329	7.619	6.843	5.593	0.731
W10 L	174.18	0.492	2.674	6.296	2.396	2.288	1.610	0.848
R	184.21	0.538	10.610	15.075	6.231	4.261	5.508	0.587
W11 L	180.02	0.513	3.607	7.963	3.312	3.136	1.653	0.715
R	193.24	0.535	27.210	19.803	6.665	6.525	5.614	0.872
W12 L	188.88	0.565	6.190	11.583	4.570	3.729	3.157	0.580
R	186.21	0.545	23.437	19.278	7.122	6.356	5.911	0.792

MORPHOMETRIC AIS DATA – 6 WEEKS

CASE NO		IOD HUE	IOD INTESNS	AREA mm^2	PERIM mm	LENGTH mm	FERET X mm	FERET Y mm	FORM FACTOR
S7	L	176.35	0.525	2.856	6.750	2.736	2.331	2.055	0.788
	R	181.82	0.463	6.860	10.142	3.769	2.987	3.538	0.838
S8	L	180.86	0.475	7.123	10.113	3.683	3.644	2.585	0.875
	R	178.25	0.484	6.176	10.816	3.990	2.606	3.835	0.663
S9	L	181.35	0.477	5.095	8.607	3.206	3.244	2.076	0.864
	R	176.39	0.548	5.969	9.757	3.902	3.623	2.521	0.788
S10	L	177.57	0.494	3.613	7.398	2.637	2.648	1.780	0.830
	R	184.23	0.439	11.240	13.108	5.136	5.042	2.733	0.822
S11	L	180.33	0.437	7.149	10.857	4.315	3.665	3.136	0.762
	R	179.04	0.475	8.254	10.813	3.933	3.877	2.585	0.887
S12	L	181.88	0.555	6.333	10.857	4.379	3.157	3.390	0.726
	R	178.54	0.560	6.047	9.570	3.568	3.559	2.182	0.830

CASE NO		IOD HUE	IOD INTESNS	AREA mm^2	PERIM mm	LENGTH mm	FERET X mm	FERET Y mm	FORM FACTOR
T2	L	Died							
	R								
T8	L	162.24	0.537	3.390	7.188	2.799	2.309	2.225	0.824
	R	208.72	0.445	29.812	22.380	7.942	6.292	7.436	0.748
T9	L	172.59	0.471	5.764	9.611	3.944	3.093	2.775	0.784
	R	203.96	0.375	20.137	20.927	6.475	5.212	6.038	0.578
T10	L	169.93	0.552	4.832	8.350	2.946	2.627	2.691	0.871
	R	200.67	0.518	16.887	15.979	6.049	3.877	5.847	0.831
T11	L	172.89	0.510	2.527	6.103	2.335	2.309	1.377	0.852
	R	232.16	0.451	15.671	15.930	5.957	3.453	5.636	0.776
T12	L	151.37	0.592	6.374	9.493	3.440	2.542	3.199	0.889
	R	239.14	0.464	20.066	17.027	5.811	5.763	5.021	0.870

APPENDIX 11
MORPHOMETRIC ANALYSIS - % COMPOSITION 6 MONTHS

CASE		TENDON	BV'S	SUTURE	OTHER
A4	L	Died			
	R				
A5	L	100	0	0	0
	R	85	11	0	4
A7	L	96	4	0	0
	R	88	9	0	3
A8	L	95	5	0	0
	R	90	6	0	4
A9	L	100	0	0	0
	R	95	5	0	0
A11	L	97	3	0	0
	R	77	7	16	0

CASE		TENDON	BV'S	SUTURE	OTHER
B1	L	100	0	0	0
	R	87	11	7	5
B3	L	98	2	2	0
	R	93	7	7	0
B4	L	94	6	6	0
	R	80	5	5	4
B8	L	95	5	5	0
	R	74	9	9	3
B9	L	89	11	11	0
	R	73	11	11	3
B10	L	91	9	9	0
	R	82	10	10	8

MORPHOMETRIC ANALYSIS - % COMPOSITION

CASE		TENDON	BV'S	SUTURE	OTHER
C2	L	98	0	0	0
	R	91	0	0	0
C3	L	100	0	0	0
	R	76	5	5	3
C5	L	Died			
	R				
C7	L	100	0	0	0
	R	95	5	0	0
C8	L	96	4	0	0
	R	78	9	13	0
C9	L	100	0	0	0
	R	88	9	0	3

CASE		TENDON	BV'S	SUTURE	OTHER
D3	L	100	0	0	0
	R	89	6	5	0
D4	L	98	2	0	0
	R	92	8	0	0
D5	L	94	6	0	0
	R	89	11	0	0
D7	L	97	3	0	0
	R	83	13	4	0
D8	L	100	0	0	0
	R	87	10	3	0
D9	L	100	0	0	0
	R	93	7	0	0

MORPHOMETRIC ANALYSIS - % COMPOSITION 6 WEEKS

CASE		TENDON	BV'S	SUTURE	OTHER
AA	L	96	4	0	0
	R	64	2	17	7
AB	L	100	0	0	0
	R	72	12	3	13
AC	L	100	0	0	0
	R	56	8	12	24
AD	L	100	0	0	0
	R	52	6	30	12
AE	L	89	11	0	0
	R	49	15	3	3
AF	L	88	12	0	0
	R	64	14	14	8

CASE		TENDON	BV'S	SUTURE	OTHER
BA	L	100	0	0	0
	R	64	27	0	9
BB	L	100	0	0	0
	R	64	17	12	7
BC	L	94	6	0	0
	R	68	17	4	11
BD	L	98	0	0	2
	R	50	16	30	4
BE	L	100	0	0	0
	R	49	28	15	8
BF	L	96	4	0	0
	R	51	20	24	8

MORPHOMETRIC ANALYSIS - % COMPOSITION

CASE		TENDON	BV'S	SUTURE	OTHER
CA	L	100	0	0	0
	R	70	14	16	0
CE	L	89	11	0	0
	R	68	28	4	0
CF	L	96	4	0	0
	R	84	16	0	0
CK	L	96	4	0	0
	R	68	9	23	0
CL	L	100	0	0	0
	R	77	11	12	0
CM	L	100	0	0	0
	R	63	28	0	9

CASE		TENDON	BV'S	SUTURE	OTHER
DA	L	100	0	0	0
	R	73	19	8	0
DD	L	93	7	0	0
	R	76	15	9	0
DE	L	100	0	0	0
	R	58	15	27	0
DK	L	97	3	0	0
	R	77	23	0	0
DL	L	96	4	0	0
	R	62	23	15	0
DM	L	100	0	0	0
	R	72	12	16	0

MORPHOMETRIC ANALYSIS - % COMPOSITION

CASE		TENDON	BV'S	SUTURE	OTHER
N1	L	99	1	-	0
	R	98	2	-	0
N2	L	100	0	-	0
	R	99	1	-	0
N3	L	98	2	-	0
	R	97	3	-	0
N5	L	100	0	-	0
	R	96	4	-	0
N11	L	99	0	-	1
	R	99	1	-	0
N12	L	99	1	-	0
	R	97	3	-	0

CASE		TENDON	BV'S	SUTURE	OTHER
S7	L	100	0	-	0
	R	99	1	-	0
S8	L	97	3	-	0
	R	96	4	-	0
S9	L	100	0	-	0
	R	97	0	-	3
S10	L	100	0	-	0
	R	99	0	-	1
S11	L	100	0	-	0
	R	100	0	-	0
S12	L	100	0	-	0
	R	100	0	-	0

MORPHOMETRIC ANALYSIS - % COMPOSITION

CASE		TENDON	BV'S	SUTURE	OTHER
W1	L	100	0	-	0
	R	93	5	-	2
W2	L	97	3	-	0
	R	94	6	-	0
W3	L	98	2	-	0
	R	92	5	-	3
W10	L	98	2	-	0
	R	92	6	-	2
W11	L	96	4	-	0
	R	93	5	-	2
W12	L	94	6	-	1
	R	88	8	-	4

CASE		TENDON	BV'S	SUTURE	OTHER
T2	L	Died			
	R				
T8	L	99	0	0	1
	R	53	33	4	10
T9	L	100	0	0	0
	R	83	19	0	8
T10	L	100	0	0	0
	R	63	25	0	12
T11	L	100	0	0	0
	R	47	23	0	30
T12	L	98	0	0	2
	R	52	36	0	12